PB-228 153

CARBON MONOXIDE REACTIONS IN THE AFTERFLAME ZONES OF ETHYLENE/OXYGEN AND ETHANE/OXYGEN FLAMES

Trilochan Singh

California University
Berkeley, California

June 1970

DISTRIBUTED BY:

NTIS
National Technical Information Service
U. S. DEPARTMENT OF COMMERCE
5285 Port Royal Road, Springfield Va. 22151

PB 228 153

CARBON MONOXIDE REACTIONS IN THE
AFTERFLAME ZONES OF
ETHYLENE/OXYGEN AND ETHANE/OXYGEN FLAMES

Trilochan Singh

Report No. TS-70-2
Grant PHS AP 00385

June, 1970

Approved by

Robert F Sawyer
Robert F. Sawyer
Associate Professor
Co-investigator

211

ABSTRACT

The kinetics of carbon monoxide disappearance in the afterflame zone of ethylene/oxygen and ethane/oxygen flames at equivalence ratios of 0.67, 0.80 and 1.0, pressures of .083 and .054 atm and temperature range of 1500 to 1700°K, supported on water-cooled rectangular flat flame burner were investigated. The composition profiles of stable species such as CO, CO_2, O_2, H_2O, N_2 and Ar were determined by subjecting the gas samples (taken with a triple walled water-cooled stainless steel probe) to mass spectrometric analysis. The profiles of hydroxyl radical, an unstable species and temperature were obtained by using ultraviolet absorption spectroscopy. Theoretical multicomponent diffusion coefficients were used for calculating the net reaction rates from the composition and temperature profiles. The uncertainty in theoretical diffusion coefficients do not affect significantly the reaction rate profiles of major stable species but result in a high uncertainty for the reaction rates of hydroxyl radical and molecular hydrogen. The measured mole fraction of hydroxyl radical shows consistent disagreement with those calculated from the equilibrium or partial equilibrium hypothesis. The overall rate of carbon monoxide disappearance and carbon dioxide appearance may be represented by simple global first order rate equation

$$-\frac{d[CO]}{dt} = k_{overall-1}[CO]$$

$$\frac{d[CO_2]}{dt} = k_{overall-2}[CO]$$

The value of $k_{overall}$ depends upon both the type of the fuel and equivalence ratio. The average values of $k_{overall-1}$ and $k_{overall-2}$ were found to be $1.49\times10^3 \exp^{-(2200/RT)}$ sec^{-1} and $1.02\times10^3\exp^{-(725/RT)} sec^{-1}$ respectively.

ja.

from 1a

The overall reaction rates for carbon monoxide and carbon dioxide were also calculated from a postulated reaction mechanism for the $CO/O_2/H_2$ system and compared with those deduced from the observed composition and temperature profiles. The recommended literature value for the rate coefficient ($k = 5.6\times10^{11} \exp^{-1080/RT}$ $cm^3\text{-mole}^{-1}\text{-sec}^{-1}$) of the reaction $CO + OH = CO_2 + H$ had to be increased by an average factor 2.6 to obtain agreement between the observed and calculated kinetic rates for carbon monoxide and carbon dioxide.

Theoretical flame structures were calculated by numerical integration of the coupled kinetic rate equations and the diffusion equations. (M) Measured temperature profiles were employed obviating the necessity for including the energy conservation relations. A consistent disagreement was obtained between the observed and calculated profiles of CO, CO_2, OH, H_2O and O_2. A systematic variation in the value of rate coefficients for various reactions and initial estimates for the radical species (H and O) concentrations leads to a good qualitative agreement between the theoretical and experimentally observed mole fraction profiles. The recommended literature value for k_{CO+OH} has to be increased by a factor of 2 which is in agreement with the overall reaction rate calculations from the postulated reaction mechanism.

ACKNOWLEDGEMENTS

The author wishes to express his sincere appreciation to Professor Robert F. Sawyer, Professor Ernest S. Starkman and Professor Laurence S. Caretto for providing guidance throughout the course of this work. Special thanks are due to the author's advisor, Professor R. F. Sawyer, for his continuous interest and encouragement.

The author would also like to thank Mr. Joseph DeCosta, Mr. Horton Stewart, Mr. Dick Jensen and other members of Hesse Hall Laboratories for their generous assistance in preparing the laboratory equipment.

Helpful discussions with fellow graduate students, in particular with Bill McLean, Norm Laurendeau, Mel Branch and Scott Samuelsen, are gratefully acknowledged.

The author is thankful to the National Air Pollution Control Administration for providing financial assistance under Grant AP-385-04 and University of California, Berkeley for awarding the University Science Fellowship in 1967-68 and a part of the computer time for this work.

Finally the author would like to thank his wife, Hardeep Singh, for her patience and forebearance.

TABLE OF CONTENTS

Page

CHAPTER 1 - Introduction 1

1.1 Introduction and Statement of the Problem 1
1.2 Approach 3
1.3 Outline of Presentation 5

CHAPTER 2 - Literature Review 7

2.1 General Survey 7
2.2 Overall Kinetics of Carbon Monoxide 8

CHAPTER 3 - Experimental Equipment and Procedure 20

3.1 Layout 20
3.2 Burner Assembly 20
3.3 Gas Supply and Flow Measurements 23
3.4 Gas Sampling 23
3.5 Mass Spectrometric Data Analysis 26
3.6 Spectroscopic System 26
3.7 External Light Source 27
3.8 Spectrograph 27
3.9 Ultraviolet Transmission Windows 29
3.10 Photoelectric Recording 29

CHAPTER 4 - Data Reduction 33

4.1 Flame Equations 33
4.2 Reaction Rate Calculations 36
4.3 Diffusion Velocity Calculations 36
4.4 Numerical Differentiation 39
4.5 Quantitative Determination of Hydroxyl Radical 39
4.6 Temperature Determination 49

CHAPTER 5 - Experimental Results 52

5.1 Data Gathering Procedure 52
5.2 Experimental Results 59

CHAPTER 6 - Overall Kinetic Interpretation 69

6.1 Overall Carbon Monoxide Disappearance/Carbon Dioxide Appearance Rates 69
6.2.A Dependence of CO/CO_2 Rates on Equivalence Ratio and Type of Fuel 89
6.2.B Comparison of Experimentally Measured and Theoretically Calculated Concentration of OH . . 95
6.3 Comparison with Other Works 98
6.4 Overall Reaction Rate for Disappearance of Oxygen 102

TABLE OF CONTENTS (Continued)

Page

CHAPTER 7 - Detailed Kinetic Interpretation 103

7.1 Outline of Approach 103
7.2 Calculation of Kinetic Reaction Rates 106
7.3 Comparison for Carbon Monoxide and Carbon Dioxide Reaction Rates 109
7.4 Reaction Rate Comparison for Oxygen, Water and Other Species 115
7.5 Theoretical Flame Structure 118

CHAPTER 8 - Conclusions 134

REFERENCES 137

APPENDIX 1 - Experimental Data 144

APPENDIX 2 - Error Analysis 156

APPENDIX 3 - Computer Program Listing 161

LIST OF ILLUSTRATIONS

Figure Title Page

2-1 Rate data for the reaction $CO + OH = CO_2 + H$ 13

3-1 Flate flame burner, subatmosphere chamber and flame observation instruments 21

3-2 Details of porous metal top flat flame burner assembly 22

3-3 Schematic diagram for gas flow 24

3-4 Triple walled, water cooled stainless steel probe . . . 25

3-5 Quartz spectral transmittance 28

3-6 Schematic layout for absorption spectroscopy 31

4-1 Temperature determination by ultraviolet absorption spectroscopy of OH for ethylene/oxygen/argon flame . 50

5-1 Mass spectrogram 55

5-2 A typical OH absorption spectrum for ethane/oxygen/argon flames 56

5-3 Carbon monoxide mole fraction profile ethylene/oxygen/argon flames, P = .054 atm, equivalence ratio = 0.81 60

5-4 Carbon dioxide mole fraction profile ethylene/oxygen/argon flames, P = .054 atm, equivalence ratio = 0.81 61

5-5 Water and hydroxyl radical mole fraction profile for ethylene/oxygen/argon flames, P = .054 atm and equivalence ratio = 0.81 62

5-6 Composition and temperature profiles for ethane/oxygen/argon flames at .083 atm pressure and equivalence ratio of 1.05. The mole fraction of argon is 0.60 63

5-7 Variation of oxygen mole fraction profile with equivalence ratio for ethane/oxygen/nitrogen flames, P = .084 atm and mole fraction of nitrogen = 0.60 64

5-8 Variation of carbon monoxide mole fraction with equivalence ratio for ethane/oxygen/nitrogen flames, P = .084 atm and mole fraction of nitrogen = 0.60 . . 65

LIST OF ILLUSTRATIONS (Continued)

Figure Title Page

5-9 Variation of carbon dioxide mole fraction with equivalence ratio for ethane/oxygen/nitrogen flames, P = .084 atm and mole fraction of nitrogen = 0.60 66

5-10 Reaction rate profiles for ethane/oxygen/argon flames at P = .083 atm and equivalence ratio = 1.05 67

6-1 Reaction order dependence with respect to oxygen for carbon monoxide disappearance rate for ethylene/oxygen flames, T = 1637±12°K 72

6-2 Reaction order dependence with respect to oxygen for carbon dioxide appearance rate for ethylene/oxygen flames 73

6-3 Reaction order dependence with respect to carbon monoxide for CO disappearance rate ethylene/oxygen flames 74

6-4 Reaction order dependence with respect to carbon monoxide for CO_2 appearance rate for ethylene/oxygen flames 75

6-5 Determination of Arrhenius parameters for $k_{overall-1}$, ethylene/oxygen flames, equivalence ratio = 0.67 (Data Group 1) 77

6-6 Determination of Arrhenius parameters for $k_{overall-2}$, ethylene/oxygen flames equivalence ratio = 0.67 (Data Group 1) 78

6-7 Determination of Arrhenius parameters for $k_{overall-1}$, ethylene/oxygen flames equivalence ratio = 0.8 (Data Group 2) 79

6-8 Determination of Arrhenius parameters for $k_{overall-2}$, ethylene/oxygen flames equivalence ratio = 0.8 (Data Group 2) 80

6-9 Determination of Arrhenius parameters for $k_{overall-1}$, ethylene/oxygen flames equivalence ratio = 1.0 (Data Group 3) 81

6-10 Determination of Arrhenius parameters for $k_{overall-2}$, ethylene/oxygen flames equivalence ratio = 1.0 (Data Group 3) 82

LIST OF ILLUSTRATIONS (Continued)

Figure Title Page

6-11 Determination of Arrhenius parameters for $k_{\text{overall-2}}$, ethane/oxygen flames equivalence ratio = 0.67 (Data Group 4) 83

6-12 Determination of Arrhenius parameters for $k_{\text{overall-1}}$, ethane/oxygen flames equivalence ratio = 0.80 (Data Group 5) 84

6-13 Determination of Arrhenius parameters for $k_{\text{overall-2}}$, ethane/oxygen flames equivalence ratio = 0.80 (Data Group 5) 85

6-14 Determination of Arrhenius parameters for $k_{\text{overall-1}}$, ethane/oxygen flames equivalence ratio = 1.0 (Data Group 6) 86

6-15 Determination of Arrhenius parameters for $k_{\text{overall-2}}$, ethane/oxygen flames equivalence ratio = 1.0 (Data Group 6) 87

6-16 Reaction order dependence with respect to hydroxyl radical for carbon monoxide disappearance rate, ethylene/oxygen flames, T = 1567±12°K 91

6-17 Reaction order dependence with respect to hydroxyl radical for carbon dioxide appearance rate, ethylene/oxygen flames, T = 1567±12°K 92

6-18 Influence of equivalence ratio on hydroxyl radical mole fraction profile, ethane/oxygen/argon flames, P = .084 atm 93

6-19 Influence of equivalence ratio on hydroxyl radical mole fraction profile, ethylene/oxygen/argon flames, P = .083 atm 94

6-20 Comparison of experimentally measured and theoretically calculated hydroxyl radical mole fraction profile, ethane/oxygen/argon flames, P = .084 atm 96

6-21 Comparison of experimentally measured and theoretically calculated hydroxyl radical mole fraction profile, ethylene/oxygen/argon flames, P = .084 atm 97

7-1 Variation of dimensionless parameter R_{∞} vs. reciprocal of temperature 113

7-2 Comparison of measured mole fraction data for H_2O with theoretical predictions, ethane/oxygen/argon flames, equivalence ratio = 1.0 and P = 0.083 atm 123

LIST OF ILLUSTRATIONS (Continued)

Figure **Title** **Page**

7-3 Comparison of measured mole fraction data for OH with theoretical predictions ethane/oxygen/argon flames, equivalence ratio 1.0 and P = .083 atm 124

7-4 Comparison of measured mole fraction data with theoretical predictions ethane/oxygen/argon flames, equivalence ratio = 0.67 and P = .083 atm 127

7-5 Comparison of measured mole fraction data with theiretical predictions ethane/oxygen/argon flames, equivalence ratio = 0.80 and P = .083 atm 128

7-6 Comparison of measured mole fraction data with theoretical predictions, ethane/oxygen/argon flames, equivalence ratio = 1.0 and P = .083 atm . . 129

7-7 Comparison of measured mole fraction data with theoretical predictions, ethylene/oxygen/argon flames, equivalence ratio = 0.67 and P = .083 atm 131

7-8 Comparison of measured mole fraction data with theoretical predictions, ethylene/oxygen/argon flames, equivalence ratio = 0.67 and P = .083 atm . . 132

LIST OF TABLES

Table Title Page

1-1 Annual emission of pollutants 2

1-2 Experimental methods for kinetic studies 4

2-1 Summary of works of various investigators 15

3-1 Principal performance characteristics of monochromator 30

4-1 List of isolated rotational lines of $^2\pi-^2\Sigma$ 0-0 transition for OH 44

4-2 Numerical values of parameters for equations (4.16)&(4.17) 46

5-1 Summary of experimental conditions 58

6-1 Experimental data groups 70

6-2 Summary of $k_{overall}$ for CO disappearance and CO_2 appearance rates (1500-1723°K temp. range) 88

6-3 Average values of R_{CO} for overall disappearance rate of CO 100

7-1 Main reactions for $H_2/CO/O_2$ system 110

7-2 Summary of R_{CO} for postulated mechanism 111

7-3 Summary of R_{CO_2} for postulated mechanism 112

7-4 Summary of R_{O_2} for postulated mechanism 116

CHAPTER 1

INTRODUCTION

1.1 Introduction and Statement of the Problem

The reliance of modern technology upon combustion is so great that the exhaust products of combustion have begun to contaminate vital resources such as water and air. The pollution of air is a very serious threat to man. We can purify water before we drink it but we must breath air as it comes to us, polluted or not. The hazards of air pollution have been demonstrated by the disasters that took place in the Meuse Valley of Belgium, in December 1930; in Donora, Pennsylvania in October 1948; in London in December 1952; and in New York City in 1953, 1962 and 1966. The long term effects of air pollution, such as increased incidence of bronchial tree diseases from the common cold to lung cancer, damage to vegetation and plants, and other effects resulting in loss of billions of dollars, are even more alarming.

Table 1-1 shows the major pollutants[1,2] and the quantity of each emitted from different sources into the atmosphere in the U.S.A. per annum. In recent years extensive research and development efforts have been directed towards reducing the concentration of pollutants noted in Table 1-1 (in order to conform to new Federal and State regulations establishing air quality standards) by controlling the post combustion processes. However, relatively little has been done towards understanding the basic combustion processes responsible for the generation and subsequent alteration of pollutant species. The need for this type of basic information is the primary motivation for this work.

From Table 1-1 we see that carbon monoxide is a major pollutant as it constitues about 50 percent of the total weight of pollutants

Table 1-1. Annual emission of pollutants, million of tons, References 1 and 2.

Pollutant	Sources					
	Central Power Plants	Industry	Motor Vehicles	Space Heating	Refuse Burning	Total Emission
CO	1	2	66	2	1	72
SO_x	12	9	1	3	1	26
Unburnt Hydrocarbon	1	4	12	1	1	19
NO_x	3	2	6	1	1	13
Particulate	3	6	1	1	1	12
Total	20	23	86	8	5	142

emitted in the U.S.A. per year. About 90 percent of CO is contributed by the exhaust gases of motor vehicles. Several experimental measurements[4,5,6] of the exhaust gases of automotive internal combustion engines and the post flame gases of pre-mixed flames of $H_2/CO/O_2$ systems have shown that (1) the concentration of CO and other pollutant species are greater than those predicted by equilibrium calculations at the corresponding temperatures and pressures, and (2) the concentrations of these pollutants are controlled by chemical kinetics. Because of its obvious importance to air pollution problems, the work reported here considers the kinetics of CO; in particular, the kinetics of CO afterburning in the post flame zones of pre-mixed flames of ethylene/oxygen and ethane/oxygen.

1.2 Approach

From the air pollution point of view the ideal system for a study of the kinetics of CO disappearance would be an internal combustion engine (reciprocating). With the present state of the art, it is very difficult, if not impossible, to monitor the concentration history of the various species during the expansion stroke. Using infrared spectroscopic techniques, Starkman and Newhall[7] have traced the concentration history of NO during the expansion process in an internal combustion engine. This work has been followed by that of Smith,[4] who has measured the concentration profile of hydroxyl radicals during the expansion stroke by using ultraviolet absorption spectroscopy. But the existence of severe temperature gradients and the uncertainties caused by turbulence and mixing of charge during the expansion process in the cylinder of an internal combustion engine limit the amount of information that can be attained, because of the mathematical

Table 1-2. Experimental methods for kinetics studies.

System	CHARACTERISTICS	TEMPERATURE RANGE
Discharge Flow Systems	Radicals produced by electric discharge suitable for simple reactions with low activation energy.	300-800°K
Photolysis	One of the reactants must be good absorber of light. Main difficulty is of identifying the primary process.	300-800°K
Shock Tube	Several termolecular reactions can be followed more clearly. Difficult experimental techniques involving observations in a small fraction of a second.	1500-8000°K
Static Reaction Vessels	Reactants heated at a controlled rate. Resulting changes of pressure, temperature and/or composition followed. Detailed kinetics tested for agreement with a few experimental parameters.	300-1000°K
Premixed Flames	Sustained by complex chemical reactions. Often difficult and ambiguous to isolate a given process. Main advantage is absence of walls which is somewhat counterbalanced at low pressures and high temperatures by the knowledge of diffusion coefficients required for all the species.	1000-2500°K
Stirred Reactions	A device in which the rates of heat and mass transfer are of such a magnitude so as to make the slowest and hence rate controlling step governed by chemical kinetics. This system has been used primarily for studying the overall kinetics of various fuels.	300-2000°K

difficulties that arise in making a meaningful kinetic analysis (such as a knowledge of the net chemical rate of change of species). In view of these difficulties, some alternate experimental systems were considered because of their past contribution to the knowledge of chemical kinetics rate data and mechanisms. The various experimental systems used for the kinetic studies have been discussed in detail by Pratt.[111] All suffer from some degree of complexity and limitations. A few of the characteristics of the various experimental systems are presented in Table 1-2.

After considering all of the systems in Table 1-2, the post flame (afterburning) zones of premixed ethane/oxygen and ethylene/oxygen laminar, low pressure flames supported on a flat flame burner were selected for the study of kinetics of CO. The primary reason for this selection was that the chemical processes occurring in these post flame zones offer a close similarity to those occurring in several practical combustors such as home furnaces, gas fired water heaters, power plants, etc. which use premixed charges of hydrocarbon fuels.

1.3 Outline of Presentation

In the following chapter, the literature review pertaining to the kinetics of carbon monoxide combustion in different experimental systems is presented. In Chapter 3, the details of the experimental apparatus are discussed. Chapter 4 outlines the flame equations used in the present study, discusses the computer techniques for their solution as well as the spectroscopic equations for the determination of hydroxyl radicals concentrations and the rotational temperature. The experimental results and data collecting procedure are presented in Chapter 5. The overall kinetic interpretations for CO, CO_2 and O_2 and comparison of the results with other works are given in Chapter 6. Chapter 7 is devoted to the detailed kinetic analysis of the experimental results. The last section of Chapter 7 is devoted to a discussion of flame structure as theoretically obtained by numerical integration of the flame equations and the kinetic equations. Possible reasons for deviation between the experimental and theoretical composition profiles are also discussed.

CHAPTER 2

LITERATURE REVIEW

2.1 General Survey

The development of the Egerton Powling[8] flat flame burner and subsequently the porous plate flat flame burner[9] has greatly facilitated the quantitative study of the microstructure of the flames. The use of these burners provides two major advantages for the study of premixed flames: (1) flat flame burners produce flames of simple one-dimensional geometry with flow perpendicular to the burner surface; (2) these provide flames of high stability since flame position is determined by heat losses from the burner surface. A large number of studies giving both qualitative and quantitative information on chemical kinetics of flames have appeared in the literature during the last 10-15 years. Two approaches have been taken for the analysis (interpretation) of chemical kinetics data:

1. Overall reaction kinetics
2. Detailed kinetics

In the first approach it is assumed that the reaction proceeds via an unknown path and the overall kinetics history of a species may be described by an empirical rate equation of the Arrhenius form:

$$\frac{d[x_i]}{dt} = k_{overall} [x_1]^a [x_2]^b \cdots [x_i]^n \qquad (2.1)$$

where x_i = concentration of ith species

$a, b, \cdots, n$ = reaction order with respect to various species

k = overall rate constant

The second approach consists of postulating a plausible mechanism describing the kinetic history of various species. The observed experimental parameters are compared with those calculated from the postulated reaction mechanism. The reaction steps and/or their rate coefficients are varied until agreement is obtained between the observed parameters and those predicted from the kinetic calculations. A few examples of this approach are discussed in the introductory part of section 7.1. The works of other investigators pertaining to the overall kinetics of carbon monoxide are reviewed in the following section.

2.2 Overall Kinetics of Carbon Monoxide

The measurements of temperature profiles through laminar flat flame zones is the simplest measurement in a flame (although perhaps the most unreliable) and hence was the first to be made. One such temperature study is that of Friedman and Burke,[10] who made use of a flat premixed laminar propane-air flame operated at low pressures so as to spread the measurement zone. The analysis of the heat release profiles showed that the chemical reaction was not complete at the end of luminous zone. Noting that the enthalpy required for conversion of propane and oxygen to carbon monoxide and water approximated the total heat release up to the end of the bright luminous zone, the authors postulated the important concept of two reaction zones for hydrocarbon flames. In the first zone (luminous or primary reaction zone) hydrocarbon is converted primarily to carbon monoxide and water, while in the second (post flame) zone, conversion of carbon monoxide to carbon dioxide takes place.

Friedman and Cypher[11] followed up the temperature measurements with the probing of concentration profiles downstream of the luminous zones of premixed propane-air flames on a flat flame burner. Mass spectrometric analysis of gas samples verified their earlier suggestion of two zone combustion for hydrocarbons. No hydrocarbons were detected in the zone sampled, but significant amounts of CO were found and the following overall rate expression of first order in CO was obtained for the disappearance of carbon monoxide.

$$-\frac{d[CO]}{dt} = 231 \times [CO] \quad \text{moles-cm}^{-3}\text{-sec}^{-1} \qquad (2.2)$$

Fenimore and Jones[12] sampled burnt gases from lean acetylene/air, methane/air, ethane/air and propane/air flames at one atmosphere pressure and the oxidation rate of carbon monoxide in the presence of ample water was found to be given by the following second order global rate expression first order in both oxygen and carbon monoxide.

$$-\frac{d[CO]}{dt} = 1\times 10^{12}\ \exp^{-24000/RT}\ [CO]\,[O_2]\ \text{moles-cm}^{-3}\text{-sec}^{-1} \qquad (2.3)$$

Some of the subsequent works of Friedman et al.[13] and Fenimore and Jones[14] deal with the effects of water addition on the burning rate of carbon monoxide in $CO/H_2/O_2$ and hydrocarbon/oxygen flames. One of the interesting results of these studies was that it apparently made no difference to the burning rate of CO if water resulted from the combustion of hydrocarbon or was added as water vapor.

Fristrom and Westenberg have published a series of papers on their studies of premixed laminar low pressure flat flames of methane and oxygen. Their work has been summarized in Reference 18. Their studies also support the theory of a double reaction zone for hydrocarbon combustion. For the post flame zone they postulated, in agreement with other workers, that carbon monoxide primarily disappears through the reaction

$$CO + OH = CO_2 + H \qquad (R.1)$$

and deduced profiles of hydroxyl radical concentrations from the rate of appearance of carbon dioxide. The deduced profile of OH was used to calculate the rate constant for the disappearance of CH_4 through the reaction

$$CH_4 + OH = CH_3 + H_2O \ .$$

By considering partial equilibrium of the reactions

$$O + H_2 = OH + H$$

$$O + O + M = O_2 + M$$

and neglecting the reverse of the reaction R.1, Fristrom and Westenberg[18] suggested the following overall rate expression for CO disappearance:

$$-\frac{d[CO]}{dt} = 4\times10^{13} \exp^{-45000/RT} [CO][H_2]^{1/2}[O_2]^{1/4} \text{ moles-cm}^{-3}\text{-sec}^{-1} \quad (2.4)$$

The postulate of two reaction zones for the combustion of hydrocarbons has also been verified by Longwell _et al._,[15] Hottel _et al._[16] and Williams _et al._[17] using stirred reactors as their experimental tool. Hottel _et al._[16,17] postulated that the overall burning rate of a hydrocarbon was governed by the rate of conversion of carbon monoxide to carbon dioxide primarily through the reaction

$$CO + OH = CO_2 + H$$

The concentrations of the radical species such as OH, H and O were obtained by partial equilibration (as suggested by the works of Bulewicz and Sudgen[19]) of the following reactions:

$$H + O_2 = OH + O$$

$$O + H_2 = OH + H$$

$$OH + H_2 = H_2O + H$$

Final equilibrium was postulated to be due to the following termolecular recombination reactions:

$$O + O + M = O_2 + M$$

$$H + H + M = H_2 + M$$

$$H + OH + M = H_2O + M$$

$$OH + OH + M = H_2 + O_2 + M$$

By making use of overall stoichoimetry for propane/air combustion, partial equilibrium hypothesis and certain other assumptions, Hottel et al.[16] were able to derive the following equation for the overall disappearance of CO

$$-\frac{d[CO]}{dt} = 2.9\times 10^{11} \exp^{-15000/RT} [CO][O_2]^{0.35}[H_2O]^{0.4} \text{moles-cm}^{-3}\text{sec}^{-1} \quad (2.5)$$

Williams, Hottel and Morgan[17] studied the combustion of methane in a well stirred reactor and obtained the following expression for the overall disappearance rate of carbon monoxide

$$-\frac{d[CO]}{dt} = 1.8\times 10^{13} \exp^{-25000/RT} [CO][O_2]^{1/2}[H_2O]^{1/2} \text{moles-cm}^{-3}\text{-sec}^{-1} \quad (2.6)$$

From a conventional flow reactor experiment, Kozlov[68] found the following expression for the disappearance of carbon monoxide

$$-\frac{d[CO]}{dt} = 1.04\times 10^{12} \exp^{-32000/RT} \frac{[CO][H_2O]^{.5}[O_2]^{.25}}{T^{2.5}} \text{moles-cm}^{-3}\text{-sec}^{-1} \quad (2.7)$$

Thus we see that different overall rate expressions for the oxidation of carbon monoxide for the same hydrocarbon fuel have been obtained in various experimental systems. But one of the common features in the combustion studies of hydrocarbons is the postulate that CO primarily disappears by the reaction R.1. This assumption has been used to infer the profiles of hydroxyl radical concentrations in several studies.[18, 22,27,28,29] The deduced profiles of OH have been used to infer the rate coefficients of the reactions of hydroxyl radical with other species such as CH_4, C_2H_2, C_2H_4, H_2 etc. But there are only a few flame studies in which the concentration of hydroxyl radical has been measured along with those of CO, CO_2 and other stable species.[30,31,32] These studies have been limited to H_2/O_2, $H_2/CO/O_2$, CH_4/O_2 and C_2H_2/O_2 systems because of their relative simplicity. The rate constant data for the reaction R.1 has been assigned different values. The published work on this rate constant is reviewed here.

Fristrom and Westenberg[18] and Fenimore and Jones[34] using flame studies and Avramenko and Lorenzo[35] using a discharge tube at low temperature, indicate a high activation energy E of the order of 7-8 kcals/mole for the reaction. From the studies of competitive reactions in mixtures of H_2, CO and O_2, Baldwin et al.[36] determined the ratio $k(OH+CO)/K(OH+H_2) = 0.31$ near 800°K as compared to the values ranging from 0.04 to 0.08 as obtained from the data of Fristrom et al.[18] and Fenimore and Jones.[34] Using estimates of $E(OH+H_2)$ as given by Kaufman and Del Greco[37] and Dixon-Lewis et al.,[38] it is found that E(OH+CO) should be close to zero. Blundell et al.[39] obtained a ratio of $k(OH+CH_4)/k(CO+OH)= 2$ at 773-800°K from the oxidation studies of CH_4 which emphasized the fate of formaldehyde and CO. Combining the above with Fenimore and Jones[40] estimate of $E(OH+CH_4) \simeq 9$ kcals/mole and Fristrom's[18] estimate of $E(OH+CH_4) \simeq 6.5$ kcals/mole it is found that $E(OH+CO) = 0-2$ kcals/mole. Wilson,[41] in a review, has suggested a value of $k(OH+CO) = 3.1\times10^{11} \exp^{-600/RT}$ $cm^3\text{-mole}^{-1}\text{-sec}^{-1}$. Browne et al.[30,42]

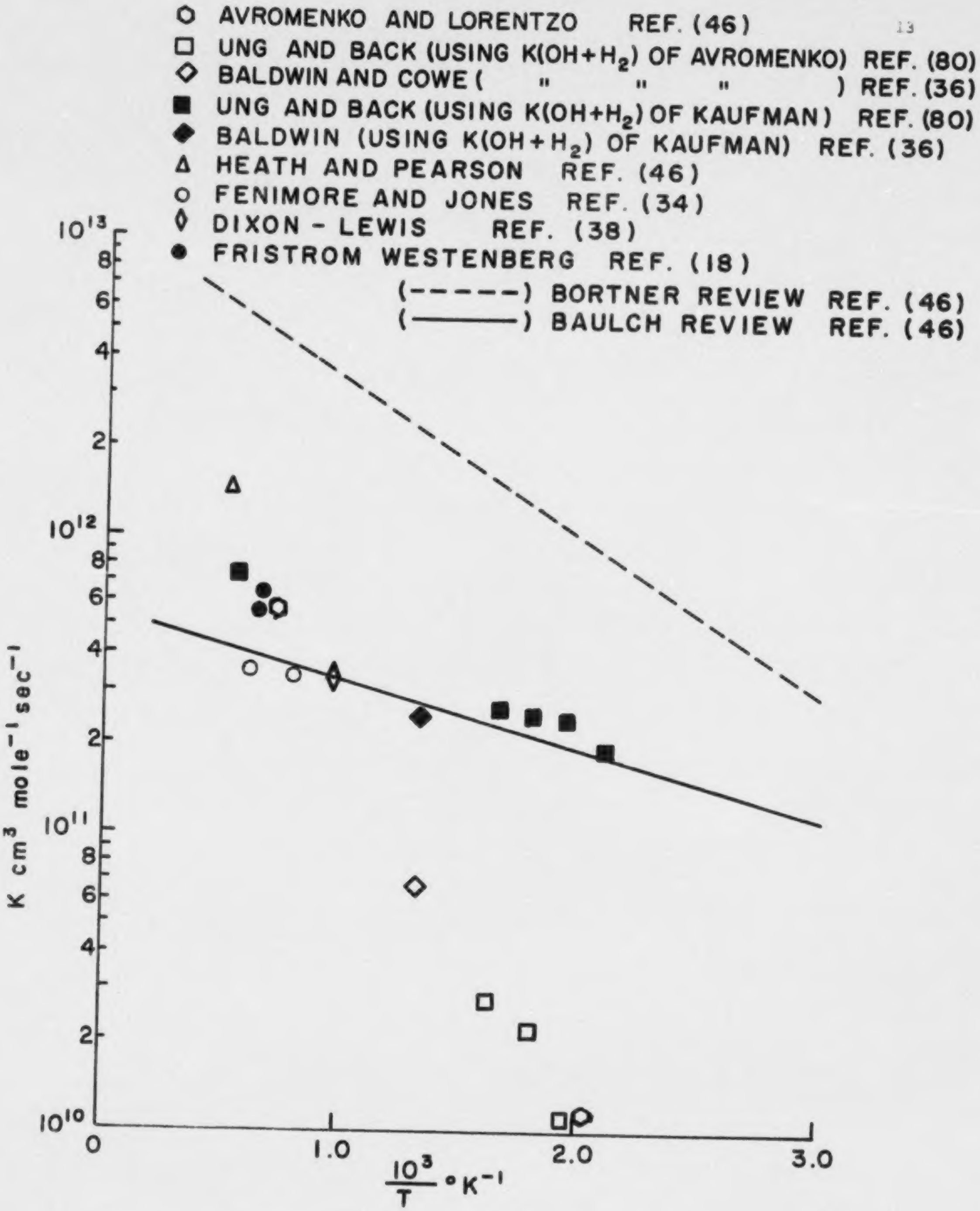

FIG. 2-1. RATE DATA FOR THE REACTION CO + OH = CO_2 + H

report a value of $k = 3.7\times10^{11} \exp^{-700/RT}$ cm^3-$mole^{-1}$-sec^{-1}. The results of Browne *et al.*[30,42] are in good agreement with the low temperature flow reactor studies of Dixon-Lewis *et al.*,[43] Greiner[44] and Wilson *et al.*[45] A critical evaluation by Baulch *et al.*[46] recommends k(OH+CO) = $5.6\times10^{11} \exp^{-1080/RT}$ cm^3-$mole^{-1}$-sec^{-1}. The available rate data for the reaction (CO+OH = CO_2+H) is plotted in Fig. 2-1. A review of the available rate data for other combustion reactions of importance to this study is presented in Reference 121.

A summary of the relevant work outlining the system, reactants, measured parameters and the results of various investigators is presented in Table 2-1. Because of the discrepancies reported in the various investigations in Table 2-1 and interest in the reaction of CO as related to the problem of air pollution, the process of conversion of CO to CO_2 has been chosen as a subject of further studies in the post flame zones of C_2H_4/O_2 and C_2H_6/O_2 flames. The experimental details are discussed in the next chapter.

Table 2-1. Summary of works of various investigators. T ≡ temperature; P ≡ pressure; ϕ ≡ equivalence ratio; x_{stable} = mole fraction stable species; V = burning velocity.

Authors	Reactants	System	Measured Parameters	Experimental Conditions	Results	Ref. No.
Friedman & Burke	C_3H_8-Air	Flat flame burner (Egerton-Pauling)	T - thermocouple	P=.059 atm T=300-1605°K	Two flame zone theory for hydrocarbon flames postulated	10
Friedman & Cypher	C_3H_8-Air	Same	T x_{stable}	Same	Global rate expression for $-\frac{d[CO]}{dt}$	11
"	$CO-O_2-N_2-H_2O$	Same	T V	P=40-100 mm T=2010° max	Global rate expression for burning velocity as function of reactant	13
Friedman & Nugent	$CO-O_2-H_2-H_2O$	Same	T x_{stable} V	T=1500-1700°K P=30.0 mm	Global rate expression for $-\frac{d[CO]}{dt}$ as function of reactant concentrations	112
Fenimore & Jones	$CO-O_2-H_2O$ C_2H_2-Air C_2H_4-Air CH_4-Air	Porous plate Flat flame burner	T x_{stable}	P=1 atms T=1700-2000°K	Global rate expression for $-\frac{d[CO]}{dt}$ obtained as fn[O_2, CO]	12
"	CH_4-O_2-Ar $C_2H_2-O_2$-Ar $C_3H_8-O_2$-Ar +D_2O trace	"	T x_{stable} [H] from [HD] profile	P=30-140 mm T=1300-1958°K	($H+O_2$=OH+O) main reaction for consumption of O_2 in H/C flame	20

Table 2-1. (Continued)

Authors	Reactants	System	Measured Parameters	Experimental Conditions	Results	Ref. No.
Fenimore & Jones	N_2O+H_2+Air $+D_2O$	Same	T x_{stable} [H] from [HD] profile	T=1260-1780 P=60-410 mm	Relative rates of $\frac{k(H_2+OH)}{k(CO+OH)}$ reported	34
"	$C_2H_4-O_2$-Air $C_2H_6-O_2$-Ar $+N_2O$	Same	T x_{stable} [OH] from $\frac{d[CO_2]}{dt}$ [H] from $\frac{d[O_2]}{dt}$	T=1400-1800 P=3-12 cm	Report k(RH+O) k(RH+H) k(RH+OH)	27
"	$C_2H_2-O_2$-CO Ar	Porous plate Flat flame burner	T x_{stable}	P=30 mm T=1000-1500°K ϕ=0.31, 2.4	Rate of (C_2H_2+O) reported after deducing [O] and [H] [OH] from $d[CO_2]/dt$ and $d[O_2]/dt$	28
"	"	"	"	P=30 mm ϕ=1.8 T=1700-2000	Rate of (C_2H_2+OH) reported for condition $[H]_{eq} > [OH]_{eq} >> [O]_{eq}$	29
Bulewitcz *et al.*	$H_2-O_2-N_2$	"	T $[H]_{photo-metrically}$	P=1 atm T=1600-2400°K	[OH] from balancing of $H+H_2O=H_2+OH$ postulated hypothesis of partial equilibrium	19

Table 2-1. (Continued)

Authors	Reactants	System	Measured Parameters	Experimental Conditions	Results	Ref. No.
Fristrom & Westenberg	CH_4-O_2 (8% fuel 92% O_2)	Egerton type Flat flame burner	T x_{stable}	P=0.1&.05 atm T=300-2000°K	[OH] deduced from d[CO_2]/dt and report k(CH_4=OH)	18
"	$C_2H_6-O_2$ $C_2H_4-O_2$ $C_2H_2-O_2$	"	T x_{stable} [H],[O] from ESR	T=729-1085 P=0.1 atms	[OH] from d[CO_2]/dt and report k(RH+OH) R = C_2H_4, C_2H_6, C_2H_2	22
Kaskan	H_2-air	Porous plate flat burner	T [OH] from u.v. abs. spect.	ϕ=1-2.5 T=1320-1698°K P=0.5-1 atms	[OH] gets partially equilibrated through OH+H_2=H_2O+H in rich H_2-air flames	23
"	"	"	T [OH]-u.v. abs. spect. [O]-from NO+O→ hν+NO_2	ϕ=.5-.95 P=0.5,1 atm T=1290-1848°K	[OH] partially equilibrated through OH+OH=H_2O+O	24
"	H_2-CO-Air	"	T [OH] from u.v. abs. spect. & glow from CO+O→ hν+CO_2	ϕ=.72-1.5 P=.3-1.0 atm T=1500-2000°K	(CO) & (OH) shown to decay by water gas equilibration	26

Table 2-1. (Continued)

Authors	Reactants	System	Measured Parameters	Experimental Conditions	Results	Ref. No.
Kaskan	H_2-Air	Porous plate flat burner	T [OH]u.v. abs. spect. [CO] from water gas equilibration	ϕ=1.1-2.9 P=.158-.325 T=1520-1880°K	[O] from partial equilibration reactions and report values of k(CO+OH)	25
Baldwin et al.	H_2-O_2-RH RH≡C_3H_8 C_2H_6 C_4H_{10}	Boric acid coated reaction vessels	[CO_2], [H_2O], [H_2] measured	T=480-540°C	Ratios $\frac{k(OH+CO)}{k(OH+H_2)}$ rate k(RH+H)	36
Blundel et al.	CH_4-O_2	"	[CO][CO_2] [H_2O] ΔP	T=500-550°C P=60-400 mm	Values of relative rates of $\frac{k(CH_4+OH)}{k(CO+OH)}$, $\frac{k(H_2CO+HO_2)}{k(HO_2+CO)}$	39
Kaufman et al.	OH+H_2+He OH+O+He OH+OH+He	Discharge flow system [OH] produced by H+NO_2=OH+NO	[OH] from u.v. abs. spectr.	T=300°K P=1-2 mm	Reports values of k(OH+OH), k(OH+H_2), k(OH+O)	37
Dixon-Lewis et al.	OH+H_2+CO	"	[OH] from ESR	P=1 mm T=300°K	"	43
"	O_2+H_2+N_2 +D_2O trace	Egerton flat flame burner	T x_{stable} [H] from [HD]	T=300-1078°K ϕ=2.0 P=1 atm	Attempted to reproduce composition profile by numerical analysis with limited success	32

Table 2-1. (Continued)

Authors	Reactants	System	Measured Parameters	Experimental Conditions	Results	Ref. No.
Dixon-Lewis et al.	$O_2+H_2+N_2$ $+N_2O$ × trace or CO_2 trace	"	"	T=1072-1573°K P=1 atms	Report values of $k(H+O_2)$, $k(H+CO)$ $k(H+N_2O)$, $k(H+CO_2)$ and $k(OH+H_2)$	38
Browne et al.	$C_2H_2-O_2-Ar/N_2$	Porous plate flat flame burner	T x_{stable} [OH] from u.v. abs. (O) for [CO+O] cont.	P=18 mm T=1000-1700°K ϕ=.42-2.5	Numerical integration of flame kinetic equations & with limited success Report $k(C_2H_2+H)$, $k(C_2H_2+OH)$ $k(C_2H_2+O)$, $k(O+H_2)$, $k(HCO+H)$, $k(HCO+M)$, $k(CO+OH)$	30
Hottel et al.	$C_3H_8-O_2-N_2$ and $CO-O_2-N_2$	Stirred reactor	x_{stable} T	ϕ=.136-1.9 P=.25-1.0 atm T=1280-1684	Global rate for appearance of (CO_2) obtained	16

CHAPTER 3

EXPERIMENTAL EQUIPMENT AND PROCEDURE

3.1 Layout

The experimental equipment used in this work primarily consists of a porous top, flat flame burner. The auxiliary equipment include a water cooled sampling probe, a Bendix time of flight mass spectrometer, rotameters, an ultraviolet light source, monochromator, and a photoelectric recording system. A schematic of the experimental setup is shown in Fig. 3-1. The radiation from a 1000 watt xenon arc lamp (light source) is focused over the surface of the burner through lens L_1. Slit is used to reduce the thickness of the incoming beam to about 1 mm as it passes over the burner surface. The emerging radiation is focused by lens L_2 onto the entrance slit of a monochromator which is connected to photoelectric recording system. The optical system is fixed and the burner is mounted on a base plate capable of movement in the vertical direction. For sub-atmospheric work, the burner is enclosed in a steel housing, which is connected to a vacuum pump at the top. Two quartz windows are provided in the side of the housing for optical measurements. Suitable openings are also provided in the housing for supporting a gas sampling probe and a thermocouple probe. Since the sampling probe and optical system is fixed in position, the up and down movement of the burner enables one to get temperature and composition profiles as functions of distance above the burner surface.

3.2 Burner Assembly

Various designs for flat flame burners have been reported in the literature.[8,9,18] The porous top design has been adopted for this work because of its relative simplicity.

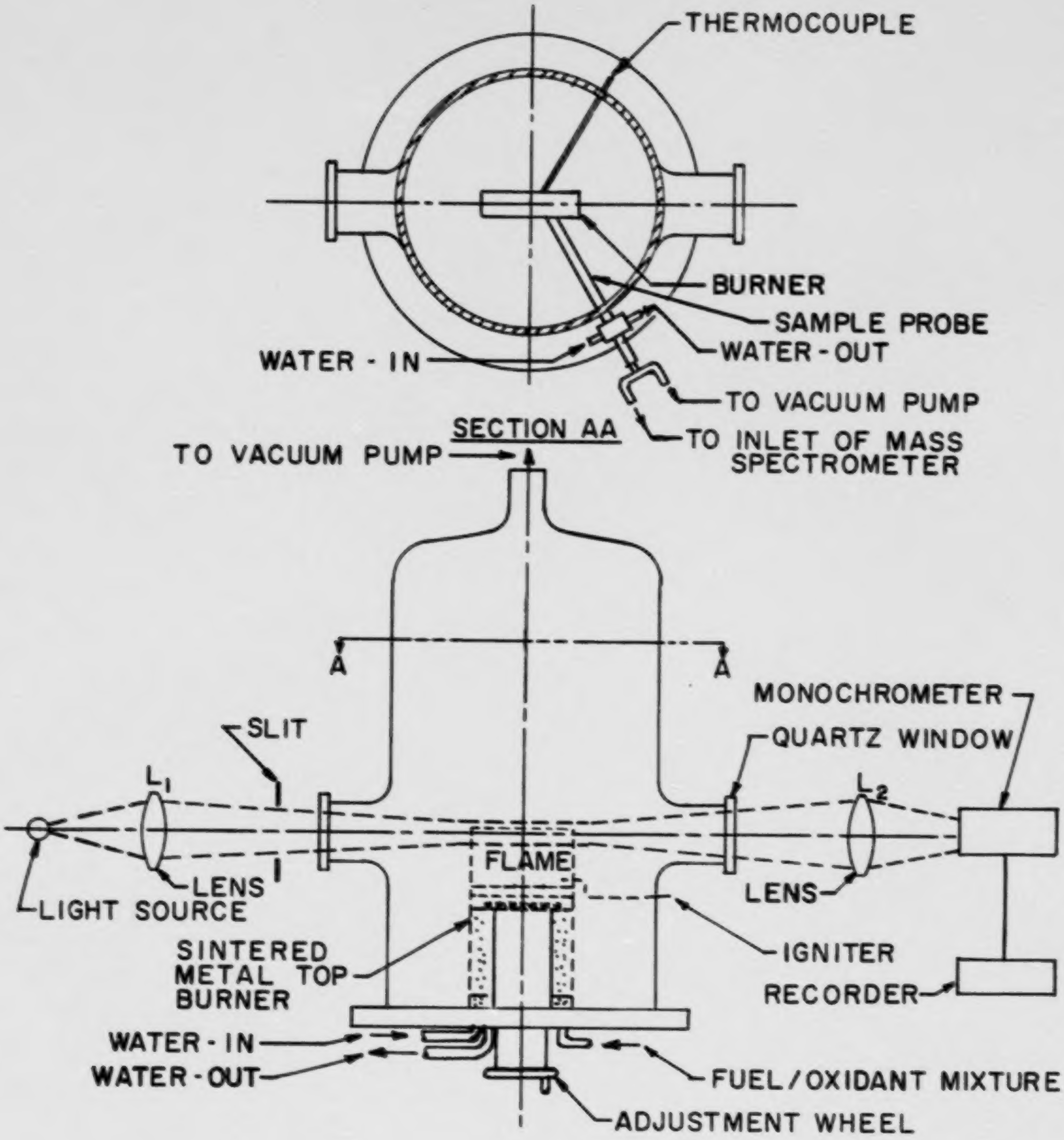

FIG. 3-1. FLAT FLAME BURNER, SUBATMOSPHERE CHAMBER AND FLAME OBSERVATION INSTRUMENTS.

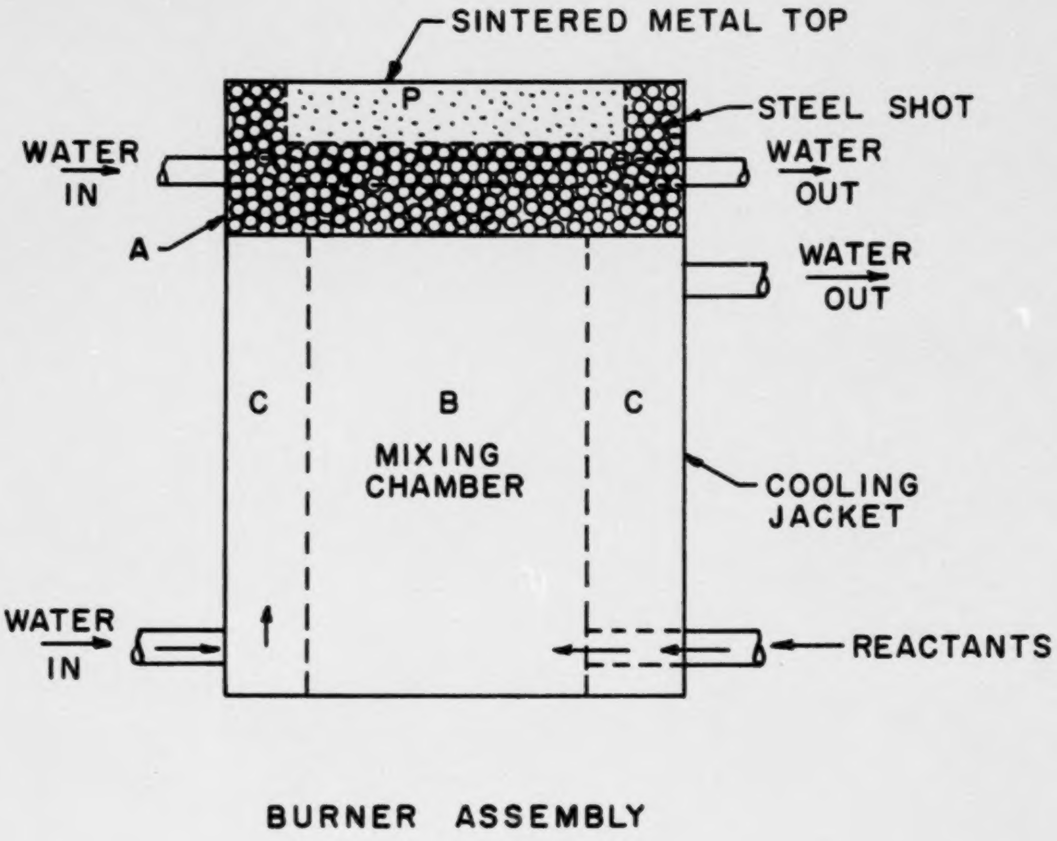

FIG. 3-2. DETAILS OF POROUS METAL TOP FLAT FLAME BURNER ASSEMBLY

The burner assembly consists of a mixing chamber B surrounded by a cooling water jacket C as shown in Fig. 3-2. The top section A is filled with 2-3 mm diameter stainless steel shots to ensure thorough mixing of the reactants. It is also embedded with a water cooled coil. A stainless steel sintered metal porous plug P ($3" \times 5"/8" \times \frac{1}{8}"$) is capped to section A. The combustible mixture is forced through the porous plug and emerges as a stream at uniform velocity.

3.3 Gas Supply and Flow Measurements

The reactant gases C_2H_6, C_2H_4, O_2, N_2 etc. are taken from commercially supplied high pressure bottles of pure grade (rated purity 99.5-99.9 percent). Each gas is passed through a constant pressure regulator which has a range of 0-30 psi before entering the calibrated rotameters for quantitative measurement of the flow. (A schematic diagram for the gas flow is shown in Fig. 3-3.) This procedure minimizes the fluctuations in pressure upstream of the rotameters due to changes in the pressure of the gas in the supply bottles. (For accurate quantitative measurements of flow by rotameters, a constant upstream pressure is necessary.) The rotameters are connected to the mixing chamber of the burner assembly on the downstream side as shown in Fig. 3-3.

3.4 Gas Sampling

The sampling probe is designed to produce a minimum of disturbance in the flame. Disturbances are caused by the withdrawal of sample as well as the size of the probe. The probe should also be capable of producing rapid cooling of the sample gases to stop the chemical reaction in order that the composition of mixture entering the mass spectrometer is very close to the true composition at the sampling point. These

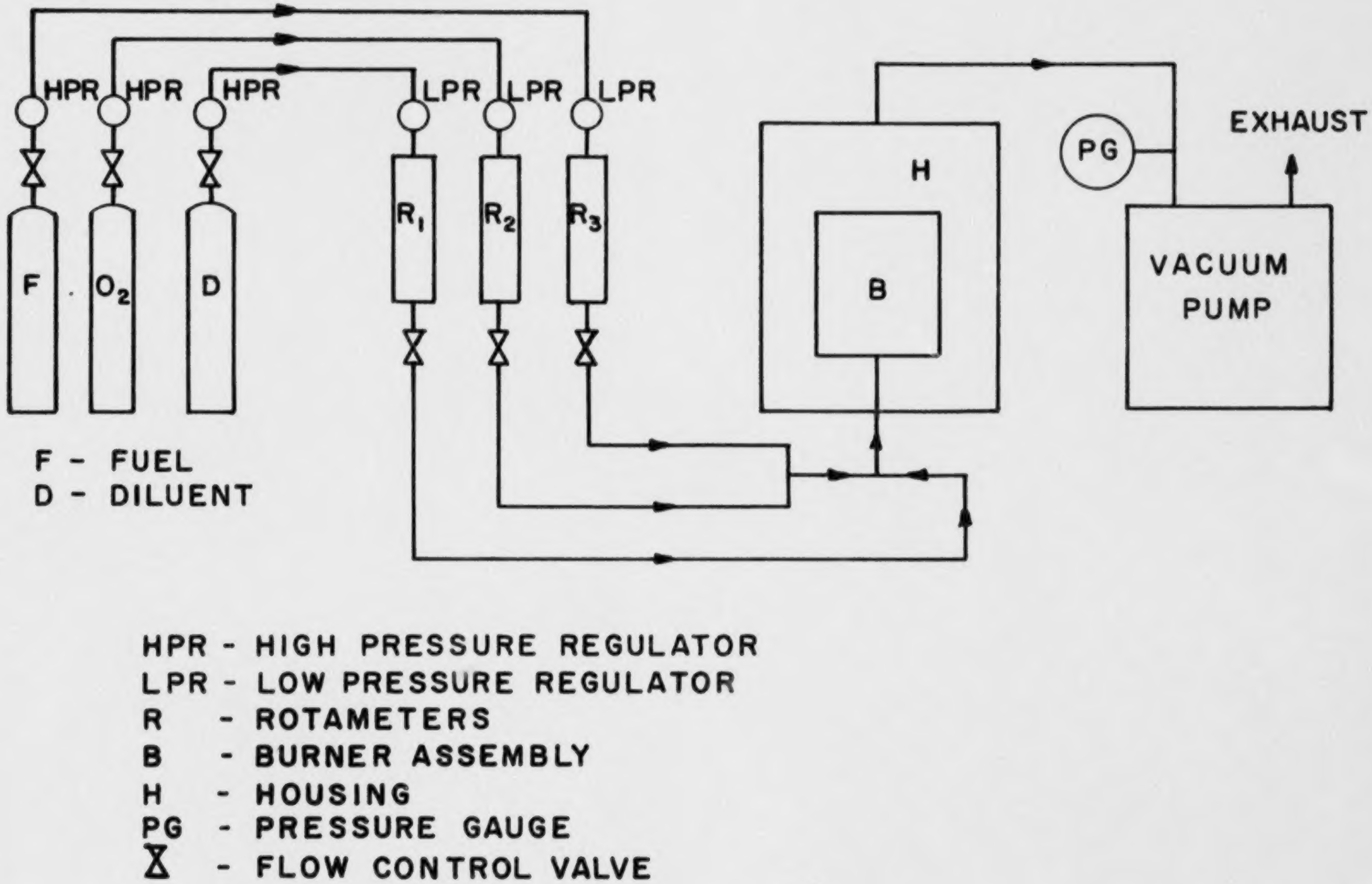

FIG. 3-3. SCHEMATIC DIAGRAM FOR GAS FLOW

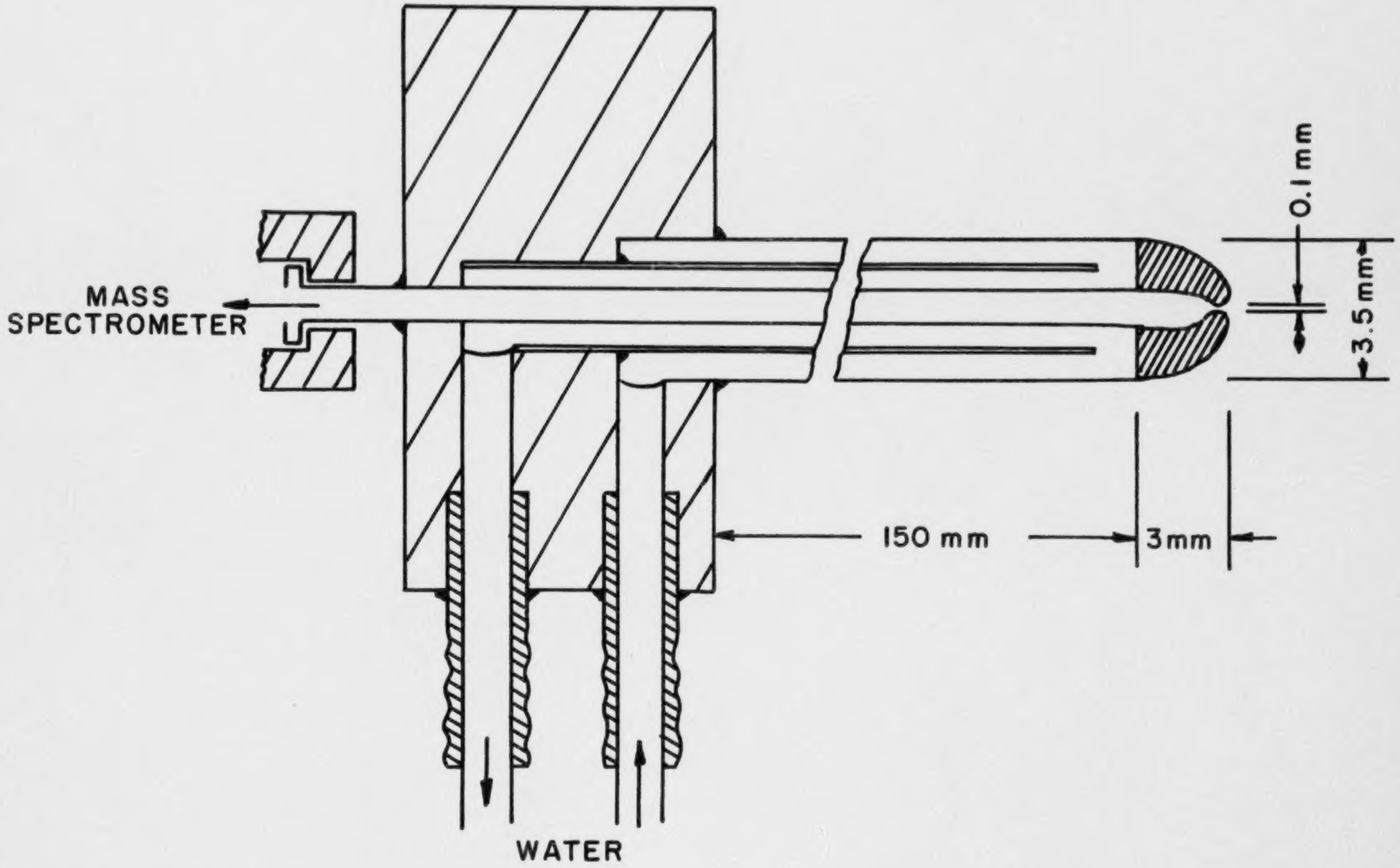

FIG. 3-4. TRIPLE WALLED, WATER COOLED STAINLESS STEEL SAMPLE PROBE

objectives are achieved by using a 3.5 mm diameter stainless steel probe of triple wall construction as shown in Fig. 3-4. The cooling water flows through the two outer annulii and the sample is withdrawn through a converging diverging inlet section of 0.10 mm inside diameter to produce rapid quenching of the gas sample. The suitability of this type of probe for flame sampling in the afterflame region has been discussed by Friedman *et al.*[11] and Fristrom and Westenberg.[18] The outlet of the probe (reduced to a pressure of 2-3 torr) is directly connected to the inlet leak valve of a Bendix Model 17-210 time of flight mass spectrometer. The output of the mass spectrometer is displayed on an oscilloscope and recorded by a strip chart recorder.

3.5 Mass Spectrometric Data Analysis

The raw data from the mass spectrometer requires the solution of an overdetermined system of linear algebraic equations (in order to obtain the mole fraction of various species). The solution to the system is obtained by the method of least squares. The computer program of McLean and Sawyer,[47] modified to include a check on the conservation of mass with respect to inlet flow rates of the reactant gases, was used for calculating the mole fraction of various species present in the flame gas sample at each point. The calibration spectra of the various species were obtained by feeding pure gases to the mass spectrometer and were checked periodically.

3.6 Spectroscopic System

Spectroscopy is an ideal system for studying radicals in flames since it does not disturb the system, as is inherent in the use of a probe. The principal limitation here is spatial resolution, which is controlled by the size of the beam at its focal point (1-2 mm). In this work, ultraviolet absorption spectroscopy has been selected for both the measurements of concentration of hydroxyl radicals and temperature. The fundamental data such as transition probabilities, energies and wave numbers of various lines for different emission bands of hydroxyl radicals are relatively well-known from the works of Dieke and Crosswhite[48] and Oldenberg and Rieke.[49] The basic instrumentation required for absorption spectroscopy will now be discussed briefly.

3.7 External Light Source

The light source should be capable of providing radiation of high intensity in the ultraviolet regime of interest in this study (3060Å-3110Å), and should be stable both in wavelength and intensity. For this purpose a high pressure 1000 watt xenon arc lamp is selected as the external light source.

3.8 Spectrograph

This is the analytical device which produces a resolved spectrum. The dispersive elements in most spectrographs is either a prism or a grating. Prism spectrographs are of short focal length. Here the length of the whole visible and ultraviolet spectrum may be only a few centimeters or less, and thus, resolution is sacrificed.

If very high resolution is required, as is necessary for discrimination of the rotational structure of complicated molecular bands, a large grating spectrograph is required. These disperse a large quantity of light and hence require very bright light sources. For general use an instrument between the two extremes suffices. Accordingly, a McPherson monochromator model 216-5 having a 0.5 meter path length with

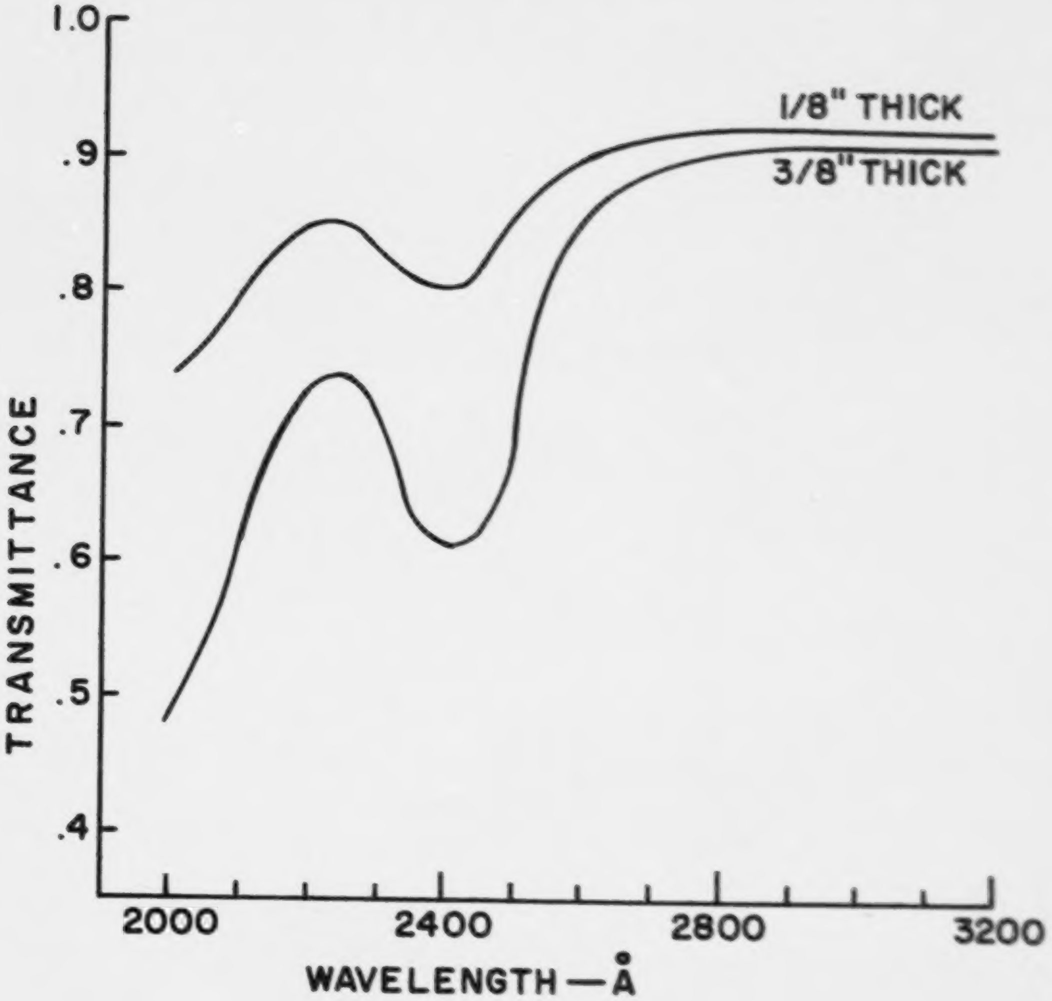

FIG. 3-5. QUARTZ SPECTRAL TRANSMITTANCE

a grating of 1200 lines/mm blazed at 3000Å in the first order was used in this work. The significant performance characteristics of the instrument for the grating used are given in Table 3-1.

3.9 Ultraviolet Transmission Windows

Two ultraviolet transmitting quartz windows are used in the burner housing along the optical path length. The first one is used for admitting radiation from the external light source (1000 watt xenon arc lamp) into the flame at low pressure. The second one is for transmission of radiation from the flame gases and the external light source, to the lens L_2 for focusing on the inlet of the monochromator. The following factors are significant in selecting a window material: (1) good transmission properties in the UV regime of light, which is of interest in this study; (2) a non-hygroscopic material, as water vapor in one of the major products of hydrocarbon combustion. Fused quartz type 102 provided by the General Electric Company meets these specifications closely and was selected from the window material. The spectral transmittance curve for the material is shown in Fig. 3-5.

3.10 Photoelectric Recording

When changes in intensity of a spectrum as a function of flame conditions are of chief consideration, the use of a photomultiplier phototube is convenient and accurate for spectroscopic measurements in a defined wavelength region. A RCA 1P 28 phototube having high spectral radiant sensitivity for 3100Å region has been used for the present study. The output of the phototube was recorded on a strip chart recorder whose input impedance is matched with that of the phototube. A schematic for the spectroscopic equipment used in the present work is shown in Fig. 3-6.

Table 3-1. Principal performance characteristics of monochromator*.

Wave length range	1050-10,000 Å
Dispersion	16.6 Å/mm
Resolution (first order) with 10μ slit	0.4 Å
Optics	f 8.7

*with 1200 lines/mm grating

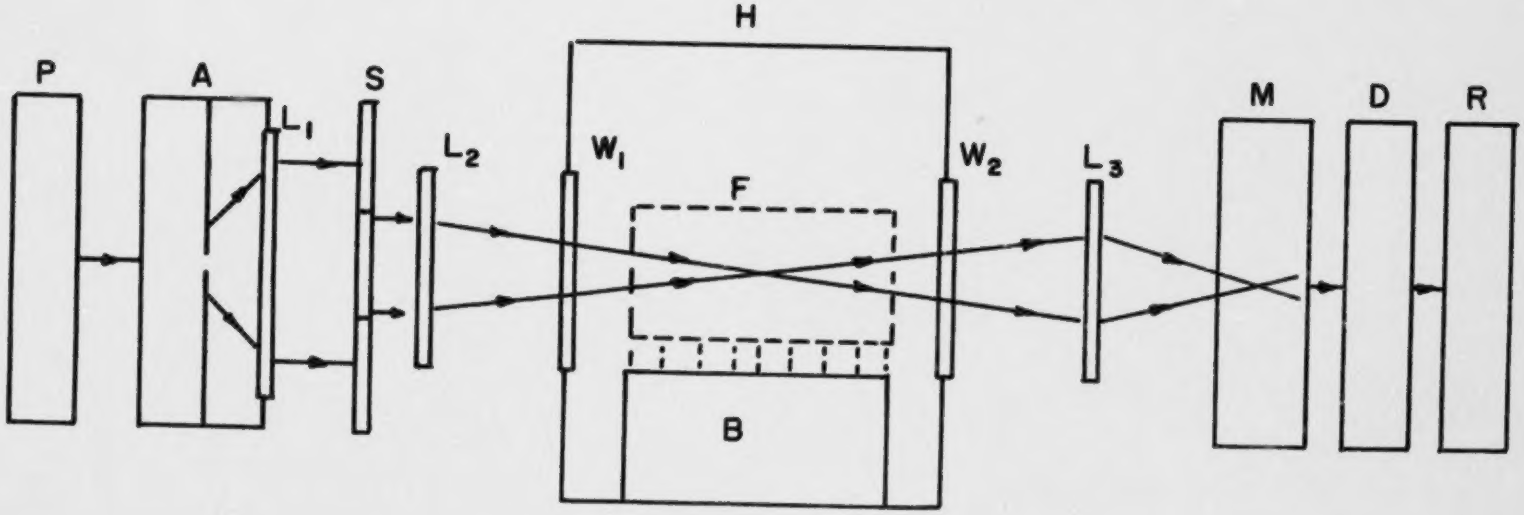

P - POWER SUPPLY FOR A
A - 1000 WATT XENON ARC LAMP
L_1 - COLLIMATING LENS
S - SLIT
L_2, L_3 - FOCUSING LENS
W_1, W_2 - QUARTZ WINDOWS

B - BURNER
F - FLAME
H - BURNER HOUSING
M - MONOCHROMATOR
D - DETECTOR (PHOTO TUBE)
R - RECORDER

FIG. 3-6. SCHEMATIC LAYOUT FOR ABSORPTION SPECTROSCOPY

The details of instrumentation used in absorption spectroscopic work and combustion experiments have been discussed by several authors.[113, 114] The details in this chapter have been kept to a minimum. The flame equations, spectroscopic equations and the procedures for data reduction are discussed in the following chapter.

CHAPTER 4

FLAME EQUATIONS AND DATA REDUCTION

The experimental procedure described in Chapter 3 enables one to obtain the composition and temperature for the post-flame-zone gases as a function of distance above the burner surface. These data have great potential for providing an insight into the chemical kinetic processes taking place in the zone under study. By appropriate application of the flame equations it is possible to determine the net chemical reaction rate for various species from the composition and temperature profiles.

4.1 Flame Equations

The use of a flat flame burner provides flames of essentially one dimensional geometry. The equations describing a steady one dimensional, premixed, laminar flame have been formulated by Hirshfelder and co-workers,[50] Fristrom and Westenberg,[18] Strehlow[51] and have been used by several workers.[10-14,30,32] It is assumed that the following conditions are fulfilled:

(1) The system is in a steady state.

(2) The system is essentially at constant pressure.

(3) Effects due to viscosity, radiation and external forces are negligible.

(4) The thermal diffusion effect is negligible.

(5) The ideal gas equations are applicable to the flow gases.

(6) The system may be considered one dimensional.

With these assumptions, the equations for laminar flames may be summarized as given below for a plane perpendicular to the flow.

Overall Continuity Equation

The equation for overall mass conservation at any point in the flame may be written as

$$\rho \ v \ A = \text{constant} = \dot{m} \tag{4.1}$$

where ρ is the density (gm/cc), v is the mass average velocity (cc/sec, A is the cross-sectional area of the bounding stream (cm^2), and $\dot{m}$ is the mass flow rate (gm/sec).

Species Continuity Equation

The equation for conservation of a particular species is given by

$$\frac{d}{dz} (N_i (v+V_i) \ A) = R_i \ A \tag{4.2}$$

where N_i is the molar density for the ith species, V_i is the diffusion velocity for the ith species, A is the cross-sectional area of the flame at the given plane, z is the distance coordinate along the direction of flame propagation, and R_i is the appearance or disappearance rate for the ith species due to chemical reaction.

Energy Conservation Equation

Ignoring thermal radiation, the energy conservation equation becomes

$$\dot{m} \ \hat{H} + A \ \Sigma \ N_i H_i V_i - A\lambda \frac{dT}{dz} = \text{constant} \tag{4.3}$$

when $\hat{H}$ is the specific enthalpy of the mixture (calories/gram), H_i the molar chemical enthalpy of the ith species (calories/gram-mole) and λ is the thermal conductivity of the mixture. The use of the energy equation has been obviated in the present study by employing the measured temperature profiles.

Diffusion Equation

The equation for the diffusion velocity for the ith species is

$$V_i = \frac{N^2}{N_i \rho} \sum_{j=1}^{j=N_s} M_j \, D^*_{ij} \frac{d}{dz} \left(\frac{N_j}{N}\right) \tag{4.4}$$

where N is the molar density of the mixture, D^*_{ij} is the multicomponent diffusion coefficient for the ith species, M_j is the molecular weight for the jth component, and N_s is the total number of species.

For some cases equation (4.4) becomes very cumbersome since the diffusion velocity of a particular species depends on a set of multicomponent diffusion coefficients each of which, in turn, depends in a complicated way on the mixture composition and the binary diffusion coefficient of all the pairs of species in the mixture. In a given system if one component is present in large excess, i.e. a diluent, then each species may be regarded as a trace in a binary mixture with the excess component. In such cases, the diffusional velocity is approximated by

$$V_i = - \frac{D_{ij}}{x_i} \frac{dx_i}{dz} \tag{4.4a}$$

where D_{ij} is the binary diffusion coefficient of species i with the excess component j and x_i is mole fraction of ith species. In cases where species i is present as a trace in a more general multicomponent mixture, Fristrom and Westenberg[28] have suggested the use of equation

$$V_i = - \frac{1}{x_i \sum\limits_{j \neq i} \frac{x_j}{D_{ij}}} \frac{dx_i}{dz} \tag{4.5}$$

for the diffusion velocity.

It is convenient in the analysis of flame structure data to make use of an additional variable called the species mass flux fraction defined by

$$G_i = \frac{N_i M_i (v+V_i)}{\rho \ v} \qquad (4.6)$$

Using G_i as a variable, the species continuity equation reduces to

$$\frac{\dot{m}}{M_i} \frac{dG_i}{dz} = R_i \ A \qquad (4.7)$$

4.2 Reaction Rate Calculations

A computer program (listed in Appendix 3) has been developed for calculating the chemical reaction rate R_i for each species by making use of equations (4.4) or (4.5), (4.6) and (4.7), and experimentally measured temperature and composition profiles. The solution of diffusion equation (4.4) and (4.5) involve certain assumptions which are discussed below.

4.3 Diffusion Velocity Calculations

To calculate the diffusion velocity from equations (4.4) or (4.5), one must calculate the diffusion coefficient and determine the composition profiles. The other variables such as N, the molar density of the mixture and ρ, the mass density are known from composition and flow measurements.

The experimental data for the diffusion coefficients of various species present in the combustion products of hydrocarbons over the temperature range of interest are relatively few.[18] As a consequence one is forced to use theoretical models for the calculation of diffusion coefficients. Fristrom and Westenberg[18] recommend the use of potential parameters for pure gases which have been determined from viscosity data and certain combination rules by which parameters for interaction of unlike molecules may be estimated from those of the respective species making up the diffusion pair. Viscosity parameters for many gases have been compiled by Hirshfelder, Curtiss, and Bird,[50] Svehla[52,53] and several others.[18,54,55]

In this study, the interaction of non-polar molecules is represented by the Lennard-Jones potential

$$\phi = 4\varepsilon[(\sigma/r)^{12} - (\sigma/r)^{6}] \tag{4.8}$$

while that of polar molecules is represented by the Stockmayer potential

$$\phi = 4\varepsilon[(\sigma/r)^{12} - (\sigma/r)^{6} + \delta(\sigma/r)^{2}] \tag{4.9}$$

Here ϕ is the potential governing the intermolecular forces, r is the distance between molecules, σ and ε are the parameters representing (roughly) a collision diameter and depth of potential well, δ is a function of the angles describing the relative orientation of the two molecules. The calculations for the diffusion coefficients D_{ij} have been made by standard kinetic theory methods,[18,50,54,55] which gives

$$D_{ij} = \frac{3(KT)^2}{16\ P\mu\ r_{ij}^{(1,1)}}$$

where K = Boltzmann constant

P = pressure

T = temperature, °K

μ = reduced mass of the colliding molecules i and j = $\frac{M_i M_j}{M_i + M_j}$

$M_i \& M_j$ = molecular weights of ith and jth species

$r_{ij}^{(\ell,s)}$ = collisional integral = $\sqrt{\frac{KT}{2\pi\mu}} \int_0^\infty e^{-j^2}\ \gamma^{2s+3}\ \Omega^{(\ell)}(g)\ d\gamma$

$\gamma = (\mu/2KT)^{1/2}\, g$

$\Omega^{(\ell)}(g)$ = collisional cross-section = $2\pi \int_0^\infty (1-\cos^\ell x)\, b\, db$

x = deflection angle after collision between ith and jth molecules

$$= \pi - b \int_{r_m}^{\infty} \frac{dr/r^2}{\sqrt{1 - \frac{b^2}{r^2} - \frac{\phi(r)}{\frac{1}{2}\mu g^2}}}$$

b = impact parameter

r = intermolecular distance at any instant

g = relative velocity of the colliding molecules

r_m = minimum intermolecular distance during the course of a collision

The values of r_{ij} for various pairs in a nondimensional form have been tabulated in Reference 50 and have been used in the present calculation. These calculations may be in error as much as 20-25 percent in the temperature range below 2000°K, but in many cases they may be more precise.[28]

The potential parameters $(\delta, \sigma, \varepsilon)$ for stable species are taken from References 50 and 53. The data for potential parameters of unstable species such as OH, O and H are very scarce. Hydrogen atom parameters are taken from the theoretical estimates of Weissman _et al._[56] and Vanderslice _et al._[57] Oxygen atom parameters are based on the results of Yun and Mason[58] for collisional integrals of dissociated air, while that for hydroxyl radicals are based on estimates of Svehla.[53] The computer program in Appendix 3 incorporates the above mentioned equations and has been used for calculating the multicomponent diffusion coefficients required for the solution of equation (4.4). This program may also be used for calculating the binary diffusion coefficients.

4.4 Numerical Differentiation

The use of equations (4.4) - (4.7) also necessitate knowledge of the derivatives of composition profiles. This can be done by approximating a function passing through the given points. The most common method of estimating a function is the approximation by an interpolating polynomial. Several interpolating polynomials, such as a Lagrangian polynomial, binomial polynomial, etc. were tried. Most of the polynomials ensured that the function passed through the given points but the profiles of the derivatives were oscillating. A cubic polynomial based on a least square fit resulted in a stable profile for the derivatives. The calculation scheme of Baer[59] for fitting of nonlinear regression functions by a least square technique was modified and incorporated into the computer program given in Appendix 3.

After calculating the diffusion coefficients (as outlined in section 4.3) and derivatives of composition profiles, equations (4.4) - (4.6) are solved to obtain mass flux fraction profile. A second cubic polynomial is fitted through the resulting profiles of mass flux fraction, whose derivatives give the net reaction rate of each species in accordance with equation (4.7).

4.5 Quantitative Determination of Hydroxyl Radical

The hydroxyl radical has a well defined band for $^2\pi-^2\Sigma$ (0-0) electronic transition with its head at 3064 Å. This band has been exhaustively analyzed by Dieke and Crosswhite[48] and fundamental data have been tabulated for most of the rotational lines belonging to this band. Learner[60] has made corrections to the relative transition probabilities for various lines by taking into account the interaction of vibrational and rotational modes. The data of Dieke and Crosswhite[48] and Learner[60] make the $^2\pi-^2\Sigma$ band very suitable for the quantitative measurement of hydroxyl radical by using absorption spectroscopy.

Theory

When a monochromatic beam of radiation of intensity I_{λ_o} passes through a homogeneous medium, the intensity of the emerging beam I_λ is related to I_{λ_o} by the Beer-Lambert Law

$$I_\lambda = I_{\lambda_o} e^{-k_\lambda X} \tag{4.10}$$

where k_λ = monochromatic absorption coefficient

X = optical path length

By considering a beam of radiation in the wavelength range of λ to $\lambda + d\lambda$ to be in equilibrium and traversing a homogeneous system. Zemansky and Mitchell[61] were able to obtain the following relationship between the absorption coefficient and Einstein coefficient for spontaneous emission

$$\int k_\lambda d\lambda = \frac{\lambda_o^4}{8\pi c} N_1 A_{21} \tag{4.11}$$

where N_1 = number per unit volume (concentration)

c = speed of light

λ_o = wavelength of the absorption line

A_{21} = Einstein coefficient for spontaneous emission from upper state 2 to lower state 1.

In deriving equation (4.11) the following assumptions were made

(1) In considering the conservation of energy, the contribution of spontaneous emission, which is in a random direction, was assumed

negligible as compared to that of induced emission and absorption in the direction of the beam.

(2) The population of the excited state, 2, was assumed negligible as compared to that of the ground state, 1. This assumption is applicable for the $^2\pi-^2\Sigma$ transition of OH as N_2/N_1 is of the order of 10^{-10} at 2000°K, if a Boltzmann distribution is assumed.

From the classical electron theory of dispersion, the optical behaviour of N_1 atoms or molecules per unit volume is represented by N_d, the ratio of the observed integrated absorption coefficient $(\int k_\lambda d\lambda)$ to that obtained by assuming that the electrons responsible for the absorption of radiation are bound to the center of the molecule by Hooke's Law type of forces. The ratio N_d/N_1 is found to be constant for a particular spectral line and is called the f-value or transition probability or oscillator strength. On this basis, the f-value of a spectral line is related to the integrated absorption coefficient by the following equation[61]

$$\int_{\text{line}} k_\lambda d\lambda = \frac{\pi e^2 \lambda^2}{mc^2} N_m f_{mn} \qquad (4.12)$$

where e = charge on electron in e.s.u. units

m = mass of electron

N_m = concentration in the lower state m

The f-values for several rotational lines of the $^2\pi-^2\Sigma$ band of OH have been measured by Oldenberg and Rieke.[49] More recent measurements of Carrington[62] support Oldenberg's[49] findings. It has been shown[23] that for those rotational lines of OH for which f-numbers were measured

$$f_{mn} = 3.07\times10^{-4} A_k/(2J+1) \qquad (4.13)$$

where A_k is the relative transition probability tabulated for all the lines by Dieke and Crosswhite[48] for transition from lower state m to upper state n, and J is the rotational quantum number in the lower state m.

In order to evaluate the integrated absorption coefficient $\int k_\lambda d\lambda$ for the spectral line, the line shape must be known. Experimentally this is possible with an instrument (spectrograph) having a resolution greater than the half width of the line. But the monochromator being used for this study has a resolution of 0.4 Å; therefore, consideration must be given to three principal factors responsible for line broadening. The first is the natural broadening due to the finite life time of the excited state and is given by

$$\nabla n = \frac{1}{2\pi \nabla t}$$

where ∇n = half width due to natural broadening

∇t = life time of excited state

This is very small for most cases and has been neglected in the present study.

The half width due to pressure broadening is given by

$$\begin{aligned} \nabla p &= Z_L/T \\ &\simeq c\sqrt{p/T} \end{aligned}$$

where Z_L = number of broadening collisions per absorbing molecule per second

p = pressure

T = temperature

c = constant

For the experimental situation in the present study with $p \approx 0.1$ atmosphere and $T \approx 1500°K$, the pressure broadening amounts to about 2.6×10^{-4} Å. This can be neglected compared to the Doppler half width (with is due to translational motion of the molecules) given by

$$\nabla_D = \frac{2}{c}\sqrt{RT/M}\ \lambda_o$$

$$= \frac{2}{3\times10^{10}}\sqrt{\frac{8.3169\times10^7\times1500}{17}} \times 3064$$

$$= 60\times10^{-4}\ \text{Å}$$

where M = molecular weight

∇_D = Doppler half width

R = universal gas constant

Thus it can be assumed that the line broadening is purely due to the Doppler effect. This assumption implies that the resolving power of the spectrography should be high enough to separate the lines being used for spectroscopic studies from other lines in the neighborhood. The McPherson Monochromator model 216.5 with a grating of 1200 lines/mm used in this study is capable of isolating 12 rotational lines (listed in Table 4.1) belonging to the $^2\pi-^2\Sigma$ electronic and 0-0 vibrational transition of OH. For a spectral line with Doppler shape the monochromatic absorption coefficient is related to the peak absorption coefficient k_o by the following equation [100,103]

$$k_\lambda = k_o \exp\left[\frac{2(\lambda-\lambda_o)}{\nabla_D}\right]^2 \qquad (4.14)$$

The absorption for a line is given by

$$A = \int_{\text{line}} \frac{I^\circ_\lambda - I_\lambda}{I^\circ_\lambda}\, d\lambda$$

Table 4-1. List of isolated rotational lines of $^2\pi-^2\Sigma$ 0-0 transition for OH, Reference 48.

Transition	Wavelength Å	Energy Level cm^{-1}
R_{2-7}	3069.17	1077.80
R_{2-4}	3074.369	429.45
R_{2-3}	3077.028	289.01
P_{1-2}	3086.390	83.70
Q_{1-6}	3087.338	767.45
Q_{1-8}	3092.394	1321.25
Q_{2-6}	3092.786	824.49
Q_{2-7}	3094.618	1077.60
Q_{1-9}	3095.342	1650.74
Q_{2-8}	3096.820	1367.56
P_{1-5}	3101.229	5543.54
Q_{2-11}	3105.603	2413.51

or

$$A = \int (1-e^{-k_\lambda X})\ d\lambda \tag{4.15}$$

from equation (4.10) and is independent of the resolution of the spectrometer, so long as the line is isolated.

Combining (4.14) and (4.15)

$$A = \int (1-e^{-k_o X \exp(-[\frac{2(\lambda-\lambda_o)}{\nabla_D}]^2)})\ d\lambda$$

Let $P \equiv k_o X$

$$W \equiv \frac{2(\lambda-\lambda_o)}{\nabla_D}$$

or

$$dW = \frac{2(d\lambda)}{\nabla_D}$$

Therefore

$$A = \int (1-e^{P \exp(-W^2)})\, d\lambda$$

$$= \frac{\nabla_D}{2} \int (1-e^{P \exp(-W^2)})\ dW$$

Expanding the exponential on the right side, interchanging the order of summation and after integrating[63] one finds

$$A = \frac{\nabla_D}{2} \sum_{n=1}^{\infty} - \frac{1}{n!} (-P)^n \int_{-\infty}^{\infty} \exp^{(-nW^2)} dW$$

or

$$B \equiv \frac{2A}{\sqrt{\pi}\, P\, \nabla_D} = \sum_{n=0}^{\infty} \frac{(-P)^n}{(n+1)!\ \sqrt{n+1}} \tag{4.16}$$

Numerical values for the dimensionless group on the left hand side have been given by Ladenburg[64] and Cowan[65] and are reproduced in Table 4-1.

For $0.1 \leq P \leq 3.0$, Penner[63] has shown that equation (4.16) may be replaced by the approximation

Table 4-2. Numerical values of parameters for equations (4.16) and (4.17).

P	B	PB	P	B	PB
0.10	0.964	0.0964	1.80	0.584	1.050
0.15	0.948	0.142	2.0	0.556	1.112
0.20	0.933	0.187	2.2	0.532	1.117
0.25	0.916	0.229	2.4	0.507	1.218
0.30	0.902	0.270	2.6	0.487	1.267
0.35	0.887	0.311	2.8	0.468	1.311
0.40	0.877	0.348	3.0	0.450	1.350
0.45	0.861	0.383	3.2	0.432	1.385
0.50	0.844	0.421	3.4	0.417	1.415
0.55	0.831	0.457	4.0	0.372	1.488
0.60	0.818	0.491	4.4	0.377	1.530
0.65	0.806	0.524	5.0	0.376	1.580
0.70	0.793	0.555	6.0	0.270	1.650
0.75	0.780	0.585	7.0	0.240	1.720
0.80	0.768	0.620	8.0	0.22	1.77
0.85	0.757	0.640	9.0	0.20	1.82
0.90	0.745	0.675	10.0	0.18	1.86
0.95	0.734	0.700	12.0	0.16	1.92
1.10	0.725	0.725	14.0	0.14	1.98
1.20	0.663	0.820	17.0	0.12	2.04
1.40	0.646	0.905	20.0	0.10	2.09
1.60	0.616	0.985			

$$B = \frac{2A}{\sqrt{\pi}\ P\ \nabla_D} \approx \exp\left[-\frac{1}{2}\sqrt{P}\ \right] \qquad (4.17)$$

with an accuracy of better than a few percent.

By measuring A, the area of the absorption line and by assuming a value of temperature one can calculate ∇_D, the Doppler width, and P and hence the peak absorption coefficient k_o from equations (4.16) and (4.17).

From (4.14), the integrated absorption coefficient for a line of Doppler shape is given by

$$\int_{\text{line}} k_\lambda d\lambda = k_o \int_{\text{line}} \exp - \left[\frac{2(\lambda-\lambda_o)}{\nabla_D}\right]^2 d\lambda$$

Kaskan[24] has shown that this integral may be approximated by

$$\int_{\text{line}} k_\lambda d\lambda = 1.065\ k_o\ \nabla_D \qquad (4.18)$$

Combining (4.12) with (4.18) one obtains

$$k_o = 3.06\times10^{16}\ \frac{\lambda_o^2}{\nabla_D}\ \frac{N_m A_k}{2J+1}$$

or

$$N_m = \frac{1}{3.06\times10^6}\ \frac{\nabla_D}{\lambda_o^2}\ \frac{(2J+1)}{A_k}\ k_o \qquad (4.19)$$

Thus, knowing k_o for an assumed value of temperature, the concentration of hydroxyl radical in the m-th state can be calculated from (4.19).

If rotational and vibrational degrees of freedom are assumed to be in equilibrium, N_{OH}, the total concentration of hydroxyl radical is related to N_m, the m-th state concentration by the Boltzmann distribution

$$N_{OH} = \frac{Z_{r-v}}{(2J+1)} \exp^{E_m/RT} N_m \qquad (4.20)$$

Combining with (4.19), we obtain

$$N_{OH} = \frac{Z_{r-v}}{3.06\times10^6} \frac{\nabla_D}{\lambda_o^2} \frac{k_o}{A_k} \exp^{E_m/RT} \qquad (4.21)$$

where J = rotational quantum number in the m-th state

Z_{r-v} = rotational vibrational partition function

E_m = energy of m-th state.

The assumption of rotational equilibrium will be justified later in this section. No direct evidence can be presented for the existence of vibrational equilibration. In the temperature range of interest (1500-1700°K) the equilibrium population of OH in the state with $V=1$ ($V \equiv$ vibrational quantum number) is less than 3 percent of that of the ground state. The characteristic time of the system (residence time of flow in a one mm thickness characteristic of the flame zone) is 2-3 orders of magnitude greater than the vibrational relaxation time of OH. In addition, the most significant reaction contributing to the production of OH in the regime under study is probably $H + O_2 = OH + O$. This is an endothermic reaction which would further tend to reduce the population of hydroxyl radical in excited state. This makes it highly probable that vibrational equilibrium exists. Moreover, a slight departure from vibrational equilibrium would not affect the total concentration of hydroxyl radical to any significant degree. Thus, the total concentration of hydroxyl radical is known from equation (4.21) for an assumed temperature. The assumed value of the temperature is compared with that calculated in section 4.6. If the two values of temperature differ by more than 50°K, a new value is assumed and the process is repeated.

4.6 Temperature Determination

The magnitude A (absorption of a line) is inferred for the 12 isolated rotational lines (listed in Table 4-1) from the spectrogram by taking the product of the half width and the height of the lines. (The registered lines are to a good approximation a triangle.) k_o is obtained from equation (4.16) by inserting the Doppler width ∇_D corresponding to an assumed temperature. The plot of log k_o/A_k vs. E_m, when the rotational degrees of freedom of OH are in equilibrium, is a straight line. The temperature is obtained from the slope of this line by making use of equation (4.21). This also justifies the rotational equilibrium assumption made for equation (4.20). Figure 4-1 shows temperature determination for two data points of $C_2H_4/O_2/Ar$ flame. These temperatures have an overall uncertainty of about ±50°K. If the calculated value of temperature does not agree within 50°K with that of assumed one, calculations are repeated with a new assumed value of the temperature.

Knowing k_o for any one isolated rotational line, the concentration of OH can be calculated from equation (4.21). In the present work k_o for the rotational line $P_{1.5}$, whose separation from the neighboring lines was largest, was used for the calculation of OH concentrationa. A computer program given in Appendix 3 was developed for carrying out these computations.

The spectroscopic temperature profiles for the initial runs obtained by the above mentioned method were compared with those measured by a 4 mil silica coated Pt-Pt/Rh-13% thermocouple assembly. It was found that thermocouple measured temperatures were lower as compared to those obtained spectroscopically by about 50-150°K. This difference is probably due to the difficulties in estimating the loss of heat by radiation to the

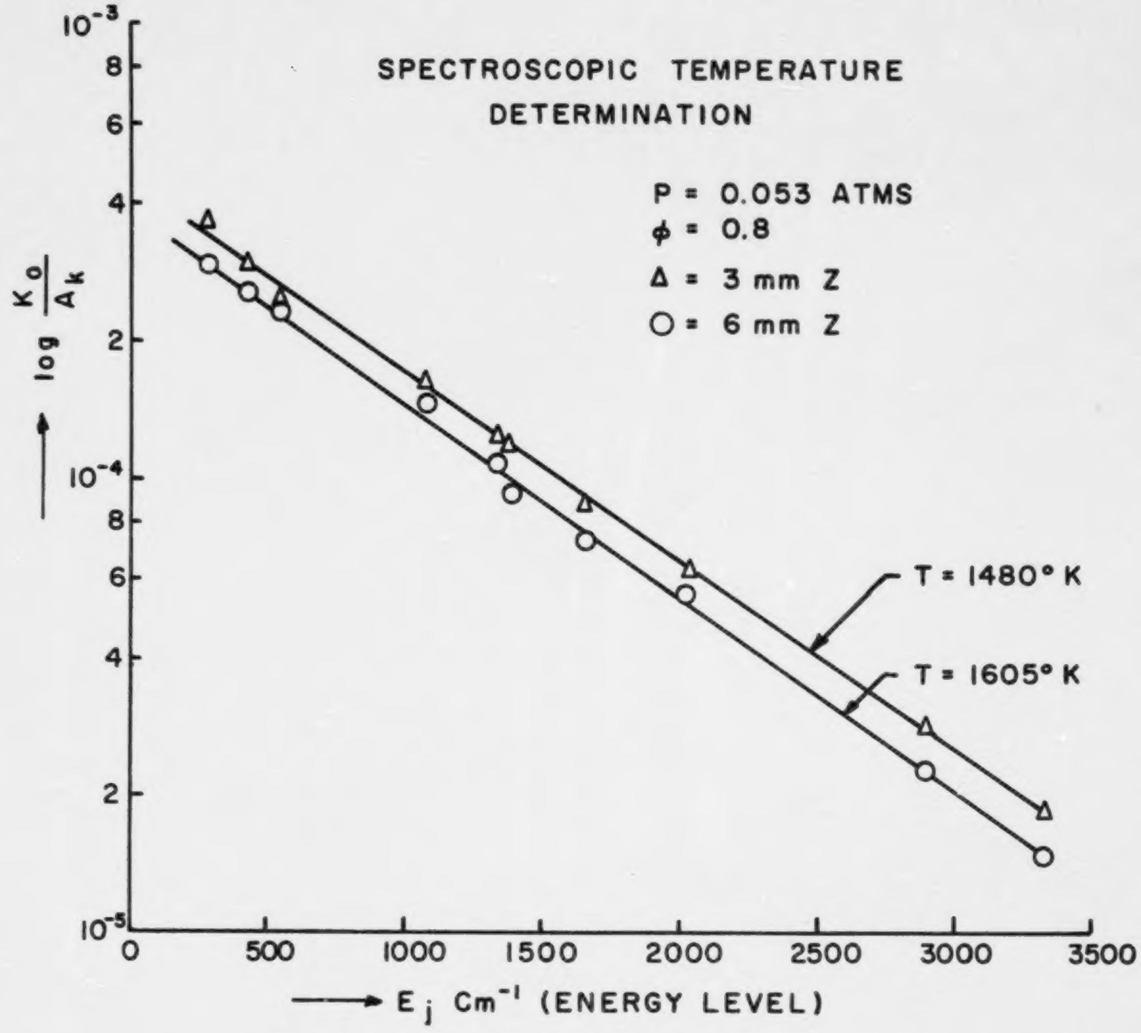

FIG. 4-1. TEMPERATURE DETERMINATION BY ULTRAVIOLET ABSORPTION SPECTROSCOPY OF OH FOR ETHYLENE/OXYGEN/ARGON FLAME

housing and by conduction to the zirconium support of the thermocouple wires. Relatively higher thermocouple temperatures were recorded by increasing the length of silicon coated thermocouple wires hanging out from the zirconium support. In all subsequent runs only spectroscopic temperatures whose validity is reasonably well established from the other works[18,23,31] reported in the literature were measured.

CHAPTER 5

EXPERIMENTAL RESULTS

5.1 Data Gathering Procedures

It has been well established[10,16,18] that in hydrocarbon-oxygen flames most of the fuel disappears by the end of a luminous zones and is converted to CO and H_2O. In the present study at a pressure of .083 atm, the luminous zone ended at a height of about 3 mm above the burner surface, while for a pressure of 0.054 atm the luminous zone continued up to a height of about 5 mm. The flame was sampled at 8 locations between 3 and 16 mm above the surface of the burner to obtain composition and temperature profiles for each flame condition. For fuel rich flames a flat geometry could not be obtained. Therefore, the present study is limited to fuel lean and stoichiometric flames. The data were recorded for the following experimental conditions:

Fuel

Ethane and ethylene were selected as fuels. Most of the hydrocarbon flame studies reported in the literature are confined to $CH_4/CO/O_2$ flames because of their simplicity. Ethane and ethylene are a step higher in the complexity of their structure as compared to methane and have been postulated to appear as intermediate species during the oxidation/combustion of several higher order hydrocarbon species.[66] C_2H_4 is an unsaturated hydrocarbon belonging to the olefinic series while C_2H_6 is a saturated hydrocarbon belonging to the paraffinic group. Their use would enable us to study the effect of structure of fuel on the burning rate of CO.

Equivalence Ratio

Three equivalence ratios, 0.67, 0.8 and 1.0, were selected for the present study. The chemical kinetic rate of a species depends upon the local composition and temperature. Thus, we would expect that this variation of composition may have a significant effect on the rate of CO reaction.

Pressure

The data were recorded at pressures of 0.054 and 0.083 atmospheres. At these pressures the burning zone was spread over a distance of 3-10 mm. The variation of pressure is expected to spread the distance over which the total change of concentrations occur but is not expected to affect the rate of change of profile per unit time.

Diluents

Argon and nitrogen were selected as diluents and their mole fraction was about 60 percent in all the runs. The change of diluent would not be expected to affect the composition and reaction rates of the reactant species. However, in the mass spectrometric analysis, N_2 has a primary peak at (mass number) m/e = 28 which coincides with that of CO. This presents some difficulty in determining the exact contribution of CO to m/e = 28, particularly at the points of low concentration of CO. Argon does not have a peak at 28 but the vacuum ion pump of the mass spectrometer is not able to pump it as rapidly as the sample enters. This results in a building up of the partial pressure of argon in the spectrometer and tends to suppress the height of other peaks and increases fluctuations in the background mass spectra. This difficulty is minimized by closing the variable leak inlet of the mass spectrometer after recording the spectrum at each data point. The averaging of the results obtained by using nitrogen and argon as diluents for the same reactant composition is expected to reduce the overall error.

A summary of the planned experimental conditions with the corresponding run numbers used in reference to the data in various figures is given in Table 5-1.

Measurements were not made for the three cases (run no. 8, 10, and 12) of ethane/oxygen/argon flames at 0.054 atm and equivalence ratios of 1.0, 0.8 and 0.67. A total of 21 cases were investigated. The repeated cases have been indicated with subscripted alphanumeric symbols in the figures.

For the analysis of stable species such as CO, CO_2, O_2, H_2O, H_2, Ar and N_2, samples were withdrawn continuously through a watercooled probe and fed to the variable leak inlet of the time of flight mass spectrometer. The mass spectra were scanned from mass number (m/e) 1 to mass number 46. All the species of interest have mass numbers in this range. Due to background electronic noise, emission from tungsten grid, and some residual gases in the flight tube of the mass spectrometer there were some background peaks at m/e = 1, 2, 16, 17, 18, 28 and 40. The recorded spectra were corrected for the background peaks before reducing the data.

The height of the background spectra at m/e = 2 was of the same order as the small contribution of the sample to the peak (m/e = 2) for all the runs. Peak 2 also showed continuous fluctuations. Thus, it became very difficult to obtain the exact contribution from the sample to m/e = 2 and this resulted in a large uncertainty for the value of the mole fraction of H_2. Similar remarks apply to the mole fraction of CO at the last 2-3 points (heights 10-16 mm above the burner surface) for most of the runs.

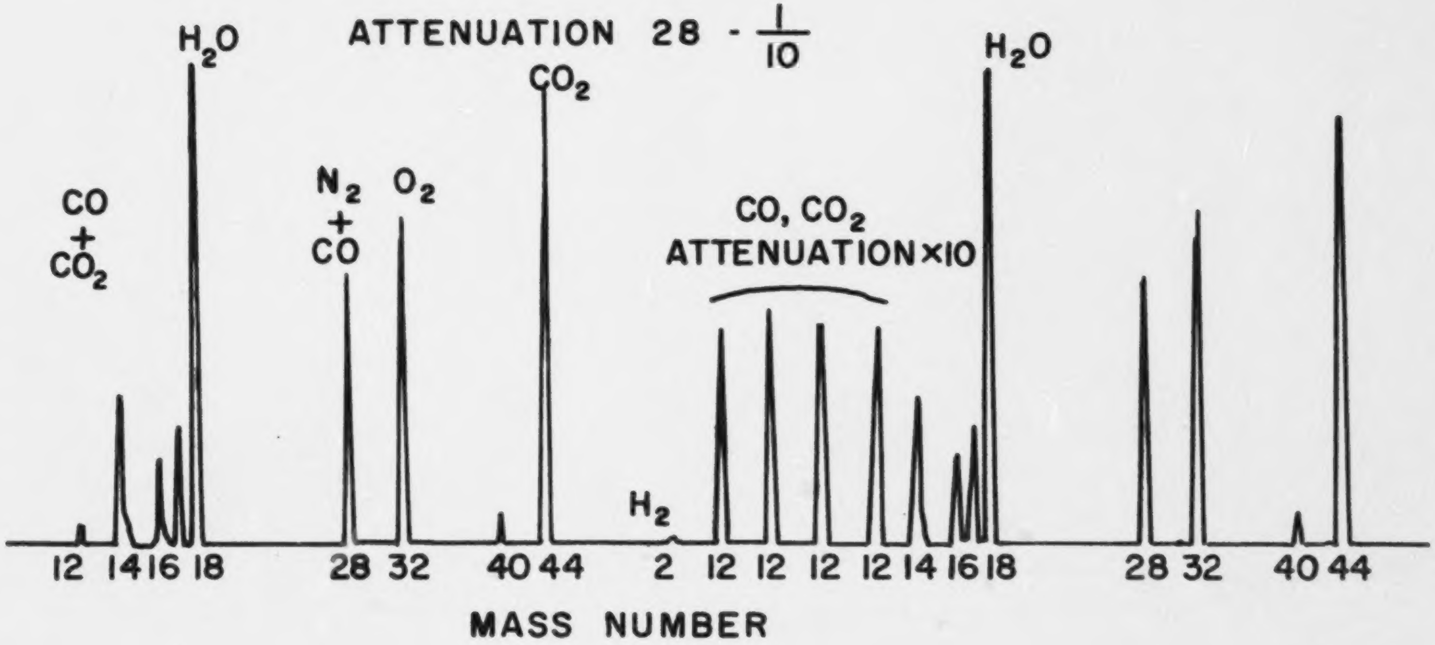

FIG. 5-1. MASS SPECTROGRAM $C_2H_6 - O_2 - N_2$ FLAMES
FUEL LEAN

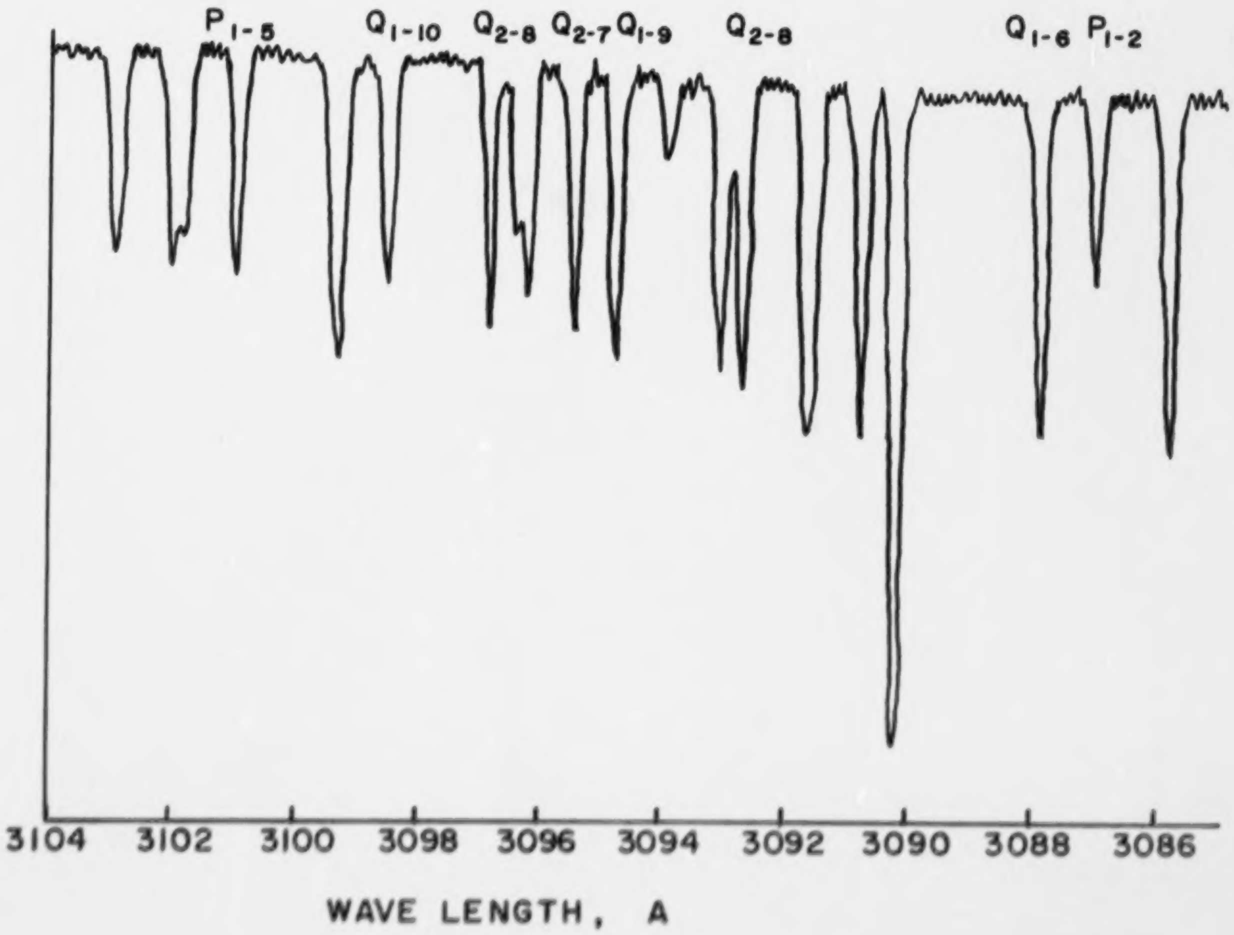

FIG. 5-2. A TYPICAL OH-ABSORPTION SPECTRUM FOR ETHANE/OXYGEN/ARGON FLAMES

At each data point the mass spectrum was scanned two or three times and the average value of the peak heights were used for obtaining the mole fraction of the species. A typical mass spectrograph for $C_2H_6/O_2/N_2$ flames repeated twice at one data point is shown in Fig. 5-1. The repeatability of the individual peaks is illustrated by 4 scannings for one of the small peaks at mass no. 12, which helps to differentiate the contribution of CO to the peak at m/e = 28 from that of N_2.

The calibration mass spectra were checked periodically by flowing pure gases through the burner at a pressure of 0.084 and 0.053 atmospheres. The samples of pure gas were fed to the inlet of the mass spectrometer via the sampling probe. This procedure tends to compensate for errors due to undetectable leaks into the system under actual operating conditions.

The ultraviolet absorption spectra for OH radicals was scanned from 3085 Å to 3110 Å at a speed of 1 Å per minute. The scanning was repeated for 2-3 points during each run. The areas of the various absorption lines in repeated scans were very close to those obtained during the first scan. Therefore, it was not considered necessary to repeat the scanning for all the points. The temperature and concentration of hydroxyl radicals were obtained from the areas of 7 out of 12 isolated lines as already outlined in Chapter 4. A typical absorption spectrum for hydroxyl radical is shown in Fig. 5-2.

The uniformity and reproducibility of the composition at a given cross section was checked by analyzing the flame with the probe placed at right angles and then parallel to the optical path on different days. A typical distribution for the mole fraction profiles of carbon monoxide, carbon dioxide, water and hydroxyl radical mole fraction are shown in

Table 5-1. Experimental conditions.

Run No.	Fuel	Diluent	Pressure (Atmospheres)	Equivalence Ratio
1	C_2H_6	N_2	0.083	0.67
2	"	Ar	"	"
3	"	N_2	"	0.80
4	"	Ar	"	"
5	"	N_2	"	1.0
6	"	Ar	"	"
7	"	N_2	0.054	0.67
8	"	Ar	"	"
9	"	N_2	"	0.8
10	"	Ar	"	"
11	"	N_2	"	1.0
12	"	Ar	"	"
13	C_2H_4	N_2	0.083	0.67
14	"	Ar	"	"
15	"	N_2	"	0.8
16	"	Ar	"	"
17	"	N_2	"	1.0
18	"	Ar	"	"
19	"	N_2	0.054	0.67
20	"	Ar	"	"
21	"	N_2	"	0.8
22	"	Ar	"	"
23	"	N_2	"	1.0
24	"	Ar	"	"

Figs. 5-3, 5-4 and 5-5. At most of the points the agreement lies between 5 to 10 percent and is considered reasonable.

5.2 Experimental Results

A typical set of composition and temperature profiles for $C_2H_6/O_2/$ Ar flames at 0.083 atm and equivalence ratio of 1.05 is shown in Fig. 5-6. The concentrations of O_2 and CO decrease up to a distance of 1.0 cm above the burner surface after which the rate of decay becomes very slow. The concentration of CO_2 increases rapidly up to a distance of 1.0 cm after which the rate of concentration change decreases considerably. The concentration of OH increases in the first part and then decreases. The concentration of H_2O and H_2 change relatively slowly. Most of the fuel has disappeared at 0.40 cm above the burner surface.

Typical variation of the mole fractions of CO, CO_2 and O_2 with equivalence ratio are shown in Figs. 5-7 to 5-9 for ethylene/oxygen flames at 0.083 atm pressure and equivalence ratio of 0.67, 0.80 and 1.0. These are in agreement with the qualitative expectations that the mole fraction of carbon monoxide and carbon dioxide are minimum for the leanest flame (equivalence ratio 0.67) and that of O_2 is minimum for a near stoichiometric flame. These changes in composition represent both chemical and diffusion effects. The mole fraction profiles are reduced to the reaction rate profiles for each species as described in Chapter 4. The diffusion velocity for the major stable species such as carbon monoxide, carbon dioxide, oxygen and water is about 5 to 20 percent of the convective flow velocity. Thus, the uncertainties in the diffusion coefficient and mole fraction do not have a significant effect on the value of mass flux fraction and consequently the net reaction rate of the major stable species. However, the diffusion velocities of molecular hydrogen and

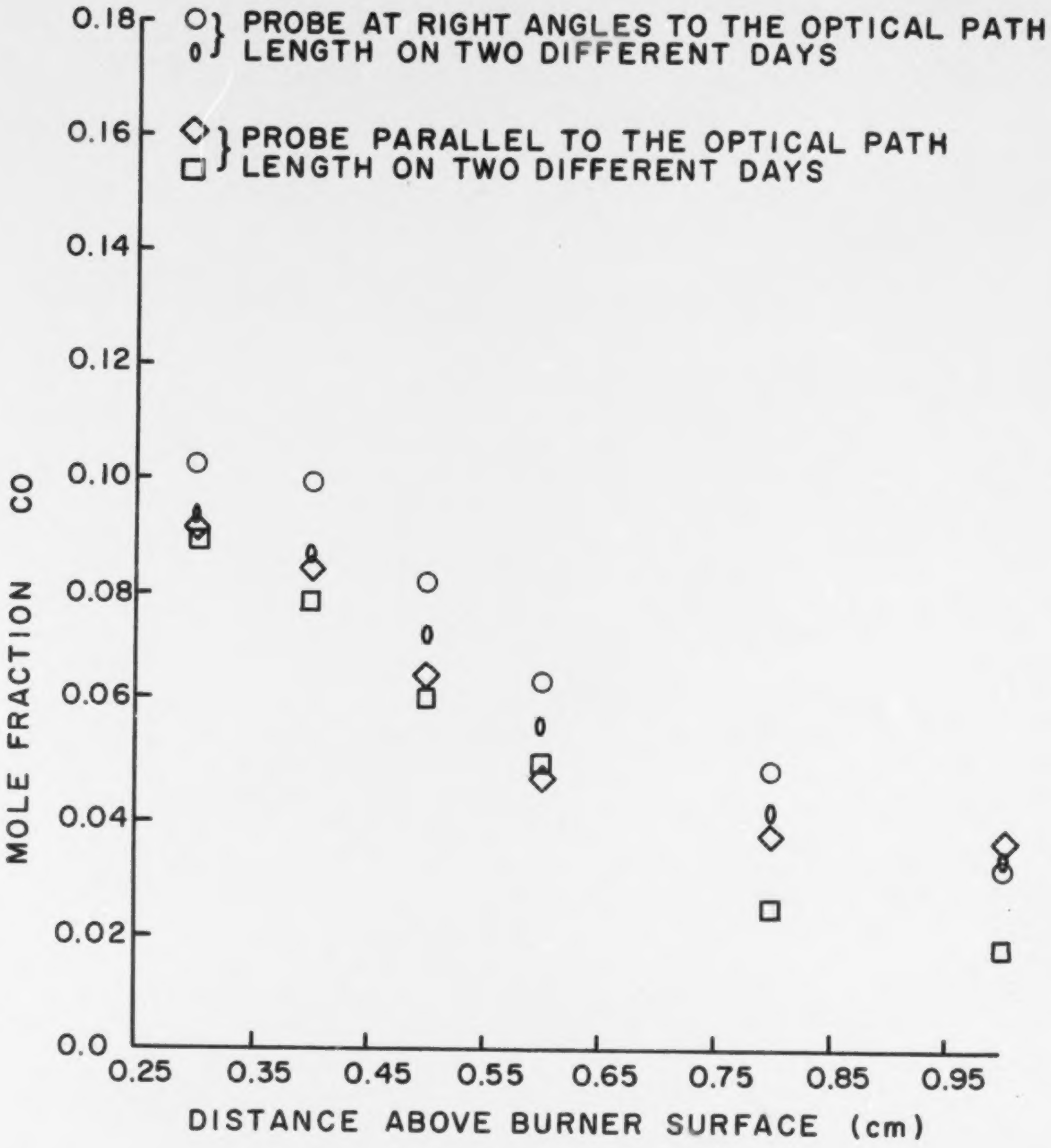

FIG. 5-3. CARBON MONOXIDE MOLE FRACTION PROFILE, ETHYLENE/OXYGEN/ARGON FLAMES P = .054 ATM AND EQUIVALENCE RATIO = 0.81

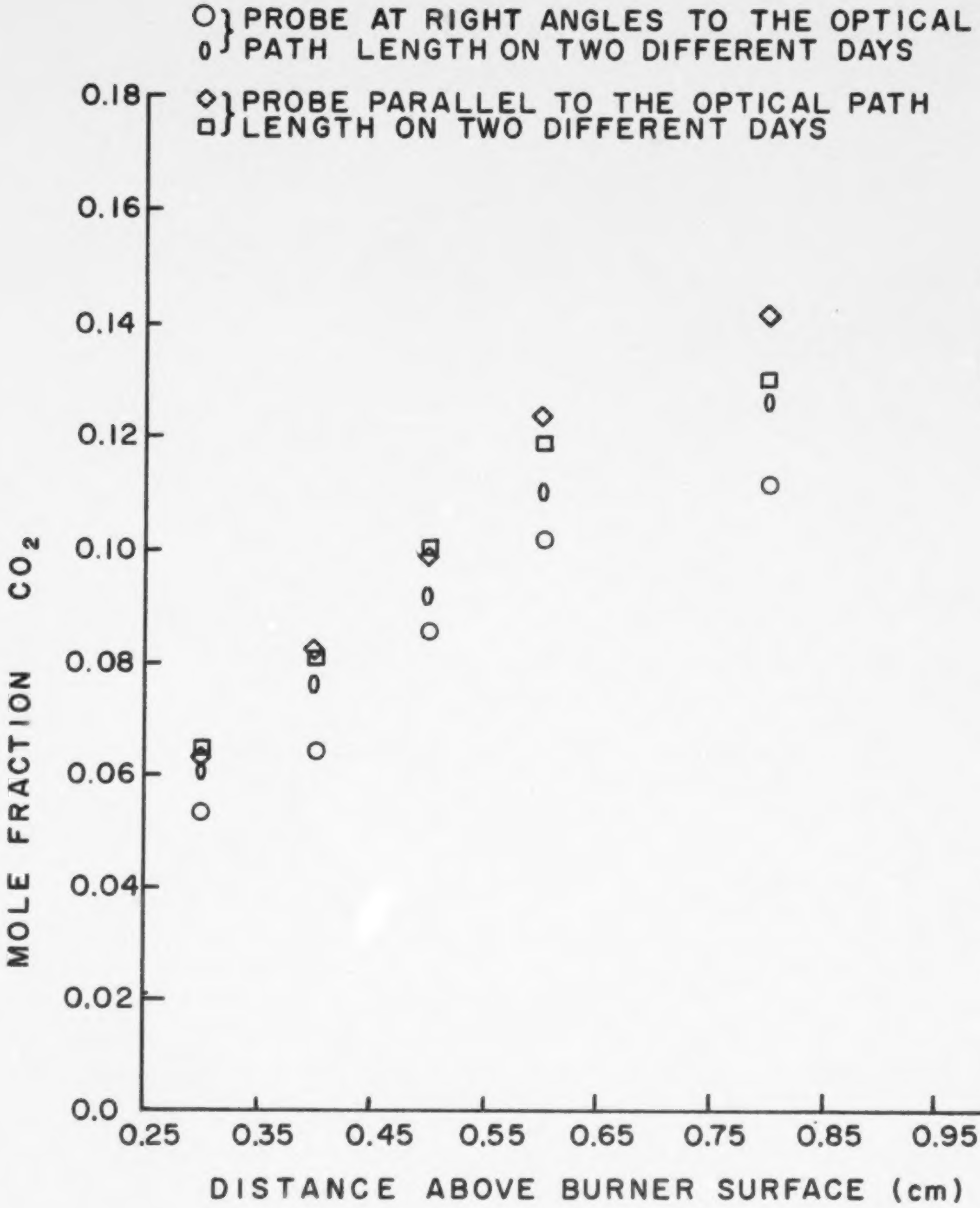

FIG. 5-4. CARBON DIOXIDE MOLE FRACTION PROFILE, ETHYLENE/OXYGEN/ARGON FLAMES, P = .054 ATM AND EQUIVALENCE RATIO = 0.81

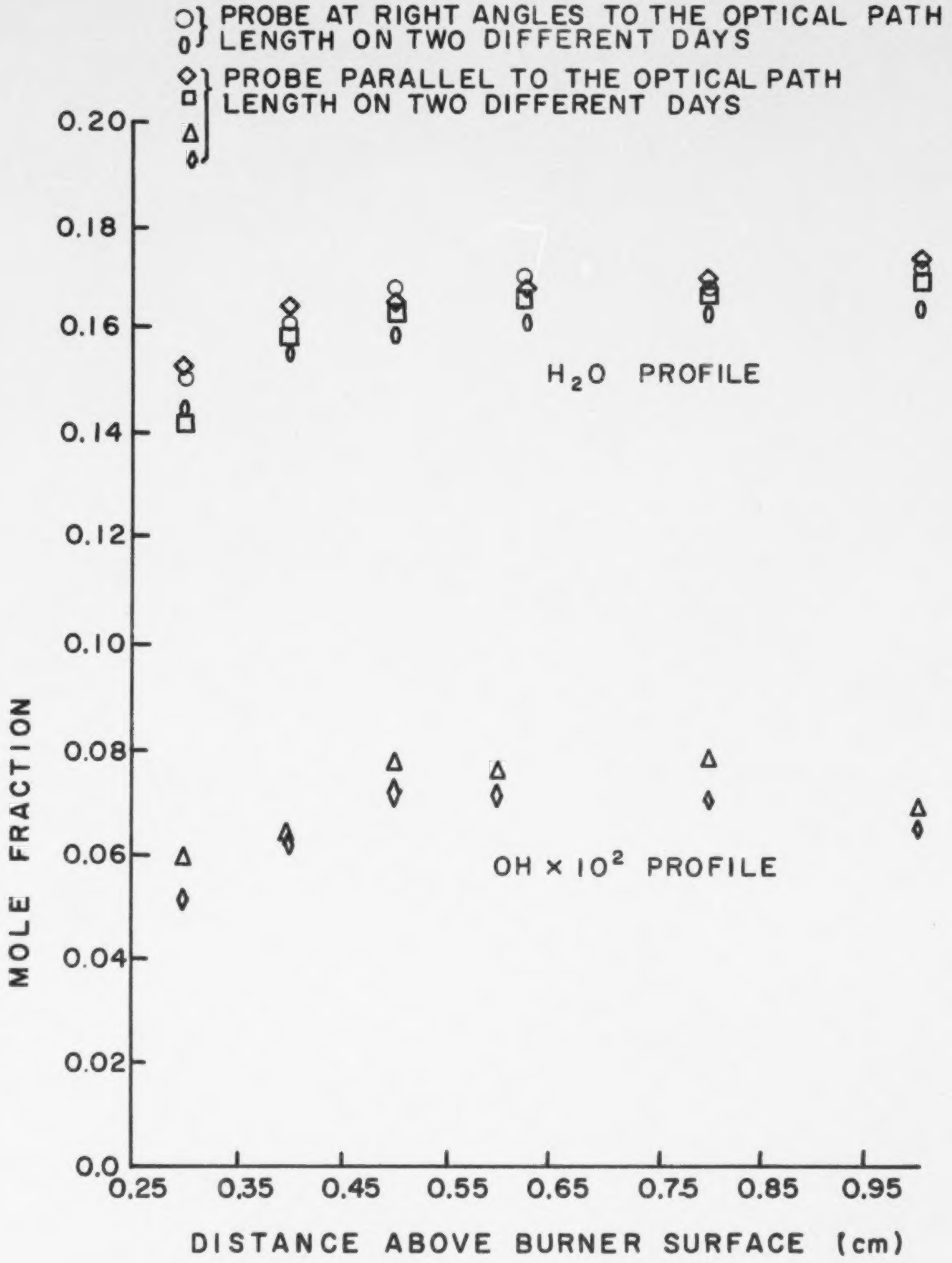

FIG. 5-5. WATER AND HYDROXYL RADICAL MOLE FRACTION PROFILES FOR ETHYLENE/OXYGEN/ARGON FLAMES, P = .054 ATM AND EQUIVALENCE RATIO = 0.81

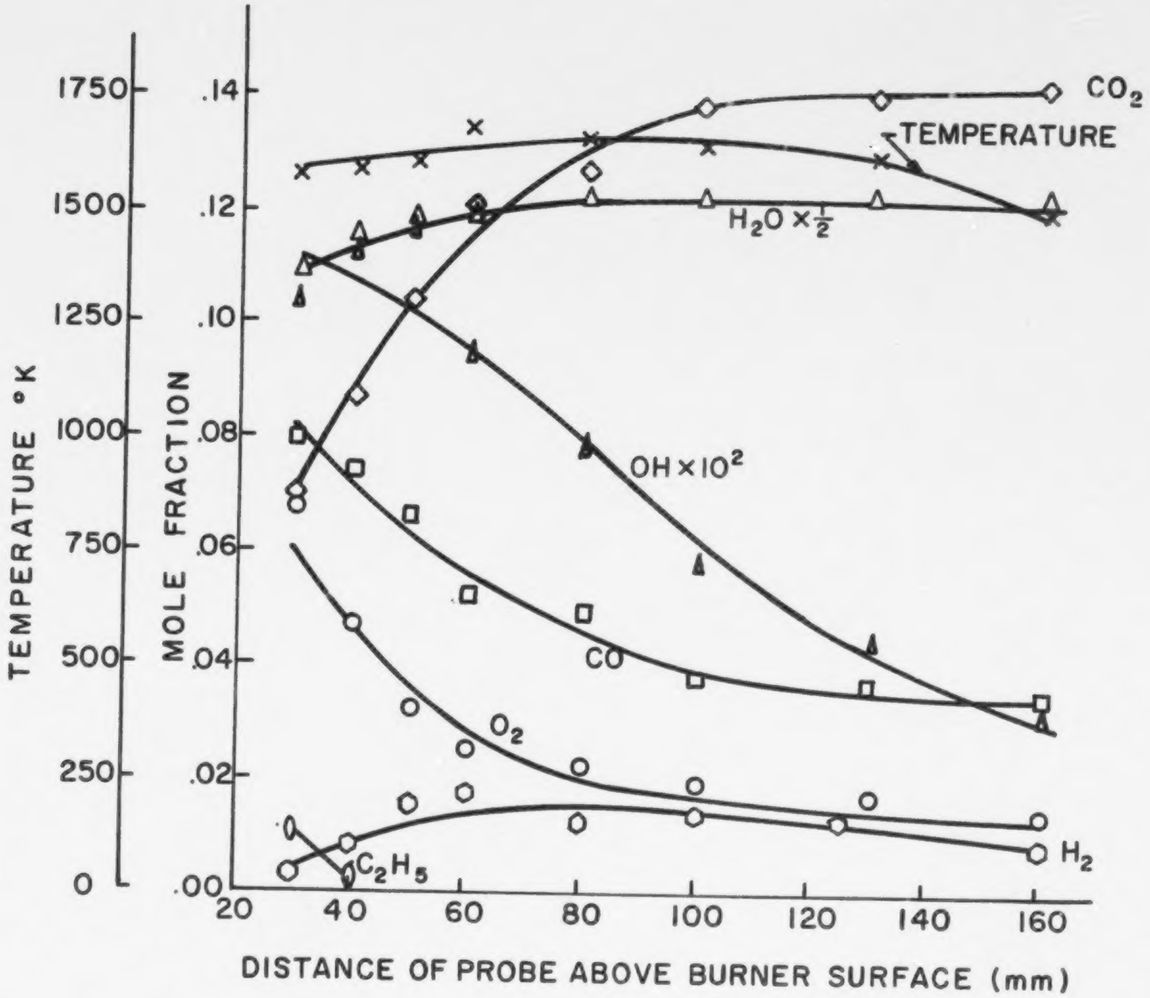

FIG. 5-6. COMPOSITION AND TEMPERATURE PROFILES FOR ETHANE/OXYGEN/ARGON FLAMES AT .083 ATM PRESSURE AND EQUIVALENCE RATIO OF 1.05. THE MOLE FRACTION OF ARGON IS 0.60.

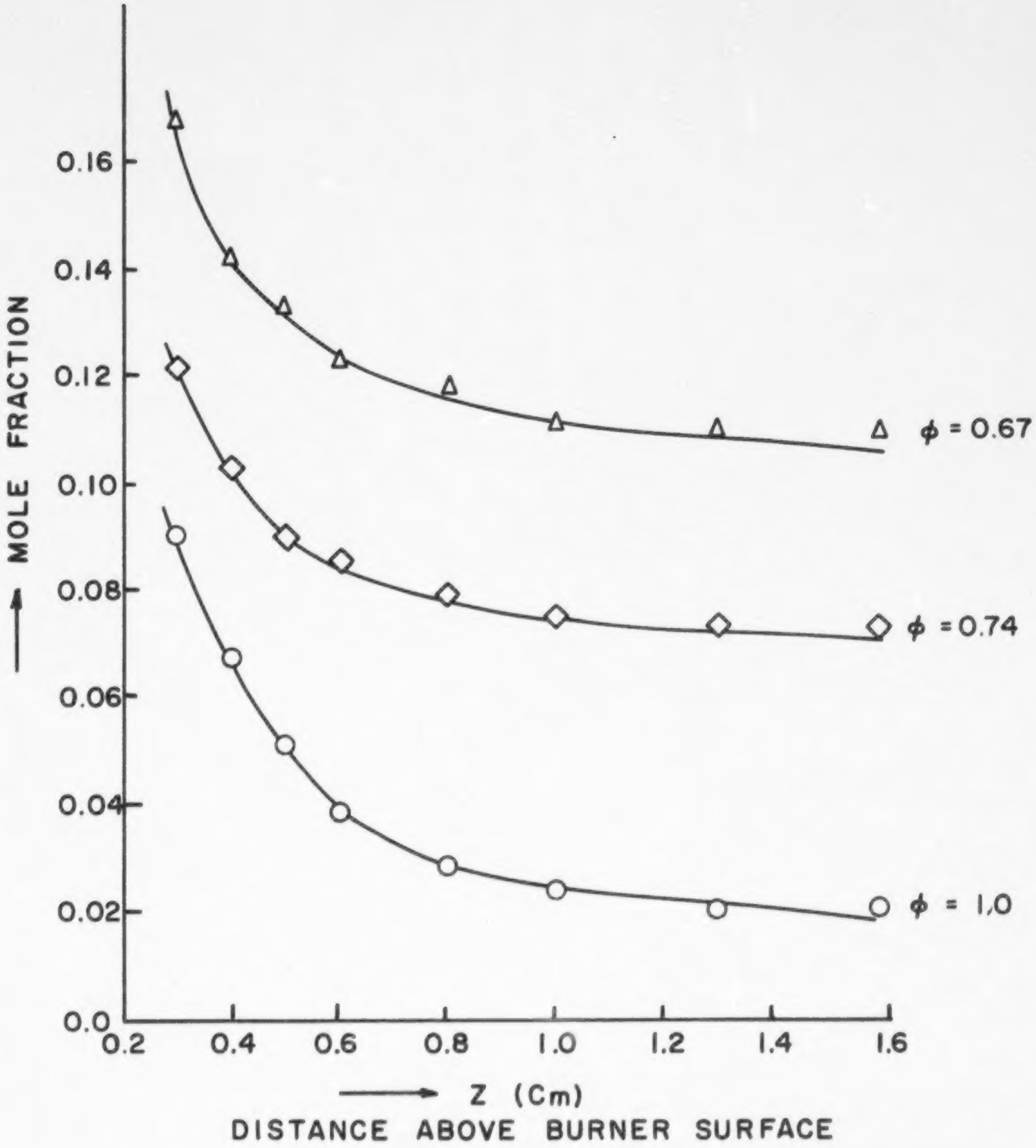

FIG. 5-7. VARIATION OF OXYGEN MOLE FRACTION PROFILE WITH EQUIVALENCE RATIO FOR ETHANE/OXYGEN/NITROGEN FLAMES, P = .084 ATM, MOLE FRACTION OF NITROGEN = 0.60

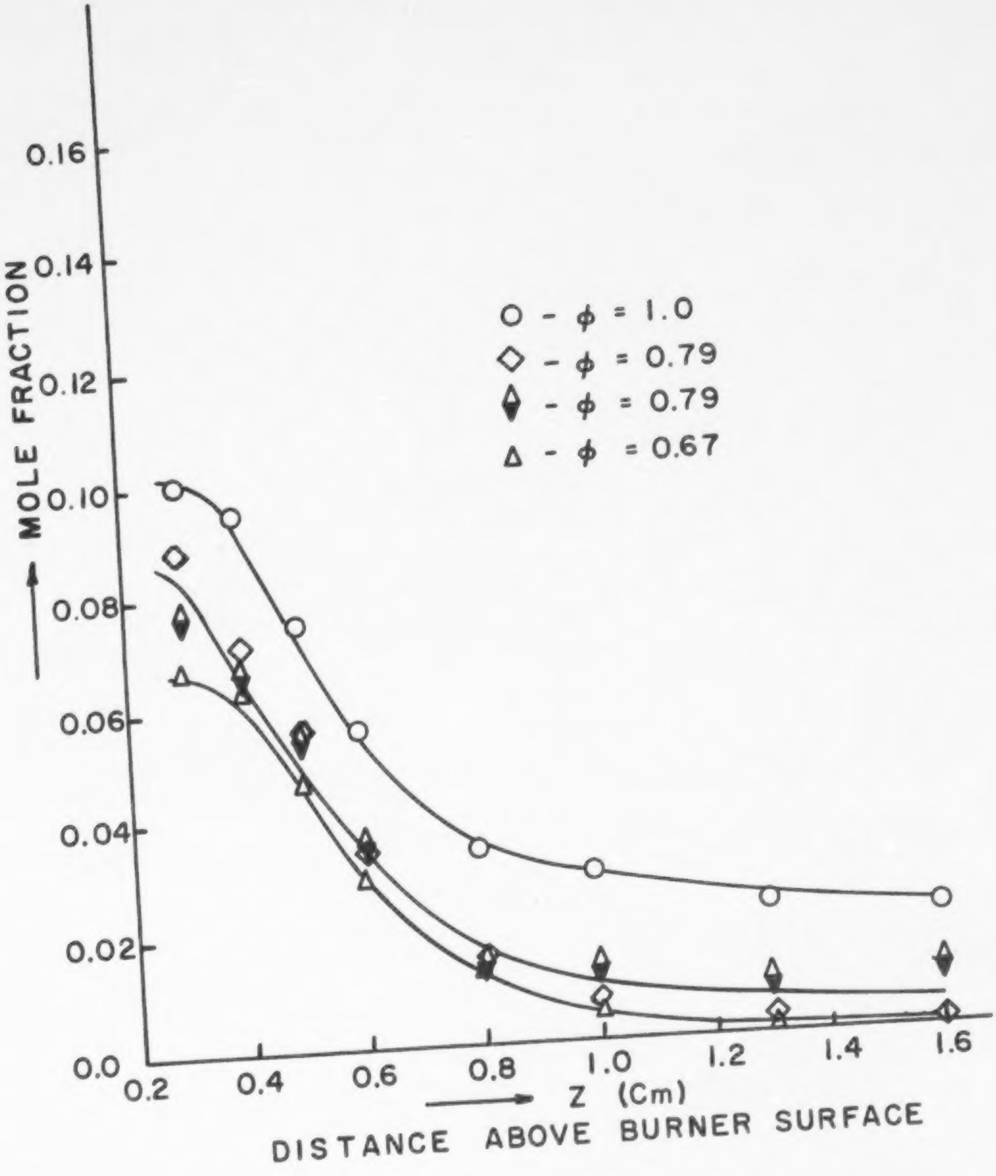

FIG. 5-8. VARIATION OF CARBON MONOXIDE MOLE FRACTION WITH EQUIVALENCE RATIO FOR ETHANE/OXYGEN/NITROGEN FLAMES, P = .084 ATM, MOLE FRACTION NITROGEN = 0.60

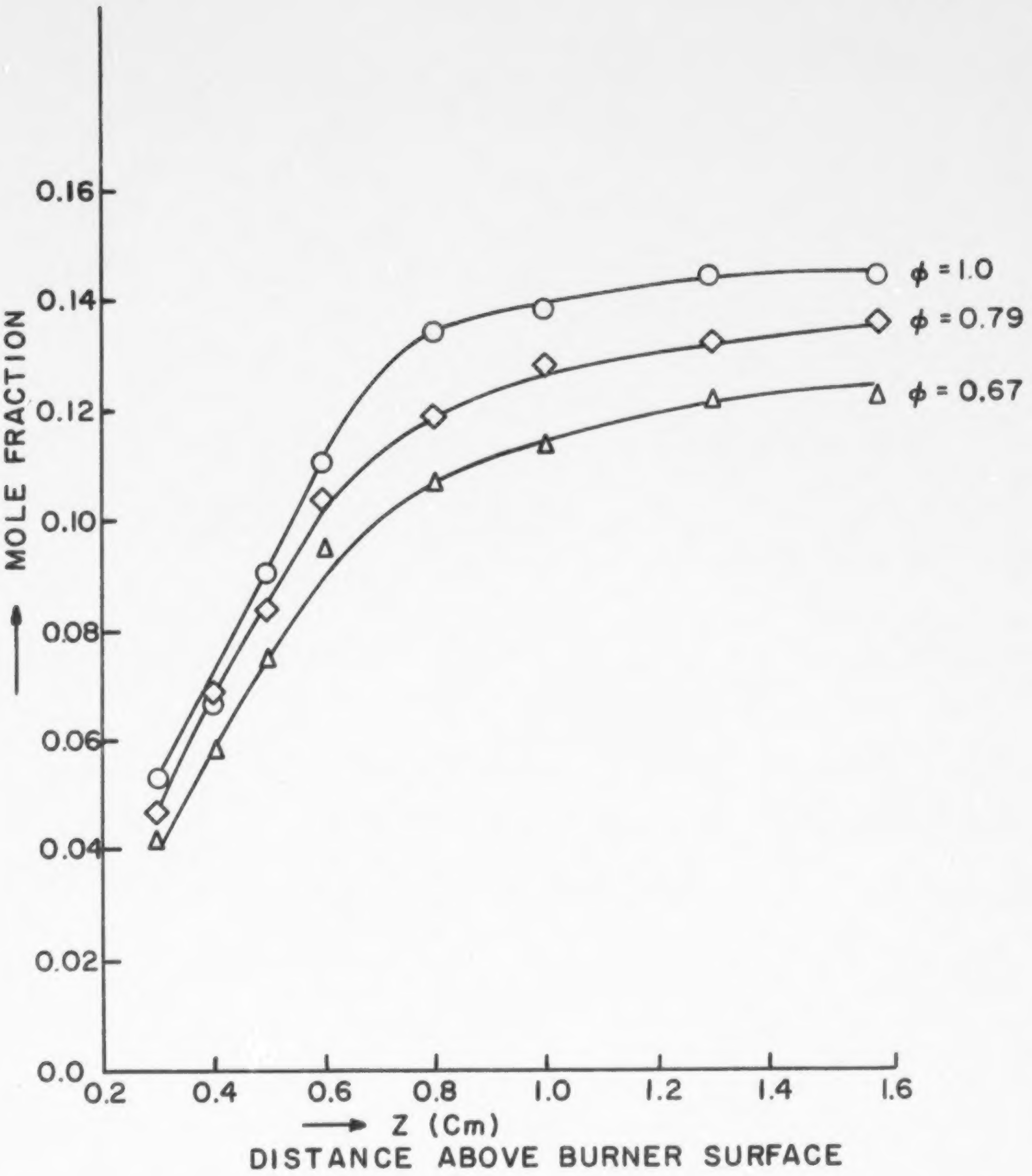

FIG. 5-9. VARIATION OF CARBON DIOXIDE MOLE FRACTION PROFILES WITH EQUIVALENCE RATIO FOR ETHANE/OXYGEN/NITROGEN FLAMES, P = .084 ATM AND MOLE FRACTION NITROGEN = 0.60

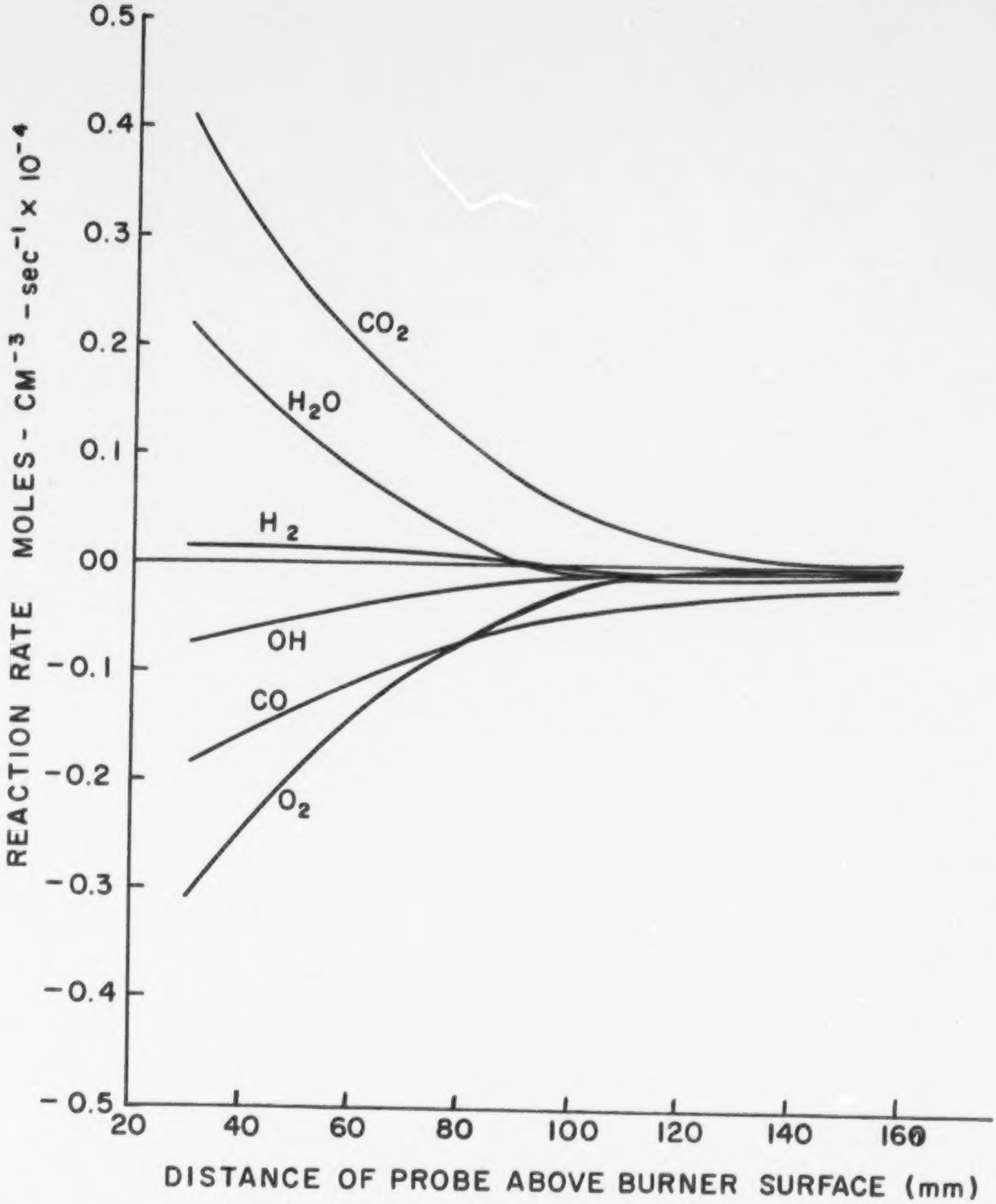

FIG. 5-10. REACTION RATE PROFILES FOR ETHANE/OXYGEN/ARGON FLAMES AT P = .083 ATM AND EQUIVALENCE RATIO = 1.05

hydroxyl radical are greater by a factor of 2 to 6 as compared to the mass flow velocity. Thus, the values of the reaction rates for these species are determined by the extent of uncertainties in the values of the diffusion coefficient and mole fraction. The reaction rate profile corresponding to the composition profiles in Fig. 5-6 are presented in Fig. 5-10. The composition profile, temperature profiles and the corresponding reaction rate profile for all runs are presented in Appendix 1. The overall kinetic analysis for the results is discussed in the following chapter.

CHAPTER 6

OVERALL KINETIC INTERPRETATION

As discussed in Chapter 2, the overall reaction rate of a species is given by the equation

$$\frac{d[X_i]}{dt} = K_{overall} [X_1]^a [X_2]^b \cdots [X_j]^n \qquad (2.1)$$

The overall reaction rate dependence for carbon monoxide, carbon dioxide and oxygen upon the initial composition, local composition and temperature is discussed in this chapter. The rate data are arranged in the six sets (listed in Table 6-1) according to the type of fuel and equivalence ratio of the reactants.

A study of Appendix 1 and Figs. 5-6 to 5-10 shows that the reaction rates of all the species approach a very small value above 1.0 cm from the top of the burner surface. The subsequent kinetic analysis is limited to the regime of 0.3 to 1.0 cm above the burner surface where significant composition changes are taking place and most of the hydrocarbon has been consumed.

6.1 Overall Carbon Monoxide Disappearance/Carbon Dioxide Appearance Rate

A review of the literature in Chapter 2 suggests the disappearance rate of carbon monoxide/appearance rate of carbon dioxide in the afterburning zone of hydrocarbon flames depend upon the local concentration of CO, CO_2 and H_2O. By making use of the equation (2.1), the rates may be expressed as:

$$-\frac{d[CO]}{dt} = K_{overall-1} [CO]^{a_1} [O_2]^{b_1} [H_2O]^{c_1} \qquad (6.1)$$

$$\frac{d[CO_2]}{dt} = K_{overall-2} [CO]^{a_2} [O_2]^{b_2} [H_2O]^{c_2} \qquad (6.2)$$

Table 6-1. Experimental data groups

Group No.	Fuel	Equivalence Ratio
1	C_2H_6	0.67
2	C_2H_6	0.80
3	C_2H_6	1.00
4	C_2H_4	0.67
5	C_2H_4	0.80
6	C_2H_4	1.00

The concentration of H_2O changes relatively slowly in the regime of the present study. Thus, $[H_2O]^c$ may be taken as constant and may be lumped together with $K_{overall}$. Studies of afterburning of CO reported in the literature[10,12,16,18] are in agreement that the reaction order with respect to carbon monoxide is unity, i.e. $a_1 = 1$ and $a_2 = 1$. Thus, initially a first order dependence is here assumed for carbon monoxide.

In order to determine the reaction order with respect to oxygen, plots of $\log - \frac{d[CO]/dt}{[CO]}$ vs. $\log [O_2]$ and $\log \frac{d[CO_2]/dt}{[CO]}$ vs. $\log [O_2]$ at T = 1637 ± 12°K are plotted in Figs. 6-1 and 6-2 respectively. The slope of these lines is zero, thus indicating that rates of CO disappearance/CO_2 appearance are independent of the concentration of O_2. In order to check the assumption of order unity with respect to carbon monoxide, plots of $\log - d[CO]/dt$ vs. $\log [CO]$ and $\log d[CO_2]/dt$ vs. $\log [CO]$ at T = 1567 ± 12°K are presented in Figs. 6-3 and 6-4. The slopes of the lines are 1.07 and 0.89, which justify a unity dependence with respect to carbon monoxide. Hence, rates of CO_2 appearance/CO disappearance in the present study may be expressed by the following apparent first order rate equations

$$- \frac{d[CO]}{dt} = K_{overall-1}[CO] \tag{6.3}$$

$$\frac{d[CO_2]}{dt} = K_{overall-2}[CO] \tag{6.4}$$

in agreement with results of Reference 10, as mentioned in Chapter 2. The Arrhenius form is now assumed for the overall rate constants $K_{overall-1}$ and $K_{overall-2}$, i.e.

$$K_{overall-1} = A_1 \exp^{-(E_1/RT)} \tag{6.5}$$

$$K_{overall-2} = A_2 \exp^{-(E_2/RT)} \tag{6.6}$$

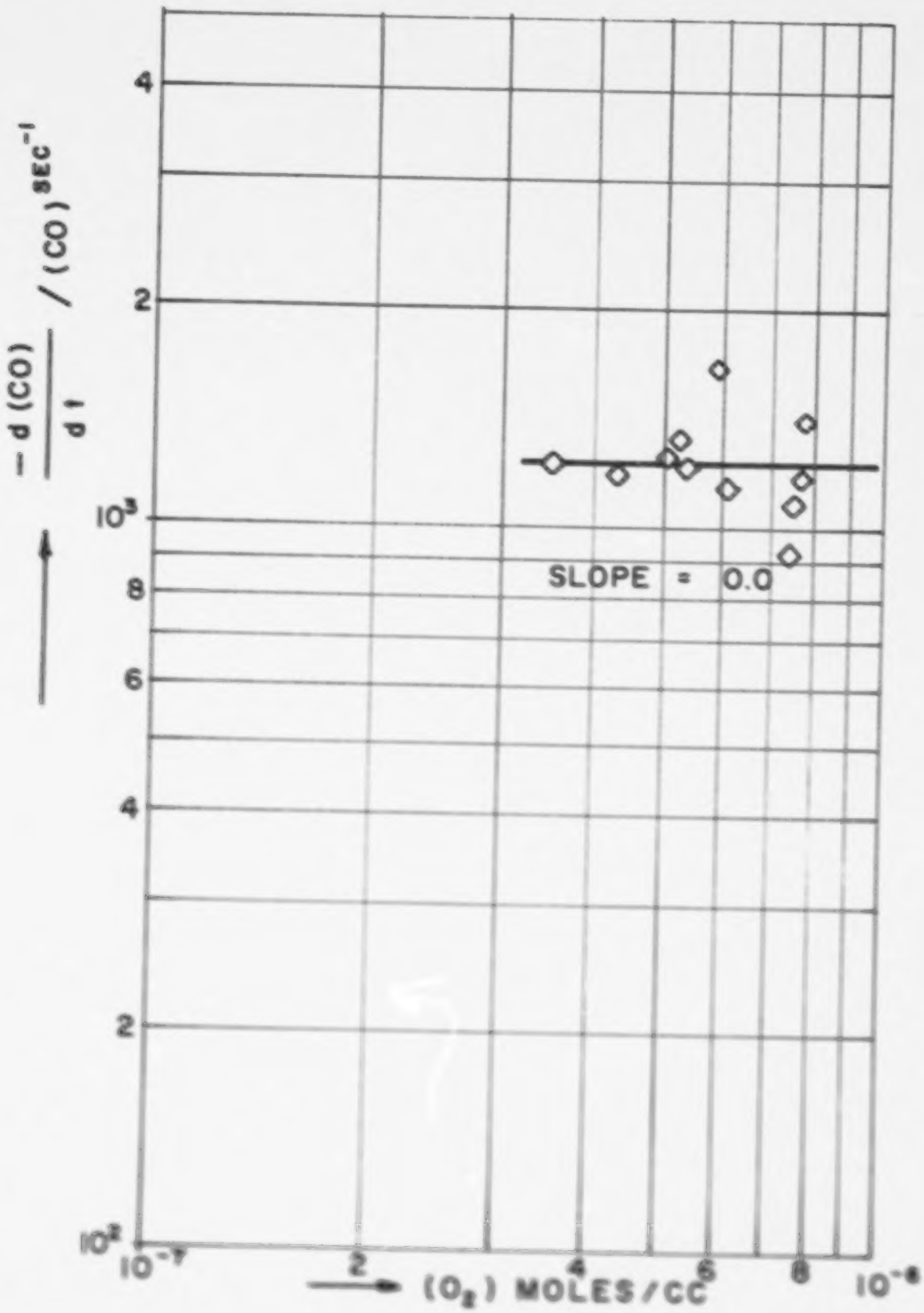

FIG. 6-1. REACTION ORDER DEPENDENCE WITH RESPECT TO OXYGEN FOR CARBON MONOXIDE DISAPPEARANCE RATE FOR ETHYLENE/OXYGEN FLAMES, T = 1637 ± 12°K

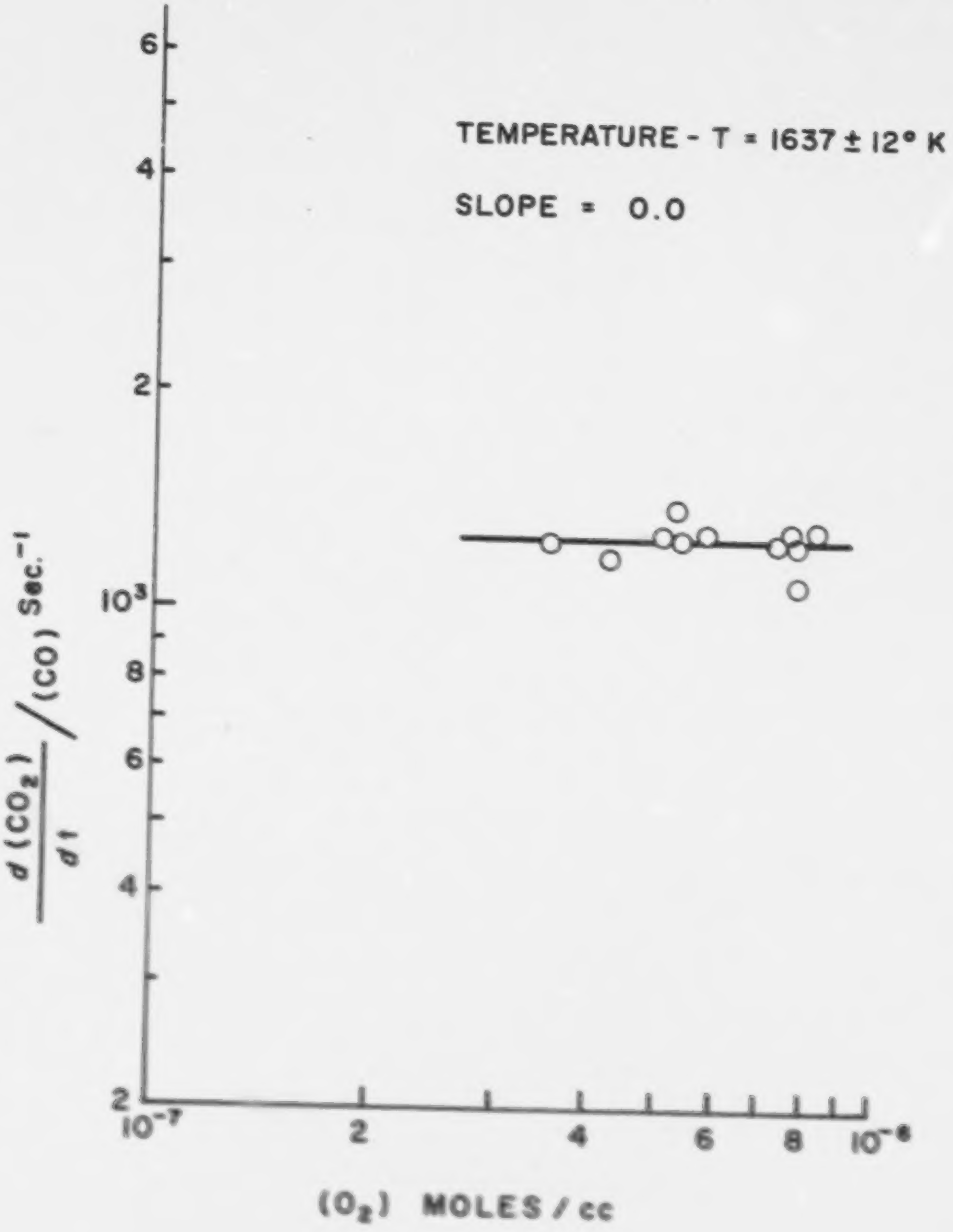

Fig. 6-2. REACTION ORDER DEPENDENCE WITH RESPECT TO OXYGEN FOR CARBON DIOXIDE APPEARANCE RATE FOR ETHYLENE/OXYGEN FLAMES

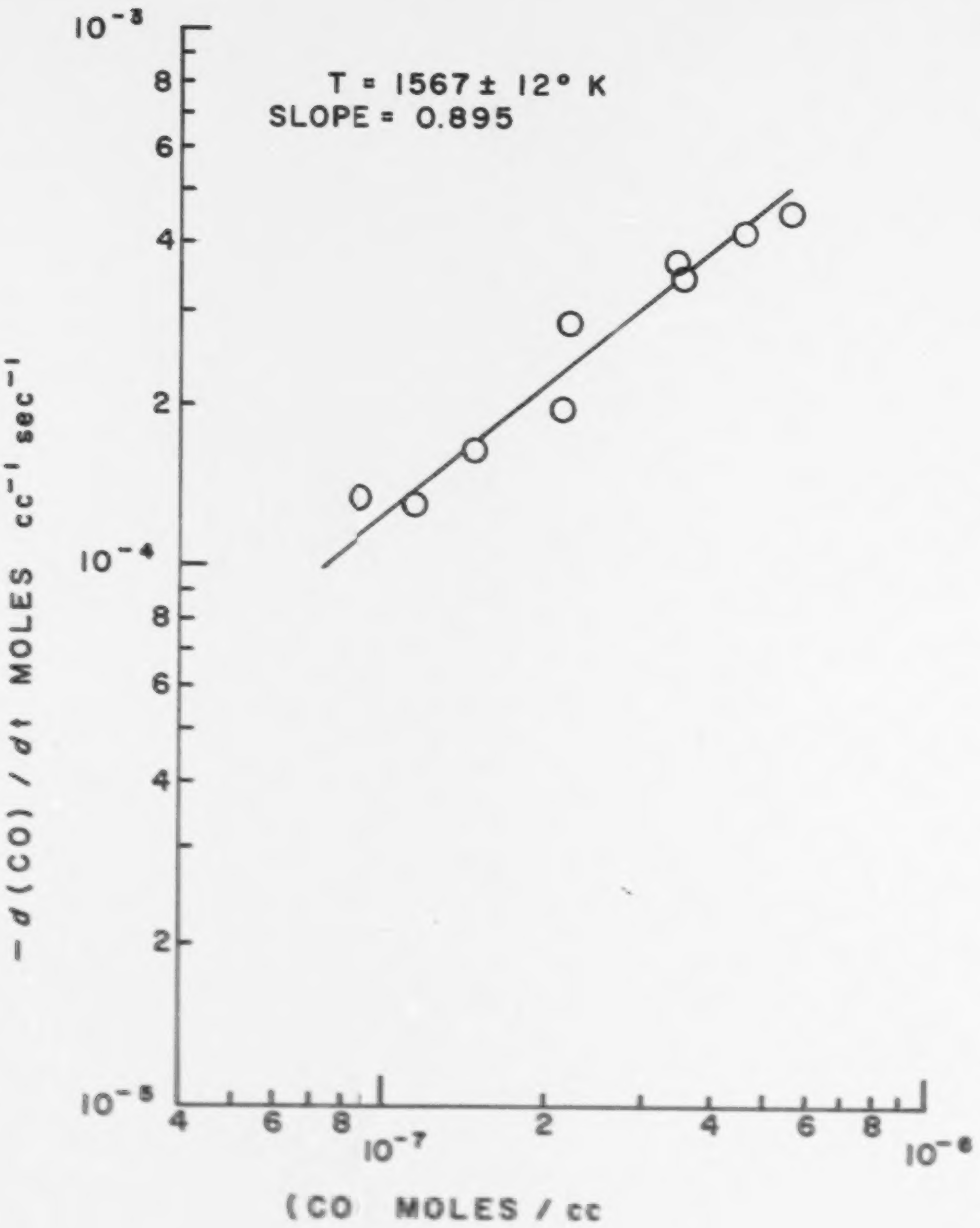

FIG. 6-3. REACTION ORDR DEPENDENCE WITH RESPECT TO CARBON MONOXIDE FOR CO DISAPPEARANCE RATE, ETHYLENE/OXYGEN FLAMES

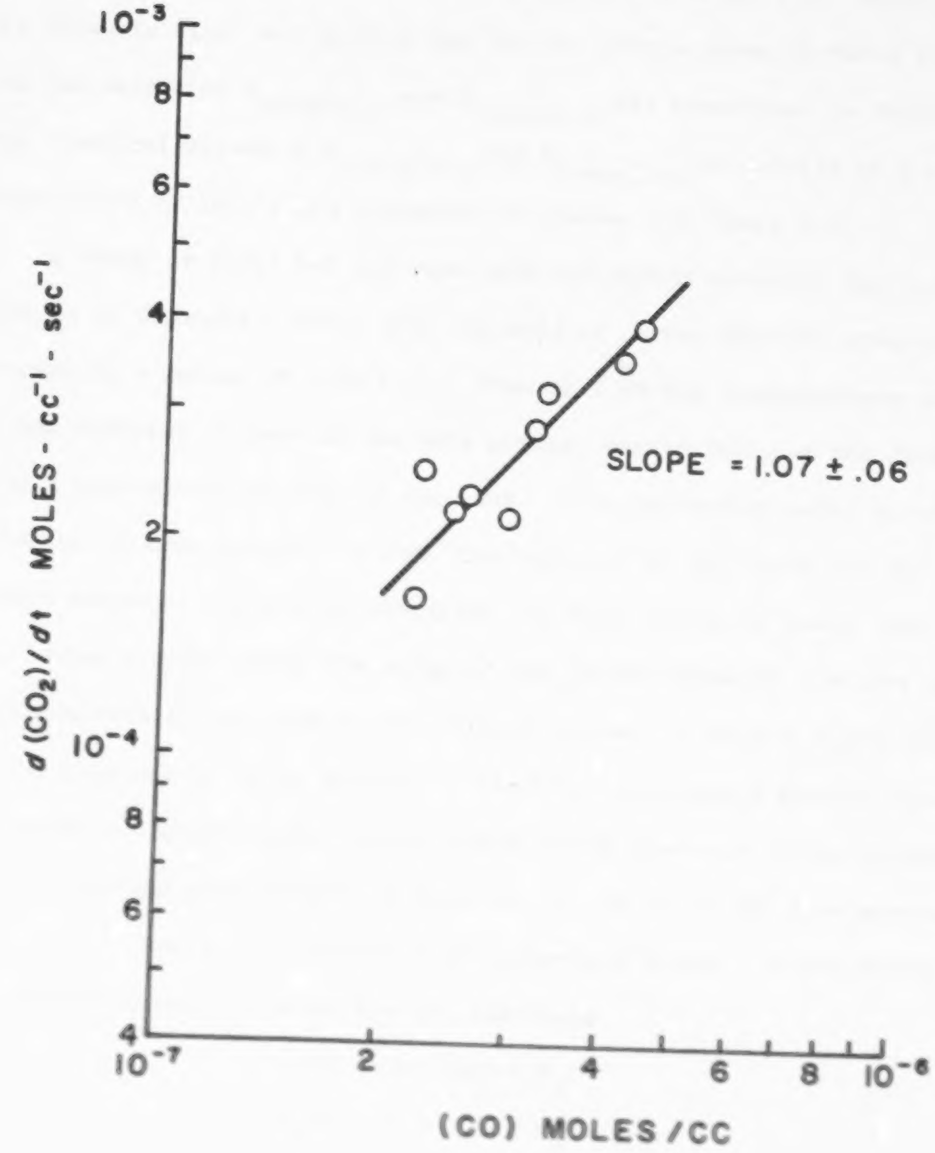

FIG. 6-4. REACTION ORDER DEPENDENCE WITH RESPECT TO CARBON MONOXIDE FOR CO_2 APPEARANCE RATE, ETHYLENE/OXYGEN FLAMES, T = 1567±12°K

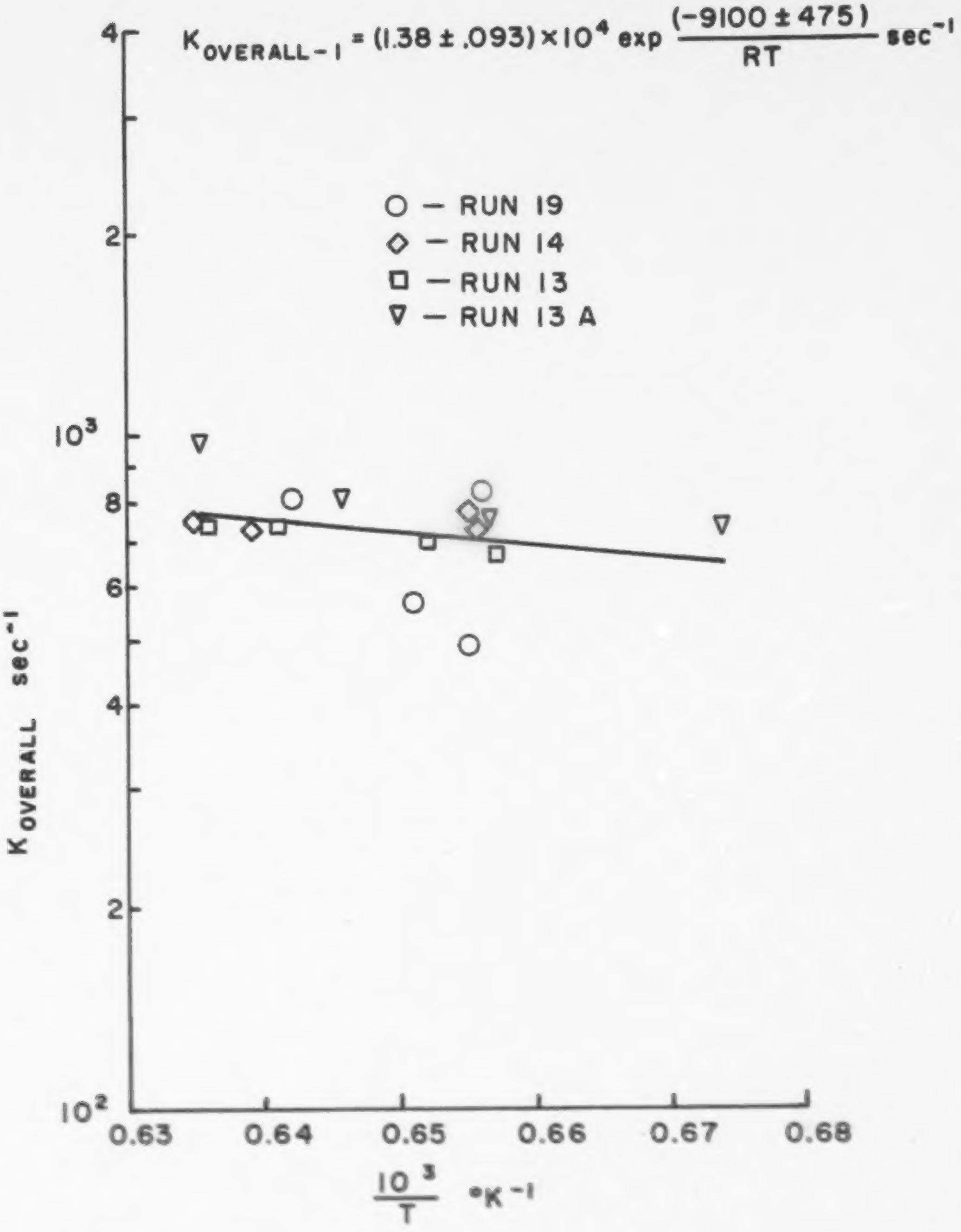

FIG. 6-5. DETERMINATION OF ARRHENIUS PARAMETERS FOR $k_{overall-1}$ ETHYLENE/OXYGEN FLAMES, EQUIVALENCE RATIO = 0.67 (DATA GROUP 1)

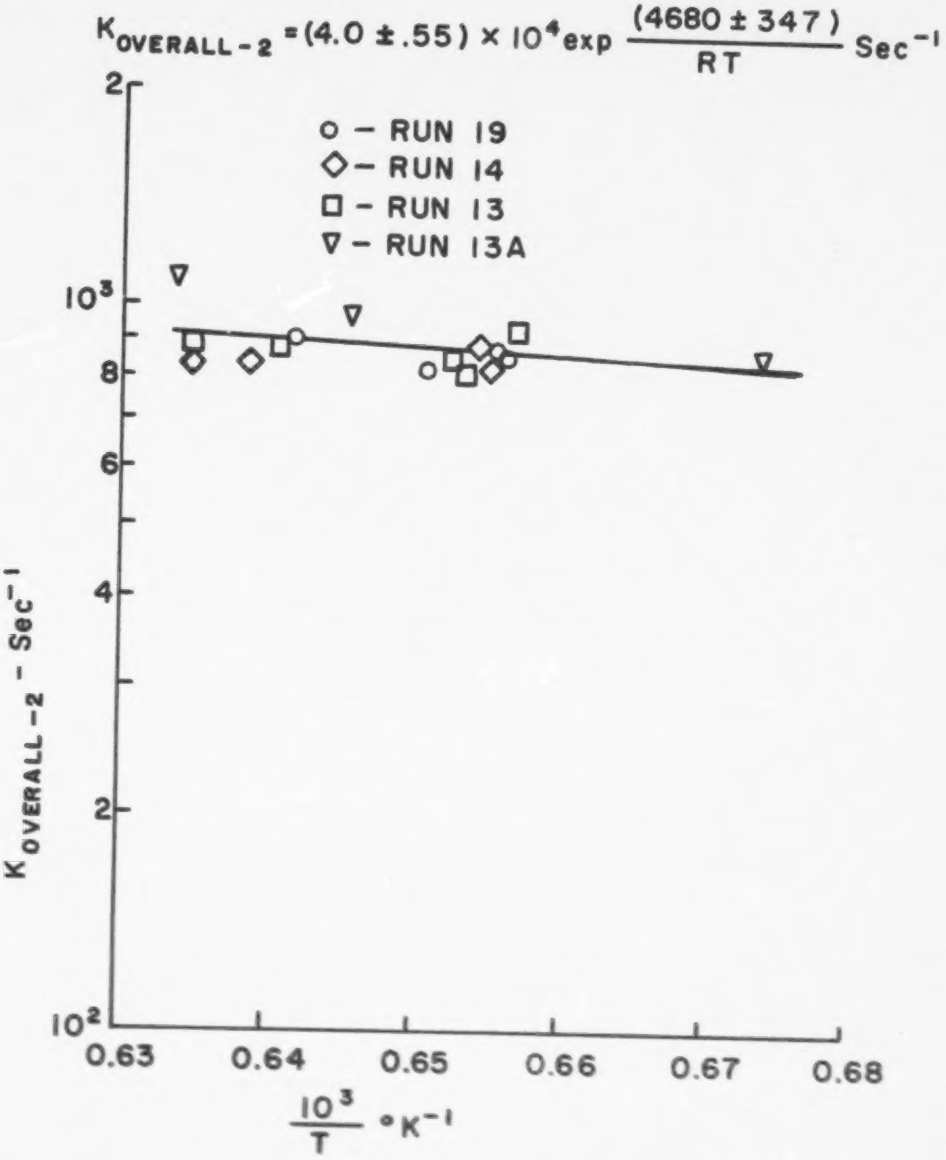

FIG. 6-6. DETERMINATION OF ARRHENIUS PARAMETERS FOR $k_{overall-2}$ ETHYLENE/OXYGEN FLAMES, EQUIVALENCE RATIO = 0.67 (DATA GROUP 1)

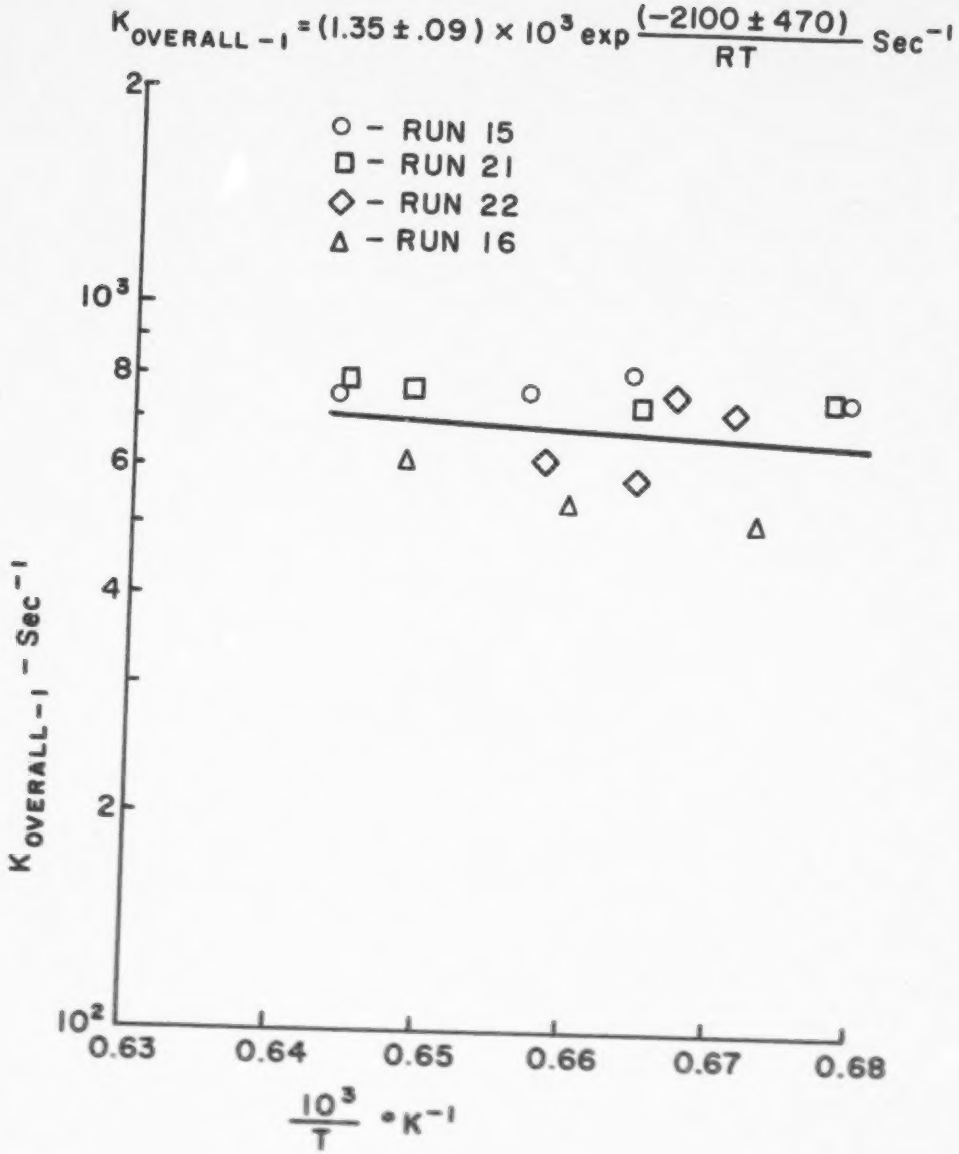

FIG. 6-7. DETERMINATION OF ARRHENIUS PARAMETERS FOR $k_{overall-1}$, ETHYLENE/OXYGEN FLAMES, EQUIVALENCE RATIO = 0.8 (DATA GROUP 2)

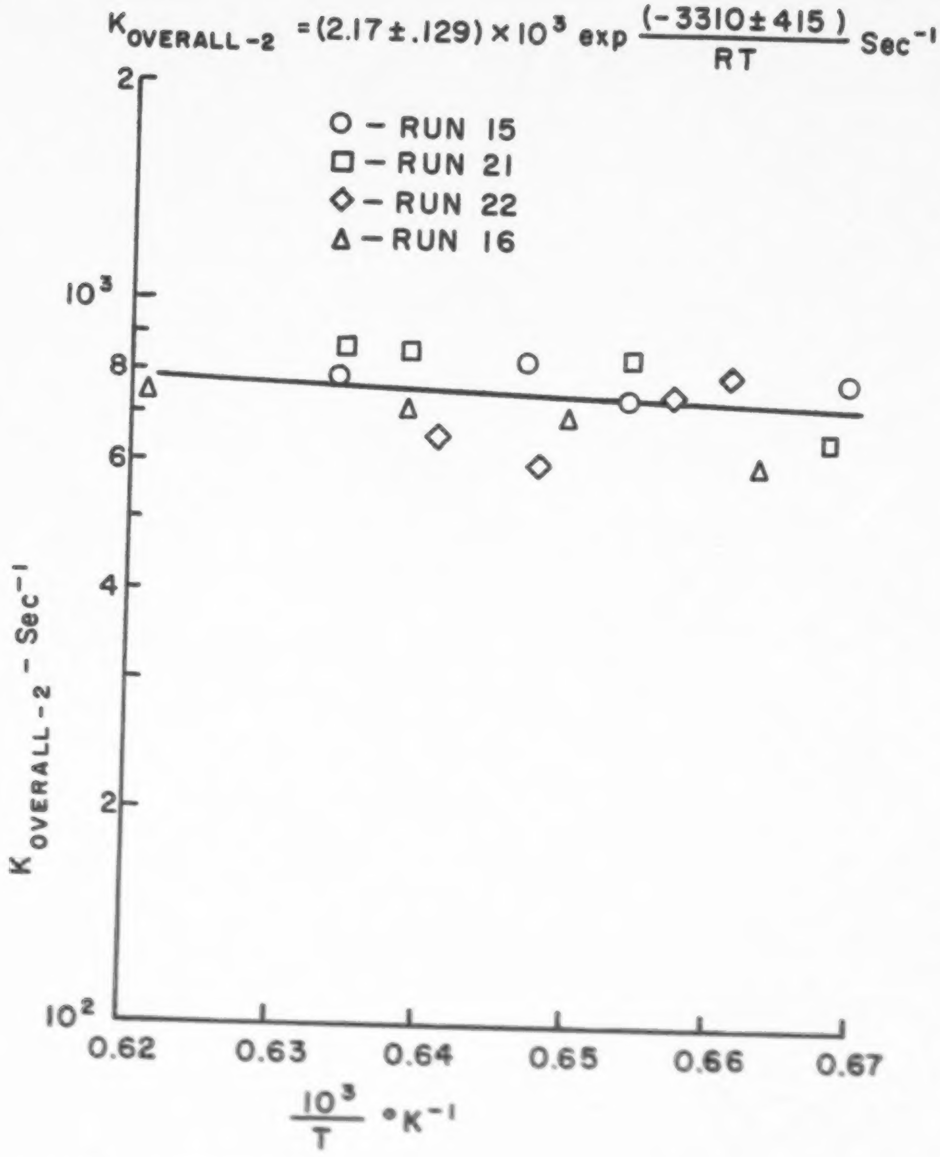

$$K_{OVERALL-2} = (2.17 \pm .129) \times 10^3 \exp \frac{(-3310 \pm 415)}{RT} \ \text{Sec}^{-1}$$

FIG. 6-8. DETERMINATION OF ARRHENIUS PARAMETERS FOR $k_{overall-2}$ ETHYLENE/OXYGEN FLAMES, EQUIVALENCE RATIO = 0.8 (DATA GROUP 2)

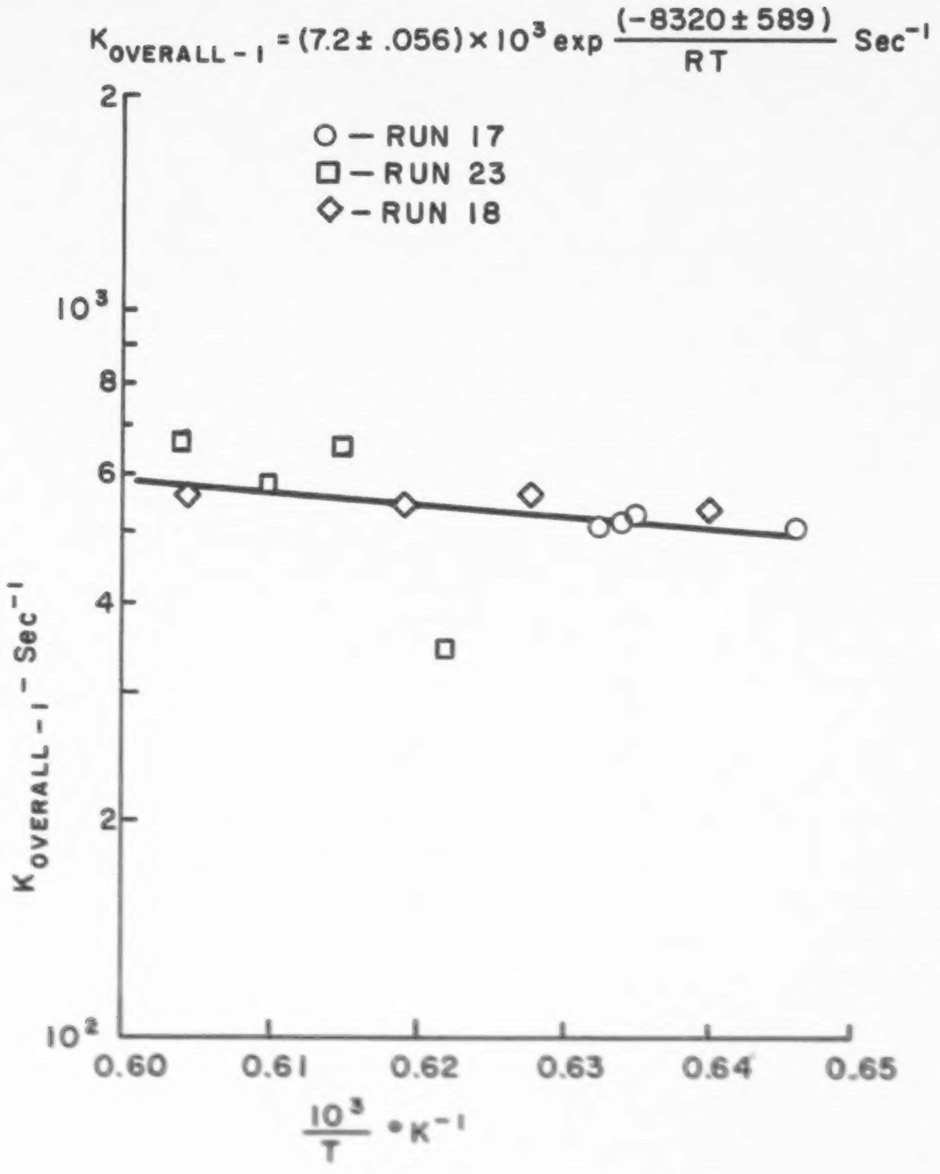

FIG. 6-9. DETERMINATION OF ARRHENIUS PARAMETERS FOR $k_{overall-1}$, ETHYLENE/OXYGEN FLAMES, EQUIVALENCE RATIO = 1.0 (DATA GROUP 3)

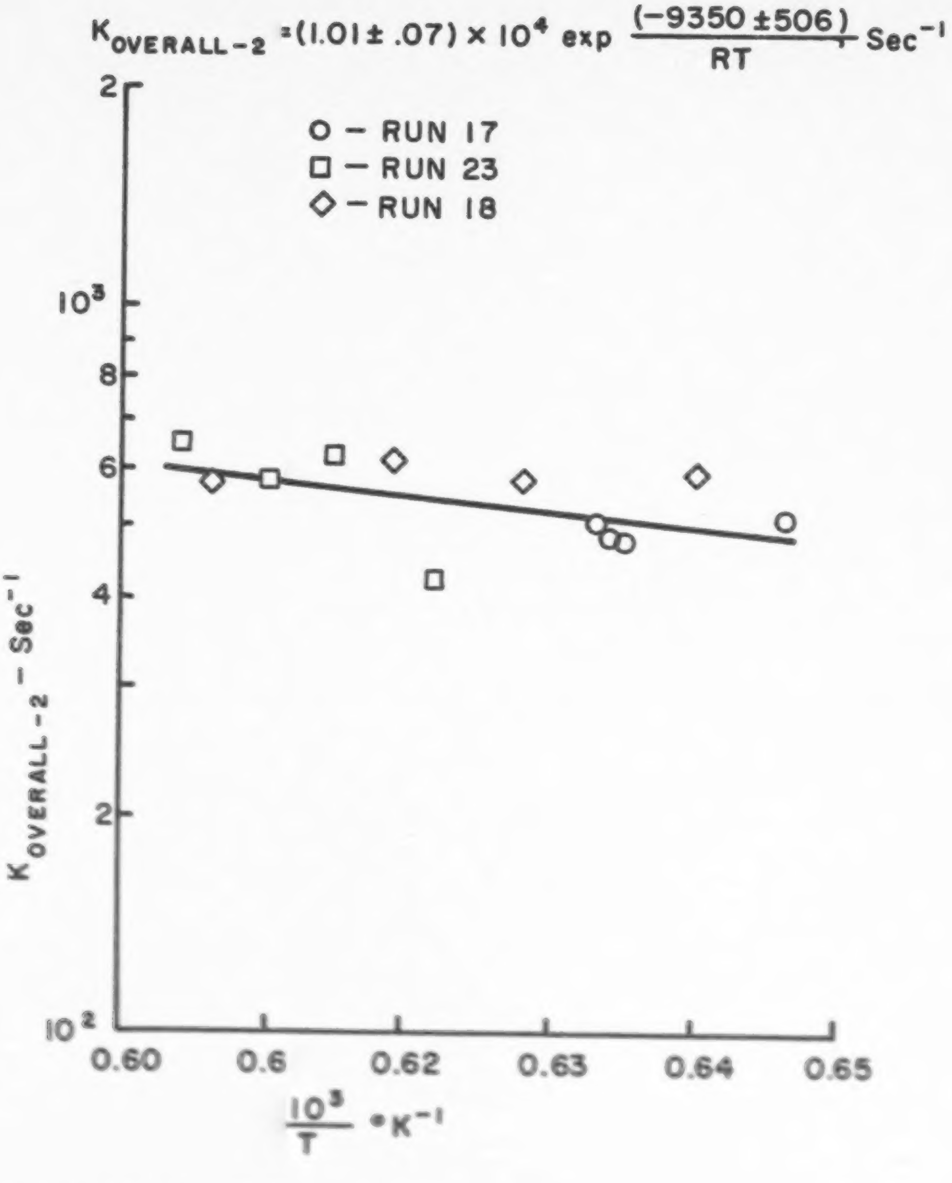

FIG. 6-10. DETERMINATION OF ARRHENIUS PARAMETERS FOR $k_{overall-2}$, ETHYLENE/OXYGEN FLAMES, EQUIVALENCE RATIO = 1.0 (DATA GROUP 3)

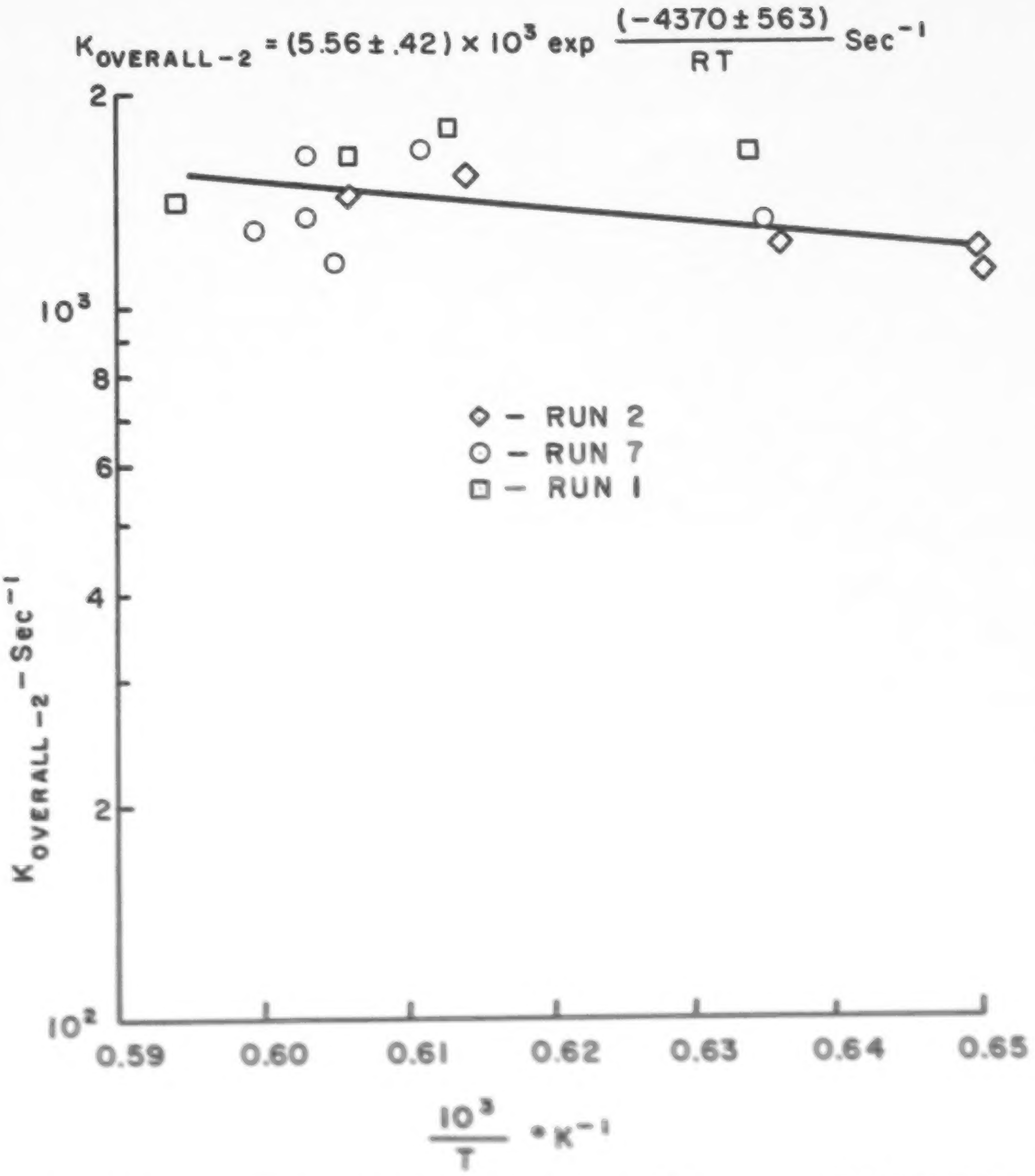

FIG. 6-11. DETERMINATION OF ARRHENIUS PARAMETER FOR $k_{overall-2}$, ETHANE/OXYGEN FLAMES, EQUIVALENCE RATIO = 0.67, (DATA GROUP 4)

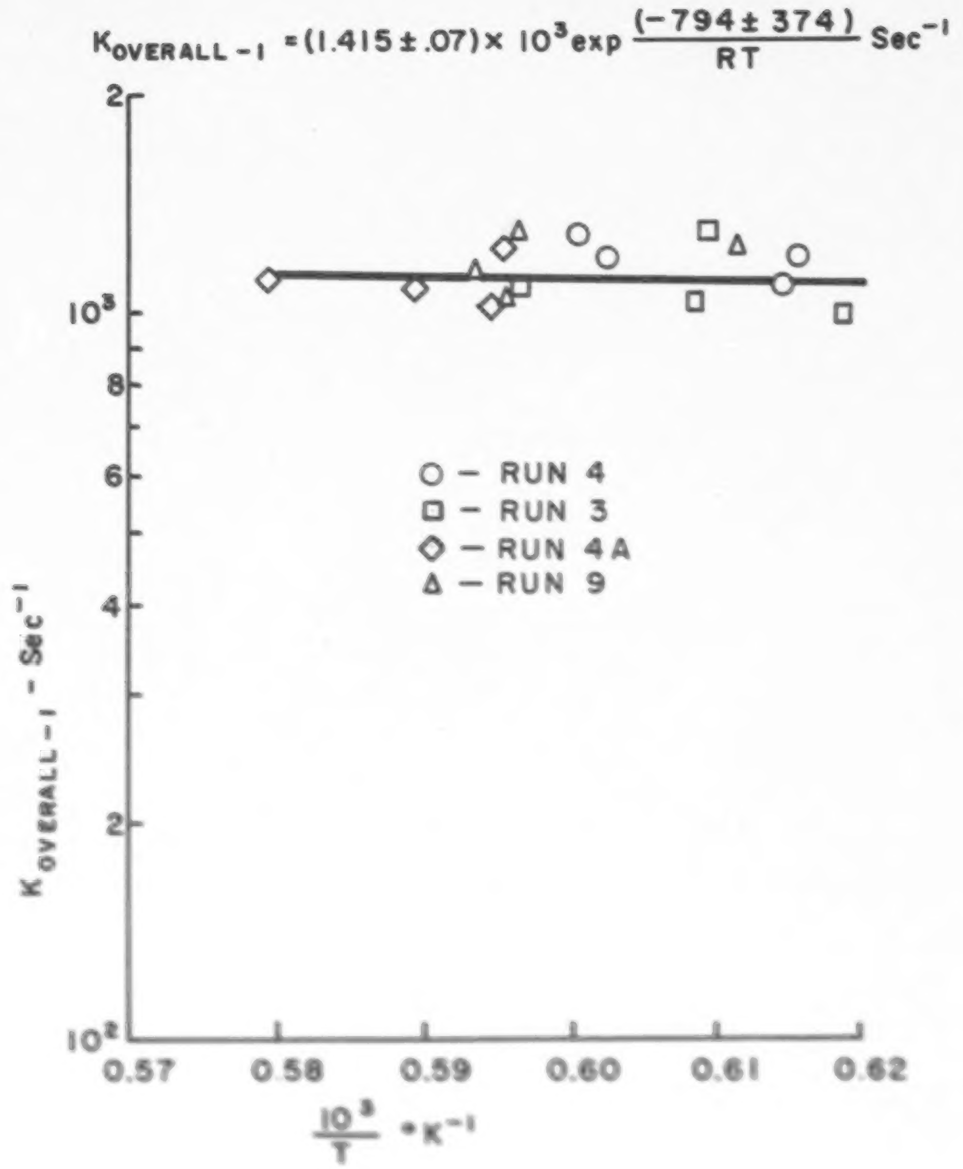

FIG. 6-12. DETERMINATION OF ARRHENIUS PARAMETERS FOR $k_{overall-1}$, ETHANE/OXYGEN FLAMES, EQUIVALENCE RATIO = 0.9 (DATA GROUP 3)

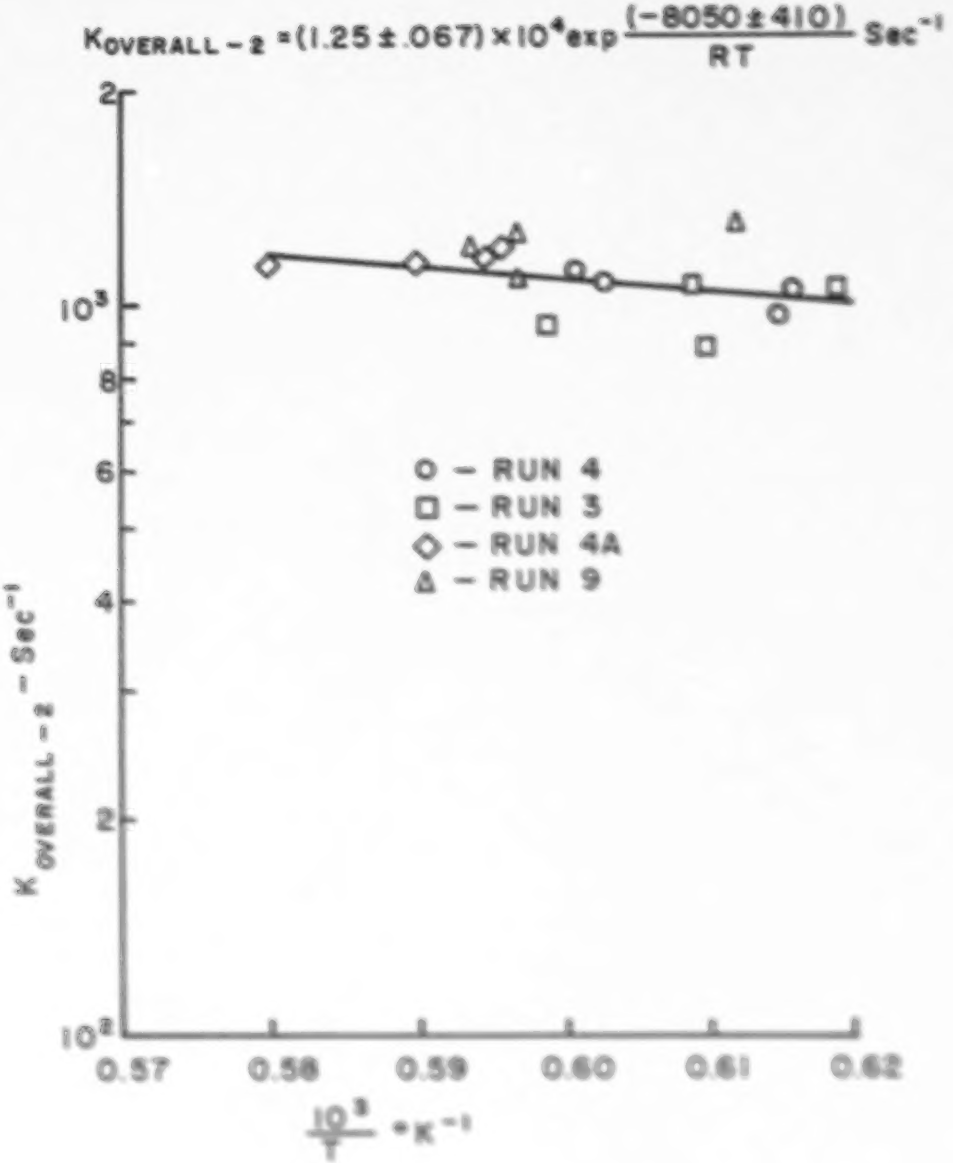

$$K_{OVERALL-2} = (1.25 \pm .067) \times 10^4 \exp\frac{(-8050 \pm 410)}{RT}\ \mathrm{Sec}^{-1}$$

FIG. 4-13. DETERMINATION OF ARRHENIUS PARAMETERS FOR $k_{overall-2}$, ETHANE/OXYGEN FLAMES, EQUIVALENCE RATIO = 1.0 (DATA GROUP 1)

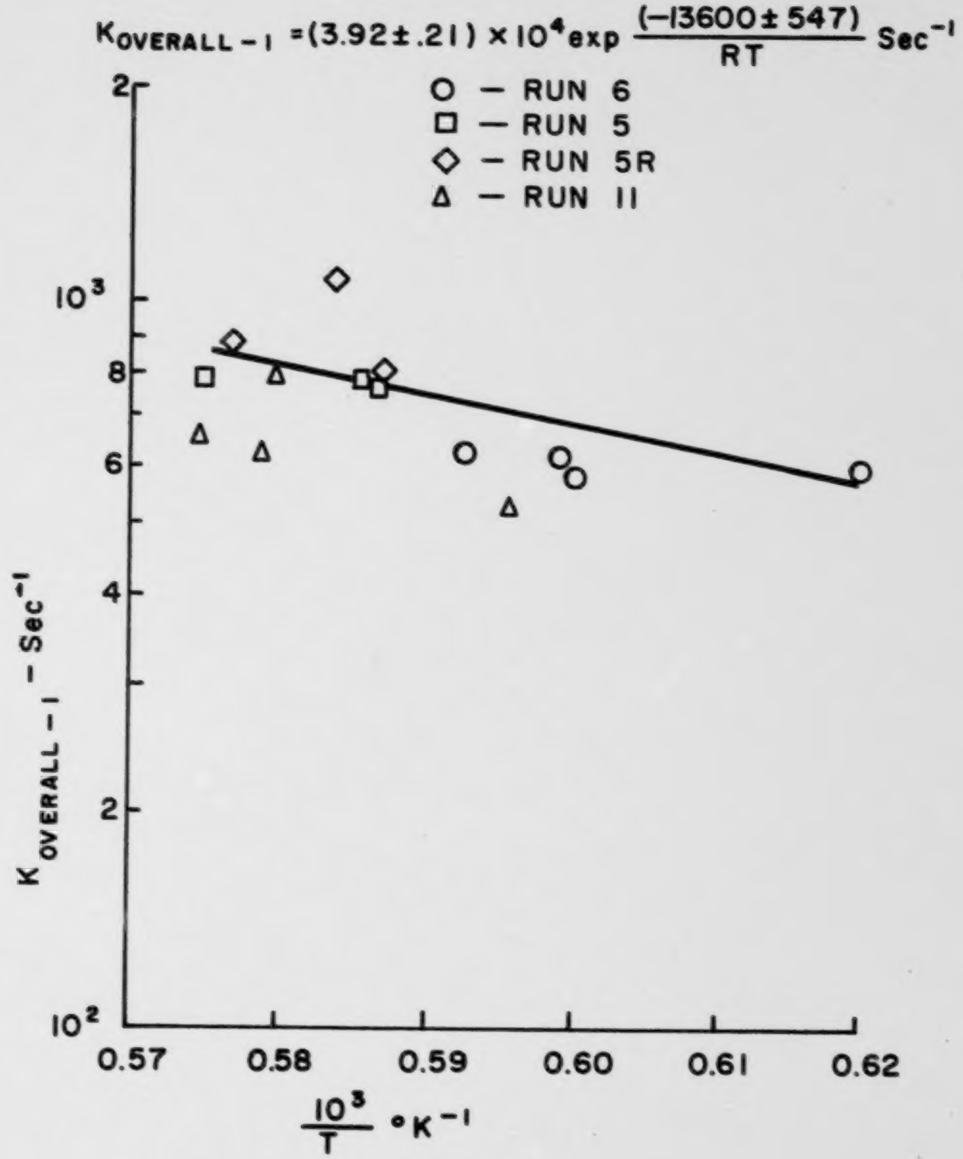

FIG. 6-14. DETERMINATION OF ARRHENIUS PARAMETERS FOR $k_{overall-1}$, ETHANE/OXYGEN FLAMES, EQUIVALENCE RATIO = 1.0 (DATA GROUP 6)

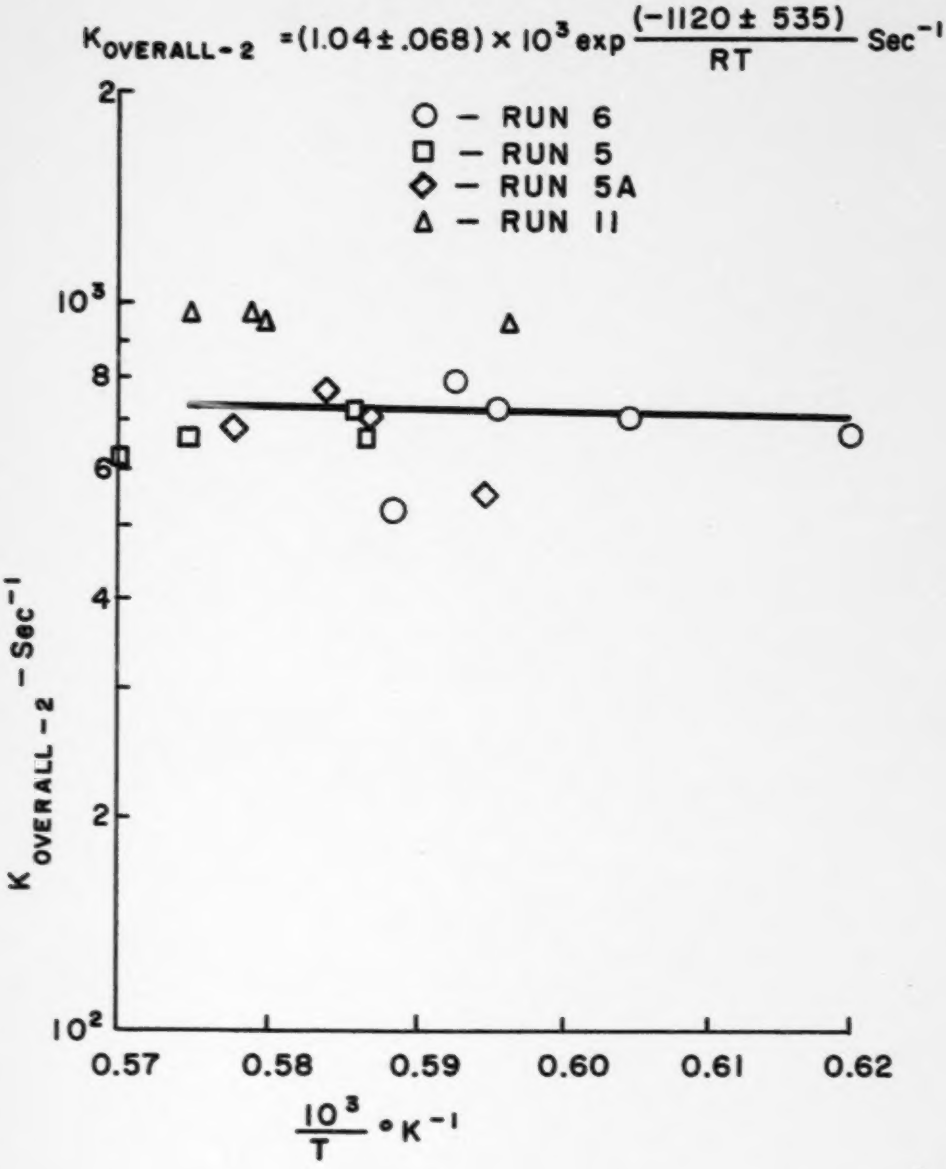

FIG. 6-15. DETERMINATION OF ARRHENIUS PARAMETERS FOR $K_{overall-2}$, ETHANE/OXYGEN FLAMES, EQUIVALENCE RATIO = 1.0 (DATA GROUP 6)

Table 6-2. Summary of $K_{overall}$ for CO disappearance and CO_2 appearance rates (1500-1723°K temp range).

Fuel	Equivalence ratio	$K_{overall}$ for (a) CO disappearance (b) CO_2 appearance sec^{-1}	$K_{overall}$ at T = 1615°K	Average OH Concentration moles/cc×10^8
C_2H_4	0.67	(a) $(1.38 \pm .093) \times 10^4 \exp \frac{(-9100 \pm 475)}{RT}$	815	.0591
		(b) $(4.0 \pm .44) \times 10^3 \exp \frac{(-4680 \pm 347)}{RT}$	943	
C_2H_4	0.80	(a) $(1.35 \pm .091) \times 10^3 \exp \frac{(-2100 \pm 470)}{RT}$	696	.0459
		(b) $(2.17 \pm .129) \times 10^3 \exp \frac{(-3310 \pm 415)}{RT}$	780	
C_2H_4	1.00	(a) $(7.1 \pm .056) \times 10^3 \exp \frac{(-8320 \pm 585)}{RT}$	538	.0252
		(b) $(1.01 \pm .068) \times 10^4 \exp \frac{(-9350 \pm 503)}{RT}$	557	
C_2H_6	0.67	(a) $(8.24 \pm .64) \times 10^2 \exp \frac{(847 \pm 590)}{RT}$	1120	.0563
		(b) $(5.56 \pm .42) \times 10^3 \exp \frac{(-4370 \pm 563)}{RT}$	1142	
C_2H_6	0.80	(a) $(1.415 \pm .07) \times 10^3 \exp \frac{(-794 \pm 374)}{RT}$	1100	.1124
		(b) $(1.25 \pm .067) \times 10^4 \exp \frac{(-8050 \pm 410)}{RT}$	1040	
C_2H_6	1.0	(a) $(3.92 \pm .21) \times 10^4 \exp \frac{(-13600 \pm 547)}{RT}$	595	.0717
		(b) $(1.04 \pm .068) \times 10^3 \exp \frac{(-1120 \pm 535)}{RT}$	707	

particularly in the immediate vicinity of the luminous zone (corresponding to the first 2-3 data points). The aforementioned reactions involve interaction between two radical/atomic species which are present in relatively small concentrations. Therefore, the net contribution of the above mentioned reactions in reducing the overall disappearance of carbon monoxide would be small.

Another factor contributing to the divergence between the disappearance rate of carbon monoxide and appearance rate of carbon dioxide could be the difficulties associated with calculating the mole fraction of carbon monoxide from the mass spectral data. As mentioned in section 5.1, these difficulties arise due to overlapping of principal peaks of N_2 and CO at m/e = 28 and increased background fluctuations at m/e = 28 when argon is used as a diluent. At present the higher uncertainty associated with the calculated value of CO mole fraction appears to be the principal reason for the disagreement between the observed CO disappearance rate and CO_2 appearance rate.

6.2.A Dependence of CO/CO_2 Rates on Equivalence Ratio and Type of Fuel

The values of $K_{overall-1}$ and $K_{overall-2}$ at 1615°K in Table 6-2 show that for a given fuel, the rate of CO disappearance/CO_2 appearance increases as we go towards the leaner fuel/oxidant mixtures. This result is in agreement with the qualitative expectation that the presence of excess oxidant results in faster and more complete burning of the fuel. The comparison for $K_{overall}$ in Table 6-2 also shows that at a given equivalence ratio, the overall rate coefficient for CO disappearance/ CO_2 appearance is greater for ethane-oxygen flames than the corresponding rate coefficient for ethylene-oxygen flames. This result is in disagreement with the results of Reference 12 where the rate of carbon monoxide disappearance in the post flame zone of hydrocarbons is reported to be independent of the nature of the fule. These two trends (dependence of $K_{overall}$ on equivalence ratio and nature of fuel) may be explained in terms of a postulate made by several experimenters that the primary path for the disappearance of CO is the reaction

$$CO + OH \rightarrow CO_2 + H \qquad \text{(R.1)}$$

$$-\frac{d[CO]}{dt} = \frac{d[CO_2]}{dt} \propto [CO]\,[OH]$$

or

$$\frac{-\frac{d[CO]}{dt}}{[CO]} = \frac{\frac{d[CO_2]}{dt}}{[CO]} \propto [OH]$$

or

$$K_{overall} \propto [OH]$$

This analytical result from the simple postulate is qualitatively supported by the experimental data as discussed below.

The plots of log $K_{overall-1}$ vs. log [OH] and log $K_{overall-2}$ vs. log [OH] for ethylene-oxygen flames at a temperature of 1567 ± 12°K are presented in Figs. 6-16 and 6-17. The slopes vary from 0.94 to 1.12 and thus confirm the proportionality of $K_{overall}$ with respect to OH. This result is also justified by comparing the variation of experimentally measured hydroxyl radical mole fraction with equivalence ratio and nature of fuel. This is done in Figs. 6-18 and 6-19. The average concentration of OH for each set is presented in the last column of Table 6-2. A study of Figs. 6-18 and 6-19 and Table 6-2 shows that for a given position and fuel, the mole fraction of hydroxyl radical increases as we go toward the leaner fuel mixtures - a trend similar to that exhibited by

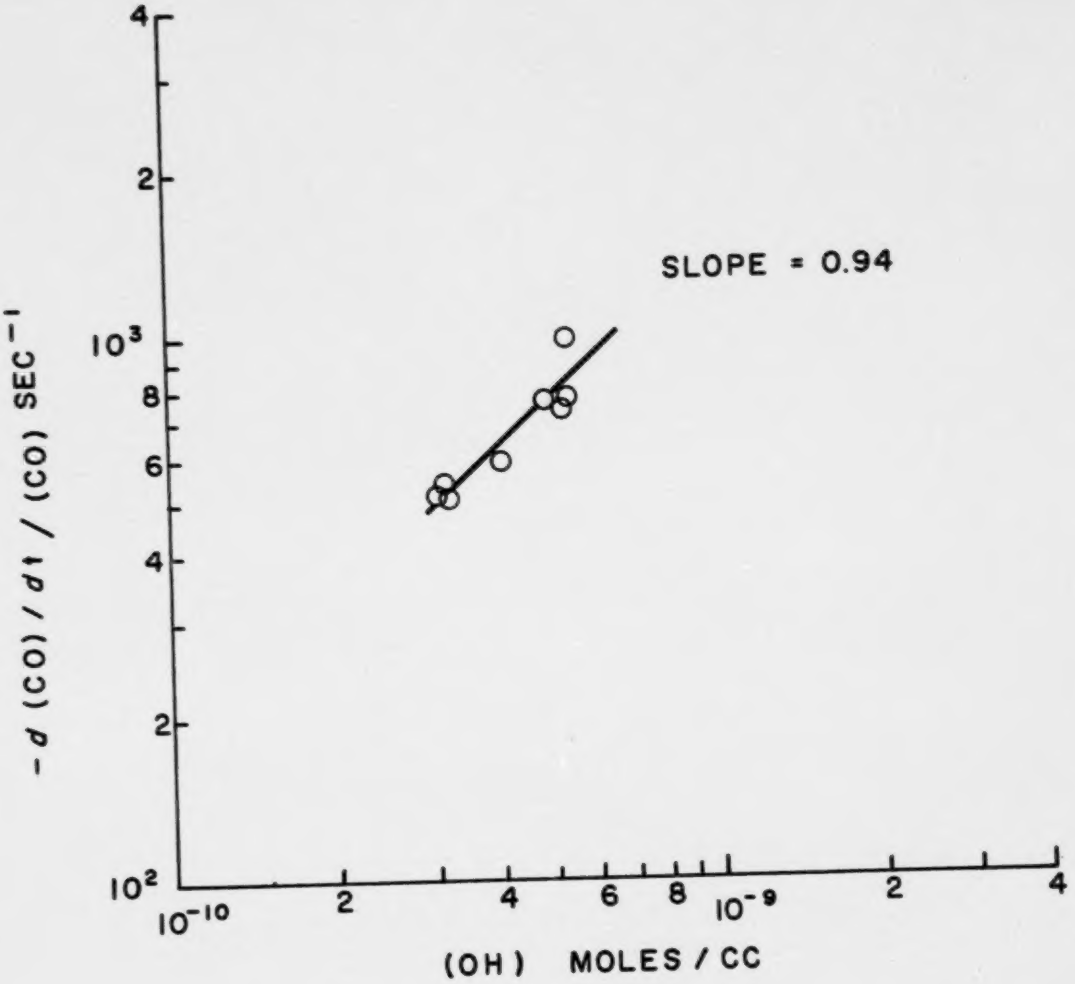

FIG. 6-16. REACTION ORDER DEPENDENCE WITH RESPECT TO HYDROXYL RADICAL FOR CARBON MONOXIDE DISAPPEARANCE, ETHYLENE/OXYGEN FLAMES, T = 1567±12°K

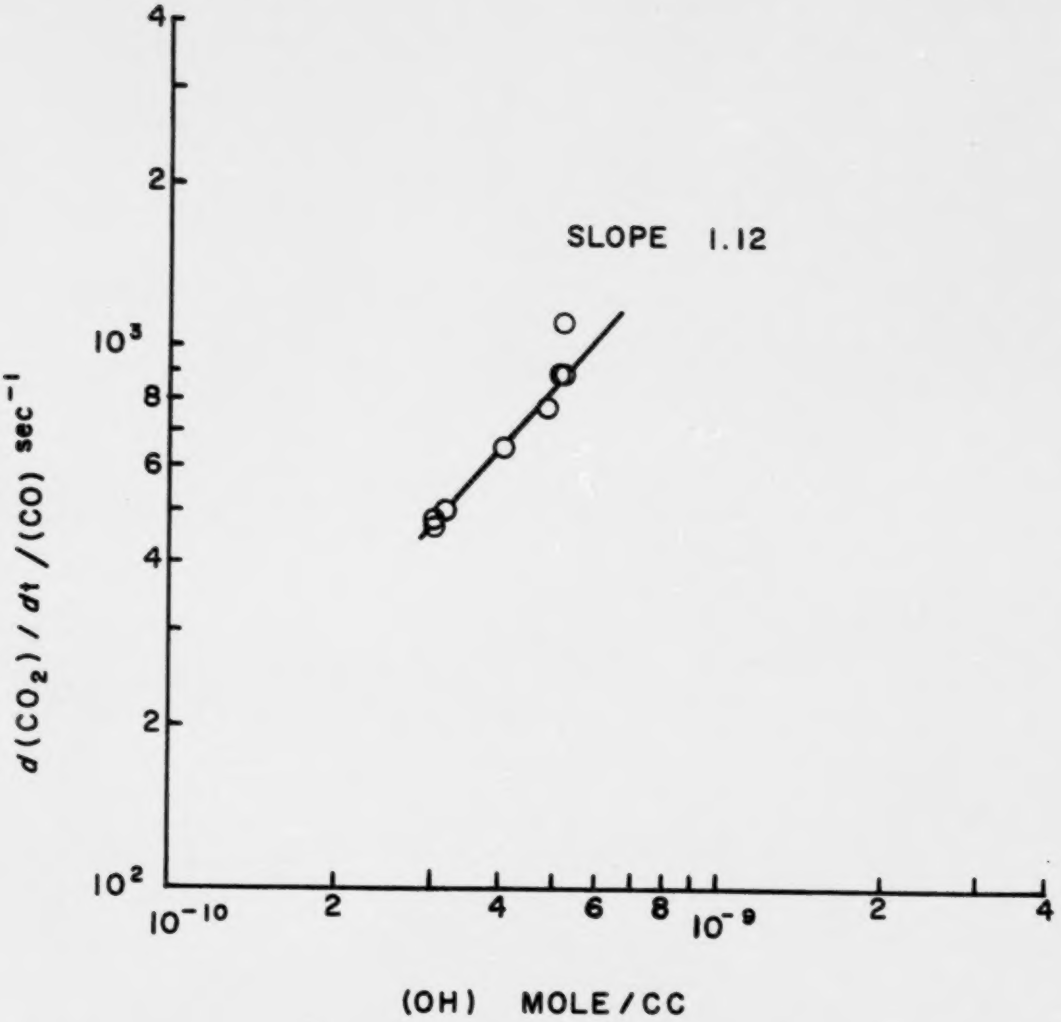

FIG. 6-17. REACTION ORDER DEPENDENCE WITH RESPECT TO HYDROXYL RADICAL FOR CARBON DIOXIDE APPEARANCE RATE, ETHYLENE/OXYGEN FLAMES, T - 1567±12°K

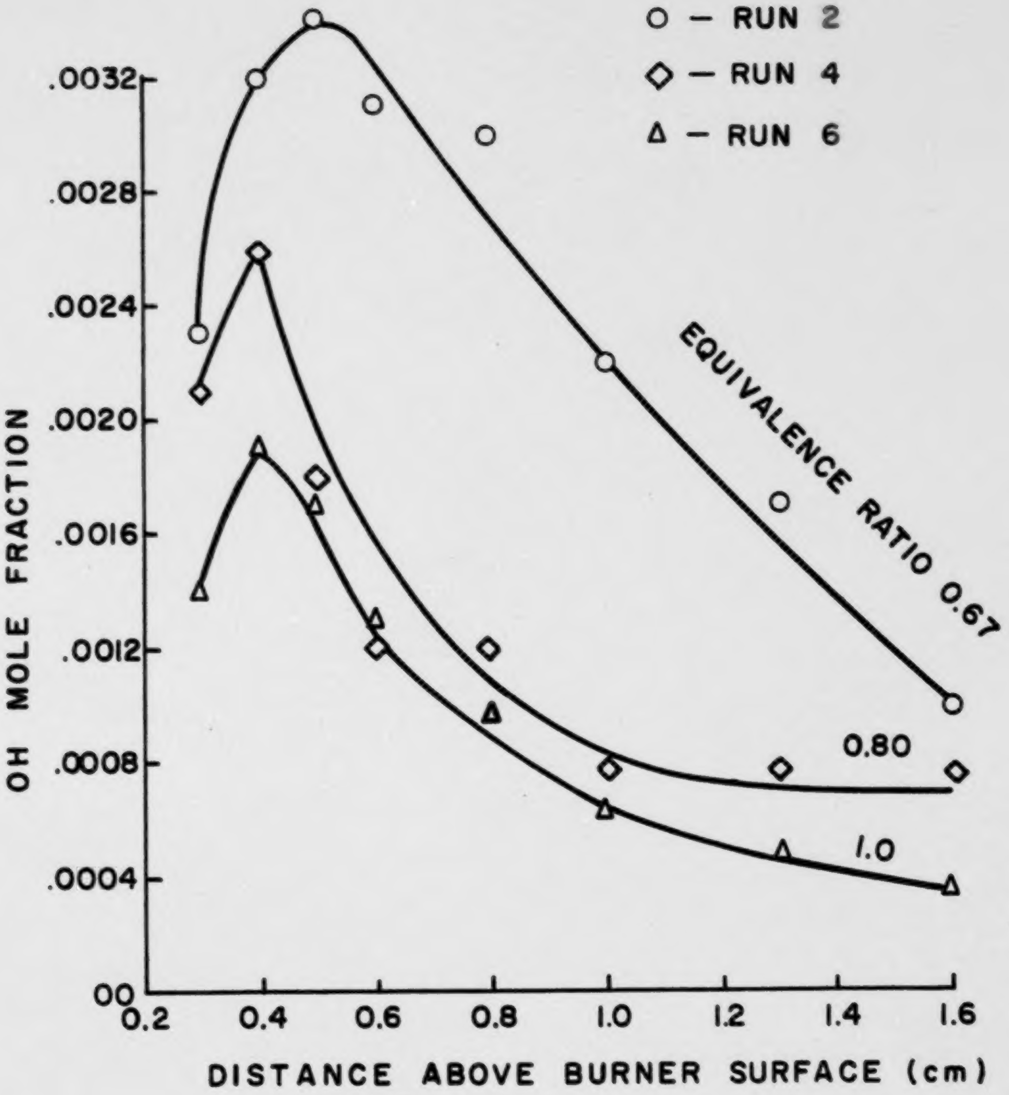

FIG. 6-18. INFLUENCE OF EQUIVALENCE RATIO ON HYDROXYL RADICAL MOLE FRACTION PROFILE, ETHANE/OXYGEN/ARGON FLAMES, P = .083 ATM

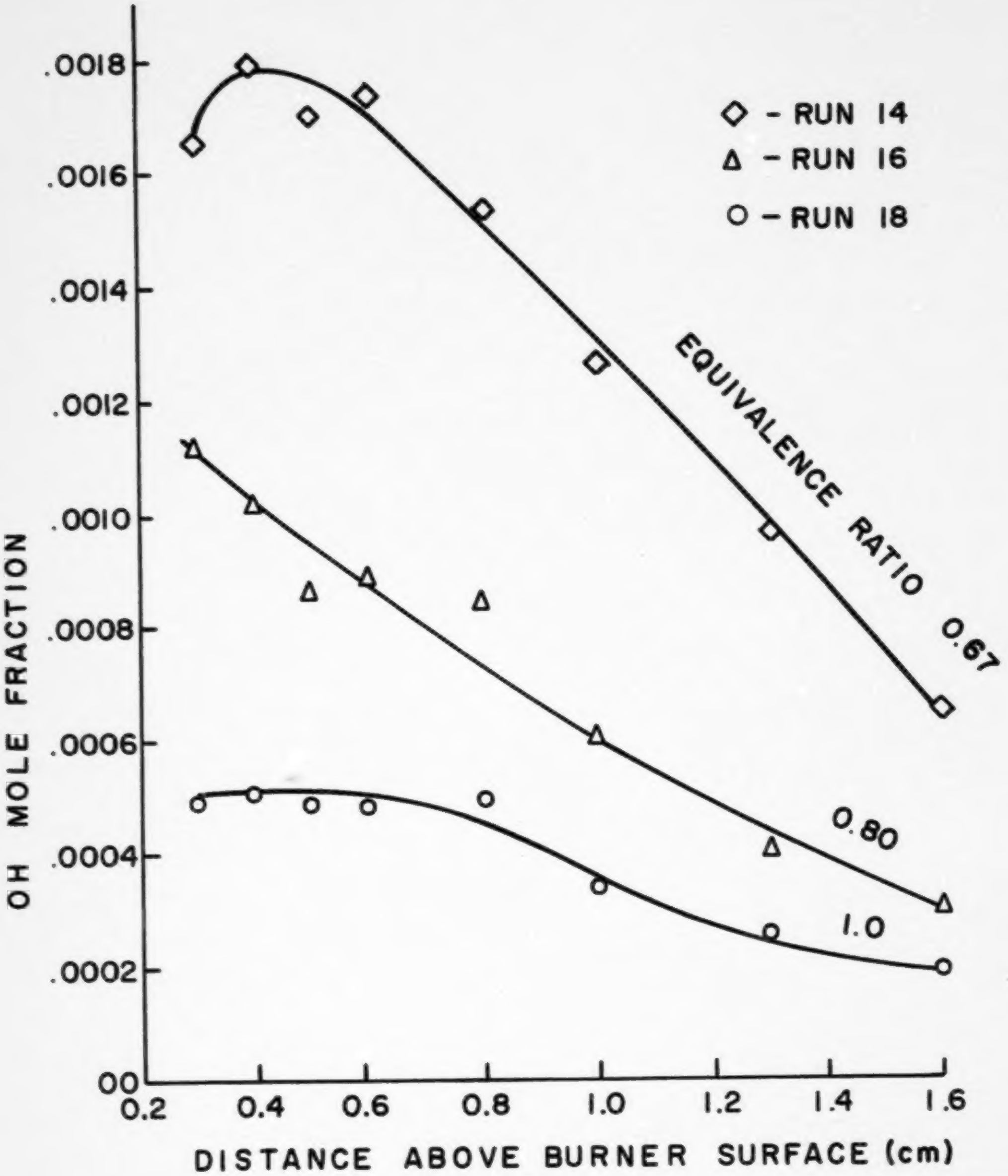

FIG. 6-19. INFLUENCE OF EQUIVALENCE RATIO ON HYDROXYL RADICAL MOLE FRACTION PROFILE ETHYLENE/OXYGEN/ARGON FLAMES, P = .083 ATM

$K_{overall}$. At a given equivalence ratio, the variation of OH concentration with respect to fuel is also similar to that of $K_{overall}$. Hence

$$K_{overall-1} \propto [OH]$$

$$K_{overall-2} \propto [OH] ,$$

which support the theoretical result obtained from the postulate that reaction R.1 is the principal path for the destruction of carbon monoxide. Thus we see that $K_{overall}$ for fuel lean mixtures is greater than that for stoichiometric mixtures. The principal reason for this difference appears to be the relatively high concentrations of hydroxyl radical and low concentration of hydrogen for fuel lean mixtures. This means the reaction R.1 is the principal path not only for the decay of carbon monoxide but also for the consumption of hydroxyl radicals. The other principal reaction ($H_2 + OH = H_2O + H$) competing for OH becomes slow. The resulting higher concentration of OH tends to make $K_{overall}$ ($\simeq k_1 \times [OH]$) higher for fuel lean mixtures.

6.2.B Comparison of Experimentally Measured and Theoretically Calculated Concentration of OH.

In the absence of experimentally measured concentration of radical species, theoretical postulates are used to infer their concentrations. Figures 6-20 and 6-21 compare the experimentally measured mole fraction of hydroxyl radical with those calculated from equilibrium considerations as well as from partial equilibrium assumption of the reactions (as suggested by Reference 16, 19 and 23)

$$H + O_2 = OH + O \qquad R.3$$

$$O + H_2 = OH + H \qquad R.5$$

The partial equilibrium assumption gives

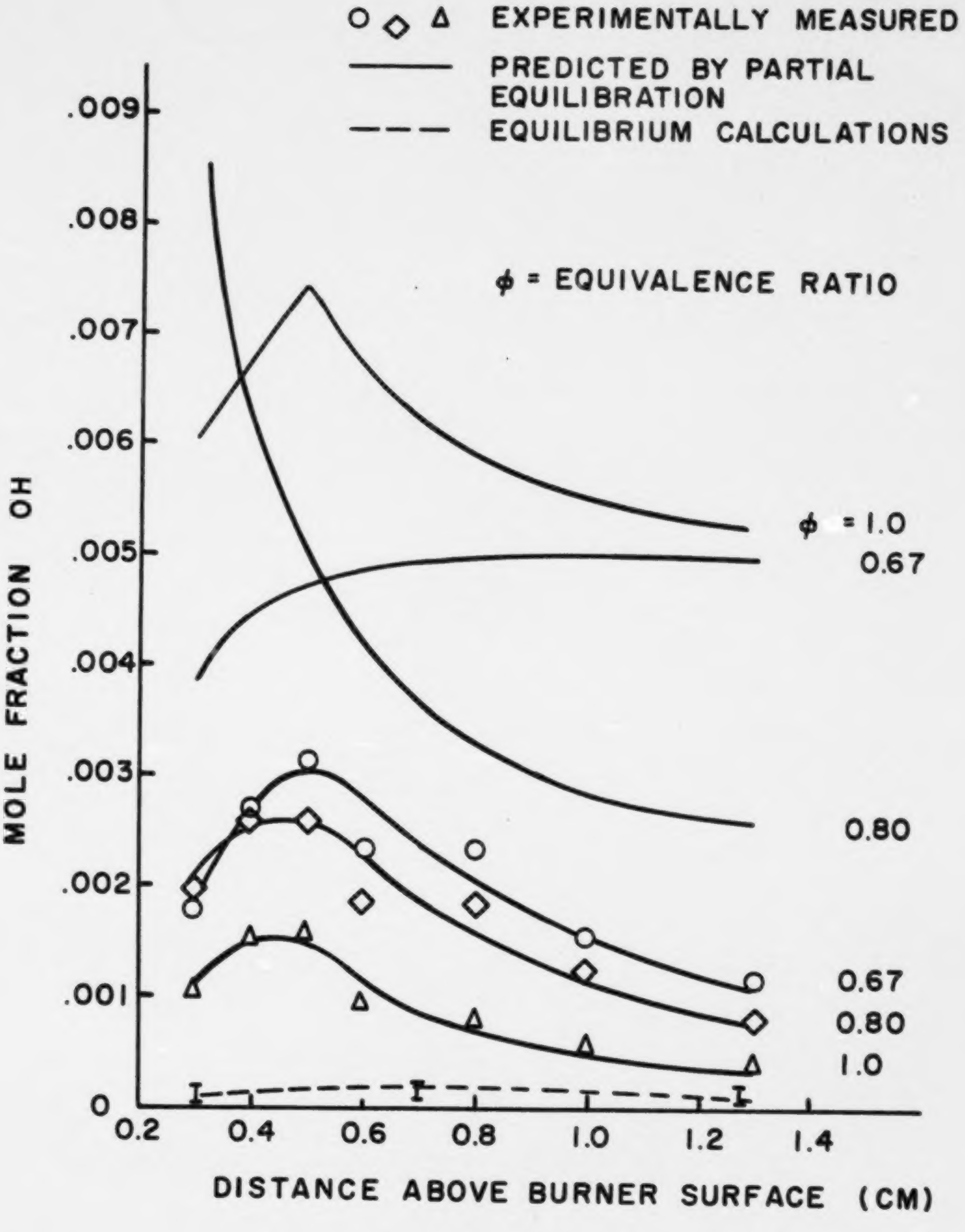

FIG. 6-20. COMPARISON OF EXPERIMENTALLY MEASURED AND THEORETICALLY CALCULATED HYDROXYL RADICAL MOLE FRACTION PROFILE, ETHANE/OXYGEN/ARGON FLAMES, P = .084 ATM

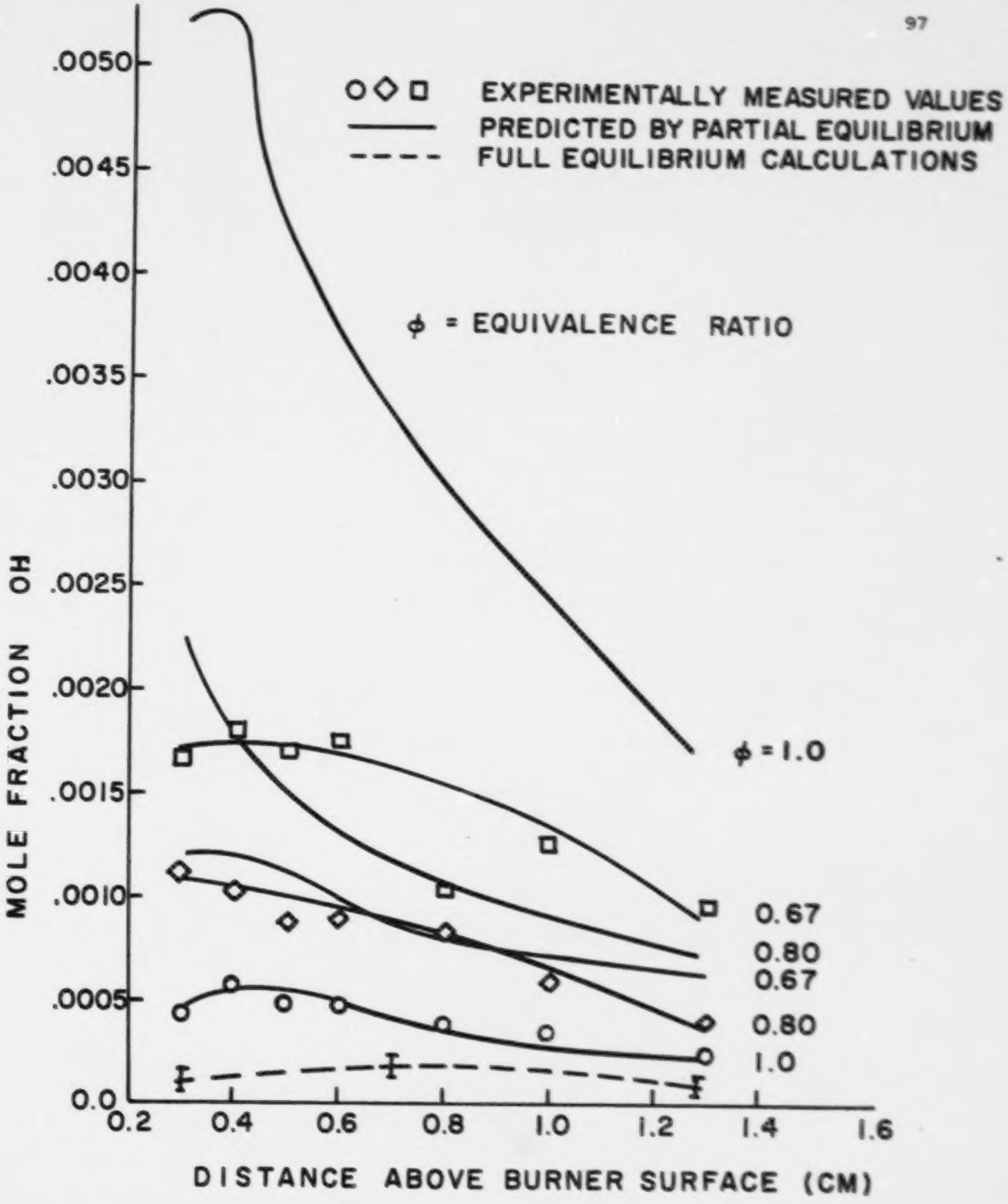

FIG. 6-21. COMPOSITION OF EXPERIMENTALLY MEASURED AND THEORETICALL
CALCULATED HYDROXYL RADICAL MOLE FRACTION PROFILE,
ETHYLENE/OXYGEN/ARGON FLAMES, P = .084 ATM

$$[OH]^2 = K_3\ K_5\ [O_2]\ [H_2] \qquad (6.7)$$

where K_3 and K_5 are the equilibrium constants for the reactions R.3 and R.5. For all cases the experimentally measured mole fraction of OH is greater than that predicted by equilibrium calculations. This is in agreement with the results of other investigators.[4,23] On the other hand, the experimentally measured OH mole fraction is less than that predicted by the partial equilibrium equation (6.7) (except for one case of ethylene/oxygen flame, equivalence ratio = 0.67). As the partial equilibrium value of [OH] is proportional to the measured value of $[H_2]$, one reason for the discrepancy between the experimental and predicted (from the partial equilibrium hypothesis) OH mole fraction may be the uncertainty involved in the measurement of molecular hydrogen concentrations. But this uncertainty alone probably cannot account for the divergence between the experimental values of hydroxyl radical mole fraction and the corresponding values calculated from the partial equilibrium hypothesis. The above discussion points out the difficulties in relying on equilibrium or partial equilibrium hypotheses for estimating hydroxyl radical concentrations.

6.3 Comparison with Other Works

The results of the present study for the overall rates of carbon monoxide disappearance are compared with the results of other investigators reviewed in Chapter 2. The various rate expressions used for comparison are reproduced below:

$$-\frac{d[CO]}{dt} = 231\times[CO]$$ Friedman and Cypher[11] (2.2)

$$-\frac{d[CO]}{dt} = 1.2\times10^{12}\exp^{-24000/RT}[CO][O_2]$$ Fenimore and Jones[12] (2.3)

$$\frac{d[CO_2]}{dt} = 2.9\times10^{10}\exp^{-15000/RT}[CO][O_2]^{.35}[H_2O]^{.4} \quad \text{Hottel } \underline{\text{et}}\ \underline{\text{al}}.^{16} \quad (2.4)$$

$$-\frac{d[CO]}{dt} = 1.8\times10^{13}\exp^{-25000/RT}[CO][O_2]^{.5}[H_2O]^{.5} \quad \text{Williams } \underline{\text{et}}\ \underline{\text{al}}.^{17} \quad (2.5)$$

$$-\frac{d[CO]}{dt} = 4\times10^{13}\exp^{-45000/RT}[CO][H_2O]^{.5}[O_2]^{.25} \quad \text{Fristrom } \underline{\text{et}}\ \underline{\text{al}}.^{18} \quad (2.6)$$

$$-\frac{d[CO]}{dt} = 1.04\times10^{12}\exp^{-32000/RT}\frac{[CO][H_2O]^{.5}[O_2]^{.5}}{T^{2.5}} \quad \text{Kozlov}^{68} \quad (2.7)$$

To facilitate this comparison a dimensionless parameter R_{CO} is defined as:

$$(R_{CO})_i = \frac{\text{Observed rate of CO disappearance (calculated from composition profiles through the use of flame equations)}}{\text{Calculated rate of CO disappearance from the ith equation}}$$

The average value of R_{CO} for each of the six sets is summarized in Table 6-3.

From the above comparison we see that the observed rate of CO disappearance in the present study agree within a factor of 1.07 to 1.75 with those predicted by Hottel *et al.*[16] However, two of the assumptions made by Hottel *et al.*[16] in deriving equation (2.4) cannot be fully justified. Neglecting the reverse of reaction R.1 implies that the concentration of CO is much greater than the corresponding equilibrium concentration of CO, i.e.

$$[CO] >> [CO]_{equil}$$

The concentration of radical species are calculated from the partial equilibrium assumption of reactions R.1 to R.10 of Table 5-4, which is not supported by the experimental measurements for OH in the present study. However, in spite of the above assumptions, these equations lead to results of the right order of magnitude. This makes it very difficult

Table 6-3. Average values of R_{CO} for overall disappearance of CO.

Fuel	Equi-valence Ratio	Friedman &[11] Cypher Flame Studies	Fenimore &[12] Jones Flame Studies	Hottel et[16] al. Stirred Reactor	Williams et[17] al. Stirred Reactor	Fristrom[10] & Westenberg Semi-Theoretical	Kozlov[68] Flow Reactor
C_2H_6	0.67	4.57 ± .989	19.5 ± 4.19	.739±.127 (1.37)*	5.76± 2.27	2.79 ± .57	.0061 (164.0)
C_2H_6	0.8	4.06 ± .44	21.15± 4.43	.624±.086 (1.61)	3.83± .93	2.286± .38	.0045 (212.0)
C_2H_6	1.0	3.13 ± .62	34.78±16.13	.589±.122 (1.70)	2.56± .69	2.29 ± .61	.00364 (275.)
C_2H_4	0.67	4.15 ±1.63	27.94±19.46	.992±.6 (1.01)	13.66±10.47	4.65 ±3.31	.0084 (119.0)
C_2H_4	0.8	2.96 ± .44	34.2 ±10.52	.811±.196 (1.25)	10.3 ± 3.64	4.05 ±1.24	.00745 (134.0)
C_2H_4	1.0	2.347± .35	32.10± .85	.590±.11 (1.725)	4.709± .86	2.72 ± .52	.00423 (232.0)

*The values in parenthesis indicate reciprocal of R_{CO}

to derive any meaningful kinetic conclusions, hence indicating, that care should be used in applying the results of a global rate expression, since these expressions are applicable to only the limited range of experimental conditions at which the expressions were derived.

Thus, considering the limitations of global rate analysis, the large values of R_{CO} (19 to 35) for Fenimore and Junes[12] are not surprising. The expression (2.3) was not supported by their subsequent study.[67]

The agreement within a factor of 2-5 (barring a few points when it is an order of magnitude) with the results of Friedman and Cypher,[11] Fristrom and Westenberg[18] and Williams et al.[17] are considered reasonable. The different values of R_{CO} obtained by using equations (2.4) and (2.5) derived by studying the combustion of propane and methane in a stirred reactor support the result of the present study that the rate of burning of CO in the afterflame zone is affected by the nature of the fuel. No satisfactory explanation can be given for the large disagreement with the results of the flow reactor studies of Kozlov.[68]

Overall, we conclude that the rate of CO disappearance/CO_2 appearance in the present study can be represented by an overall first order rate equation

$$\frac{d[CO_2]}{dt} = K_{overall-1}\,[CO] \tag{6.3}$$

$$-\frac{d[CO]}{dt} = K_{overall-2}\,[CO] \tag{6.4}$$

The values of $K_{overall-1}$ and $K_{overall-2}$ are functions of the equivalence ratio and the nature of the fuel.

6.4 Overall Reaction Rate for Disappearance of Oxygen

The reaction rate dependence of the rate of oxygen disappearance with respect to oxygen and carbon monoxide was considered at various temperatures. The reaction order with respect to oxygen and carbon monoxide varied with temperature. One of the reasons for this variation may be the absence of a single elementary slow reaction which controls the disappearance of oxygen. Therefore, it was not possible to derive a global reaction rate expression for the disappearance of oxygen.

The reaction rates of carbon monoxide, carbon dioxide and oxygen are discussed in terms of detailed kinetics in the next chapter.

CHAPTER 7

DETAILED KINETICS INTERPRETATION

7.1 Outline of Approach

As discussed in Chapter 2, the detailed kinetics approach for the interpretation of flat flame type of data consists of postulating a detailed reaction path for describing the kinetic history of various species. This method has been employed by various workers using different experimental techniques. In most cases a few experimental parameters are obtained and a detailed reaction mechanism is postulated. The observed parameters are then compared with those calculated from the postulated reaction mechanism. A few examples of the typical approach are discussed briefly below.

Seery and Bowman[69,70] measured the induction times for the oxidation of methane behind a reflected shock wave. Using a high temperature 17-step oxidation mechanism for methane, established by the flame work of Fristrom et al.[18] and Fenimore,[71] Seery and Bowman[69] compared the calculated induction times to those observed experimentally. By carrying out a parametric study for the values of rate constants for different reactions Seery and Bowman[69] eliminated 5 reactions (as the variation in the rate coefficients of these 5 reactions by several orders of magnitudes did not affect the induction time) and postulated an additional reaction from the low temperature methane oxidation studies of Enikolopyan.[69] The resulting 13-step mechanism gave good agreement between the observed and calculated values of the induction times.

Browne et al.[42] used optical inferometry to measure the density field behind a normal shock wave in H_2/O_2, $H_2/N_2/O_2$ and $H_2/CO/O_2$ mixtures diluted with argon. Density profiles based on various sets of kinetics were generated with the aid of a one dimensional reactive flow analysis. A set of kinetic coefficients was obtained which gave good agreement between the analytical and experimental profiles. A similar approach has been used by several other workers[18,72,73] using a shock tube.

Baldwin et al.[36,74,75] have studied a variety of $C_xH_y/O_2/N_2$ mixtures reacting in aged boric acid coated vessels at temperatures between 500 and 550°C. The resulting mixture of reactants and products were analyzed after varying intervals of time. The corresponding changes in pressure were also recorded. Detailed reaction mechanisms were postulated. The use of radical species concentration was avoided in the calculation of time-rate-of-change of the observed species concentrations by calculating the relative rates of two reactions, e.g. $k_1[CO][OH]/k_2[CH_4][OH]$, and by comparing this combination with the experimentally observed relative rates. In other cases, a steady state assumption was made for the intermediate unstable species. A similar approach has been taken by Blundell et al.[39] for studying the rates of radical reactions in methane oxidation.

Jenkins et al.[76] have used an adiabatic stirred reactor to study the combustion mechanism of hydrogen/oxygen mixtures containing steam as a diluent in the temperature range of 1330-1560°K. The measured flame temperatures under different operating conditions have been compared to those calculated from an assumed mechanism. Values of five reaction rate constants reported in the literature were modified until quantitative agreement was obtained between the calculated and observed temperature. This procedure has two obvious limitations; first, the reaction scheme postulated may or may not be a comprehensive one, and second, the variations considered may or may not be the only adjustments to the rate constants which will give the same measure of agreement between observed and predicted temperatures.

Browne _et_ _al_.[30] obtained profiles of concentration of stable species, the concentrations of the unstable species C_2, CH and OH and temperature by probing premixed flames of $C_2H_2/O_2/N_2/Ar$ supported on a porous plate flat burner at subatmospheric pressure. A detailed reaction mechanism was postulated. The system of kinetic, state and flame equations were then numerically integrated to analytically predict the concentration profiles. For fuel rich flames, good agreement was obtained between the predicted and observed composition profiles in the luminous zone but the agreement was not good for fuel lean flames in the same region. This is one of the few studies where an attempt has been made to obtain agreement between the detailed structure of a flame obtained both theoretically and experimentally.

In the present study two approaches have been taken for interpreting the results in terms of detailed kinetics. The first approach consists of postulating a reaction mechanism. The kinetic (theoretical) reaction rates are calculated from the postulated reaction mechanism and are compared with those computed from the experimentally observed concentration and temperature profile using flame equations as outlined in Chapter 4 (referred to as observed rates in the latter part of the discussion). The second approach consists of calculating the flame structure (composition profiles) by numerical integration of the diffusion equations and kinetic equations resulting from the postulated mechanism. The predicted mole fraction profiles are compared with those measured experimentally. This approach is discussed in section 7.5. The first approach is discussed below.

7.2 Calculation of Kinetic Reaction Rates

From the literature review[18,30,39,42] of Chapter 2, a reaction mechanism for $CO/O_2/H_2$ system at high temperature (1000-1500°K) was selected as follows:

$CO + OH \xrightarrow{k_1} CO_2 + H$ (R.1)

$CO_2 + H \xrightarrow{k_2} CO + OH$ (R.2)

Primary path for CO disappearance.

$H + O_2 \xrightarrow{k_3} OH + O$ (R.3)

$O + OH \xrightarrow{k_4} H + O_2$ (R.4)

$O + H_2 \xrightarrow{k_5} OH + H$ (R.5)

$OH + H \xrightarrow{k_6} O + H_2$ (R.6)

$H_2 + OH \xrightarrow{k_7} H_2O + H$ (R.7)

$H_2O + H \xrightarrow{k_8} H_2 + OH$ (R.8)

$OH + OH \xrightarrow{k_9} H_2O + O$ (R.9)

$H_2O + O \xrightarrow{k_{10}} OH + OH$ (R.10)

Chain propagating and chain branching reactions for intermediate radical species, H, OH and O.

$O + O + M \xrightarrow{k_{11}} O_2 + M$ (R.11)

$H + H + M \xrightarrow{k_{12}} H_2 + M$ (R.12)

$H + OH + M \xrightarrow{k_{13}} H_2O + M$ (R.13)

$O + H + M \xrightarrow{k_{14}} OH + M$ (R.14)

$CO + O + M \xrightarrow{k_{15}} CO_2 + M$ (R.15)

Termolecular recombination reaction.

By making use of reactions R.1 to R.15 the reaction rate for the different species are given below:

$$\frac{d[CO]}{dt} = - k_1[CO][OH] + k_2[CO_2][H] - k_{15}[CO][O][M]$$

$$\begin{aligned}\frac{d[OH]}{dt} = & - k_1[CO][OH] + k_2[CO_2][H] + k_3[H][O_2] - k_4[O][OH] + k_5[O][H_2] \\ & - k_6[H][OH] - k_7[H_2][OH] + k_8[H_2O][H] - k_9[OH][OH] + k_{10}[H_2O][O] \\ & - k_{13}[H][OH][M] + k_{14}[O][H][M]\end{aligned}$$

$$\frac{d[CO_2]}{dt} = k_1[CO][OH] - k_2[CO_2][H] + k_{15}[CO][O][M]$$

$$\frac{d[O_2]}{dt} = - k_3[H][O_2] + k_4[O][OH] + k_{11}[O][O][M]$$

$$\frac{d[H_2]}{dt} = - k_5[O][H_2] + k_6[H][OH] - k_7[H_2][OH] + k_8[H][H_2O] + k_{12}[H][H][M]$$

$$\frac{d[H_2O]}{dt} = k_7[H_2][OH] - k_8[H][H_2O] + k_9[OH][OH] - k_{10}[H_2O][O] + k_{13}[H][OH][M]$$

In order to calculate the reaction rates from the above equations we need to know the concentration of atomic oxygen and atomic hydrogen. These concentrations have not been measured experimentally in the present work. Three approaches have been used in the literature to estimate the concentration of O and H.

As mentioned earlier, Kaskan[23,26] and Bulewizc et al.[19] have suggested that chain branching and chain propagating reactions R.3 to R.10 are fast and are partially equilibrated (i.e. maintain equilibrium between themselves). Based on this assumption, the concentrations of O and H are given by the following expressions

$$[H] = \frac{k_7 k_4 k_6}{k_8 k_3 k_5} \frac{[OH]^3}{[H_2O][O_2]} = \frac{K_7}{K_3 K_5} \frac{[OH]^3}{[H_2O][O_2]} \qquad (7.1)$$

$$[O] = \frac{k_9}{k_{10}} \frac{[OH]^2}{[H_2O]} = K_9 \frac{[OH]^2}{[H_2O]} \tag{7.2}$$

where K_3, K_5, K_7 and K_9 are the equilibrium constants for the reactions R.3, R.5, R.7 and R.9.

Fenimore and Jones[71] have suggested that in hydrocarbon/oxygen flames, O_2 primarily disappears through the reaction R.3. Their suggestiong has been partially supported by more recent works of Browne _et al._[39,42] and Bowman _et_ _al._[69,70] By neglecting the reverse of reaction R.3, the concentration of H is given by

$$[H] = \frac{-\frac{d[O_2]}{dt}}{k_3[O_2]} \tag{7.3}$$

The third approach for the estimation of concentration of H and O is the steady state approximation. This leads to the following equation for the concentration of O and H.

$$[O] = \frac{k_3[H][H_2] + k_6[H][OH] + k_9[OH]^2}{k_4[OH] + k_5[H_2] + k_{10}[H_2O] + k_{15}[CO][M]} \tag{7.4}$$

$$[H] = \frac{k_1[CO][OH] + k_4[H_2][OH] + k_7[H_2][OH] + k_5[O][H_2]}{k_2[CO_2] + k_3[O_2] + k_8[H_2O] + k_6[OH] + k_{13}[O][M] + k_{14}[OH][M]} \tag{7.5}$$

Calculations were carried out for the reaction rates of various species by using reaction scheme R.1 to R.15 and the following equations for the concentrations of H and O atoms.

$\left.\begin{matrix}7.4\\7.5\end{matrix}\right\}$ Scheme A

$\left.\begin{matrix}7.1\\7.2\end{matrix}\right\}$ Scheme B

$\left.\begin{matrix}7.2\\7.3\end{matrix}\right\}$ Scheme C

The values of the rate coefficients for various reactions used in the present study have been obtained from an extensive literature review.[121] A summary of this review is presented in Table 7-1. To facilitate the comparison, a dimensionless parameter R_i is again used which is defined as follows:

$$(R)_i = \frac{\text{observed reaction rate for ith species}}{\text{calculated kinetic rate for ith species}}$$

7.3 Comparison for Carbon Monoxide and Carbon Dioxide Reaction Rates

The average values of the dimensionless parameters R_{CO} and R_{CO_2} for the six sets of data are tabulated in Tables 7-2 and 7-3. The values in column D of Tables 7-2 and 7-3 were obtained by neglecting the reverse of reaction R.1. The values of R_{CO} varies from 1.12 to 3.84 with an overall average of 2.63 by using four different schemes for the calculations of kinetic rates of carbon monoxide. This deviation between the kinetic rates and those reduced from the flame equations can be attributed to the following factors:

a) Overall uncertainty of the experiment including data reduction.

b) Alternative path for the disappearance of carbon monoxide.

c) Uncertainty in the value of rate constant for the reaction $CO + OH = CO_2 + H$.

From the error analysis in Appendix 2, the overall experimental uncertainty lies between 20 to 30 percent. This cannot account for the observed disagreement between kinetic and observed rates of carbon monoxide disappearance.

The second factor concerning the alternative path was considered. The comparison of the values of R_{CO} for scheme D as compared to those obtained by using calculation schemes A, B and C show that the backward

Table 7-1. Main reactions for $H_2/CO/O_2$ system $k = AT^b exp^{-E/RT}$, Reference 121.

Reaction	Coefficients A	b	E calories/ mole
$CO + OH \rightarrow CO_2 + H$	5.6×10^{11}	0	1,080
$CO_2 + H \rightarrow CO + OH$	5.6×10^{13}	0	23,500
$H + O_2 \rightarrow OH + O$	2.94×10^{14}	0	16,300
$OH + O \rightarrow O_2 + H$	1.3×10^{13}	0	0
$H_2 + OH \rightarrow H_2O + H$	1.29×10^{13}	0	4,600
$H + H_2O \rightarrow H_2 + OH$	8.41×10^{13}	0	20,100
$O + H_2 \rightarrow OH + H$	1.74×10^{13}	0	9,450
$OH + H \rightarrow O + H_2$	7.33×10^{12}	0	7,300
$OH + OH \rightarrow H_2O + O$	5.75×10^{12}	0	780
$H_2O + O \rightarrow OH + OH$	5.75×10^{13}	0	18,000
$H + H + M \rightarrow H_2 + M$	1.0×10^{18}	-1.0	0
$O + O + M \rightarrow O_2 + M$	1.25×10^{18}	-0.9	0
$O + H + M \rightarrow OH + M$	3×10^{14}	0	0
$H + OH + M \rightarrow H_2O + M$	1.17×10^{17}*	0	0
$CO + O + M \rightarrow CO_2 + M$	6.0×10^{13}	0	0

*at 2040°K with $M = H_2O$

units $k = cm^{(n-1)\times 3} - mole^{(1-n)} - sec^{-1}$

n = molecularity of reaction

Table 7-2. Summary of R_{CO} for postulated mechanism.

Fuel	Equivalence ratio	A [H] from steady state hypothesis	B [H] from partial equilibrium hypothesis	C [H] from $-\frac{d[O_2]}{dt}$	D Reversed (CO+OH) neglected
C_2H_4	0.67	2.11±1.04	1.98±0.78	2.12±0.94	2.01±0.81
	0.8	3.47±1.15	3.25±1.13	3.70±1.15	3.25±1.17
	1.0	3.36±1.99	3.08±1.89	3.64±2.24	3.08±1.00
C_2H_6	0.67	1.42±0.65	1.12±0.46	1.33±0.58	1.15±0.47
	0.8	2.42±0.31	2.37±0.87	2.57±0.86	2.54±0.91
	1.0	3.66±1.69	3.21±1.91	3.84±1.71	3.19±1.76
Overall Average		2.55	2.51	2.86	2.67

Table 7-3. Summary of R_{CO_2} for postulated mechanism

Fuel	Equivalence ratio	A [H] from steady state hypothesis	B [H] from partial equilibrium hypothesis	C [H] from $-\frac{d[O_2]}{dt}$	D Reversed (CO+OH) neglected
C_2H_4	0.67	2.48±1.08	2.33±1.15	2.67±0.97	2.32±1.08
	0.8	3.63±1.34	3.40±1.23	3.85±1.38	3.38±1.19
	1.0	3.51±1.82	3.23±1.71	3.79±1.52	3.21±1.70
C_2H_6	0.67	1.73±0.85	1.59±0.80	1.92±1.07	1.59±0.80
	0.8	2.37±1.01	2.38±0.69	2.66±0.71	2.57±0.69
	1.0	3.75±1.72	3.51±0.87	3.57±1.52	3.50±0.86
Overall Average		2.91	2.74	3.07	2.72

$$R_{CO} = \frac{\text{OBSERVED RATE OF CO DISAPPEARANCE}}{\text{CALCULATED CO RATE FROM (CO+OH) REACTION}}$$

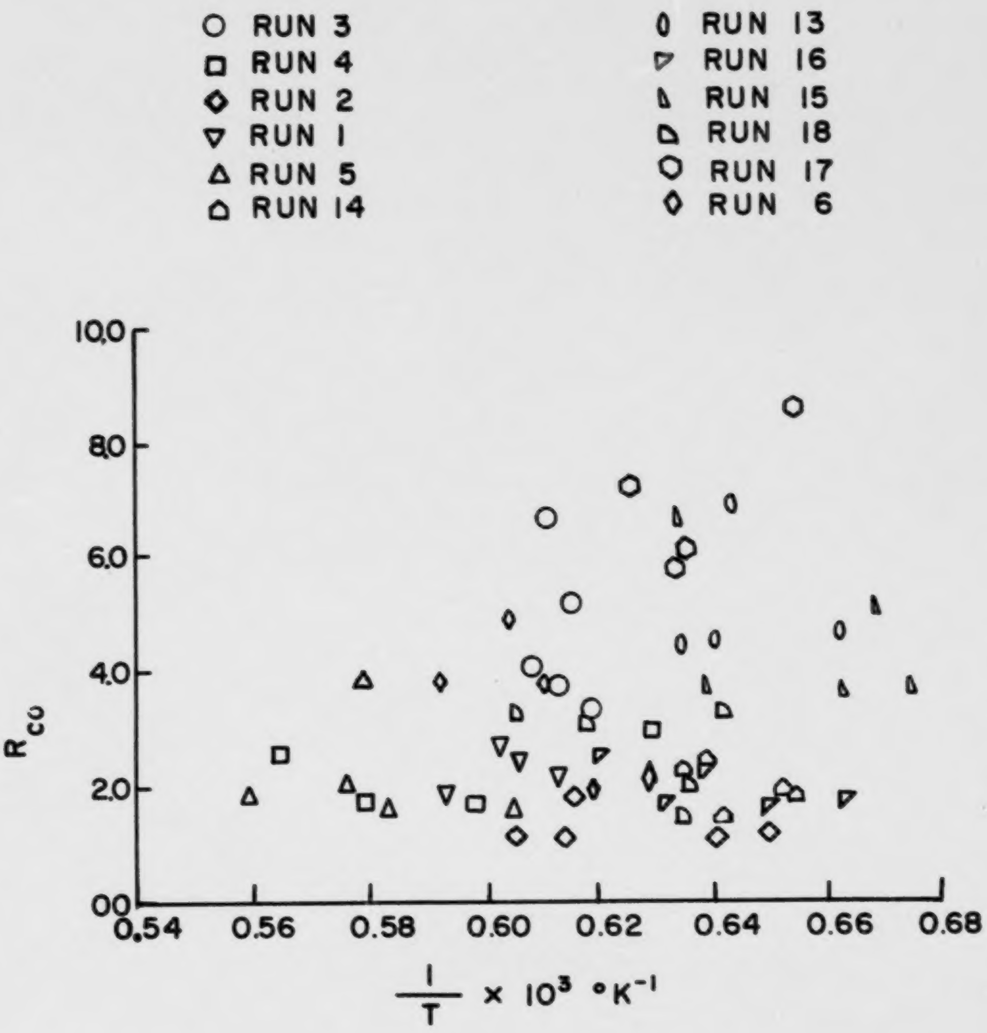

FIG. 7-1. VARIATION OF DIMENSIONLESS PARAMETER R_{CO} vs. RECIPROCAL OF TEMPERATURE

reaction $CO_2 + H = CO + OH$ is not important in the regime of present study.

The concentration of atomic H varies by one to three orders of magnitude in schemes A, B and C of the calculations. But this does not affect the values of R_{CO} by more than 10 to 15 percent. This may be an additional indication that the reverse of reaction R.1 is not significant in the regime under consideration.

From the study of oxidation of methane at 800°K in the static reaction vessel[39] and shock tube studies of $H_2/O_2/CO$ mixtures,[42] the following reaction has been suggested as an additional path for the disappearance of CO

$$H + O_2 + M = HO_2 + M \qquad (R.16)$$

$$HO_2 + CO = CO_2 + OH \qquad (R.17)$$

Calculations for the kinetic reaction rates and R_{CO} were made by including the reactions R.16 and R.17 in the reaction mechanism and by using a steady state approximation for calculating the concentration of H, O and HO_2. This did not affect the value of R_{CO} by more than three to five percent. Thus, these reactions do not seem to play a significant role in the disappearance of CO. One reason for this may be that HO_2 is very unstable at high temperature and consequently its concentration at the flame temperature is expected to be very low.

In the absence of experimentally measuring the mole fraction of atomic oxygen, it is not possible to determine the exact contribution of reaction R.15 to the disappearance of CO. The exclusion of reaction R.15 from one set of calculations did not change the value of R_{CO} by more than five percent. This indicates that the reaction $CO + O + M \rightarrow CO_2 + M$

is not significant in the kinetics of CO disappearance. This is in agreement with other works[16,25,26,7] where it was concluded that the reaction R.15 is important in the burning of CO only in the absence of water.

In the absence of a measured profile for other species, it is not considered justified to consider other alternative paths. Thus, at present, the disagreement between observed rate of carbon monoxide disappearance and those calculated from the reaction scheme may be attributed primarily to the uncertainty in the value of rate constant for reaction R.1. The literature recommended value[46]

$$k_{CO+OH} = (5.6 \pm .8) \times 10^{11} \exp^{-(1080\pm500/RT)} \ cm^3\text{-}mole^{-1}\text{-}sec^{-1}$$

has to be increased by an average factor of 2.63 to match the observed data in the present study.

R_{CO_2} exhibits a similar behavior to that of R_{CO} except that the value of R_{CO_2} is greater than that of R_{CO} at most of the data points. The possible reasons for this difference have already been discussed in section 6.2.

7.4 Reaction Rate Comparison for Oxygen, Water and Other Species

The average values of R_{O_2} calculated according to schemes A, B and C are listed in Table 7-4. From this table we see that for scheme B, the value of R_{O_2} varies from -114 to 38. The negative values indicate lack of even qualitative agreement. This indicates that the estimates of atomic hydrogen obtained from the partial equilibrium hypothesis is too low to account for the disappearance of O_2 through the reaction R.3

$$H + O_2 \xrightarrow{k_3} OH + O$$

Table 7-4. Summary of R_{O_2} for postulated mechanism.

Fuel	Equivalence ratio	A [H] and [O] from steady state hypothesis	B [H] and [O] from partial equilibrium	C [H] from $-\frac{d[O_2]}{dt}$ and [O] from partial equilibrium
C_2H_4	0.67	1.92±0.69	38.08±17.4	2.26±1.23
	0.80	1.63±0.85	77.12±36.6	1.65±0.15
	1.0	1.85±0.97	-114.20± 9.4	1.47±0.14
C_2H_6	0.67	1.78±1.02	-93.90±14.3	1.50±0.37
	0.80	0.91±0.21	-79.26±89.1	0.96±0.21
	1.0	0.76±0.38	-29.50±11.2	1.05±0.24

The value of rate constant k_4 for the reverse of reaction R.3 is greater than that of k_3 by an order of magnitude at most of the points. The lower estimates of atomic hydrogen concentrations lead to small positive values for the kinetic rates of molecular oxygen. The experimentally observed oxygen concentration profiles indicate a negative reaction rate. Thus, this leads to large negative values of R_{O_2}. This once again points out the difficulty of relying on the partial equilibration hypothesis for the concentration of radical species.

Scheme C gives values of R_{O_2} varying from 0.96 to 2.26. This is to be expected as the values of atomic hydrogen are estimated from the observed rate of disappearance of oxygen which is assumed to take place through the forward part of reaction R.3. The hypothesis of steady state gives values of R_{O_2} varying from 0.76 to 1.92, which may be considered a reasonable agreement between the observed rates and calculated rates for the disappearance of oxygen. Thus, the steady state hypothesis for estimates of radical species appears to be good for matching the observed rates of oxygen disappearance.

The values of R_{H_2O}, R_{H_2} and R_{OH} were also calculated according to the three schemes of calculation stated above. The value of R_{H_2O} varies from 0.107 to 2.35 if the partial equilibrium hypothesis is used for estimates of [H] and [O]. The steady state hypothesis leads to values of R_{H_2O} varying from -0.195 to 2.70. Negative values occur at the initial one or two data points for a few runs. If we exclude these points, the values of R_{H_2O} have a range of 0.197 to 2.7 (i.e. the agreement between the observed rates and calculated kinetic rates of water is within a factor of 5 using scheme A for estimates of atomic hydrogen and oxygen concentrations).

The values of R_{H_2} and R_{OH} vary by one to three orders of magnitude in all the three calculation schemes, A, B, and C. The primary reason for the large discrepancy between the observed reaction rates and those calculated for kinetic equations for hydrogen and hydroxyl radical is the higher uncertainty involved in the calculation of mass flux fraction profile of these species. This has been discussed earlier in Chapter 6.

Thus we see that reaction scheme R.1 to R.15 gives qualitative agreement for the observed reaction rates of CO, CO_2, O_2 and H_2O for more than 90 percent of the data points in the afterflame zone of ethane/oxygen and Ethylene/oxygen flames. The quantitative agreement is within a factor of 5 depending upon the hypothesis used for estimating the concentration of atomic oxygen and atomic hydrogen. In the absence of measured profiles for radical species such as atomic hydrogen, atomic oxygen and formaldehyde which may be present in the immediate vicinity of luminous zone and lack of reliable diffusion data, particularly for radical species, it is not considered justified to derive new values of the kinetic rate constants for the various reactions to match the observed rates in the present study. The numerous unknowns may result in more than one set of the values of kinetic rate coefficients which would account for the observed rate data. The alternative approach for interpreting the results in terms of detailed kinetics is discussed in the next section.

7.5 Theoretical Flame Structure

As mentioned in section 7.1, the alternative approach involves numerical integration of flame equations to predict the concentration profiles of various species. The predicted values of the concentrations are compared with those measured experimentally. To facilitate the integration, the flame equation of Chapter 4 is used in the following form:

Species Conservation Equation

$$\frac{dG_i}{dz} = R_i \frac{M_i}{\dot{m}} \qquad (4.6)$$

Diffusion Equation

Following Hirshfelder et al.,[81] the diffusion equation (4.4) may also be rearranged to express the derivatives of mole fractions in terms of mass flux fraction, mole fraction and binary diffusion coefficients

$$\frac{dx_i}{dz} = \frac{\dot{m}}{N} \sum \frac{x_i M_i G_j - x_j M_j G_i}{M_i M_j \ D_{ij}} \qquad (7.6)$$

Using ideal gas equation of state, (7.6) becomes

$$\frac{dx_i}{dz} = \frac{\dot{m}RT}{P} \sum \frac{x_i M_i G_j - x_j M_j G_i}{M_i M_j \ D_{ij}} \qquad (7.7)$$

Equation (4.6) is related to the stoichiometry of the reactions through the following expression

$$R_j = \sum_{r=1}^{r=R_R} (\nu''_{jr} - \nu_{jr}) \ k_r \ \left(\frac{P}{RT}\right)^{n_r} \ \pi_{i=1}^{i=N_S} \ (x_i)^{\nu'_{ir}} \qquad (7.8)$$

where R_j = reaction rate of jth species

ν'_{jr}, ν''_{jr} = forward and backward stoichiometric coefficients for jth species in the rth reaction

k_r = rate coefficient for rth reaction

$n_r = \sum_{i=1}^{N_S} \nu'_{ir}$

R_R = total number of reactions

N_S = total number of species including third bodies

Combining the equations (4.6) and (7.8)

$$\frac{dG_i}{dz} = \frac{M_i}{\dot{m}} \sum_{r=1}^{r=R_R} (\nu''_{ir} - \nu'_{ir})\; k_r \left(\frac{P}{RT}\right)^{n_r} \prod_{j=1}^{j=N_S} (x_j)^{\nu'_{ir}} \qquad (7.9)$$

The necessity of using the energy equation has been obviated by making use of experimentally measured temperature profile. Equations (7.9) and (7.7) are suitable for numerical integration. For each species appearing in the postulated mechanism, the two nonlinear differential equations, (7.7) and (7.9) have to be solved simultaneously to predict the composition profile.

Numerical Integration Techniques

In choosing a numerical method to integrate the system of equations, consideration must be given to accuracy, stability and machine time. The numerical techniques available for the solution of the set of chemical kinetic equations fall into two main classes:

(1) Explicit Method

The main characteristic of an explicit method of numerical integration is that the value of a dependent variable at a forward step is only a function of the values of the dependent variables at the previous step. Representative of this method of solution is the widely used Runge-Kutta method (R.K. Method). The step size for the R.K. Method must be of the order of the local time constants to insure a stable solution. The R.K. Method requires only one previous point for continuing the solution and thus is self-starting.

(2) Implicit Method

An implicit method differs from an explicit method in that the value of a dependent variable at the forward point depends not only on the values of variables at the previous point but also on the values of the variables at the forward step under consideration. One of the essential steps in this method is that the dependent variables are expanded about the forward point. The derivatives are linearized and the resulting equations are solved with an implicit scheme. The implicit methods are not self starting as compared to the explicit method and hence another method such as Runge Kutta method is required to start the solution. One of the representative schemes of this method is the predictor corrector method. In References 116 to 118, the numerical techniques of integration are discussed. No one particular method is best suited for the solution of all types of problems. The stability of the integration method, accuracy and machine time are the main considerations in choosing a particular method.

In the present study, both the Runge Kutta method[119] and predictor corrector method[116] were tried initially. The Runge Kutta method was found to take more computing time as compared to the predictor-corrector method for a given step size and accuracy. For subsequent runs, the predictor corrector method was used. The computer subroutine is presented in Appendix 3.

Nine species appear in the reaction scheme R.1 to R.15 postulated in section 7.2. Accordingly, eighteen first order nonlinear differential equations have to be solved simultaneously to predict the composition profiles. The initial value of the mole fraction and mass flux fraction of all the nine species are required to start the integration. The concentrations of atomic oxygen and atomic hydrogen were not measured in the present study. The steady state hypothesis was used for estimating the initial concentration of atomic oxygen and atomic hydrogen. The initial slopes for H and O were taken to be zero as implied by the steady state hypothesis. The measured values of mole fraction x_i, the corresponding slopes dx_i/dz, temperature T and diffusion coefficient D_{ij} were used to calculate the value of the initial mass flux fraction, G_i, from equation (7.9). The integration is started 0.4 cm above the burner surface (where most of the hydrocarbon fuel has disappeared) and stopped at 0.8 cm above the burner surface (where the reaction rate of most of the species approach a very small value). The value of rate coefficients for the various reaction rates were obtained from Reference 121.

The initial results of numerical integration using reactions R.1 to R.15 exhibited the following trends:

The mole fraction of water was decreasing and that of OH was increasing at a rapid rate with respect to distance above the burner surface (z) as shown by curve C of Fig. 7-2 and curve D of Fig. 7-3. The experimentally measured mole fraction of water increased very slowly with z while the mole fraction of hydroxyl radical first increased and then decreased with z. One of the probably reasons for this behavior was found to be the high uncertainty for the rate coefficient of the reaction

$$OH + OH = H_2O + O \qquad (R.9)$$

The available rate data for this reaction have been obtained in the low temperature range of 300-400°K. The contribution of the reaction R.9 to the kinetic rate of production (R_{H_2O}) of water is quite high. This increases the slope of the H_2O flux fraction profile. The larger value of flux fraction of water at the next step results in a lower value of the water mole fraction profile in accordance with equations (7.9) and (7.7). Similar reasoning apply for the increase in the mole fraction profile of hydroxyl radical. The elimination of reaction R.9 improved

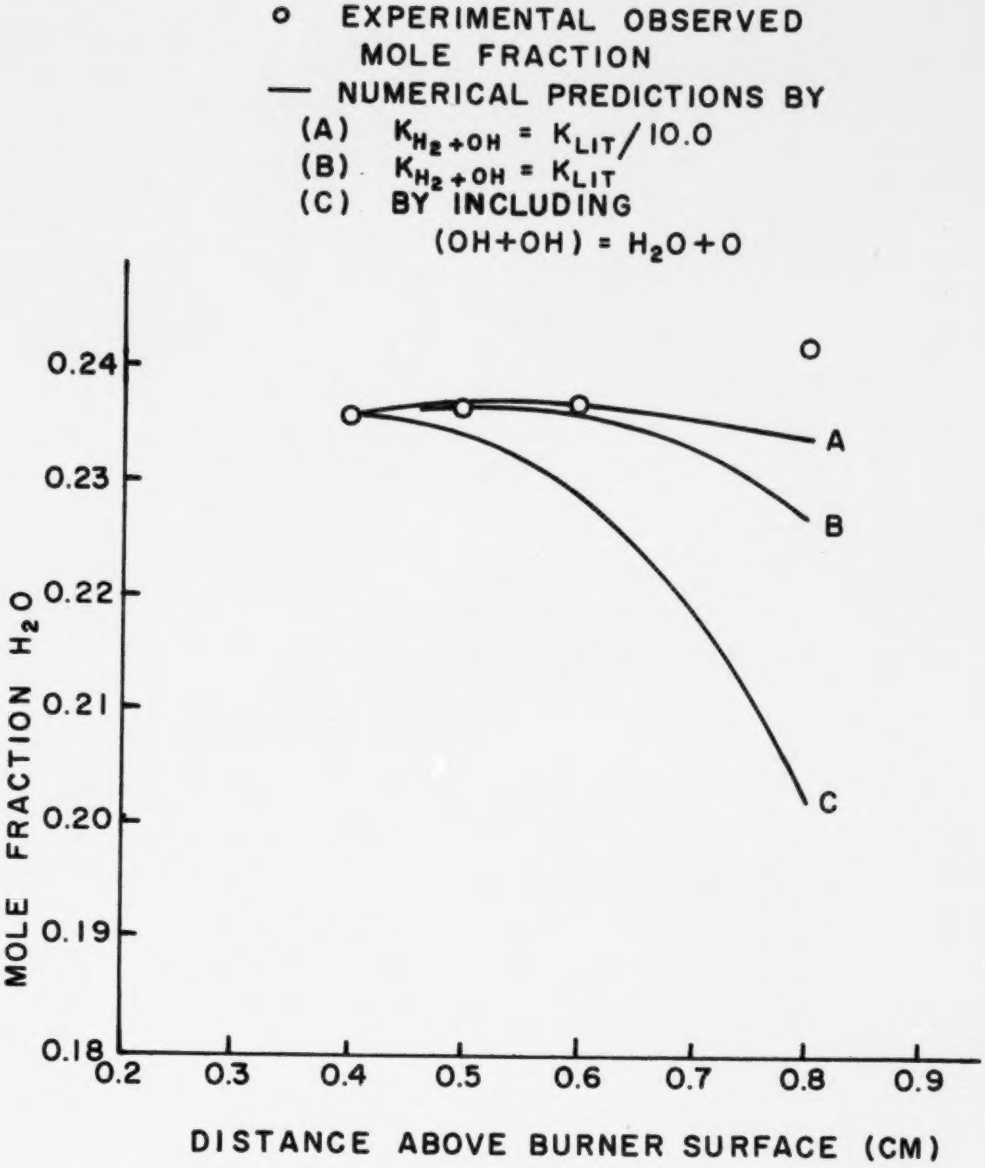

FIG. 7-2. COMPARISON OF MEASURED MOLE FRACTION DATA FOR H_2O WITH THEORETICAL PREDICTIONS, ETHANE/OXYGEN/ARGON FLAMES, EQUIVALENCE RATIO = 1.0 AND P = .083 ATM

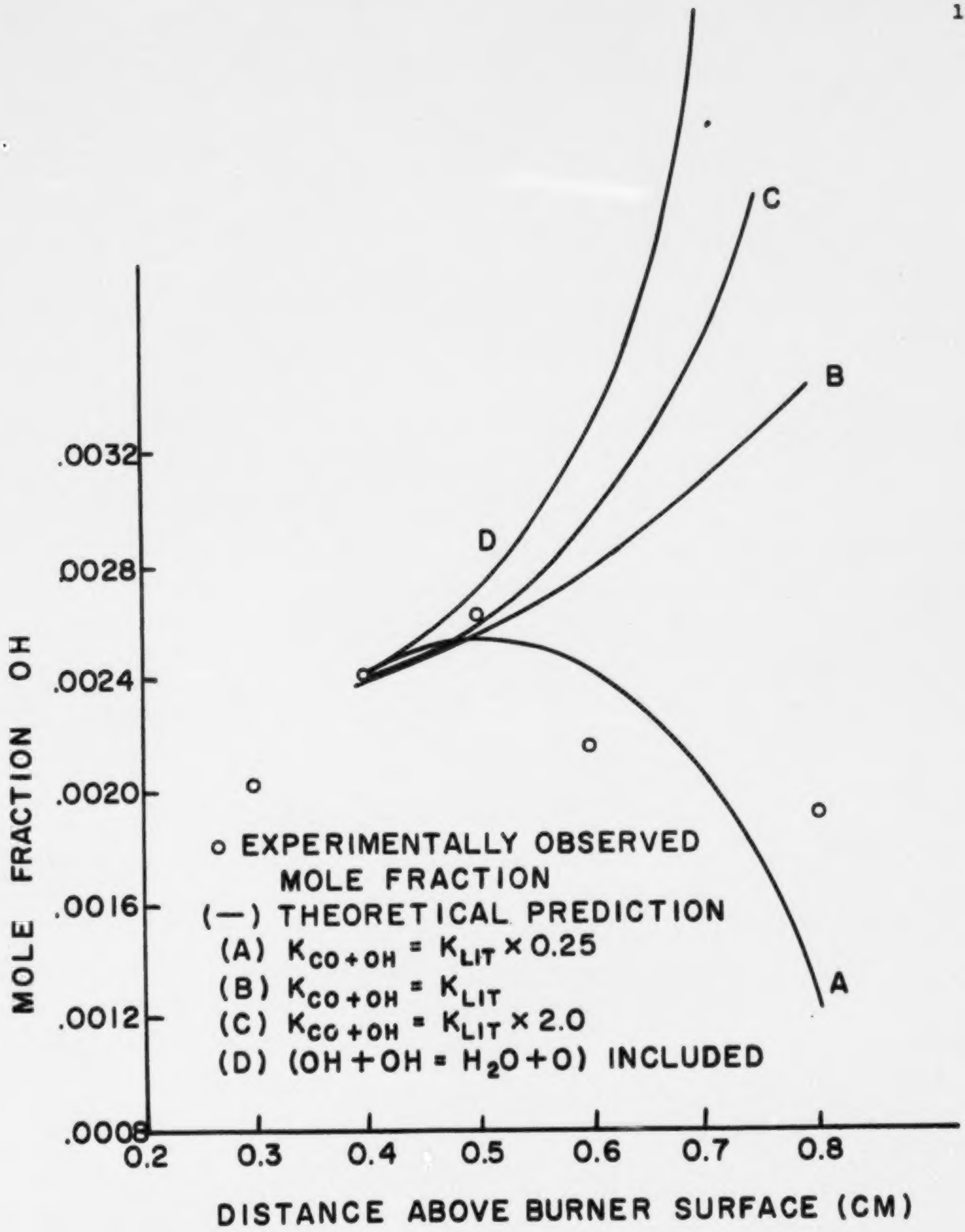

FIG. 7-3. COMPARISON OF MEASURED MOLE FRACTION DATA FOR OH WITH THEORETICAL PREDICTIONS ETHANE/OXYGEN/ARGON FLAMES, EQUIVALENCE RATIO = 1.0 AND P = .083 ATM

the trend for water (curve B, Fig. 7-2), which decreased relatively much slower.

After neglecting the reaction R.9 and its reverse, the remaining deviation between the experimental and predicted value of mole fraction of H_2O could result from the reaction $H_2 + OH = H_2O + H$ in the reaction scheme R.1 to R.15. This leads one to consider the following two alternatives:

1) To consider some alternative reactions such as

$$H + O_2 + M = HO_2 + M$$

$$HO_2 + H \quad = \cdots = H_2O + O$$

The inclusion of these reactions introduces additional uncertainties such as knowledge of concentrations of HO_2, H_2O_2, etc., the diffusion coefficients and rate data for these reactions.

2) The second alternative is that the value of rate coefficient for $H_2 + OH = H_2O + H$ reaction recommended in the literature is too high for the regime under consideration. Dixon-Lewis et al.[120] have reported deviations of up to ± 3 for ln A (A is pre-exponential factor for the rate coefficient) of reaction R.5. The value of the rate coefficients for reaction R.5 and its reverse were decreased by an order of magnitude. The resulting mole fraction profile of water (curve A, Fig. 7-2) agreed closely with the experimental values at the first three points and deviated by about 3 percent at the last point. The rate of increase of hydroxyl radical mole fraction was also relatively slower as shown by curve C in Fig. 7-3. The kinetic rate of hydroxyl radical is also controlled by the reactions R.1, R.2, R.3, R.4, R.7 and R.8.

The reaction R.1 is the primary path for the production of carbon dioxide. Using the value of $k_{CO+OH} = 5.6\times10^{10} \exp^{-1080/RT}$ cm^3-$mole^{-1}$-sec^{-1} as recommended in the literature, equations (7.7) and (7.9) were solved numerically for the reaction scheme R.1 to R.8 and R.11 to R.15. The mole fraction of carbon dioxide first increased up to z = 0.6 cm and then started to decrease slowly for fuel lean flames as shown by curve A of Fig. 7-4 and Fig. 7-5. For stoichiometric flame (equivalence ratio = 1.0), the mole fraction CO_2 continued to increase and overshoot the experimentally measured value at z = 0.8 cm by about 17 percent. The comparison of observed reaction rates and kinetic reaction rates for CO/CO_2 in section 7.3 suggested that the value of rate coefficient for reaction R.1 should be increased by a factor 1.2 - 3.84 to account for the observed data. Accordingly the rate coefficient of reaction R.1 and its reverse were increased by a factor of 2.0. The results of this integration are shown by curve C in Figs. 7-4, 7-5 and 7-6. This results in good agreement for the observed and predicted mole fraction profile of CO_2 for the stoichiometric flame (equivalence ratio = 1.0). However, for fuel lean ethane/oxygen flames, the slope of predicted CO_2 mole fraction profile becomes negative immediately after z = 0.6 cm which is in disagreement with the experimentally measured mole fraction profile of CO_2. The corresponding profile for carbon monoxide exhibits similar behavior but with a slope of negative sign as compared to that for CO_2 profile at a given position. These observations suggest that a higher value of rate coefficient for the reaction R.1 lead to better qualitative agreement for CO/CO_2 profiles in stoichiometric flames while the literature recommended value of k ($CO + OH = CO_2 + H$) gives better agreement for fuel lean flames.

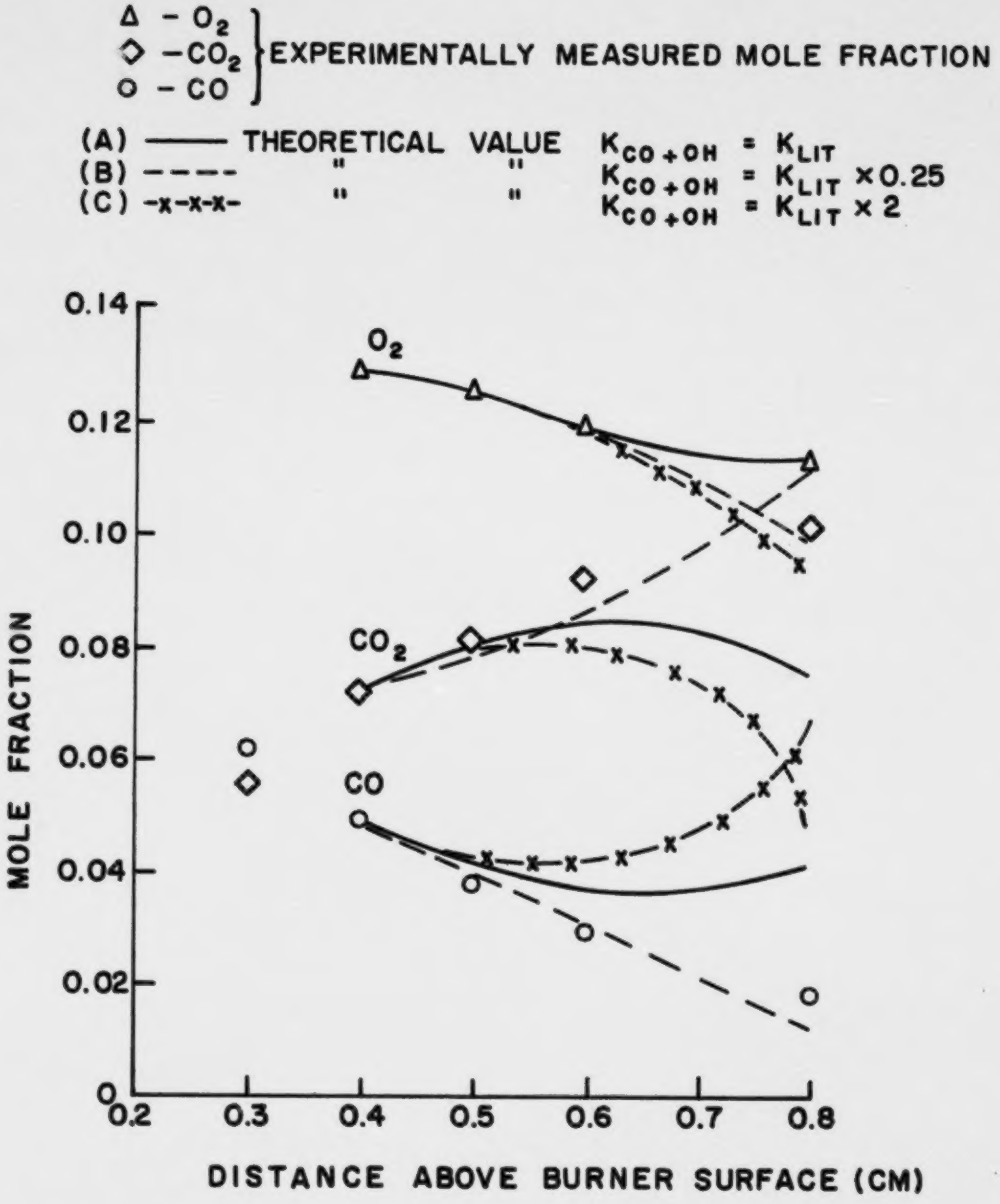

FIG. 7-4. COMPARISON OF MEASURED MOLE FRACTION DATA WITH THEORETICAL PREDICTIONS, ETHANE/OXYGEN/ARGON FLAMES, EQUIVALENCE RATIO = 0.67 AND P = .083 ATM

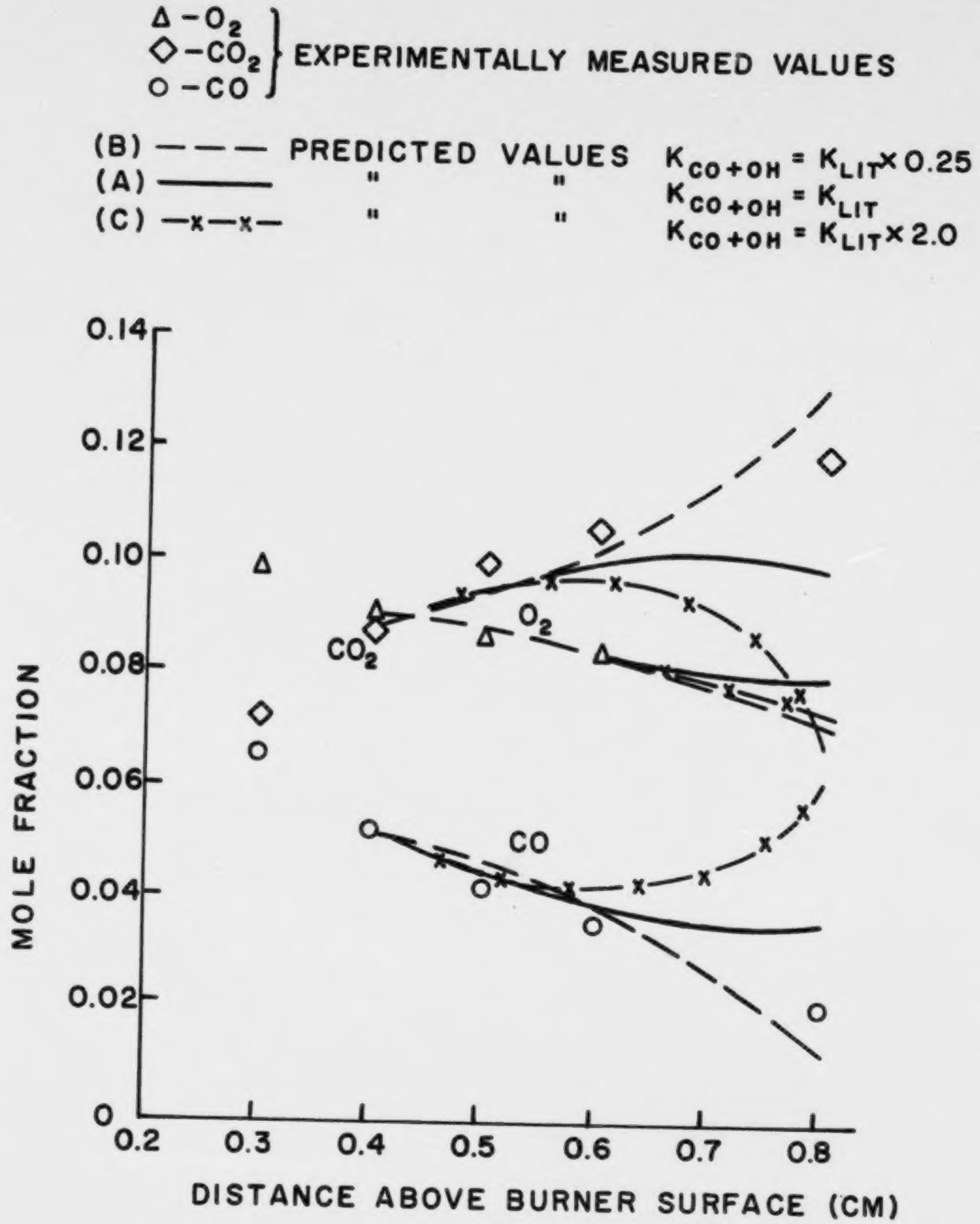

FIG. 7-5. COMPARISON OF MEASURED MOLE FRACTION DATA WITH THEORETICAL PREDICTIONS ETHANE/OXYGEN/ARGON FLAMES, EQUIVALENCE RATIO = 0.67 AND P = .083 ATM

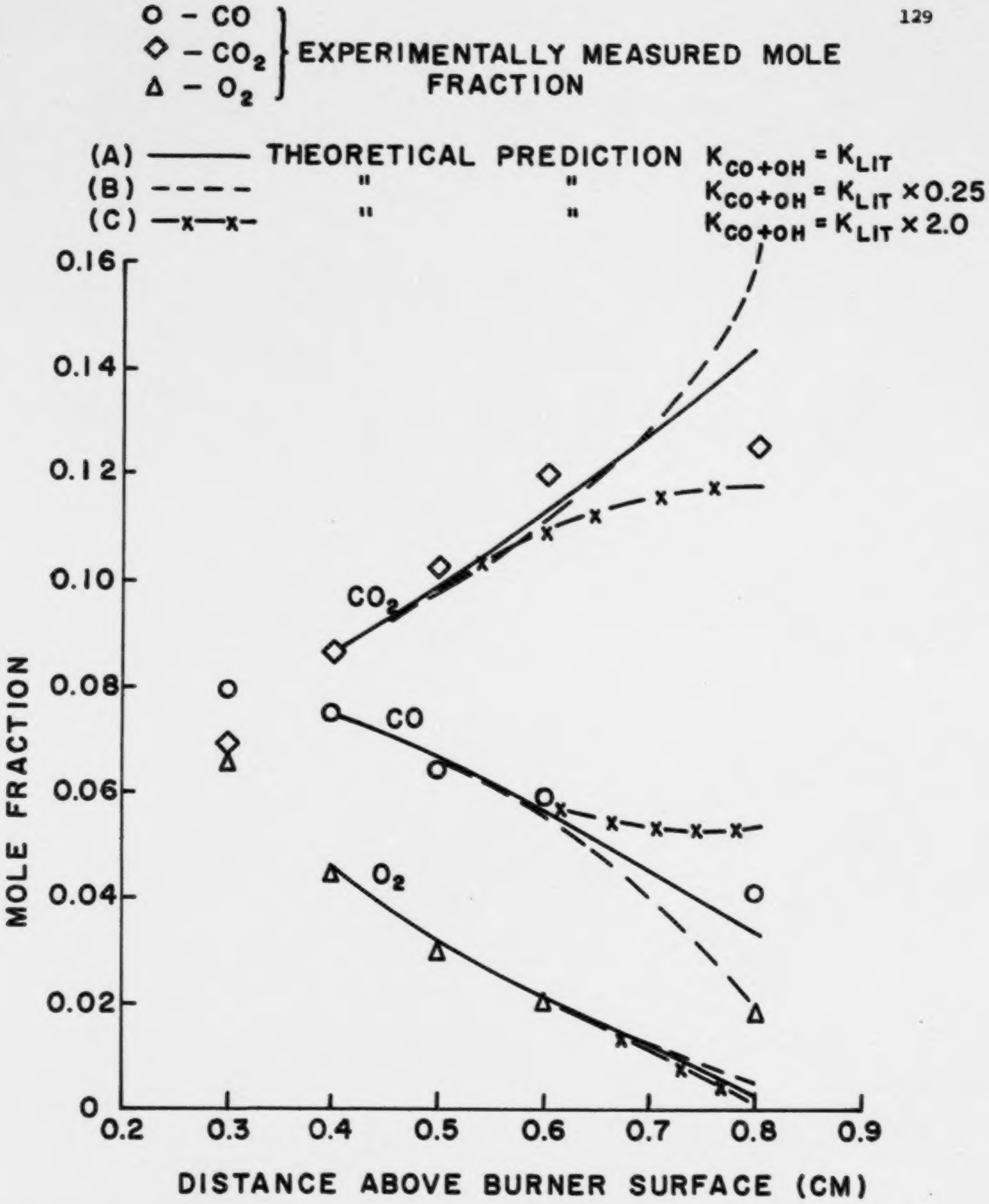

FIG. 7-6. COMPARISON OF MEASURED MOLE FRACTION DATA WITH THEORETICAL PREDICTIONS, ETHANE/OXYGEN/ARGON FLAMES, EQUIVALENCE RATIO = 1.0 AND P = .083 ATM

Using the aforementioned values of k(CO_2 + OH), the mole fraction profile of hydroxyl radical continuously increases with z and jumps to very high values of the order of one percent or more after z = 0.6 cm. The main reason for this was found to be high negative kinetic rates for OH. If the value of $k_{CO+OH} = k_{literature} \times 0.25$ is used, the kinetic rates for OH radical takes on small negative values. The resulting profile of OH exhibits a negative slope at z = 0.5 cm as shown by curve A in Fig. 7-3. The decreased value of k_{CO+OH} results in monatomically decreasing/increasing slopes for CO/CO_2 profiles, which is in sharp conflict with the experimental observation. This would suggest that rate of OH production through the reaction R.3 and R.5 are too slow to balance for the consumption of OH through the reaction R.1 and R.7.

Reaction R.3 is the primary path for the disappearance of molecular oxygen in the present reaction scheme. The steady state estimates of atomic hydrogen used in the aforesaid calculations result in monatomically decreasing slope of O_2 profile, which (as shown by curve C in Fig. 7-4, 7-5 and curve B in Fig. 7-7) does not agree with the experimentally observed profiles of O_2. This would suggest that the kinetic rate of O_2 decay is also relatively slow. One of the reasons for this disagreement may be that the steady state estimate for atomic hydrogen concentration is too low. The other could be the uncertainty in the rate coefficient of reaction R.3 which is relatively well known. The steady state estimate of atomic hydrogen concentration was increased by a factor of three. This resulted in better qualitative as well as quantitative agreement between experimental and predicted profiles for molecular oxygen as shown by curve A in Fig. 7-4 as well as in Fig. 7-5 and 7-7. The predicted profiles of hydroxyl radical also showed a

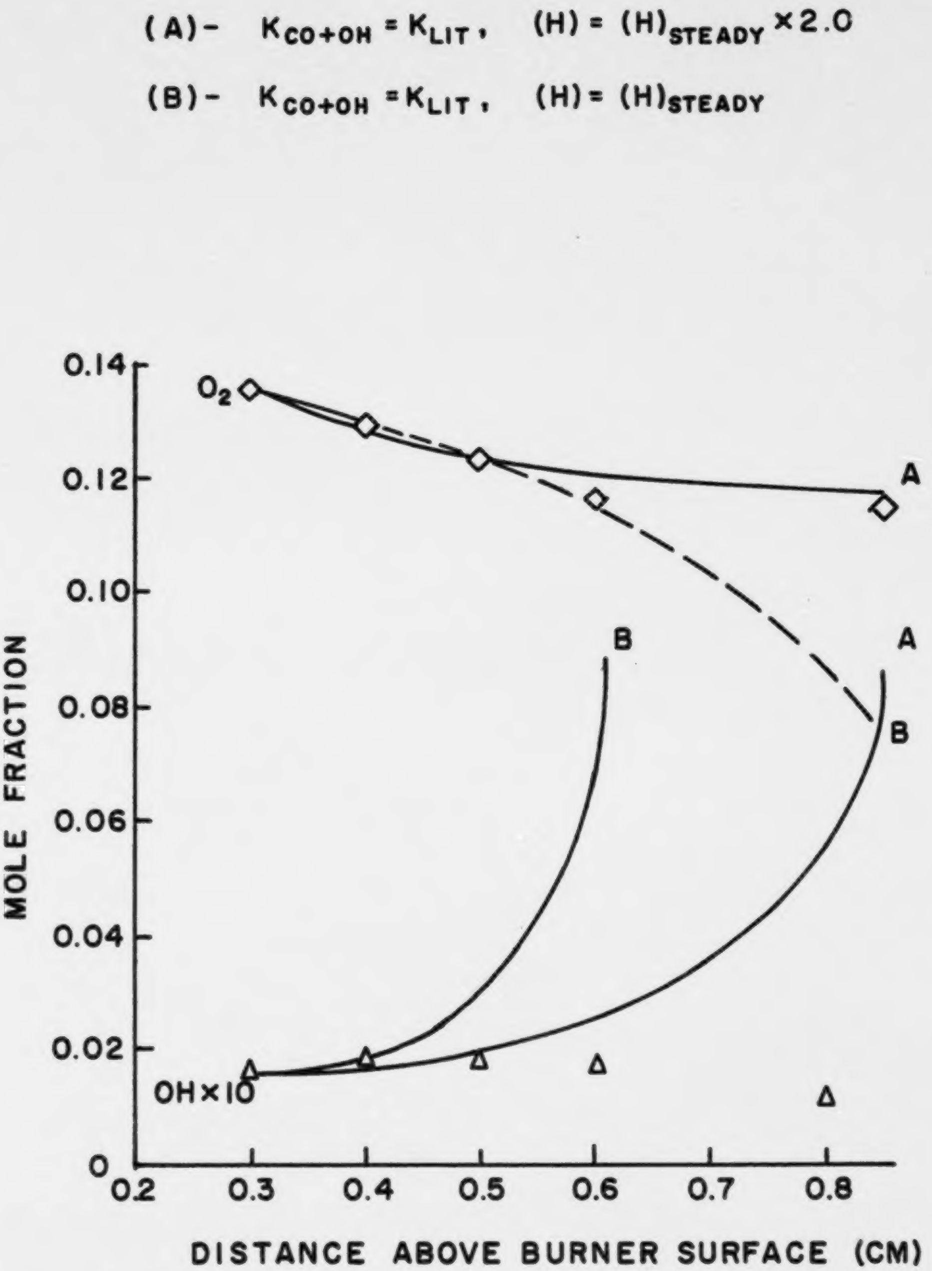

FIG. 7-7. COMPARISON OF MEASURED MOLE FRACTION DATA WITH THEORETICAL PREDICTIONS ETHYLENE/OXYGEN/ARGON FLAMES, EQUIVALENCE RATIO = 0.67 AND P = .083 ATM

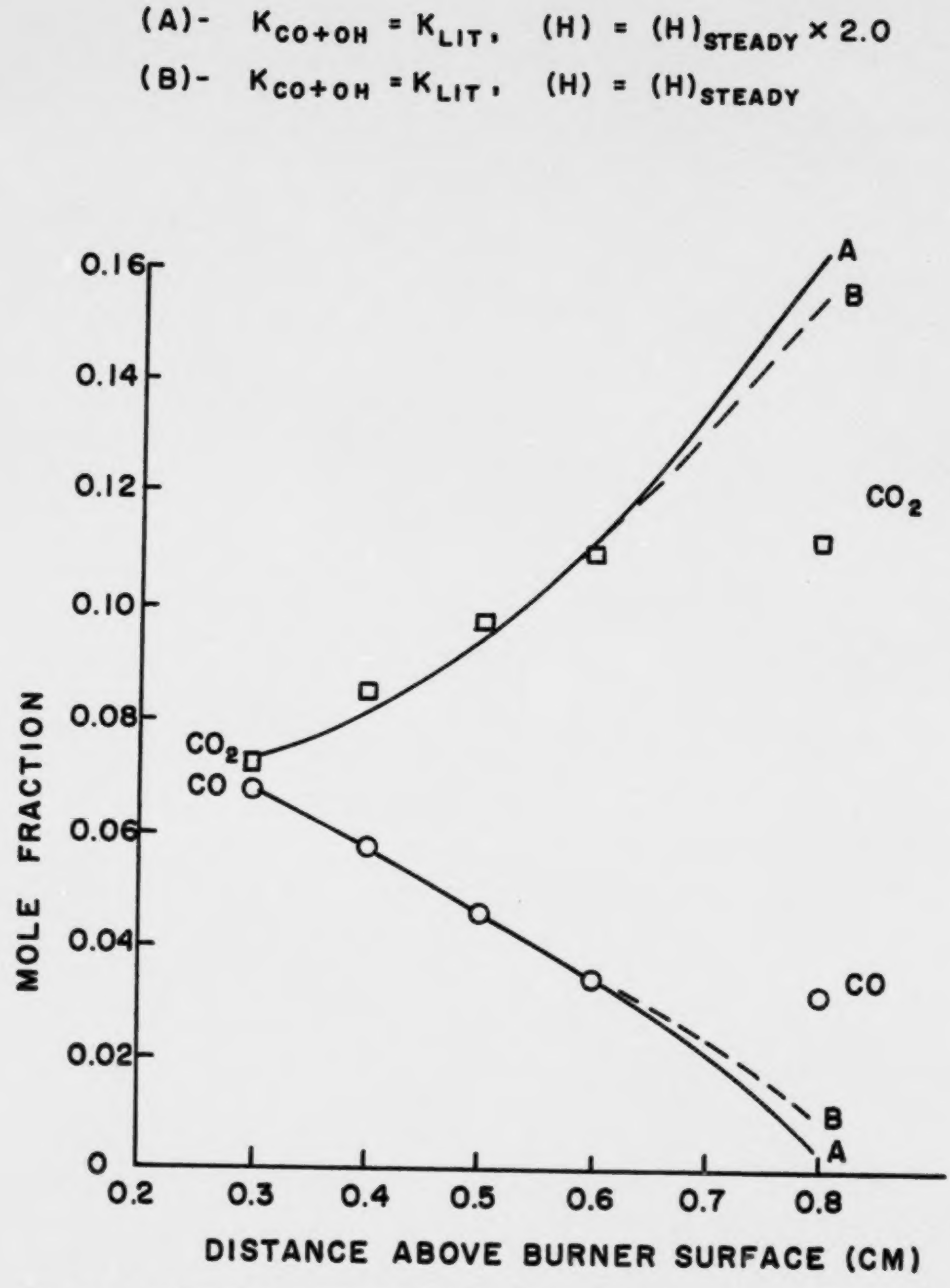

FIG. 7-8. COMPARISON OF MEASURED MOLE FRACTION DATA WITH THEORETICAL PREDICTIONS, ETHYLENE/OXYGEN/ARGON FLAMES, EQUIVALENCE RATIO = 0.67 AND P = .083 ATM

relatively better qualitative agreement with the measured ones as shown in Fig. 7-3. The effects of changing the steady state estimate of H on the profiles of CO and CO_2 were almost negligible as shown in Fig. 7-8.

The change in the initial estimate of atomic oxygen affects the profile of molecular hydrogen. It is not possible to make a meaningful comparison for H_2, as the measured profile has a high uncertainty.

In short it may be concluded:

1) The reaction scheme R.1 - R.15 after neglecting reaction R.9 and its reverse gives good qualitative agreement between the experimentally measured and predicted mole fraction profiles of CO, CO_2, O_2, H_2O and OH if

   a) $k_{CO+OH} = 1.12\times10^{12}\ \exp^{-1080/RT}$ cc-mole^{-1}-sec^{-1} (greater by a factor of two as compared to the recommended literature value)

   b) $k_{H_2+OH} = 1.5\times10^{12}\ \exp^{-5000/RT}$ cc-mole-sec (smaller by an order of magnitude as compared to the recommended literature value)

   c) Steady state estimate of [H] is increased by a factor of two to three.

2) Quantitative agreement between the predicted and experimentally measured mole fraction profiles for various species is primarily a matter of choosing the right combination of the values of rate coefficients of various reactions (known to probably ±100 percent in most cases), the diffusion coefficients (known to probably ±25 percent) and estimates of radical species distribution (the largest uncertainty in the present calculations).

CHAPTER 8

CONCLUSIONS

The kinetics of carbon monoxide disappearance in the after flame zone of ethylene/oxygen and ethane/oxygen flames at equivalence ratios of 0.67, 0.8 and 1.0, pressure of 0.083 and 0.054 atmosphere and temperature range of 1500-1700°K supported on a water-cooled porous plate top rectangular flat flame burner have been investigated. The composition profiles of stable species such as CO, CO_2, O_2, H_2O, N_2 and Ar have been investigated by subjecting the gas samples (taken with a triple walled water cooled stainless steel probe) to mass spectrometric analysis. The profiles of hydroxyl radical (an unstable species) and temperature are obtained by using ultraviolet absorption spectroscopy. Theoretical multicomponent diffusion coefficients are used for calculating the net reaction rates (referred to as observed rate in the discussion) from the composition and temperature profiles. The uncertainty in theoretical diffusion coefficients do not affect significantly the reaction rates profiles of major stable species but result in a high uncertainty for the reaction rates of hydroxyl radical and molecular hydrogen. The following statements sum up the conclusion drawn from this work.

(1) The overall rate of carbon monoxide disappearance/carbon dioxide appearance may be represented by a simple global rate expression first order in carbon monoxide

$$-\frac{d[CO]}{dt} = k_{overall-1}[CO]$$

$$\frac{d[CO_2]}{dt} = k_{overall-2}[CO]$$

$k_{overall}$ is a function of the nature of the fuel and equivalence ratio. For a given fuel $k_{overall}$ increases as one goes towards leaner fuel mixtures (up to equivalence ratio of 0.67 studied in the present work) and at the same equivalence ratio, $k_{overall}$ is greater for ethane flames as compared to ethylene flames.

(2) The average concentration of hydroxyl radical also increases as one goes to fuel lean mixtures for a given fuel. For the same equivalence ratio the average concentration of hydroxyl radical is greater for ethane/oxygen flames as compared to that for ethylene/oxygen flames.

(3) The measured mole fraction of hydroxyl radical shows consistent disagreement with those calculated from the equilibrium or partial equilibrium hypothesis.

(4) The similarity in the variation trends of $k_{overall}$ and hydroxyl radical concentration as well as the first order dependence on OH for carbon monoxide disappearance rates support the postulate that the primary path for the disappearance of CO is the reaction

$$CO + OH = CO_2 + H \qquad (R.1)$$

(5) A reaction mechanism for $CO/O_2/H_2$ system, which includes both fast bimolecular reactions as well as slow termolecular recombination reactions, is selected. The rate coefficients are taken from a review of the available rate data in the literature. Theoretical (kinetic) reaction rates are calculated from the reaction mechanism for each species and compared with the observed rates. The disagreement between the observed rates of carbon monoxide disappearance/carbon dioxide appearance and those calculated from the reaction mechanism may be attributed primarily to the uncertainty in the value of rate coefficient for reaction R.1. The literature recommended value for

$$k_{CO+OH} = (5.6\pm.8)\times10^{11}\exp^{-1080\pm500/RT}\ cm^3\text{-}mole^{-1}\text{-}sec^{-1}$$

has to be increased by an average factor of 2.63 to match the observed data.

(6) Using the postulated reaction mechanism, good qualitative agreement is also obtained between the observed and calculated reaction rates for O_2 and H_2O for more than 90 percent of the data points in the present study. The quantitative agreement is within a factor of 5 depending upon the hypothesis used for estimating the concentration of unknown radical species H and O. The agreement between the observed and theoretical reaction rates is poor for H_2 and OH due to high uncertainty involved in the calculation of diffusion velocity for these species.

(7) Conclusions (5) and (6) are also supported by the theoretical flame structure calculations carried out by numerical integration of the coupled kinetic rate equations (using postulated reaction mechanism) and the diffusion equation. Measured temperature profiles were employed obviating the necessity for including the energy conservation relations. A consistent disagreement is obtained between the calculated and observed mole fraction profiles of CO, CO_2, O_2, H_2O and OH. A systematic variation in the value of rate coefficients for various reactions and the initial estimates for the radical species (H and O) concentration lead to a good qualitative agreement between the theoretical and experimentally observed mole fraction profiles.

(8) The quantitative agreement between the predicted and experimentally observed mole fraction profiles of various species is primarily a matter of right combination of the values of rate coefficients of various reactions (known to probably ±100 percent in most cases), diffusion coefficients (known to probably ±25 percent) and estimates of radical species distribution (the largest uncertainty in the present calculations).

REFERENCES

1. U.S. Department of Commerce Publication, "The Automobile and Air Pollution," Part II, December 1967.

2. U.S. Department of Public Health Publication, "Compilation of Air Pollution Emission Factors," No. 99-AP-42.

3. Public Health Service, "A Digest of State Air Pollution Laws," Public Health Service Publication No. 711, U.S. Department of Health, Education and Welfare, Washington, D.C.

4. Smith, D. S., "Spectroscopic Investigation of Hydroxyl Radical Concentrations of End Gas Temperature in a Cyclic Combustion Process," Report No. TS-69-2, April 1969, College of Engineering, University of California, Berkeley, California.

5. Starkman, E. S., Twelfth Symposium (International) on Combustion, p. 593, The Combustion Institute, 1969.

6. Newhall, H. K., Twelfth Symposium (International) on Combustion, p. 603, The Combustion Institute, 1969.

7. Newhall, H. K. and Starkman, E. S., "Direct Spectroscopic Determination of Nitric Oxide in Reciprocating Engine Cylinders," SAE Paper 670122, 1967.

8. Powling, J., "The Flat Flame Burner," Sec. 2.1 in J. Surugue (ed.), Experimental Methods in Combustion Research, Pergamon Press, New York (1961).

9. Kaskan, W. E., Sixth Symposium (International) on Combustion, p. 134, Reinhold, 1957.

10. Friedman, R. and Burke, E. J: Chem. Phys, 22, 824 (1954).

11. Friedman, R. and Cypher, J. A.: J. Chem. Phys. 23, 1857 (1955).

12. Fenimore, C. P. and Jones, W. E.: J. Phys. Chem., 61, 651 (1957).

13. Friedman, R. and Cypher, J. A.: J. Chem. Phys., 25, 448 (1956).

14. Fenimore, C. P. and Jones, W. E.: J. Phys. Chem., 62, 693 (1958).

15. Longwell, J. P. and Weiss, M. A.: Ind. and Engg. Chem., Vol. 47, No. 8, 1634 (1954).

16. Hottel, H. C., Williams, G. C., Nerheim, N. M. and Schneider, G. R.: Tenth Symposium (International) on Combustion, p. 111, The Combustion Institute, 1965.

17. Williams, G. C., Hottel, H. C., and Morgan, A. C.: Twelfth Symposium (International) on Combustion, p. 913, The Combustion Institute, 1969.

18. Fristrom, R. M. and Westenberg, A. A.: Flame Structure, McGraw-Hill, 1965.

19. Bulewizc, E. M. and Sngden, T. M.: Trans. Faraday Soc., 54, 1855 (1958).

20. Fenimore, C. P. and Jones, G. W.: J. Phys. Chem., 62, 693 (1958).

21. Fenimore, C. P. and Jones, G. W.: J. Phys. Chem., 63, 1834 (1959).

22. Westenberg, A. A. and Fristrom, R. M.: Tenth Symposium (International) on Combustion, p. 473, The Combustion Institute, 1965.

23. Kaskan, W. E.: Combustion and Flame, 2, 229 (1958).

24. Kaskan, W. E.: Combustion and Flame, 2, 286 (1958).

25. Kaskan, W. E.: Combustion and Flame, 3, 39 (1959).

26. Kaskan, W. E.: Combustion and Flame, 3, 49 (1959).

27. Fenimore, C. P. and Jones, G. W.: Ninth Symposium (International) on Combustion, p. 597, Academic Press, 1963.

28. Fenimore, C. P. and Jones, G. W.: J. Chem. Phys., 39, 1514 (1963).

29. Fenimore, C. P. and Jones, G. W.: J. Chem. Phys., 41, 1887 (1964).

30. Browne, W. G., Porter, R. P., Verlin, J. D. and Clark, A. H.: Twelfth Symposium (International) on Combustion, p. 1035, The Combustion Institute, 1969.

31. Bonne, N., Grewer, Th. and Wagner, H. G.: Z. Physik. Chem. (Frankfurt) 26, 93 (1960).

32. Dixon-Lewis, G. and Williams, A.: Ninth Symposium (International) on Combustion, p. 576, Academic Press, 1963.

34. Fenimore, C. P. and Jones, G. W.: J. Phys. Chem., 62, 1578 (1958).

35. Avramenko, L. I. and Lorenzo, R. V. (Kolesnikova) Zh. Fiz. Khim., 24, 207 (1950).

36. Baldwin, R. R., Jackson, D., Walker, R. W., and Webster, S. J., Tenth Symposium (International) on Combustion, p. 423, The Combustion Institute, 1965.

37. Kaufman, F. and Del Greco, F. P.: Ninth Symposium (International) on Combustion, p. 659, Academic Press, 1963.

38. Dixon-Lewis, G., Sutton, M. M. and Williams, A.: Tenth Symposium (International) on Combustion, p. 495, The Combustion Institute, 1965.

39. Blundell, R. V., Cook, W. G. A., Hoare, D. E. and Milnes, G. S.: Tenth Symposium (International) on Combustion, P. 445, The Combustion Institute, 1965.

40. Fenimore, C. P. and Jones, G. W.: J. Phys. Chem., 65, 2200 (1961).

41. Wilson, W. E., "A Critical Review of the Combustion Reactions of the Hydroxyl Radicals," 1967 Spring Meeting, Western States Section, the Combustion Institute, LaJolla, California.

42. Browne, W. G., White, D. R. and Smookler, G. R.: Twelfth Symposium (International) on Combustion, p. 557, The Combustion Institute, 1969.

43. Dixon-Lewis, G., Wilson, W. E. and Westenberg, A. A.: J. Chem. Phys., 44, 2877 (1966).

44. Greiner, N. R.: J. Chem. Phys., 46, 2795 (1967).

45. Wilson, W. E. and O'Donovan, J. J.: J. Chem. Phys., 47, 5455 (1967).

46. Baulch, D. L., Drysdale, D. D. and Lloyd, A. C.: "High Temperature Reaction Rate Data," Dept. of Phys. Chem. Report, The University Leeds 2, England, No. 1, May 1968.

47. McLean, W. J. and Sawyer, R. F.: "Mas Spectrometer Data Reduction and Error Analysis," College of Engineering, University of California, Berkeley, Report No. TS-67-4 (August 1967).

48. Dueke, G. H. and Crosswhite, H. M.: J. Quant. Spectr. Radiative Transfer, 2, 97 (1962).

49. Oldenberg, O. and Rieke, E. F.: J. Chem. Phys., 6, 439 (1939) and 12, 351 (1944).

50. Hirshfelder, J. O., Curtiss, C. F. and Bird, R. B.: "The Molecular Theory of Gases and Liquids," John Wiley and Sons Inc., 1964.

51. Strehlow, R.: "Fundamentals of Combustion," International Text Book Co., 1968.

52. Svehla, R.:"Estimated Viscosities and Conductivities of Gases at High Temperature," NASA, Technical Report R-132 (1962).

53. Svehla, R.: "Thermodynamic and Transport Properties for the Hydrogen-Oxygen System," NASA-SP 3011 (1964).

54. Mason, E. A. and Monchic, L.: J. Chem. Phys., 36, 2746 (1962).

55. Monchic, L. and Mason, E. A.: J. Chem. Phys., 35, 1676 (1961).

56. Weissman, S. and Mason, E. A.: J. Chem. Phys., 36, 794 (1962).

57. Vanderslice, J. T., Weissman, S., Mason, E. A. and Fallon, R. J.: Phys. Fluids, 5, 155 (1962).

58. Yun, K. S. and Mason, E. A.: Phys. Fluids, 5, 380 (1962).

59. Baer, R. M.: "G2 CAL NLIN" Computer Centre Library, University of California, Berkeley, June 1967.

60. Learner, R.C.M.: Proc. Roy. Soc. (London) A269, 311 (1962).

61. Mitchel, A. C. and Zemansky, M. W.: Resonance Radiation and Excited Atoms, pp. 92-106, Cambridge University Press, 1961.

62. Carrington, T.: J. Chem. Phys. 30, 1087 (1959) and 31, 1243 (1959).

63. Penner, S. S.: "Quantitative Molecular Spectroscopy and Gas Emissivities," Chapter 3 and 4, Addison-Wesley, 1959.

64. Ladenburg, Z.: Physik, 65, 200 (1930).

65. Cowan, R. D. and Dieke, G. H.: Rev. Mod. Phys., 20, 418 (1948).

66. Minkoff, G. J. and Tipper, C. F. H.: Chemistry of Combustion Reactions, Buttersworth and Co. Ltd., London (1962).

67. Fenimore, C. P. and Jones, G. W.: J. Phys. Chem. 62, 1578 (1958).

68. Kozlov, G. I.: Seventh Symposium (International) on Combustion, p. 142, Butterworths (1959).

69. Seery, D. J. and Bowman, C. T.,"An experimental and analytical study of methane oxidation behind shock waves," United Aircraft Laboratories, East Hartford, Connecticut 06108, 1969.

70. Bowman, C. T. and Seery, D. J.: "Ignition mechanism of hydrocarbon fuels-methane and acetylene," Western States Section, The Combustion Institute, Palo Alto, California, Fall 1968.

71. Fenimore, C. P." Chemistry in Premixed Flames, International Encyclopedia of Physical Chemistry and Chemical Physics, Topic 19 Gas Kinetics, Vol. 5, McMillan, New York (1964).

72. Schott, G. L. and Kinsey, J. L.: J. Chem. Phys., 29, 1177, 1958.

73. Gardiner, W. C. and Kistikowsky, G. R.: J. Chem. Phys., 35, 1765 (1965).

74. Baldwin, R. R. and Cowe, D. W.: Trans. Faraday Soc., 58, 1768 (1962).

75. Baldwin, R. R.: Ninth Symposium (International) on Combustion, p. 667, Academic Press, 1963.

76. Jenkins, D. R., Yumlu, V. S. and Spalding, D. B.: Eleventh Symposium (International) on Combustion, p. 779, The Combustion Institute, 1967.

77. Fenimore, C. P. and Jones, G. W.: J. Phys. Chem., 63, 1834 (1959).

78. Glass, C. P., Kistiakowsky, G. B., Michael, I. V. and Niki, H.: J. Chem. Phys., 42, 608 (1965).

79. Gutmand, D., Harwidge, D. E., Dougherty, F. A. and Lutz, R. W.: J. Chem. Phys., 47, 4400, 1967.

80. Ung, Y. M. and Back, R. A.: Can. J. Chem., 42, 753 (1964).

81. Fenimore, C. P. and Jones, G. W.: J. Phys. Chem., 65, 993 (1961).

82. Clyne, M. A. A. and Thrush, B. A.: Proc. Roy. Soc. (london), A 275, 544 (1963).

83. Baldwin, R. R.: Trans. Faraday Soc., 52, 1344 (1956).

84. Wong, E. L. and Potter, A. E.: J. Chem. Phys., 39, 2211 (1963).

85. Kaufman, F.: Annls. Geophys. 20, 106 (1964).

86. Del Greco, F. P. and Kaufman, F.: Discuss. Faraday Soc., 33, 128 (1962).

87. Wise, H., Ablow, C. M. and Sancier, K. M.: J. Chem. Phys., 41, 3569 (1964).

88. Hoare, D. E.: "Reactions of Gaseous Hydroxyl Radicals," Nature, 194, 283 (1962).

89. Rink, J. P.: J. Chem. Phys., 34, 1942 (1961).

90. Sutton, E. A.: J. Chem. Phys., 36, 2923 (1962).

91. Patch, W. P.: J. Chem. Phys., 36, 1919 (1962).

92. Jacobs, T. A., Geidt, R. R. and Cohen, N.: J. Chem. Phys., 47, 54 (1967).

93. Kretschmer, C. B. and Petersen, H. L.: J. Chem. Phys., 39, 1772 (1963).

94. Larkin, F. S. and Thrush, B. A.: Tenth Symposium (International) on Combustion, 397, The Combustion Institute (1965).

95. Dixon-Lewis, G., Sutton, M. M. and Williams, A.: Discussion Faraday, Soc., 33, 205 (1962).

96. Halstead, C. J. and Jenkins, D. R.: Twelfth Symposium (International) on Combustion, p. 979, The Combustion Institute, 1969.

97. Byron, S. R.: J. Chem. Phys., 34, 1942 (1961).

98. Schexnayder, C. J. and Evans, J. S.: NASA Report TR-R108 (1961).

99. Wray, K. L.: J. Chem. Phys., 37, 1254 (1962).

100. Camac, M. and Vaughan, A.: J. Chem. Phys., 34, 460 (1961).

101. Kiefer, J. H. and Lutz, R. W.: J. Chem. Phys., 42, 1709 (1965).

102. Morgan, J. E. and Schiff, H. I.: J. Chem. Phys., 38, 1495 (1963).

103. Getzinger, R. W.: Eleventh Symposium (International) on Combustion, p. 117, The Combustion Institute, 1967.

104. Dixon-Lewis, G. and Williams, A.: Eleventh Symposium (International) on Combustion, p. 951, The Combustion Institute, 1967.

105. Klein, R., McNebsy, J. R., Scheer, M. D. and Schoen, L. J.: J. Chem. Phys., 30, p. 58 (1954).

106. Greiner, N. R.: J. Chem. Phys., 45, 99 (1966).

107. Wilson, W. E. and Westenberg, A. A.: Eleventh Symposium (International) on Combustion, p. 1143, The Combustion Institute, 1967.

108. Baldwin, R. R., Norris, A. C. and Walker, R. W.: Eleventh Symposium (International) on Combustion, p. 889, The Combustion Institute, 1967.

109. Wilson, W. E., O'Donovan, J. T. and Fristrom, R. M.: Twelfth Symposium (International) on Combustion, p. 929, The Combustion Institute, 1969.

110. Schofield, K.: Planet Space Science, 15, 643 (1967).

111. Pratt, G. L.: "Gas Kinetics," Chapter 2, John Wiley, London, 1969.

112. Friedman, R. and Nugent, R. C.; Seventh Symposium (International) on Combustion, p. 311, Butterworths, London (1959).

113. Ladenburg, R. W., Lewis, B., Pease, R. N. and Taylor, H. S.: "Physical Measurements in Gas Dynamics and Combustion," Princeton University Press, Princeton, New Jersey (1954).

114. Surgue, J.: "Experimental Methods in Combustion Research," AGAR, Pergamon Press, 1961.

115. Bevington, P. R.: "Data Reduction and Error Analysis for the Physical Sciences," McGraw-Hill, 1969.

116. Lomax, H.: "An Operational Unification of Finite Difference Methods for Numerical Integration of Ordinary Differential Equations," NASA TR R-262, May 1967.

117. Emanuel, G.: "Numerical Analysis of Stiff Equations," Aerospace Corporation Report Tdv-269 (4230-20)-3, AD-431750, January, 1964.

118. Purgalis, P. and Sawyer, R. F.: "General Formulation and Numerical Solution of Reaction Rate Problems," Report No. TS-68-4, College of Engineering, Univ. of California, Berkeley, July 1968.

119. Hayes, J. K.: "D2 BC RKIN Runge-Kutta Integration of Differential Equations," Computer Centre, University of Califoria, Berkeley, August 1966.

120. Dixon-Lewis, G., Sutton, M. N. and Williams, A.: Trans. Faraday Soc., 61, 235 (1965).

121. Singh, T. and Sawyer, R. F.: "Review of Rate Data for $CO/H_2/O_2$ System Reactions," College of Engineering, Report No. TS-70-3 University of California, Berkeley, 1970.

APPENDIX 1

Experimental Data

APPENDIX 1

```
          COMPOSITION.TEMPERATURE AND REACTION RATE PROFILES
          Z= DISTANCE ABOVE BURNER SURFACE
          PHI= EQUIVALENCE RATIO
          FR= MOLE FRACTION
          CR= CHEMICAL REACTION RATE MOLES CM-3 SEC-1
          P= PRESSURE ATMOSPHERES
          TEMP= TEMPERATURE DEGREE KELVIN


                              RUN NO  1
             P          C2H6       O2          N2          AR          PHI
           .0830       .0657      .3381       .5972     0.           .6700

Z(CM)     .3000E+00  .4000E+00  .5000E+00  .6000E+00  .8000E+00  .1000E+01
TEMP      .1658E+04  .1683E+04  .1650E+04  .1630E+04  .1575E+04  .1675E+04
O2   FR   .1687E+00  .1424E+00  .1335E+00  .1233E+00  .1183E+00  .1119E+00
     CR  -.4518E-04 -.3627E-04 -.2832E-04 -.2133E-04 -.1025E-04 -.3030E-05
CO   FR   .6714E-01  .5394E-01  .3727E-01  .2776E-01  .1680E-01  .1010E-01
     CR  -.4312E-04 -.3485E-04 -.2749E-04 -.2105E-04 -.1095E-04 -.4520E-05
CO2  FR   .4246E-01  .5920E-01  .7597E-01  .8959E-01  .1068E+00  .1136E+00
     CR   .5450E-04  .4566E-04  .3759E-04  .3026E-04  .1789E-04  .8540E-05
H2O  FR   .1618E+00  .1829E+00  .1853E+00  .1879E+00  .1870E+00  .1806E+00
     CR   .4253E-04  .3138E-04  .2154E-04  .1301E-04 -.1200E-06 -.8020E-05
H2   FR   .6281E-02  .4794E-02  .3311E-02  .2767E-02  .2758E-02  .3149E-02
     CR   .6000E-07 -.5900E-06 -.1260E-05 -.1960E-05 -.3470E-05 -.5110E-05
M    FR   .5461E+00  .5462E+00  .5539E+00  .5614E+00  .5679E+00  .5850E+00
     CR   .1987E-04  .1728E-04  .1479E-04  .1241E-04  .7980E-05  .3990E-05
OH   FR   .2991E-02  .3822E-02  .3494E-02  .6598E-02  .3732E-02  .2481E-02
     CR   .2280E-05  .1160E-05  .1500E-06 -.7500E-06 -.2210E-05 -.3240E-05


                              RUN NO 2
             P          C2H6       O2          N2          AR          PHI
           .0830       .0642      .3362     0.           .5996       .6700

Z(CM)     .3000E+00  .4000E+00  .5000E+00  .6000E+00  .8000E+00  .1000E+01
TEMP      .1538E+04  .1570E+04  .1650E+04  .1628E+04  .1623E+04  .1612E+04
O2   FR   .1458E+00  .1313E+00  .1273E+00  .1213E+00  .1163E+00  .1148E+00
     CR  -.2679E-04 -.2071E-04 -.1535E-04 -.1072E-04 -.3620E-05  .5800E-06
CO   FR   .6297E-01  .5070E-01  .3545E-01  .2439E-01  .1615E-01  .1328E-01
     CR  -.4439E-04 -.3577E-04 -.2806E-04 -.2125E-04 -.1033E-04 -.3020E-05
CO2  FR   .5467E-01  .7129E-01  .8416E-01  .9654E-01  .1069E+00  .1076E+00
     CR   .5032E-04  .4031E-04  .3134E-04  .2342E-04  .1072E-04  .2210E-05
H2O  FR   .1720E+00  .1784E+00  .1815E+00  .1809E+00  .1814E+00  .1816E+00
     CR   .8620E-05  .6190E-05  .4090E-05  .2320E-05 -.2700E-06 -.1570E-05
H2   FR   .1072E-02  .1452E-02  .9802E-03  .1506E-02  .1708E-02  .1735E-02
     CR  -.4980E-05 -.4500E-05 -.4000E-05 -.3490E-05 -.2420E-05 -.1280E-05
M    FR   .5616E+00  .5675E+00  .5688E+00  .5738E+00  .5779E+00  .5791E+00
     CR   .5200E-05  .4920E-05  .4590E-05  .4220E-05  .3350E-05  .2310E-05
OH   FR   .1697E-02  .2648E-02  .3158E-02  .2347E-02  .2347E-02  .1539E-02
     CR  -.4590E-05 -.3780E-05 -.3050E-05 -.2400E-05 -.1320E-05 -.5600E-06
```

```
                              RUN NO 3

            P            C2H6          O2            N2          AR            PHI
          .0840        .0735         .3266         .5994     0.              .7900

Z(CM)     .3000E+00    .4000E+00    .5000E+00    .6000E+00    .8000E+00    .1000E+01
TEMP      .1615E+04    .1640E+04    .1673E+04    .1637E+04    .1624E+04    .1610E+04
O2   FR   .1187E+00    .1023E+00    .9124E-01    .8515E-01    .7718E-01    .7444E-01
     CR  -.3807E-04   -.3046E-04   -.2360E-04   -.1749E-04   -.7500E-05   -.5100E-06
CO   FR   .7145E-01    .5719E-01    .4524E-01    .3470E-01    .1808E-01    .1150E-01
     CR  -.3330E-04   -.2858E-04   -.2422E-04   -.2020E-04   -.1323E-04   -.7650E-05
CO2  FR   .6885E-01    .8374E-01    .9617E-01    .1044E+00    .1219E+00    .1278E+00
     CR   .3255E-04    .2757E-04    .2303E-04    .1894E-04    .1208E-04    .7000E-05
H2O  FR   .1852E+00    .2005E+00    .2023E+00    .2027E+00    .2036E+00    .2051E+00
     CR   .1705E-04    .1246E-04    .8470E-05    .5100E-05    .1700E-06   -.2330E-05
H2   FR   .1061E-01    .4419E-02    .2083E-02    .2139E-02    .1009E-02    .1026E-02
     CR  -.2249E-04   -.1915E-04   -.1594E-04   -.1283E-04   -.6960E-05   -.1550E-05
M    FR   .5522E+00    .5585E+00    .5701E+00    .5769E+00    .5842E+00    .5858E+00
     CR   .2227E-04    .1889E-04    .1577E-04    .1293E-04    .8020E-05    .4190E-05
OH   FR   .1128E-02    .1418E-02    .1191E-02    .1224E-02    .1146E-02    .6970E-03
     CR  -.7810E-05   -.6830E-05   -.5850E-05   -.4870E-05   -.2890E-05   -.8800E-06
```

```
                              RUN NO 4

            P            C2H6          O2            N2          AR            PHI
          .0830        .0735         .3267     0.              .5997         .7900

Z(CM)     .3000E+00    .4000E+00    .5000E+00    .6000E+00    .8000E+00    .1000E+01
TEMP      .1624E+04    .1656E+04    .1664E+04    .1624E+04    .1592E+04    .1606E+04
O2   FR   .9849E-01    .9029E-01    .8656E-01    .8365E-01    .7891E-01    .7382E-01
     CR  -.8210E-05   -.6910E-05   -.5760E-05   -.4750E-05   -.3160E-05   -.2150E-05
CO   FR   .6531E-01    .5476E-01    .4342E-01    .3344E-01    .2040E-01    .1234E-01
     CR  -.4087E-04   -.3395E-04   -.2769E-04   -.2211E-04   -.1295E-04   -.6470E-05
CO2  FR   .7225E-01    .8663E-01    .9922E-01    .1060E+00    .1196E+00    .1663E+00
     CR   .3479E-04    .3057E-04    .2649E-04    .2254E-04    .1504E-04    .8080E-05
H2O  FR   .1951E+00    .2032E+00    .2060E+00    .2072E+00    .2101E+00    .2103E+00
     CR   .1394E-04    .1050E-04    .7460E-05    .4810E-05    .6900E-06   -.1880E-05
H2   FR   .7374E-02    .3126E-02    .1947E-02    .1499E-02    .1172E-02    .1416E-02
     CR  -.3640E-05   -.3220E-05   -.2960E-05   -.2850E-05   -.3100E-05   -.3970E-05
M    FR   .5631E+00    .5655E+00    .5661E+00    .5672E+00    .5708E+00    .5740E+00
     CR  -.5560E-05   -.5020E-05   -.4410E-05   -.3730E-05   -.2130E-05   -.2500E-06
OH   FR   .2030E-02    .2610E-02    .2612E-02    .1873E-02    .1849E-02    .1240E-02
     CR   .5310E-05    .3220E-05    .1440E-05   -.5000E-07   -.2110E-05   -.2950E-05
```

```
                              RUN NO 4A

            P            C2H6        O2           N2           AR           PHI
          .0842         .0655       .2871      0.             .6474        .7950

Z(CM)     .3000E+00   .4000E+00   .5000E+00   .6000E+00   .8000E+00   .1000E+01
TEMP      .1676E+04   .1723E+04   .1694E+04   .1679E+04   .1685E+04   .1623E+04
O2   FR   .9257E-01   .8141E-01   .7335E-01   .6903E-01   .6479E-01   .6385E-01
     CR  -.2689E-04  -.2056E-04  -.1497E-04  -.1011E-04  -.2580E-05   .2010E-05
CO   FR   .6699E-01   .5718E-01   .4421E-01   .3242E-01   .2400E-01   .1408E-01
     CR  -.3644E-04  -.3049E-04  -.2509E-04  -.2023E-04  -.1212E-04  -.6180E-05
CO2  FR   .6957E-01   .8431E-01   .9788E-01   .1077E+00   .1194E+00   .1247E+00
     CR   .4411E-04   .3633E-04   .2931E-04   .2304E-04   .1274E-04   .5450E-05
H2O  FR   .1824E+00   .1899E+00   .1945E+00   .1958E+00   .1985E+00   .1997E+00
     CR   .1592E-04   .1262E-04   .9700E-05   .7150E-05   .3200E-05   .7500E-06
H2   FR   .3371E-02   .2925E-02   .1857E-02   .2207E-02   .1868E-02   .1569E-02
     CR  -.7370E-05  -.5910E-05  -.4500E-05  -.3170E-05  -.6800E-06   .1550E-05
M    FR   .5982E+00   .5998E+00   .6027E+00   .6037E+00   .6043E+00   .6037E+00
     CR   .1640E-05   .1980E-05   .2230E-05   .2380E-05   .2390E-05   .2010E-05
OH   FR   .4680E-02   .8942E-02   .8250E-02   .2751E-02   .2452E-02   .2305E-02
     CR  -.5100E-05  -.4240E-05  -.3430E-05  -.2680E-05  -.1360E-05  -.2500E-06


                              RUN NO 5

            P            C2H6        O2           N2           AR           PHI
          .0840         .0922       .3073        .6005      0.           1.0200

Z(CM)     .3000E+00   .4000E+00   .5000E+00   .6000E+00   .8000E+00   .1000E+01
TEMP      .1702E+04   .1768E+04   .1732E+04   .1712E+04   .1689E+04   .1672E+04
O2   FR   .7198E-01   .5457E-01   .3887E-01   .2810E-01   .2156E-01   .1826E-01
     CR  -.3995E-04  -.3243E-04  -.2550E-04  -.1918E-04  -.8350E-05   .7000E-07
CO   FR   .9447E-01   .8351E-01   .6430E-01   .4341E-01   .2373E-01   .1326E-01
     CR  -.4526E-04  -.3936E-04  -.3376E-04  -.2846E-04  -.1875E-04  -.1024E-04
CO2  FR   .5715E-01   .7747E-01   .9871E-01   .1107E+00   .1227E+00   .1310E+00
     CP   .3972E-04   .3230E-04   .2575E-04   .2006E-04   .1129E-04   .6000E-05
H2O  FR   .1870E+00   .2017E+00   .2187E+00   .2238E+00   .2267E+00   .2253E+00
     CR   .2447E-04   .1860E-04   .1355E-04   .9330E-05   .3370E-05   .7000E-06
H2   FR   .3597E-01   .3747E-01   .2357E-01   .2075E-01   .1683E-01   .1691E-01
     CR  -.8232E-04  -.6915E-04  -.5657E-04  -.4457E-04  -.2233E-04  -.2440E-05
M    FR   .5361E+00   .5451E+00   .5556E+00   .5629E+00   .5701E+00   .5759E+00
     CR   .4750E-05   .6140E-05   .7250E-05   .8090E-05   .8960E-05   .8730E-05
OH   FR   .1355E-02   .1962E-02   .1736E-02   .1295E-02   .9570E-03   .6240E-03
     CR  -.2157E-04  -.1832E-04  -.1513E-04  -.1199E-04  -.5890E-05  -.3000E-07
```

```
                              RUN NO 5A

           P            C2H6         O2           N2           AR           PHI
         .0840        .0922        .3073        .6005      0.           1.0200

Z(CM)     .3000E+00   .4000E+00   .5000E+00   .6000E+00   .8000E+00   .1000E+01
TEMP      .1703E+04   .1753E+04   .1737E+04   .1706E+04   .1675E+04   .1649E+04
O2   FR   .6768E-01   .5181E-01   .3973E-01   .2892E-01   .2696E-01   .2532E-01
     CR -.2875E-04  -.2227E-04  -.1653E-04  -.1153E-04  -.3740E-05   .1100E-05
CO   FR   .1007E+00   .9540E-01   .7496E-01   .5664E-01   .3471E-01   .3015E-01
     CR -.4668E-04  -.3932E-04  -.3263E-04  -.2661E-04  -.1659E-04  -.9250E-05
CO2  FR   .5340E-01   .6687E-01   .9013E-01   .1102E+00   .1247E+00   .1328E+00
     CR   .3979E-04   .3428E-04   .2916E-04   .2444E-04   .1617E-04   .9470E-05
H2O  FR   .1778E+00   .1918E+00   .2009E+00   .2123E+00   .2144E+00   .2188E+00
     CR   .2775E-04   .2196E-04   .1678E-04   .1222E-04   .4940E-05   .1400E-06
H2   FR   .4959E-01   .4946E-01   .4471E-01   .3717E-01   .4021E-01   .3508E-01
     CR -.1921E-04  -.1792E-04  -.1662E-04  -.1529E-04  -.1258E-04  -.9780E-05
M    FR   .5199E+00   .5272E+00   .5375E+00   .5448E+00   .5476E+00   .5523E+00
     CR   .1376E-04   .1148E-04   .9310E-05   .7260E-05   .3490E-05   .1800E-06
OH   FR   .1355E-02   .1962E-02   .1736E-02   .1295E-02   .9570E-03   .6240E-03
     CR -.7120E-05  -.6330E-05  -.5570E-05  -.4820E-05  -.3410E-05  -.2080E-05
```

```
                              RUN NO 6

           P            C2H6         O2           N2           AR           PHI
         .0830        .0922        .3072      0.                .6006      1.0050

Z(CM)     .3000E+00   .4000E+00   .5000E+00   .6000E+00   .8000E+00   .1000E+01
TEMP      .1685E+04   .1653E+04   .1676E+04   .1611E+04   .1589E+04   .1599E+04
O2   FR   .6967E-01   .4730E-01   .3273E-01   .2597E-01   .2253E-01   .1988E-01
     CR -.2703E-04  -.2157E-04  -.1666E-04  -.1233E-04  -.5340E-05  -.6200E-06
CO   FR   .9786E-01   .8664E-01   .6676E-01   .5246E-01   .4980E-01   .3773E-01
     CR -.3728E-04  -.3077E-04  -.2485E-04  -.1955E-04  -.1075E-04  -.4380E-05
CO2  FR   .5848E-01   .7816E-01   .1047E+00   .1214E+00   .1261E+00   .1381E+00
     CR   .4618E-04   .3715E-04   .2910E-04   .2202E-04   .1079E-04   .3460E-05
H2O  FR   .2169E+00   .2318E+00   .2365E+00   .2376E+00   .2451E+00   .2439E+00
     CR   .1268E-04   .9120E-05   .6080E-05   .3560E-05   .7000E-07  -.1360E-05
H2   FR   .3352E-02   .8572E-02   .1590E-01   .1851E-01   .1264E-01   .1419E-01
     CR -.1490E-05  -.2000E-05  -.2300E-05  -.2400E-05  -.2000E-05  -.7800E-06
M    FR   .5486E+00   .5448E+00   .5445E+00   .5468E+00   .5472E+00   .5497E+00
     CR -.5200E-05  -.4070E-05  -.3060E-05  -.2180E-05  -.7700E-06   .1500E-06
OH   FR   .1040E-02   .1133E-02   .1194E-02   .9470E-03   .7910E-03   .5840E-03
     CR -.1090E-04  -.9500E-05  -.8120E-05  -.6760E-05  -.4080E-05  -.1470E-05
```

```
                                 RUN NO 11

              P            C2H6         O2           N2           AR           PHI
            .0560         .0921       .3062        .6017      0.            1.0527

Z(CM)     .5000E+00   .6000E+00   .8000E+00   .1000E+01   .1300E+01   .1600E+01
TEMP      .1722E+04   .1739E+04   .1726E+04   .1677E+04   .1622E+04   .1617E+04
O2   FR   .5581E-01   .4530E-01   .2833E-01   .2231E-01   .1754E-01   .1572E-01
     CR -.1142E-04 -.8100E-05 -.3250E-05 -.7800E-06 -.1550E-05 -.7690E-05
CO   FR   .1104E+00   .9220E-01   .5648E-01   .3983E-01   .3243E-01   .2903E-01
     CR -.3433E-04 -.2352E-04 -.1371E-04 -.8510E-05 -.3520E-05 -.5520E-05
CO2  FR   .5691E-01   .7373E-01   .1109E+00   .1252E+00   .1343E+00   .1387E+00
     CR   .4160E-04   .3504E-04   .2187E-04   .1514E-04   .3700E-05 -.4370E-05
H2O  FR   .2271E+00   .2374E+00   .2403E+00   .2415E+00   .2379E+00   .2404E+00
     CR   .2453E-04   .1807E-04   .7350E-05 -.4500E-06 -.6670E-05 -.6320E-05
H2   FR   .2110E-01   .1317E-01   .1122E-01   .7838E-02   .1038E-01   .9552E-02
     CR -.1540E-04 -.1206E-04 -.6800E-05 -.3420E-05 -.1910E-05 -.4650E-05
M    FR   .5288E+00   .5381E+00   .5525E+00   .5616E+00   .5669E+00   .5656E+00
     CR   .1777E-04   .1606E-04   .1234E-04   .8220E-05   .1310E-05 -.6490E-05
OH   FR   .7295E-03   .6750E-03   .7122E-03   .5174E-03   .5073E-03   .4932E-03
     CR   .4010E-05   .3180E-05   .1590E-05   .6000E-07 -.2110E-05 -.4120E-05


                                 RUN NO 13

              P            C2H4         O2           N2           AR           PHI
            .0840         .0739       .3258        .6002      0.             .6806

Z(CM)     .3000E+00   .4000E+00   .5000E+00   .6000E+00   .8000E+00   .1000E+01
TEMP      .1482E+04   .1521E+04   .1548E+04   .1573E+04   .1534E+04   .1512E+04
O2   FR   .1523E+00   .1387E+00   .1297E+00   .1238E+00   .1193E+00   .1169E+00
     CR -.2708E-04 -.2101E-04 -.1565E-04 -.1099E-04 -.3810E-05   .5400E-06
CO   FR   .7864E-01   .6566E-01   .5066E-01   .3357E-01   .2016E-01   .1699E-01
     CR -.4020E-04 -.3340E-04 -.2726E-04 -.2180E-04 -.1289E-04 -.6660E-05
CO2  FR   .5471E-01   .7305E-01   .8976E-01   .1059E+00   .1198E+00   .1230E+00
     CR   .4852E-04   .3995E-04   .3223E-04   .2533E-04   .1406E-04   .6140E-05
H2O  FR   .1297E+00   .1374E+00   .1399E+00   .1399E+00   .1403E+00   .1404E+00
     CR   .1045E-04   .7860E-05   .5570E-05   .3590E-05   .5700E-06 -.1190E-05
H2   FR   .5261E-02   .4326E-02   .3456E-02   .2393E-02   .2285E-02   .2291E-02
     CR -.6400E-05 -.5380E-05 -.4420E-05 -.3530E-05 -.1920E-05 -.5500E-06
M    FR   .5768E+00   .5798E+00   .5858E+00   .5940E+00   .5973E+00   .5998E+00
     CR   .1023E-04   .9340E-05   .8400E-05   .7420E-05   .5320E-05   .3040E-05
OH   FR   .4890E-03   .7530E-03   .8260E-03   .8480E-03   .5100E-03   .3720E-03
     CR -.1140E-05 -.1130E-05 -.1090E-05 -.1020E-05 -.8200E-06 -.5200E-06
```

```
                              RUN NO 13A

               P            C2H4          O2           N2         AR           PHI
             .0840          .0739        .3258        .6002     0.           .6806

Z(CM)      .3000E+00     .4000E+00     .5000E+00     .6000E+00     .8000E+00     .1000E+01
TEMP       .1521E+04     .1532E+04     .1559E+04     .1573E+04     .1551E+04     .1537E+04
O2    FR   .1475E+00     .1382E+00     .1290E+00     .1254E+00     .1191E+00     .1159E+00
      CR  -.2058E-04    -.1633E-04    -.1256E-04    -.9280E-05    -.4180E-05    -.1010E-05
CO    FR   .7680E-01     .6192E-01     .4862E-01     .3972E-01     .2871E-01     .1873E-01
      CR  -.3450E-04    -.2873E-04    -.2352E-04    -.1889E-04    -.1130E-04    -.5980E-05
CO2   FR   .5561E-01     .7262E-01     .8967E-01     .9962E-01     .1124E+00     .1226E+00
      CR   .4225E-04     .3508E-04     .2860E-04     .2281E-04     .1330E-04     .6540E-05
H2O   FR   .1286E+00     .1334E+00     .1369E+00     .1397E+00     .1414E+00     .1426E+00
      CR   .1031E-04     .8230E-05     .6380E-05     .4740E-05     .2110E-05     .3600E-06
H2    FR   .4342E-02     .4991E-02     .3336E-02     .2060E-02     .1646E-02     .1799E-02
      CR  -.4670E-05    -.4060E-05    -.3480E-05    -.2920E-05    -.1880E-05    -.9400E-06
M     FR   .5842E+00     .5875E+00     .5911E+00     .5922E+00     .5956E+00     .5973E+00
      CR   .1740E-05     .2070E-05     .2280E-05     .2390E-05     .2250E-05     .1670E-05
OH    FR   .4890E-03     .7530E-03     .8260E-03     .8480E-03     .5100E-03     .3720E-03
      CR  -.7200E-06    -.7500E-06    -.7700E-06    -.7600E-06    -.6600E-06    -.4700E-06
```

```
                              RUN NO 14

               P            C2H4          O2           N2            AR           PHI
             .0830          .0734        .3277     0.              .5989        .6715

Z(CM)      .3000E+00     .4000E+00     .5000E+00     .6000E+00     .8000E+00     .1000E+01
TEMP       .1525E+04     .1525E+04     .1563E+04     .1574E+04     .1554E+04     .1562E+04
O2    FR   .1356E+00     .1290E+00     .1233E+00     .1171E+00     .1155E+00     .1143E+00
      CR  -.1392E-04    -.1078E-04    -.8020E-05    -.5670E-05    -.2130E-05    -.1700E-06
CO    FR   .6743E-01     .5775E-01     .4581E-01     .3428E-01     .3235E-01     .2960E-01
      CR  -.3458E-04    -.2779E-04    -.2164E-04    -.1651E-04    -.6940E-05    -.2290E-05
CO2   FR   .7252E-01     .8507E-01     .9776E-01     .1105E+00     .1119E+00     .1149E+00
      CR   .3976E-04     .3220E-04     .2484E-04     .1848E-04     .7970E-05     .2580E-05
H2O   FR   .1436E+00     .1475E+00     .1481E+00     .1503E+00     .1502E+00     .1504E+00
      CR   .4290E-05     .3410E-05     .2630E-05     .1950E-05     .8900E-06     .2200E-06
H2    FR   .1186E-03     .1043E-03     .1101E-03     .7357E-04     .5737E-04     .5687E-04
      CR  -.1500E-06    -.1400E-06    -.1200E-06    -.1000E-06    -.7000E-07    -.4000E-07
M     FR   .5801E+00     .5807E+00     .5851E+00     .5880E+00     .5902E+00     .5908E+00
      CR   .3410E-05     .3210E-05     .2960E-05     .2660E-05     .1930E-05     .1000E-05
OH    FR   .1660E-02     .1805E-02     .1704E-02     .1755E-02     .1017E-02     .1267E-02
      CR  -.9300E-06    -.8500E-06    -.7700E-06    -.6900E-06    -.5300E-06    -.3600E-06
```

```
                          RUN NO 15

            P           C2H4        O2          N2          AR          PHI
          .0830       .0859       .3131       .6009     0.            .8120

Z(CM)     .3000E+00   .4000E+00   .5000E+00   .6000E+00   .8000E+00   .1000E+01
TEMP      .1493E+04   .1545E+04   .1576E+04   .1528E+04   .1576E+04   .1571E+04
O2   FR   .9856E-01   .8906E-01   .8062E-01   .7503E-01   .7075E-01   .6954E-01
     CR  -.2821E-04  -.2217E-04  -.1674E-04  -.1195E-04  -.4220E-05   .1010E-05
CO   FR   .7690E-01   .6881E-01   .5402E-01   .3972E-01   .2863E-01   .1659E-01
     CR  -.3953E-04  -.3453E-04  -.2643E-04  -.2163E-04  -.1512E-04  -.6900E-05
CO2  FR   .8427E-01   .1016E+00   .1197E+00   .1355E+00   .1476E+00   .1512E+00
     CR   .4115E-04   .3739E-04   .2728E-04   .1940E-04   .1149E-04   .3920E-05
H2O  FR   .1481E+00   .1571E+00   .1597E+00   .1613E+00   .1608E+00   .1617E+00
     CR   .9800E-06   .2900E-06  -.2500E-06  -.6300E-06  -.9500E-06  -.6500E-06
H2   FR   .7354E-02   .6665E-02   .4485E-02   .4132E-02   .4412E-02   .3950E-02
     CR  -.3005E-04  -.2579E-04  -.2161E-04  -.1753E-04  -.9650E-05  -.2140E-05
M    FR   .5707E+00   .5755E+00   .5833E+00   .5887E+00   .5933E+00   .5970E+00
     CR  -.4560E-05  -.1890E-05   .3400E-06   .2160E-05   .4510E-05   .5160E-05
OH   FR   .5410E-03   .7990E-03   .7750E-03   .4520E-03   .4920E-03   .4590E-03
     CR  -.9770E-05  -.8530E-05  -.7290E-05  -.6060E-05  -.3600E-05  -.1150E-05
```

```
                          RUN NO 16

            P           C2H4        O2          N2          AR          PHI
          .0840       .0875       .3126     0.            .6007       .8360

Z(CM)     .3000E+00   .4000E+00   .5000E+00   .6000E+00   .8000E+00   .1000E+01
TEMP      .1508E+04   .1537E+04   .1610E+04   .1564E+04   .1573E+04   .1485E+04
O2   FR   .9408E-01   .8470E-01   .7575E-01   .7049E-01   .6792E-01   .6582E-01
     CR  -.2140E-04  -.1724E-04  -.1342E-04  -.9960E-05  -.4070E-05   .4200E-06
CO   FP   .7879E-01   .6623E-01   .5266E-01   .4209E-01   .3621E-01   .2681E-01
     CR  -.2690E-04  -.2419E-04  -.2048E-04  -.1696E-04  -.8750E-05  -.5870E-05
CO2  FR   .8524E-01   .9864E-01   .1143E+00   .1265E+00   .1332E+00   .1396E+00
     CR   .3208E-04   .3031E-04   .2441E-04   .1947E-04   .1133E-04   .3770E-05
H2O  FR   .1607E+00   .1672E+00   .1703E+00   .1723E+00   .1731E+00   .1742E+00
     CR   .1240E-05   .6100E-06   .1400E-06  -.1700E-06  -.3000E-06   .2100E-06
H2   FR   .6286E-03   .4027E-03   .2416E-03   .1989E-03   .1941E-03   .1634E-03
     CR  -.2277E-04  -.1941E-04  -.1609E-04  -.1280E-04  -.6350E-05  -.5000E-07
M    FR   .5825E+00   .5827E+00   .5868E+00   .5886E+00   .5895E+00   .5898E+00
     CR  -.2000E-05  -.1170E-05  -.4400E-06   .2000E-06   .1160E-05   .1720E-05
OH   FR   .1188E-02   .1028E-02   .8590E-03   .8820E-03   .8470E-03   .6000E-03
     CR  -.9030E-05  -.7760E-05  -.6500E-05  -.5250E-05  -.2780E-05  -.3600E-06
```

```
                               RUN NO 17

             P          C2H4        O2          N2         AR          PHI
           .0840       .1000      .3000       .6000     0.          1.0000

Z(CM)      .3000E+00  .4000E+00  .5000E+00  .6000E+00  .8000E+00  .1000E+01
TEMP       .1548E+04  .1578E+04  .1577E+04  .1573E+04  .1525E+04  .1447E+04
O2   FR    .7779E-01  .5317E-01  .4252E-01  .3370E-01  .3099E-01  .2739E-01
     CR   -.2817E-04 -.2297E-04 -.1823E-04 -.1395E-04 -.6780E-05 -.1450E-05
CO   FR    .9619E-01  .8231E-01  .6801E-01  .5453E-01  .4235E-01  .3462E-01
     CR   -.3203E-04 -.2725E-04 -.2285E-04 -.1883E-04 -.1192E-04 -.6530E-05
CO2  FR    .8567E-01  .1014E+00  .1237E+00  .1395E+00  .1479E+00  .1587E+00
     CR    .3270E-04  .2678E-04  .2149E-04  .1682E-04  .9360E-05  .4400E-05
H2O  FR    .1652E+00  .1808E+00  .1826E+00  .1826E+00  .1846E+00  .1841E+00
     CR    .3200E-05  .1600E-05  .3100E-06 -.6900E-06 -.1790E-05 -.1710E-05
H2   FR    .3552E-02  .4840E-02  .3871E-02  .3399E-02  .3329E-02  .3173E-02
     CR   -.3068E-04 -.2673E-04 -.2284E-04 -.1901E-04 -.1152E-04 -.4270E-05
M    FR    .5709E+00  .5756E+00  .5856E+00  .5951E+00  .5943E+00  .5984E+00
     CR    .9980E-05  .8200E-05  .6630E-05  .5250E-05  .3100E-05  .1740E-05
OH   FR    .4390E-03  .5090E-03  .4830E-03  .4830E-03  .3780E-03  .3570E-03
     CR   -.1414E-04 -.1222E-04 -.1034E-04 -.8520E-05 -.5010E-05 -.1690E-05


                               RUN NO 18

             P          C2H4        O2          N2         AR          PHI
           .0830       .0996      .3001     0.            .6002       .9960

Z(CM)      .3000E+00  .4000E+00  .5000E+00  .6000E+00  .8000E+00  .1000E+01
TEMP       .1561E+04  .1592E+04  .1649E+04  .1615E+04  .1579E+04  .1548E+04
O2   FR    .6875E-01  .5645E-01  .4441E-01  .2685E-01  .1953E-01  .1851E-01
     CR   -.1706E-04 -.1375E-04 -.1077E-04 -.8120E-05 -.3820E-05 -.8600E-06
CO   FR    .9119E-01  .7931E-01  .7201E-01  .5853E-01  .4733E-01  .4260E-01
     CR   -.3150E-04 -.2842E-04 -.2460E-04 -.1979E-04 -.6660E-05 -.3090E-05
CO2  FR    .9046E-01  .1100E+00  .1190E+00  .1375E+00  .1506E+00  .1559E+00
     CR    .3500E-04  .2903E-04  .2560E-04  .2237E-04  .1051E-04  .4460E-05
H2O  FR    .1799E+00  .1900E+00  .1905E+00  .1988E+00  .2006E+00  .2012E+00
     CR    .1426E-04  .1149E-04  .8990E-05  .6760E-05  .3120E-05  .5500E-06
H2   FR    .8084E-03  .1087E-02  .1217E-02  .7295E-03  .4073E-03  .4991E-03
     CR    .9000E-07 0.         -.7000E-07 -.1300E-06 -.2300E-06 -.2800E-06
M    FR    .5769E+00  .5770E+00  .5730E+00  .5779E+00  .5817E+00  .5815E+00
     CR   -.1720E-05 -.7500E-06  .6000E-07  .7200E-06  .1560E-05  .1780E-05
OH   FR    .5000E-03  .5110E-03  .4890E-03  .4940E-03  .4980E-03  .3420E-03
     CR   -.1050E-05 -.9700E-06 -.8900E-06 -.8100E-06 -.6200E-06 -.4200E-06
```

```
                              RUN NO 19

           P          C2H6       O2          N2          AR          PHI
         .0550       .0644     .3401       .5950     0.            .6700

Z(CM)    .5000E+00  .6000E+00  .8000E+00  .1000E+01  .1300E+01  .1600E+01
TEMP     .1635E+04  .1658E+04  .1651E+04  .1623E+04  .1614E+04  .1601E+04
O2   FR  .1619E+00  .1432E+00  .1317E+00  .1261E+00  .1234E+00  .3193E+00
     CR  .1096E-03  .4831E-04 -.3256E-04 -.5792E-04  .8120E-05  .1991E-03
CO   FR  .6918E-01  .6053E-01  .4795E-01  .3579E-01  .1979E-01  .1618E-01
     CR -.2714E-04 -.2331E-04 -.1566E-04 -.8020E-05  .3420E-05  .1484E-04
CO2  FR  .4370E-01  .5177E-01  .6466E-01  .7656E-01  .9353E-01  .9427E-01
     CR  .4737E-04  .3971E-04  .2258E-04  .3060E-05 -.3070E-04 -.6984E-04
H2O  FR  .1626E+00  .1809E+00  .1832E+00  .1821E+00  .1817E+00  .4043E+00
     CR  .2091E-03  .1243E-03  .1460E-05 -.5903E-04 -.3283E-04  .1337E-03
H2   FR  .1044E-01  .5801E-02  .4173E-02  .4260E-02  .4059E-02  .4260E-02
     CR  .1145E-03  .8654E-04  .2306E-04 -.5045E-04 -.1795E-03 -.3312E-03
M    FR  .5476E+00  .5495E+00  .5600E+00  .5663E+00  .5698E+00  .9233E-02
     CR -.2208E-03 -.1169E-03  .2383E-04  .7493E-04 -.1644E-04 -.3094E-03
OH   FR  .1314E-02  .1446E-02  .1399E-02  .7900E-03  .9840E-03  .1011E-02
     CR  .5583E-04  .4154E-04  .1103E-04 -.2208E-04 -.7661E-04 -.1370E-03
```

```
                              RUN NO 20

           P          C2H4       O2          N2          AR          PHI
         .0555       .0739     .3263     0.            .5998       .6790

Z(CM)    .5000E+00  .6000E+00  .8000E+00  .1000E+01  .1300E+01  .1600E+01
TEMP     .1523E+04  .1557E+04  .1578E+04  .1491E+04  .1490E+04  .1502E+04
O2   FR  .1530E+00  .1457E+00  .1338E+00  .1272E+00  .1229E+00  .1219E+00
     CR -.2344E-04 -.1913E-04 -.1186E-04 -.6400E-05 -.1600E-05 -.8800E-06
CO   FR  .7786E-01  .6287E-01  .3581E-01  .1839E-01  .9077E-02  .6323E-02
     CR -.4580E-04 -.3844E-04 -.2560E-04 -.1522E-04 -.4290E-05  .1070E-05
CO2  FR  .6043E-01  .7493E-01  .1028E+00  .1216E+00  .1310E+00  .1339E+00
     CR  .4311E-04  .3650E-04  .2479E-04  .1510E-04  .4340E-05 -.1900E-05
H2O  FR  .1267E+00  .1326E+00  .1326E+00  .1326E+00  .1314E+00  .1315E+00
     CR  .6200E-05  .3530E-05 -.3600E-06 -.2310E-05 -.1580E-05  .3510E-05
H2   FR  .2526E-02  .1921E-02  .1870E-02  .1915E-02  .2041E-02  .2048E-02
     CR -.7700E-06 -.5500E-06 -.2100E-06 -.1200E-06  .9000E-07 -.1000E-06
M    FR  .5779E+00  .5807E+00  .5916E+00  .5963E+00  .6019E+00  .6027E+00
     CR  .1510E-05  .1710E-05  .1880E-05  .1750E-05  .9700E-06 -.4800E-06
OH   FR  .5860E-03  .6180E-03  .7450E-03  .5970E-03  .5310E-03  .4460E-03
     CR  .2000E-06  .1100E-06 -.2000E-07 -.9000E-07 -.1000E-06  .2000E-07
```

```
                                RUN NO 23

              P            C2H4         O2           N2          AR            PHI
            .0555         .0999        .2998        .6002      0.             .9990

Z(CM)      .5000E+00    .6000E+00    .8000E+00    .1000E+01    .1300E+01    .1600E+01
TEMP       .1624E+04    .1654E+04    .1637E+04    .1607E+04    .1573E+04    .1556E+04
O2   FR    .6224E-01    .5774E-01    .4760E-01    .4141E-01    .3699E-01    .3424E-01
     CR  -.1043E-04   -.8330E-05   -.4730E-05   -.1960E-05    .6500E-06    .1410E-05
CO   FR    .1005E+00    .8114E-01    .7287E-01    .5711E-01    .5421E-01    .5134E-01
     CR  -.2769E-04   -.2199E-04   -.1743E-04   -.8320E-05    .7700E-06    .4360E-05
CO2  FR    .8653E-01    .1041E+00    .1191E+00    .1346E+00    .1381E+00    .1393E+00
     CR    .2623E-04    .2135E-04    .1748E-04    .1011E-04    .3730E-05    .2970E-05
H2O  FR    .1629E+00    .1690E+00    .1718E+00    .1718E+00    .1716E+00    .1721E+00
     CR    .7990E-05    .5850E-05    .2630E-05    .7700E-06    .5800E-06    .3480E-05
H2   FR    .1323E-01    .1023E-01    .1035E-01    .8643E-02    .8213E-02    .8721E-02
     CP  -.1759E-04   -.1430E-04   -.7740E-05   -.1230E-05    .8450E-05    .1804E-04
M    FR    .5732E+00    .5758E+00    .5771E+00    .5824E+00    .5868E+00    .5949E+00
     CR  -.5560E-05   -.3460E-05    .8000E-07    .2730E-05    .5040E-05    .5340E-05
OH   FR    .6010E-03    .6523E-03    .4920E-03    .4430E-03    .3750E-03    .3060E-03
     CR  -.5770E-05   -.4560E-05   -.2220E-05    .3000E-07    .3240E-05    .6260E-05
```

APPENDIX 2

Error Analysis

Error is defined as "the difference between a calculated or observed value and the true value." Usually, of course, the true value is not known, so we can consider only estimates of the errors inherent in the estimate. The various types of errors and the methods for determining the corresponding uncertainties have been discussed in detail by Bevington.[115] In this section, the estimates of uncertainties in the absolute values of temperature, mole fraction and reaction rates of various species due to probable errors in the experimental values have been obtained from the root mean square error (r.m.s.) defined as:

$$E_F \equiv \left\{ \sum_i \left(\frac{\partial \ \ln F}{\partial \ \ln Y_i} \frac{dY_i}{Y_i} \right)^2 \right\}^{1/2}$$

Mole Fraction of Stable Species

The mole fraction of stable species have been obtained by subjecting the gas samples to a mass spectrometric analysis. The r.m.s. error in the mole fraction of the species (a function of calibration spectra, flow measurements, accuracy of mass spectra and residual vector in the solution of overdetermined set of linear equations) is discussed in reference 47. The numerical values of the standard error vary from 3 to 10 percent for various species except H_2 at different positions. The average value of about 7 percent is considered a reasonable estimate for the uncertainty in the mole fraction of various stable species. The corresponding values of uncertainty for H_2 vary from 30 to 100 percent.

Mole Fraction of Hydroxyl Radical and Temperature

The concentration of hydroxyl radical is given by equation (4.21)

$$N_{OH} = \frac{z_{r-v}}{3.06\times10^{6}} \; \frac{\nabla_D}{\lambda_o^2} \; \frac{k_v}{A_k} \exp^{E_m/RT}$$

$$N_i = X_i \frac{P}{R_u T}$$

$$X_{OH} = \left(\frac{z_{r-v}}{3.06\times10^{6}} \; \frac{R_u}{A_k} \; \frac{1}{\lambda_o^2}\right)\frac{T}{P} \, k_o \, \nabla_D \exp^{E_m/RT}$$

Let $$Z_F \equiv \frac{z_{r-v}}{3.06\times10^{6}} \; \frac{R_u}{A_k} \; \frac{1}{\lambda_o^2}$$

= constant incorporating the fundamental properties such as transition probability partition function etc.

$$E_{OH}^2 = \left(\frac{dx_{OH}}{x_{OH}}\right)^2 = \left(\frac{dZ_F}{Z_F}\right)^2 + \left(\frac{dP}{P}\right)^2 + \left(\frac{dT}{T}\right)^2 + \left(\frac{d(\nabla_D)}{\nabla_D}\right)^2 + \left(\frac{d(k_o)}{k_o}\right)^2 + \frac{E_m}{RT^2}\left(\frac{dT}{T}\right)^2$$

The last term is negligible as compared to the first 4 terms as it is 4-6 orders of magnitude smaller.

$\frac{dZ_F}{Z_F}$ = uncertainty in the fundamental data such as transition particles, energy level, partition function 5 to 10 percent

$\leqq 0.10$

$\frac{d(\nabla_D)}{\nabla_D} \simeq$ uncertain in Doppler width proportional to the square root of temperature

$\simeq \frac{1}{2}\,(dT/T)$

$\frac{dk_o}{k_o}$ = uncertainty in the peak absorption coefficient and is function of resolution of the instrument, measurement of absorption line, optical path length

$\leq .20$

$\frac{dP}{P} \simeq$ uncertainty in pressure

$\simeq .02$

$$\frac{dT}{T} \simeq \frac{100}{1500} \simeq .07$$

$$E_{xOH}^{2} = .0100 + .0400 + .0056 + .0025 = 575$$

$$E = .24 \simeq 24 \text{ percent}$$

Uncertainty in the Reaction Rate

The reaction rate of a species is given by the equation 4.7

$$R_i = \frac{R_u v_u}{AM_i} \frac{dG_i}{dz}$$

Combining with (4.6)

$$R_i = \frac{R_u v_u}{AM_i} \frac{d}{dz} [\frac{N_i M_i}{R_u} (v + V_i)] = \frac{P}{ART} \frac{d}{dz} [x_i (v + V_i)]$$

$$E_{R_i}^{2} = (\frac{dP}{P})^2 + (\frac{dT}{T})^2 + \frac{d[\frac{d}{dz}(x_i(v+V_i))]^2}{[\frac{d}{dz}[x_i(v+V_i)]]^2}$$

The diffusion velocity V_i is given by the equation 4.5

$$V_i = - \frac{1}{x_i \Sigma \frac{x_j}{D_{ij}}} \frac{dx_i}{dz}$$

or $$E_{V_i}^{2} = (\frac{dx_i}{x_i})^2 + \frac{[d(\Sigma \frac{x_j}{D_i})]^2}{(\Sigma \frac{x_j}{D_{ij}})^2} + [\frac{d(\frac{dx_i}{dz})}{\frac{dx_i}{dz}}]^2$$

As seen from the previous section

$$\left(\frac{dx_i}{x_i}\right)^2 \simeq (.07)^2 = .0049$$

The uncertainty in the diffusion coefficients is of the order of 20 percent. Therefore

$$\left[\frac{d\left(\Sigma \frac{x_j}{D_{ij}}\right)}{\Sigma \frac{x_j}{D_{ij}}}\right]^2 = (.07)^2 + (.20)^2 = .0449$$

The derivatives of the mole fraction are taken by fitting a polynomial through the concentration profiles. The accuracy of curve fit varies from 5 to 20. Thus

$$\left[\frac{d\left(\frac{dx_i}{dz}\right)}{\frac{dx_i}{dz}}\right]^2 \simeq (.20)^2 \simeq .04$$

Hence

$$E_{V_i}^2 = .0049 + .0449 + .040$$

or $$E_{V_i} = 30 \text{ percent}$$

The magnitude of V_i is less than 20 percent as compared to v, the mass average velocity for all the species except H_2 and OH. Thus the uncertainty in absolute velocity $(v+V_i)$ is of the order 6 to 7 percent. Thus the uncertainty due to 3rd term of $E_{R_i}^2$ becomes

$$\left[\frac{d\left[\frac{d}{dz}\left(x_i(v+V_i)\right)\right]}{\frac{d}{dz}\left(x_i(v+V_i)\right)}\right]^2 = (.07)^2 + (.06)^2 + (.20)^2 = .0495$$

Hence

$$E_{R_i}^2 \simeq .0004 + .0049 + .0495$$

or $E_{R_i} \simeq 23.1$ percent

The uncertainties for the reaction rates of H_2 and OH are much higher.

APPENDIX 3

PROGRAM RATES FOR CALCULATION OF REACTION RATES

```
      PROGRAM RATES(INPUT,OUTPUT,PUNCH)
      INTEGER CNTROL(10),BDIM
      REAL B(12,5),Z(8,20),A(12,12),FR(20,20),XT(20),DF(20,20),
     2VA(20,20),RR(20,20),V(20),DDX(20,20),DXD(20),Y(20),PMLWT(20),
     3 GSUM(20),G(20,20),GM(20,20),FFR(20,20),SPECIE(10)

C     B= UNKNOWN COEFFICIENTS FOR THE FITTING FUNCTION
C     Z= NO OF VARIABLES FOR FITTING FUNCTION
C     FR= MOLE FRACTION ARRAY, XT= TEMPERATURE ARRAY, DF= DIFFUSION COEFFICIENT
C     ARRAY, VA= ABSOLUTE VELOCITY ARRAY, DDX,DXD= DERIVATIVES ARRAY,
C     Y= MOLE FRACTION ARRAY, PMLWT= MOLECULAR WEIGHT  OF MIXTURE ARRAY
C     G= FLUX FRACTION PROFILE ARRAY, S= COLLISIONAL DIAMETER
C     E= DEPTH OF ENERGY WELL FOR INTER MOLECULAR POTENTIAL
C     DELTA=ADDITIONAL TERM FOR POLAR MOLECULAR INTERACTION UN 6-12 POTENTIAL
C     W= MOLECULAR WEIGHT OF SPECIES ARRAY

      COMMON/GEL/SPECIE
      COMMON/PROPS/S(20),E(20),W(20),DELTA(20)
C     INTERMOLECULAR POTENTIAL DATA
    1 CONTINUE
      READ 201, JST,JPTV
      READ 605,NCASE,M,FUEL
      PRINT 606,NCASE,FUEL
C     FLOW  MEASUREMENT DATA
      READ 701,FLWCH,FLWO2,FLWAR,AREA
      SM = FLWO2+ FLWCH
      FRO = FLWO2/SM
      FRCH= FLWCH/SM
      READ 703, ROWCH, ROWO2, ROWAR
      READ 205, P, R
      SM= FLWO2+ FLWCH+ FLWAR
C     CALCULATIONS OF INITIAL MOLE FRACTION OF REACTANTS
      FR1 = FLWCH/SM
      FR2= FLWO2/SM
      FR3= FLWAR/SM
      ROW = (FR1* ROWCH+FR2*ROWO2+ FR3*ROWAR)*P
       WO= FR1*W(4)+FR2*W(1)+FR3*W(7)
      VO= SM/(AREA*60.0)
      READ 705, NS, FHPK, FCPK
C     CALCULATION OF MASS FRACTION OF ELEMENTS IN REACTANTS
      XMFC= FR1*12.*FCPK/WO
      XMFH = FR1*FHPK/WO
      XMFO = FR2*32./WO
      XMFA= FR3*W(7)/WO
      PHI= (FHPK/4.0+FCPK)*FR1/FR2
C     CALCULATIONS OF MOLE FRACTION OF VARIOUS SPECIES FROM MASS SPECT DATA
      CAL3 MSDATA(FR,XMFC,XMFH,XMFO,XMFA)
   62 READ 201,(CNTROL(I),I=1,10)
      MDIM=8
      NDIM=20
      BDIM=12
    3 FO9MAT (8F10.4)                                                   NLIN 600
       NB = IABS(CNTROL(1))                                             NLIN 660
       IF (NB .EQ. 0)   STOP                                            NLIN 670
       NPTS = IABS(CNTROL(2))                                           NLIN 680
       NVARS = IABS(CNTROL(3))                                          NLIN 690
       LIMIT = IABS(CNTROL(4))                                          NLIN 700
       PRINT 4, (CNTROL(I), I=1,10), NB,NPTS,NVARS,LIMIT                NLIN 710
       IF (CNTROL(5) .EQ. 0)   PRINT 11                                 NLIN 720
       IF (CNTROL(5) .GE. 4)   PRINT 10                                 NLIN 730
       IF (MOD(CNTROL(5),2) .NE. 0)   PRINT 9                           NLIN 740
       IF (CNTROL(6) .EQ. 0)   PRINT 16                                 NLIN 750
       IF (CNTROL(6) .NE. 0)   PRINT 12                                 NLIN 760
       IF (CNTROL(10) .EQ. 0)   PRINT 15                                NLIN 770
       IF (CNTROL(10) .NE. 0)   PRINT 14                                NLIN 780
       PRINT 8, MDIM, NDIM, BDIM                                        NLIN 820
                                                                        NLIN 830
     C          35H  MOST TEN PER CENT PER ITERATION      )             NLIN1010
       IF (CNTROL(8) .EQ. 1)   PRINT 27                                 NLIN 170
       IF (CNTROL(8) .EQ. 2)   PRINT 37                                 NLIN 180
       IF (CNTROL(8) .EQ. 3)   PRINT 47                                 NL+N 1 0
       IF (CNTROL(8) .EQ. 4)   PRINT 57                                 NLIN 200
       IF (CNTROL(8) .EQ. 5)   PRINT 6  7                               NLIN 210
      READ 3,(B(IB),IB=1,NB)
       PRINT 7                                                          NLIN 800
       PRINT 3, (B(I), I=1,NB)                                          NLIN 810
C INDEPENDET VARIABLE DISTANCE ABOVE BURNER SURFACE DATA
      READ 202,(Z(2,I),I=1,NPTS)
      READ 204,(XT(IT),IT=1,NPTS)
      DO 602 IS=1,NS
      READ 451, SPECIE(IS)
  602 CONTINUE
      PR=P/R
      DO 71 I=1,NPTS
       SSUM=0.0
      DO 72 IS=1,NS
      SSUM=SSUM+W(IS)*FR(IS,I)
   72 CONTINUE
      PMLWT(I)=SSUM
C     CALCULATIONS OF FLOW VELOCITY
      V(I)= XT(I)*WO*VO*(300.*SSUM)
   71 CONTINUE
      DO 312 I=1,NPTS
      IF (PMLWT(I)-44.0) 312,312,63
  312 CONTINUE
C     HYDROXYL RADICAL DATA
      NS= NS+1
      READ 401,(FR(NS,I),I=1,NPTS)
      DO 23 IS=1,NS
      DO 20 I=JST,JPTS
      L=I
      Z(1,L)=FR(IS,I)
   20 CONTINUE
C     FITTING FUNCTION FOR CONCENTRATION PROFILES
       CALL GAUSS(CNTROL,B,Z,MDIM,NDIM,BDIM,A)
      DO 193 I=JST,JPTS
       L=I
      DDX(IS,L)=B(2)+2.*B(3)*Z(2,L)+3.*B(4)*(Z(2,L)**2)
      FFR(IS,L)=B(1)+B(2)*Z(2,L)+B(3)*(Z(2,L)**2)+B(4)*(Z(2,L)**3)
  193 CONTINUE
      PRINT 192,(DDX(IS,I),I=1,NPTS)
      PRINT 192,(FFR(IS,I),I=1,NPTS)
      PRINT 192,(FR(IS,I),I=1,NPTS)
   23 CONTINUE
      IN=JST
   53 T=XT(IN)
       L=IN
      DO 251 IS=1,NS
       Y(IS)= FR(IS,IN)
  251 CONTINUE
C     CALCULATION OF DIFFUSION COEFFICIENTS
      CALL DMULTI(DF,P,T,Y,NS)
      DO 55 IS=1,NS
      PRIST 52,(DF(IS,JS),JS=1,NS)
   55 CONTINUE
      DO 162 IS=1,NS
      DRSUM= 0.0
      DO 163 JS=1,NS
      DRSUM= DRSUM+W(JS)*DF(IS,JS)*DDX(JS,L)
  163 CONTINUE
C     CALCULATION OF ABSOLUTE VELOCITY
      VA(IS,IN)=DRSUM/(PMLWT(IN)*FR(IS,IN))+V(IN)
  162 CONTINUE
      PRINT 76,(VA(IS,IN),IS=1,NS)
      IN=IN+1
      IF(IN-JPTS)53,53,54
   54 CONTINUE
      DO 155 I=1,NPTS
       GM(3,I)= 1.0/XT(I)
  155 CONTINUE
       PRINT 153,(GM(3,I),I=JST,JPTS)
      DO 154 IS=1,NS
C     CALCULATION OF MASS FLUX FRACTION PROFILE
   22 DO 81 I=JST,JPTS
      L=I
      Z(1,L)=FR(IS,I)*VA(IS,I)*W(IS)/(V(I)*PMLWT(I))
   81 CONTINUE
C     FITTING FUNCTION FOR MASS FLUX FRACTION PROFILE
       CALL GAUSS(CNTROL,B,Z,MDIM,NDIM,BDIM,A)
      DO 41 I=JST,JPTS
      L=I
C     CALCULATION OF REACTION RATES
      DXD(L) =  B(2)+2.*B(3)*Z(2,L)+3.*B(4)*(Z(2,L)**2)
      FFR(IS,L)=B(1)+B(2)*Z(2,L)+B(3)*(Z(2,L)**2)+B(4)*(Z(2,L)**3)
       RR(IS,L)=ROW*VO*DXD(L)/W(IS)
   41 CONTINUE
   94 FORMAT(1X,*RATES *,10(2X,E11.4)/)
  154 CONTINUE
      IF(W(7).EQ.28.) GO TO 533
      IF(W(7).EQ.40.) GO TO 532
  532 FR4= FR3
      FR3=0.0
      GO TO 535
  533 FR4=0.0
  535 PRINT 531
      PRINT 536,P,FR1,FR2,FR3,FR4,PHI
      PUNCH 541,P,FR1,FR2,FR3,FR4,PHI
      PRINT 537
  531 FORMAT(1X,2X,*P*,8X,*C2H46*,5X,*O2*,8X,*N2*,8X,*AR*,8X,*PHI*/)
      DO 322 I= JST,NPTS
      L=I
       PRINT 538,Z(2,L),(FR(IS,I),IS=1,NS),XT(I)
       PRINT 94,(RR(IS,L),IS=1,NS)
  322 CONTINUE
      PUNCH 263,(Z(2,I),I=1,8)
       PUNCH 263,(XT(I), I=JST,JPTS)
  263 FORMAT(10F8.3)
      DO 156 IS=1,NS
      PUNCH 544,SPECIE(IS)
      PUNCH 545,(FR(IS,I),I=JST,JPTS)
       PUNCH 545,(RR(IS,I),I=1,6)
  156 CONTINUE
  545 FORMAT(8F10.8)
  544 FORMAT(A10)
C     SUM4ATION OF MASS FLUX FRACTION
      DO 82 I=1,NPTS
      RSU4=0.0
      DO 181 IS=1,NS
      RSU4= RSUM+G(IS,I)
  181 CONTINUE
      GSUM(I)= RSUM
   82 CONTINUE
      PRINT 83,(GSUM(I), I=1,NPTS)
      READ 61,MN
   42 CONTINUE
      IF(MN.EQ.2) GO TO 1
    4  FORMAT  (32H1 NONLINEAR REGRESSION CONTROLS       1016 //         NLIN 610
     1    30H NUMBER OF PARAMETERS                   I12 /               NLIN 620
     2    30H NUMBER OF DATA POINTS                  I12 /               NLIN 630
     3    30H NUMBER OF VARIABLES                    I12 /               NLIN 640
     4    30H LIMIT ON NUMBER/ITERATIONS             I12 /     )         NLIN 650
    7  FORMAT (42H0 STARTING GUESSES FOR THE PARAMETERS B(J)   )         NLIN 910
    8  FORMAT (48H0 NONLINEAR REGRESSION ARRAY DECLARATIONS ARE        / NLIN 920
     1  4H  Z( I2,  1H, I3,  8H) AND B(  I2, 1H) /1H0)                   NLIN 930
                                                                         NLIN 940
    9  FORMAT (53H CNTROL(5) .NE. 0 (MOD 2), SO PRINT INPUT DATA.       )NLIN 950
   10  FORMAT (53H CNTROL(5) .GE. 4, SO PRINT MATRICES FOR NORMAL EQS. )NLIN 960
   11 FORMAT (* CNTROL(5) = 0, SO NO INTERMEDIATE OUTPUT *)              NLIN 970
   12  FORMAT (* CNTROL(6) .NE. 0, SO MINIMIZE RELATIVE LEAST SQUARES.*)NLIN 980
   14  FORMAT (52H CNTROL(10) NONZERO, PARAMETERS CAN CHANGE BY AT      /NLIN1000
   15  FORMAT (* CNTROL(10) = 0, SO UNCONSTRAINED PARAMETER CHANGES *)  NLIN1020
   16  FORMAT (* CNTROL(6) = 0, SO MINIMIZE LEAST SQUARES *)            NLIN1030
   27  FORMAT (*0 TERMINATION DUE TO RELATIVE CHANGE OF LESS THAN *,/,  NLIN 230
     1  *    1.0E-8 IN AVERAGE SUM OF SQUARES.  THE SUM OF SQUARES *,/  NLIN 240
     2  *    HAS BEEN REDUCED. *)                                        NLIN 250
   37  FORMAT (*0 TERMINATION DUE TO NEGLIGIBLE CHANGE IN SUM/SQUARES *)NLIN 260
   47  FORMAT (*0 TERMINATION DUE TO LIMIT ON NUMBER OF ITERATIONS *)   NLIN 270
   51 FORMAT(1H0,*Y(IS)*,10F8.6)
   52 FOR4AT(1X,*DF*,10(1X,E11.4))
   57  FORMAT (*0 TERMINATION DUE TO SINGULARITY OF NORMAL EQS *)       NLIN 280
   61 FORMAT(I1)
```

```
 67  FORMAT (*0 TERMINATION DUE TO NEGLIGIBLE CHANGE IN PARAMETERS.*)
 75 FORMAT(1H0,*V(I)*,10(2X,F8.3))
 76 FORMAT(1X,*VA(IS,IN)*, 10(1X,E11.4))
 83 FORMAT(1H0,*GSM*,9(1X,E11.4))
 93 FORMAT(1H0,*GI/FR*,9(1X,E11.4))
130 FORMAT(1H1)
158 FORMAT(1X,*DCO/CO*,8(2X,E11.4)/)
175 FORMAT(1H0,*PMLWT*,9(1X,E11.4))
192 FORMAT(1H0,*DDX/FFR*,10(2X,F8.6))
201 FORMAT( 10I6)
202 FORMAT(10F8.4)
204 FORMAT(10F8.3)
208 FORMAT(1H0,*FRMSANL*,10(2X,F8.6))
274 FORMAT( 1X,*TEMP*,10(2X,F8.3))
401 FORMAT(8F10.8)
402 FORMAT(1X,*OHCONC*,10(2X,F8.6))
451 FORMAT(A10)
536 FORMAT(1X,5(F5.4,5X),F6.4/)
537 FORMAT(1X,2X,*Z*,9X,*O2*,11X,*CO*,11X,*CO2*,10X,*C2H *,10X,*H2O*,
   1 10X,*H2*,12X,*M*,10X,*OH*,8X,*TEMP*/)
513 FORMAT(1H0,*P R*, F10.6,2X,F10.6)
538 FORMAT(1X,F6.4,2X,8(E11.4,2X),F6.1/)
541 FORMAT(10F8.6)
605 FORMAT(2I5,A10)
606 FORMAT(1X,*CASE NO=*, I4,2X, A10)
701 FORMAT(8F10.4)
702 FORMAT( 1H0,*FLW*,4F10.4)
703 FORMAT( 5F10.7)
704 FORMAT( 1H0, *ROW*,5F10.8)
706 FORMAT(1X,*FR1 2 3 ROW V*,6(2X,F9.6))
707 FORMAT(1H0,*XMF C H O A*,4F9.6)
 63 STOP
    END


      SUBROUTINE SETUP(CNTROL,B,Z,A,SUMSQ,MDIM,NDIM,BDIM)
      INTEGER   CNTROL(8), BDIM
      REAL  A(BDIM,BDIM), B(BDIM,4), Z(MDIM,NDIM)
CALCULATE THE TERMS IN THE MATRIX EQUATION      A * X = C
COMPUTE ONLY THE SUM OF SQUARES IF CNTROL(10) NEGATIVE, SINCE THE GAUSS
CYCLE DID NOT REDUCE THE SUM OF SQUARES..............................
      JJ = IABS(CNTROL(1))
      IF (CNTROL( 8) .EQ. -1)   GO TO 6
      DO 5  J=1,JJ
      B(J,3) = 0.0
      DO 5  K=1,JJ
    5 A(J,K) = 0.0

    6 CONTINUE
      NUMBER = IABS(CNTROL(2))
      SUMSQ = 0.0

      DO 15  N=1,NUMBER
      YC = YCOMP(N,B,Z,MDIM)
      ZN = Z(1,N)
      DEL Y = ZN - YC
      IF (CNTROL(6) .GT. 0  .AND. ZN .NE. 0.0)   DEL Y = DEL Y / ZN
 67  FORMAT (*0 TERMINATION DUE TO NEGLIGIBLE CHANGE IN PARAMETERS.*) NLIN 290
 75 FORMAT(1H0,*V(I)*,10(2X,F8.3))
 76 FORMAT(1X,*VA(IS,IN)*, 10(1X,E11.4))
 83 FORMAT(1H0,*GSM*,9(1X,E11.4))
 93 FORMAT(1H0,*GI/FR*,9(1X,E11.4))
130 FORMAT(1H1)
158 FORMAT(1X,*DCO/CO*,8(2X,E11.4)/)
175 FORMAT(1H0,*PMLWT*,9(1X,E11.4))
192 FORMAT(1H0,*DDX/FFR*,10(2X,F8.6))
201 FORMAT( 10I6)
202 FORMAT(10F8.4)
204 FORMAT(10F8.3)
208 FORMAT(1H0,*FRMSANL*,10(2X,F8.6))
274 FORMAT( 1X,*TEMP*,10(2X,F8.3))
401 FORMAT(8F10.8)
402 FORMAT(1X,*OHCONC*,10(2X,F8.6))
451 FORMAT(A10)
536 FORMAT(1X,5(F5.4,5X),F6.4/)
537 FORMAT(1X,2X,*Z*,9X,*O2*,11X,*CO*,11X,*CO2*,10X,*C2H *,10X,*H2O*,
   1 10X,*H2*,12X,*M*,10X,*OH*,8X,*TEMP*/)
513 FORMAT(1H0,*P R*, F10.6,2X,F10.6)
538 FORMAT(1X,F6.4,2X,8(E11.4,2X),F6.1/)
541 FORMAT(10F8.6)
605 FORMAT(2I5,A10)
606 FORMAT(1X,*CASE NO=*, I4,2X, A10)
701 FORMAT(8F10.4)
702 FORMAT( 1H0,*FLW*,4F10.4)
703 FORMAT( 5F10.7)
704 FORMAT( 1H0, *ROW*,5F10.8)
706 FORMAT(1X,*FR1 2 3 ROW V*,6(2X,F9.6))
707 FORMAT(1H0,*XMF C H O A*,4F9.6)
 63 STOP
    END
```

```
      SUBROUTINE SETUP(CNTROL,B,Z,A,SUMSQ,MDIM,NDIM,BDIM)                NLIN1080
      INTEGER   CNTROL(8), BDIM                                          NLIN1090
      REAL  A(BDIM,BDIM), B(BDIM,4), Z(MDIM,NDIM)                        NLIN1100
CALCULATE THE TERMS IN THE MATRIX EQUATION      A * X = C                NLIN1110
COMPUTE ONLY THE SUM OF SQUARES IF CNTROL(10) NEGATIVE, SINCE THE GAUSS NLIN1120
CYCLE DID NOT REDUCE THE SUM OF SQUARES...........................       NLIN1130
      JJ = IABS(CNTROL(1))                                               NLIN1140
      IF (CNTROL( 8) .EQ. -1)   GO TO 6                                  NLIN1150
      DO 5  J=1,JJ                                                       NLIN1160
      B(J,3) = 0.0                                                       NLIN1170
      DO 5  K=1,JJ                                                       NLIN1180
    5 A(J,K) = 0.0                                                       NLIN1190
                                                                         NLIN1200
    6 CONTINUE                                                           NLIN1210
      NUMBER = IABS(CNTROL(2))                                           NLIN1220
      SUMSQ = 0.0                                                        NLIN1230
                                                                         NLIN1240
      DO 15  N=1,NUMBER                                                  NLIN1250
      YC = YCOMP(N,B,Z,MDIM)                                             NLIN1260
      ZN = Z(1,N)                                                        NLIN1270
      DEL Y = ZN - YC                                                    NLIN1280
      IF (CNTROL(6) .GT. 0  .AND. ZN .NE. 0.0)   DEL Y = DEL Y / ZN      NLIN1290
      IF (CNTROL(6) .LT. 0  .AND. YC .NE. 0.0)   DEL Y = DEL Y / YC
      SUMSQ = SUMSQ + DEL Y ** 2
      IF (CNTROL(8) .LE. -1)   GO TO 15
      DO 10  K=1,JJ
      B(K,4) = DERIV(K,N,B,Z,MDIM)
      IF (CNTROL(6) .GT.0 .AND. ZN .NE. 0.0)   B(K,4) = B(K,4) / ZN
      IF (CNTROL(6) .LT. 0 .AND. YC .NE. 0.0)   B(K,4) = B(K,4) / YC
      B(K,3) = B(K,3) + B(K,4) * DEL Y
   10 CONTINUE
      DO 14  J=1,JJ
      DO 14  K=J,JJ
   14 A(J,K) = A(J,K) + B(J,4) * B(K,4)
   15 CONTINUE
      IF (CNTROL(8) .LE. -1)   RETURN

      DO 20  K=2,JJ
      L = K - 1
      DO 20  J=1,L
   20 A(K,J) = A(J,K)

      DO 35  I=1,JJ
      DENOM = ABS(A(I,I))
      DO 25  J=2,JJ
   25 DENOM = AMAX1(DENOM,ABS(A(I,J)))
      IF (DENOM.LE. 0.0)   DENOM = 1.0
      DO 30  K=1,JJ
   30 A(I,K) = A(I,K)/DENOM
   35 B(I,3) = B(I,3)  , DENOM

      RETURN
      END


      SUBROUTINE GAUSS (CNTROL, B, Z, MDIM,NDIM,BDIM, A)
      INTEGER   CNTROL(8), BDIM
      REAL   A(BDIM,BDIM), B(BDIM,4), Z(MDIM,NDIM)

    2 FORMAT (114H0CYCLE    SUM OF SQUARES      ************************
     1********** B(J)  PARAMETERS **********************************/ )

      EPS = 1.0E-7
      MWAY = 1
      NN = 0
      DTRMNT = 0.0
C1LL TO YCOMP HERE IS TO PERMIT ONE-TIME WRITING OF HOLLERITH TITLE....
      DUMMY = YCOMP(1,B,Z,MDIM)
      JJ = IABS(CNTROL(1))
      NUMBER = CNTROL(2)
      LIMIT = IABS(CNTROL(4))
      L = CNTROL(5)
      LL = L * (L - 1) * (L - 5)
      IF (LL .NE. 0)  PRINT 2
      CNTROL(7) = NN
      CNTROL(8) = 0
      DO 3  J=1,JJ
    3 B(J,2) = B(J,1)
```

```
       SCALE = 1.0
       MARK10 = CNTROL(10)

   10  CALL       SETUP(CNTROL,B,Z,A,SUMSQ,MDIM,NDIM,BDIM)

       IF (MWAY .NE. 2)   GO TO 12
       PRINT  13
   13  FORMAT (*0 THE FOLLOWING NORMAL EQUATIONS ARE SINGULAR *)
       CALL DMPMAT(CNTROL,BDIM,A,B(1,3))
       CNTROL(8) = 4
       GO TO 15

   12  IF (CNTROL(5) .GE. 4)   CALL DMPMAT(CNTROL,BDIM,A,B(1,3))
       IF (CNTROL(5) .GE. 4)   PRINT 2
       IF (NN .EQ. 0)   SQMIN = SUMSQ
       IF (NN .EQ. 0)   START = SUMSQ
       IF (SCALE .LT. 1.0)   NN = -NN
       IF (LL .NE. 0)   PRINT 14, NN, SUMSQ, (B(J,1), J=1,JJ)
   14  FORMAT (1H0,I4, E21.9, G22.8,4G16.8/(G48.8,4G16.8))
       NN = IABS(NN)
       NN = NN + 1
       CNTROL(7) = NN
       IF (NN .LE. LIMIT)   GO TO 20
       CNTROL(8) = 3
   15  DO 16  J=1,JJ
   16  B(J,1) = B(J,2)
       RETURN

   20  IF (NN .EQ. 1)   GO TO 40
       IF (SUMSQ .LT. SQMIN)   GO TO 34
   25  TEST = ABS((SUMSQ - SQMIN)/ SQMIN)
       IF (TEST .GT. EPS)   GO TO 30
       IF (CNTROL(8) .LE. 0)   CNTROL(8) = 2
CNTROL(8) = 2  SIGNALS THAT SUM OF SQUARES CHANGES NEGLIGIBLY..........
       GO TO 15

   30  IF (SUMSQ .LT. SQMIN)   GO TO 34
       CNTROL(8) = -1
       SCALE = 0.1 * SCSLE
CHOP CORRECTION SINCE IT APPEARS TOO LARGE............................
       DO 31  J=1,JJ
   31  B(J,5) = SCALE * B(J,5)
       GO TO 49

   34  DO 35  J=1,JJ
   35  B(J,2) = B(J,1)
       SQMIN = SUMSQ
       CNTROL(8) = 1
       IF (SCALE .LT. 1.0) CALL SETUP(CNTROL,B,Z,A,SUMSQ,MDIM,NDIM,BDIM)
       SCALE = 1.0

   40  CONTINUE
 CALCULATE SOLUTION FOR NORMAL EQUATIONS
       MWAY =  LINEQS(BDIM,JJ,A,B(1,3),DTRMNT,B(1,4))
       IF (MWAY .EQ. 2)   GO TO 10
 CORRECTIONS ARE STORED IN B(J,5) SINCE B(J,3) IS CHANGED BY SET-UP......
       DO 42  J=1,JJ
   42  B(J,5) = B(J,3)
CHECK WHETHER NEW CORRECTIONS ARE NEGLIGIBLE...........................
       DO 44 J=1,JJ
       DENOM = ABS(B(J,2))
       IF (DENOM .LT. 1.0E-7)   DENOM = 1.0
       TEST = ABS(B(J,3) - B(J,2)) / DENOM
   44  IF (TEST .GT. 1.0E-8)   GO TO 45
       CNTROL(8) = 5
      GO TO 15
   45  IF (CNTROL(10) .EQ. 0)   GO TO 49
       DO 47  J=1,JJ
       IF (ABS(B(J,5)) .LT. 0.05*ABS(B(J,2)))  GO TO 47
       B(J,5) = 0.05 * SIGN(B(J,2), B(J,5))
   47  CONTINUE

CORRECT THE CURRENT VALUES OF THE PARAMETERS.......................
   49  DO 50  J=1,JJ
   50  B(J,1) = B(J,2) + B(J,5)
       GO TO 10
       END



       SUBROUTINE FINALE(CNTROL, B, Z, MDIM,NDIM)
       DIMENSION   Z(MDIM,NDIM), B(1)
       INTEGER   CNTROL(8)
      COMMON/SPR/ SUM SQ
       JJ = IABS(CNTROL(1))
       NUMBER = IABS(CNTROL(2))
       AV = 0.0
       AV1 = 0.0
       AV2 = 0.0
       DEL MAX = 0.0
       REL MAX = 0.0
       REL AV = 0.0
       YMAX = 0.0
       ZMAX = 0.0
       ZZMAX = 0.0
       SUM SQ = 0.0
       RELSMSQ = 0.0
       N = 1
       PRINT 1, CNTROL(7), (B(J), J=1,JJ)
    1  FORMAT (8H1 AFTER       I3,      12H  ITERATIONS    /
     C          45H0 THE MINIMIZING VALUES OF THE PARAMETERS ARE //
     1  (1X,5E15.7))
       PRINT 2
    2  FORMAT(//118H0********************************************************
     1***************************************************************/)
       IF (CNTROL(6) .EQ. 1)   PRINT 3
       IF (CNTROL(6) .NE. 1)   PRINT 4
    3  FORMAT (94H0NUMBER              Y OBSERVED      Y CALCULATED
     1OBS - CALC       (OBS - CALC) / OBS          /)
    4  FORMAT (94H0NUMBER              Y OBSERVED      Y CALCULATED
     1OBS - CALC       (OBS - CALC) / CALC         /)

       DO 10  N=1,NUMBER
       YC = YCOMP(N,B,Z,MDIM)
      ZN = Z(1,N)                                                       NLIN2960
      DEL Y = ZN - YC                                                   NLIN2970
      SUM SQ = SUM SQ + DEL Y**2                                        NLIN2980
      AV = AV + DELY                                                    NLIN2990
      AV2 = AV2 + ABS(DEL Y)                                            NLIN3000
      CHECK = ABS(DEL Y)                                                NLIN3010
      IF (CHECK .GT. ABS(DEL MAX))     MARK  = N                        NLIN3020
      IF (CHECK .GT. ABS(DEL MAX))     DEL MAX = DEL Y                  NLIN3030
      ABS DEL = CHECK                                                   NLIN3040
      ABSVAL = ABS(DELY)                                                NLIN3050
      SAVE = DEL Y                                                      NLIN3060
    7 CONTINUE                                                          NLIN3070
      IF (CNTROL(6) .LE. 0  .AND. YC .NE. 0.0)   DEL Y = DEL Y / YC     NLIN3080
      IF (CNTROL(6) .EQ. 1  .AND. ZN .NE. 0.0)   DEL Y = DEL Y / ZN     NLIN3090
      RELSMSQ = RELSMSQ + DELY**2                                       NLIN3100
      REL AV = REL AV + DEL Y                                           NLIN3110
      CHECK = ABS(DEL Y)                                                NLIN3120
      IF (CHECK .GT. ABS(REL MAX))     MARK1 = N                        NLIN3130
      IF (CHECK .GT. ABS(REL MAX))     REL MAX = DEL Y                  NLIN3140
      ABSRAT = ABS(DEL Y)                                               NLIN3150
      AV1 = AV1 + DEL Y                                                 NLIN3160
      AV2 = AV2 + ABSRAT                                                NLIN3170
      PRINT 5,N,Z(1,N),YC,SAVE,DEL Y                                    NLIN3180
    5 FORMAT (I5,E23.5,E17.5,2E19.5)                                    NLIN3190
   10 CONTINUE                                                          NLIN3200
                                                                        NLIN3210
      D = NUMBER                                                        NLIN3220
      AV = AV/D                                                         NLIN3230
      AV1 = AV1/D                                                       NLIN3240
      AV2 = AV2/D                                                       NLIN3250
      RTMNSQ = SQRT(SUMSQ/D)                                            NLIN3260
      PRINT 11,  AV, AV1, AV2, DEL MAX, MARK, REL MAX, MARK1,           NLIN3270
     1         RTMNSQ, SUM SQ, RELSMSQ                                  NLIN3280
   11 FORMAT (30H0  AVERAGE DEVIATION          E14.5/                   NLIN3290
     1        30H     AVERAGE REL DEV          E14.5/                   NLIN3300
     2        30H     AVE ABS REL DEV          E14.5/                   NLIN3310
     3 30H   MAXIMUM DEVIATION          E14.5, 6X, 10H AT POINT       I4/NLIN3320
     4 30H   MAXIMUM REL DEV            E14.5, 6X, 10H AT POINT       I4/NLIN3330
     5        30H   ROOT MEAN SQUARE DEVIATION E14.5/                   NLIN3340
     6        30H   FINAL SUM OF SQUARES       E14.5/                   NLIN3350
     7        30H   RELATIVE SUM/SQS           E14.5)                   NLIN3360
  108 FORMAT (5F20.5)                                                   NLIN3370
  109 FORMAT (//)                                                       NLIN3380
  110 FORMAT (I20, F20.8)                                               NLIN3390
      RETURN                                                            NLIN3400
      END                                                               NLIN3410



                                                                        NLIN3420
      FUNCTION LINEQS(M,N,A,B,DTRMNT,Z)                                 NLIN3430
      COMMON  CNTROL                                                    NLIN3440
      INTEGER   CNTROL(8)                                               NLIN3450
      REAL   A(M,M), B(M), Z(M)                                         NLIN3460
COMPUTE SOLUTION OF NORMAL EQS BY GAUSSIAN ELIMINATION, PARTIAL PIVOTINGNLIN3470
      I=M                                                               NLIN3480
      EPS = 1.0E-30                                                     NLIN3490
      NM1=N-1                                                           NLIN3500
      DO 40 J=1,NM1                                                     NLIN3510
      J1=J+1                                                            NLIN3520
C=. FIND ELEMENT OF COL J, ROWS J-N, WHICH HAS MAX ABSOLUTE VALUE.      NLIN3530
      LMAX=J                                                            NLIN3540
      RMAX=ABS(A(J,J))                                                  NLIN3550
      DO 8 K=J1,N                                                       NLIN3560
      RNEXT=ABS(A(K,J))                                                 NLIN3570
      IF (RMAX .GE. RNEXT) GO TO 8                                      NLIN3580
      RMAX=RNEXT                                                        NLIN3590
      LMAX=K                                                            NLIN3600
    8 CONTINUE                                                          NLIN3610
      IF (LMAX .NE. J) GO TO 10                                         NLIN3620
C=. MAX ELEMENT IN COLUMN IS ON DIAGONAL                                 NLIN3630
        IF (ABS(A(J,J)) .LT. EPS)   GO TO 94                            NLIN3640
        GO TO 20                                                        NLIN3650
C=. MAX ELEMENT IS NOT ON DIAGONAL. EXCHANGE ROWS J AND LMAX.            NLIN3660
   10 DO 12 L=J,N                                                       NLIN3670
      W=A(J,L)                                                          NLIN3680
      A(J,L)=A(LMAX,L)                                                  NLIN3690
      A(LMAX,L)=W                                                       NLIN3700
   12  CONTINUE                                                         NLIN3710
       W = B(J)                                                         NLIN3720
       B(J) = B(LMAX)                                                   NLIN3730
   14  B(LMAX) = W                                                      NLIN3740
       DTRMNT = -DTRMNT                                                 NLIN3750
C.. ZERO COLUMN J BELOW THE DIAGONAL.                                    NLIN3760
   20 Z(J)=1./A(J,J)                                                    NLIN3770
      DO 30 K=J1,N                                                      NLIN3780
      IF (A(K,J)) 22,30,22                                              NLIN3790
   22 W=-Z(J)*A(K,J)                                                    NLIN3800
      DO 24 L=J1,N                                                      NLIN3810
      A(K,L)=W*A(J,L)+A(K,L)                                            NLIN3820
   24  CONTINUE                                                         NLIN3830
   26  B(K) = W * B(J) + B(K)                                           NLIN3840
   30 CONTINUE                                                          NLIN3850
   40 CONTINUE                                                          NLIN3860
                                                                        NLIN3870
        IF (ABS(A(N,N)) .LT. 1.0E-30)   GO TO 94                        NLIN3880
C.. OBTAIN SOLUTION BY BACK SUBSTITUTION.                                NLIN3910
   42 Z(N)=1./A(N,N)                                                    NLIN3890
                                                                        NLIN3900
       B(N) = Z(N) * B(N)                                               NLIN3920
      DO 60 K=1,NM1                                                     NLIN3930
      J=N-K                                                             NLIN3940
      J1=J+1                                                            NLIN3950
      W=0.                                                              NLIN3960
      DO 56 I=J1,N                                                      NLIN3970
       W = A(J,I) * B(I) + W                                            NLIN3980
   56  CONTINUE                                                         NLIN3990
   58  B(J) = (B(J) - W) * Z(J)                                          NLIN4000
   60 CONTINUE                                                          NLIN4010
                                                                        NLIN4020
C=. EVALUATE DETERMINANT.                                                NLIN4030
      MDSW=1                                                            NLIN4040
CAN SKIP THE EVALUATION OF THE DETERMINANT BY PRE-SETTING TO ZERO...... NLIN4050
        IF (DTRMNT .EQ. 0.0)   GO TO 74                                 NLIN4060
   70 DO 72 J=1,N
   72 DTRMNT=DTRMNT*A(J,J)                                              NLIN4070
   74  LINEQS = 1                                                       NLIN4080
   80  CONTINUE                                                         NLIN4090
       RETURN                                                           NLIN4100
C                                                                       NLIN4110
CONTINUE HERE FOR SINGULAR OR NEAR-SINGULAR CASE....................    NLIN4120
   94  LINEQS = 2                                                       NLIN4130
       DTRMNT=0.                                                        NLIN4140
       GO TO 80                                                         NLIN4150
       END                                                              NLIN4160
                                                                        NLIN4170

        SUBROUTINE DMPMAT(CNTROL,M,A,C)
        INTEGER   CNTROL(1)                                             NLIN4180
        REAL   A(M,M), C(M)                                             NLIN4190
                                                                        NLIN4200
        IF (CNTROL(10) .EQ. -1)   RETURN                                NLIN4210
        JJ = CNTROL(1)                                                  NLIN4220
        PRINT 1, CNTROL(7)                                              NLIN4230
                                                                        NLIN4240
    1  FORMAT (15H0 AT ITERATION  I3,                                   NLIN4250
     1 59H, IN THE MATRIX EQUATION  A X = C, THE ROWS OF C AND A ARE  / NLIN4260
     3115H  J        C(J)          ********************  A(J,K)  *****NLIN4270
     4**************************************************  )            NLIN4280
                                                                        NLIN4290
        DO 2  J=1,JJ                                                    NLIN4300
    2   PRINT 3, J, C(J), (A(J,K), K=1,JJ)                              NLIN4310
    3   FORMAT (1H I2, E15.5, E20.5,4E15.5/ (E38.5,4E15.5) )            NLIN4320
                                                                        NLIN4330
        PRINT 4                                                         NLIN4340
    4   FORMAT (1X)                                                     NLIN4350
        RETURN                                                          NLIN4360
        END                                                             NLIN4370
                                                                        NLIN4380
                                                                        NLIN4390


       FUNCTION DERIV(K,N,B,Z,MDIM)
       REAL    B(1), Z(MDIM,1)                                          NLIN4400
                                                                        NLIN4410
COMPUTE FINITE DIFFERENCE APPROXIMATIONS TO PARTIAL DERIVATIVES IN      NLIN4420
CASE THIS ROUTINE IS NOT SUPPLIED BY USER.......................        NLIN4430
                                                                        NLIN4440
       J = K                                                            NLIN4450
       H = 0.00001 * ABS(B(J))                                          NLIN4460
       IF (H .LT. 1.0E-5)   H = 1.0E-5                                  NLIN4470
       BJ = B(J)                                                        NLIN4480
       B(J) = BJ + H                                                    NLIN4490
       Y2 = YCOMP(N,B,Z,MDIM)                                           NLIN4500
       B(J) = BJ - H                                                    NLIN4510
       Y1 = YCOMP(N,B,Z,MDIM)                                           NLIN4520
       B(J) = BJ                                                        NLIN4530
       DERIV = (Y2 - Y1) / (2.0* H)                                     NLIN4540
       RETURN                                                           NLIN4550
       END                                                              NLIN4560
                                                                        NLIN4570
```

```
      SUBROUTINE STOCK (TSTAR, DELMAX)
      DIMENSION T(65), D(9)
      COMMON/STKMYR/N1, N2, N3, T1, T2, T3, M1, M2, M3, D1, D2, D3, TT,
     1              DD
      DATA (T(I), I = 1, 65)/0.1, 0.2, 0.3, 0.4, 0.5, 0.6, 0.7, 0.8, 0.9
     1,    1.0, 1.2, 1.4, 1.6, 1.8, 2.0, 2.5, 3.0, 3.5, 4.0, 5.0, 6.0,
     2     7.0, 8.0, 9.0, 10.0, 12.0, 14.0, 16.0, 18.0, 20.0, 25.0,
     3     30.0, 35.0, 40.0, 50.0, 75.0, 100.0, 28*1000.0/
      DATA (D(I), I = 1, 9)/0.0, 0.25, 0.5, 0.75, 1., 1.5, 2., 2.5, 5./
      TT = TSTAR
      DD = DELMAX
      IF ((TSTAR .GE. T(1)) .AND. (TSTAR .LE. T(37)) .AND. (DELMAX .GE.
     1D(1)).AND. (DELMAX .LE.D(8))) GO TO 1
      PRINT 2, TSTAR, DELMAX
    2 FORMAT (*-  E R R O R    CALL FOR STOCKMAYER (12-6-3) COLLISION IN
     1TEGRALS WITH TSTAR = * E12.4, * AND DELTA MAX = * E12.4/* IS OUT O
     2F RANGE OF 0.1 .LE. TSTAR .LE. 100.0 AND 0.0 .LE. DELTA MAX .LE. 2
     3.5. ALL INTEGRALS WILL BE SET EQUAL TO 1.*)
      N1 = 0
      RETURN
    1 N1 = 1
      N2 = 65
   30 N21 = N2 - N1
      IF (TSTAR .GE. T(N1) .AND. TSTAR .LE. T(N2)) GO TO 10
      IF (N21 .EQ. 1) GO TO 20
      N1 = N2
      N2 = N2 + N21/2
      GO TO 30
   10 IF (N21 .EQ. 1) GO TO 40
      N2 = N1 + N21/2
      GO TO 30
   20 N1 = N2
      N2 = N2 + 1
   40 N3 = N2 + 1
      IF (N2.LE. 36) GO TO 142
      N3 = N2
      N2 = N1
      N1 = N1 - 1
  142 T1 = T(N1)
      T2 = T(N2)
      T3 = T(N3)
      IF (DELMAX .EQ. 0.0) RETURN
      M1 = 1
      M2 = 9
  130 M21 = M2 - M1
      IF (DELMAX .GE. D(M1) .AND. DELMAX .LE. D(M2)) GO TO 110
      IF (M21  .EQ. 1) GO TO 120
      M1 = M2
      M2 = M2 + M21/2
      GO TO 130
  110 IF (M21 .EQ. 1) GO TO 140
      M2 = M1 + M21/2
      GO TO 130
  120 M1 = M2
      M2 = M2 + 1
```

```
140 M3 = M2 + 1
    IF (M2 .LE. 7) GO TO 141
    M3 = M2
    M2 = M1
    M1 = M1 - 1
141 D1 = D(M1)
    D2 = D(M2)
    D3 = D(M3)
    RETURN
    END


    SUBROUTINE OMDIFF(OMEGA)
    DIMENSION O(8,37)
    COMMON/STKMYR/N1, N2, N3, T1, T2, T3, M1, M2, M3, D1, D2, D3,
   1              TSTAR, DELMAX
    DATA (O(I), I = 1, 176)/4.0079, 4.002, 4.655, 5.521, 6.454, 8.214,
   1     9.824, 11.31, 3.13, 3.164, 3.355, 3.721, 4.198, 5.23, 6.225,
   2     7.16, 2.6494, 2.657, 2.77, 3.002, 3.319, 4.054, 4.785, 5.483,
   3     2.3144, 2.32, 2.402, 2.572, 2.812, 3.386, 3.972,4.539,2.0661,
   4     2.073, 2.14, 2.278, 2.472, 2.946, 3.437, 3.918, 1.8767,1.885,
   5     1.944, 2.06, 2.225, 2.628, 3.054, 3.474, 1.7293, 1.738,1.791,
   6     1.893, 2.036, 2.388, 2.763, 3.137, 1.6122, 1.622, 1.670,
   7     1.760, 1.886, 2.198, 2.535, 2.872, 1.5175, 1.527,1.572,1.653,
   8     1.765, 2.044, 2.349, 2.657, 1.4398, 1.45, 1.49, 1.564, 1.665,
   9     1.917, 2.196, 2.478, 1.3204, 1.33, 1.364, 1.425, 1.509, 1.72,
   *     1.956, 2.199, 1.2336, 1.242, 1.272, 1.324, 1.394,1.573,1.777,
   1     1.99, 1.1679, 1.176, 1.202, 1.246, 1.306, 1.461, 1.639,1.827,
   2     1.1166, 1.124, 1.146, 1.185, 1.237, 1.372, 1.53,1.698,1.0753,
   3     1.082, 1.102, 1.135, 1.181, 1.3, 1.441, 1.592, 1.0006, 1.005,
   4     1.02, 1.046, 1.08, 1.17, 1.278, 1.397, .95003, .9538, .9656,
   5     .9852, 1.012, 1.082, 1.168, 1.265, .91311, .9162,.9256,.9413,
   6     .9626, 1.019, 1.09, 1.17, .88453, .8871, .8948, .9076, .9252,
   7     .9721, 1.031, 1.098, .84277, .8446, .8501, .8592,.8716,.9053,
   8     .9483, .9984, .81827, .8142, .8183, .8251, .8344,.8598,.8927,
   9     .9316, .78976, .7908, .794, .7993, .8066, .8265, .8526,.8836/
    DATA (O(I), I = 177, 296)/.77111, .772, .7745, .7788, .7846,.8007,
   1     .8219, .8474, .75553, .7562, .7584, .7619, .7667, .78, .7976,
   2     .8189, .7422, .7428, .7446, .7475, .7515, .7627, .7776,.7957,
   3     .72022, .7206, .722, .7241, .7271, .7354, .7464, .76, .7254,
   4     .7029, .7039, .7055, .7078, .7142, .7228, .7334, .68776,.688,
   5     .6888, .6901, .6919, .697, .704, .7125, .6751, .6753, .676,
   6     .677, .6785, .6827, .6884, .6955, .66405, .6642, .6648,.6657,
   7     .6669, .6704, .6752, .6811, .64136, .6415, .6418,.6425,.6433,
   8     .6457, .649, .6531, .6235, .6236, .6239, .6243, .6249, .6267,
   9     .6291, .6321, .60882, .6089, .6091, .6094, .6099,.6112,.6131,
   *     .6154, .5964, .5964, .5966, .5969, .5972, .5983, .5998,.6017,
   1     .57626, .5763, .5764, .5766, .5768, .5775,.5785,.5798,.54146,
   2     .5415, .5416, .5416, .5418, .5421, .5424, .5429, .51803,
   3     .5181, .5182, .5184, .5184, .5185, .5186, .5187/
    IF (N1 .NE. 0) GO TO 1
    OMEGA = 1.0
    RETURN
  1 IF (DELMAX .EQ. 0.0) GO TO 3
    CALL FITLAG(TSTAR, T1, T2, T3, O(M1,N1), O(M1,N2), O(M1,N3), O1)
    CALL FITLAG(TSTAR, T1, T2, T3, O(M2,N1), O(M2,N2), O(M2,N3), O2)
```

```
      CALL FITLAG(TSTAR, T1, T2, T3, O(M3,N1), O(M3,N2), O(M3,N3), O3)
      CALL FITLAG(DELMAX, D1, D2, D3, O1, O2, O3, BIGO)
      GO TO 4
    3 CALL FITLAG (TSTAR, T1, T2, T3, O(1,N1), O(1,N2), O(1,N3), BIGO)
    4 OMEGA = BIGO
      RETURN
      END



      SUBROUTINE DMULTI (D, P, T, Y, N)

CALCULATES MULTICOMPONENT DIFFUSION COEFFICIENTS

      COMMON/PROPS/S(20), E(20), W(20), DELTA(20)
      DIMENSION D(20,20),XD(20,20),Y(20),ZZ(20),X(20,20)
      DIMENSION F(20,20)
      F1 = 0.002628 * T**1.5/P
      IF ( N .EQ. 1) GO TO 100
      N1 = N - 1
      DO 1 I = 1, N1
      I1 = I + 1
      DO 2 J = I1, N
      WIJ = W(I) * W(J) * 2.0/(W(I) + W(J))
      TSTAR = T/SQRT(E(I) * E(J))
      SIJ = (S(I) + S(J))/2.0
      DIJ = SQRT(DELTA(I) * DELTA(J)) * (SQRT(S(I) * S(J))/SIJ)**3
      CALL STOCK (TSTAR, DIJ)
      CALL OMDIFF(OM11)
      DIJ =F1/(SQRT(WIJ) * SIJ**2 * OM11)
      XD(I,J) = Y(J)/DIJ
      XD(J,I) = Y(I)/DIJ
    2 CONTINUE
    1 CONTINUE
      IF (N .EQ. 2) GO TO 200
      DO 3 I = 1, N
      SUM = 0.0
      DO 4 J = 1, N
      IF (I .EQ. J) GO TO 4
      SUM = SUM + XD(I,J)
    4 CONTINUE
      ZZ(I)= SUM/W(I)
    3 CONTINUE
      DO 5 I = 1, N
      F(I,I) = 0.0
      X(I,I) = 0.0
      YI = Y(I)
      ZI=ZZ(I)
      DO 6 J = 1, N
      IF (I .EQ. J) GO TO 6
      F(I,J) = YI/Y(J) * XD(I,J) + W(J) * ZI
      X(I,J) = F(I,J)
    6 CONTINUE
    5 CONTINUE
      SUM = 0.0
      DO 7 I = 1, N
      SUM = SUM + Y(I) * W(I)
```

```
  7 CONTINUE
    DETF = DTRMNT(20, N,X,ZZ)
    SUM = SUM/DETF
    DO 10 I = 1, N
    D(I,I) = 0.0
    IP1 = I + 1
    IM1 = I - 1
    DO 20 K = 1, IM1
    DO 21 L = 1, IM1
    X(K,L) = F(K,L)
 21 CONTINUE
    DO 22 L = IP1, N
    X(K,L-1) = F(K,L)
 22 CONTINUE
 20 CONTINUE
    DO 23 K = IP1, N
    DO 24 L = 1, IM1
    X(K-1,L) = F(K,L)
 24 CONTINUE
    DO 25 L = IP1, N
    X(K-1, L-1) = F(K,L)
 25 CONTINUE
 23 CONTINUE
    FII= DTRMNT(20,N1,X,ZZ)
    DO 30 J = 1, N
    IF (I .EQ. J) GO TO 30
    JP1 = J + 1
    JM1 = J - 1
    DO 31 K = 1, JM1
    DO 32 L = 1, IM1
    X(K,L) = F(K,L)
 32 CONTINUE
    DO 33 L = IP1, N
    X(K,L-1) = F(K,L)
 33 CONTINUE
 31 CONTINUE
    DO 35 K = JP1, N
    DO 36 L = 1, IM1
    X(K-1,L) = F(K,L)
 36 CONTINUE
    DO 37 L = IP1, N
 37 X(K-1,L-1) = F(K,L)
 35 CONTINUE
    FACTOR = (-1)**(I + J)
    FIJ = FACTOR*DTRMNT(20,N1,X,ZZ)
    D(I,J) = SUM * (FIJ - FII)/W(J)
 30 CONTINUE
 10 CONTINUE
    RETURN
100 TSTAR = T/E(1)
    CALL STOCK(TSTAR, DELTA(1))
    CALL OMDIFF(OM11)
    D(1,1) = F1/(SQRT(W(1)) * S(1)**2 * OM11)
    RETURN
200 D(1,1) = 0.0
    D(2,2) = 0.0
    D(1,2) = Y(2)/XD(2,2)
```

```
      D(2,1) = D(1,2)
      RETURN
      END


      FUNCTION DTRMNT(M, N,AB,ZZ)
CALCULATES DETERMINANT OF N BY N UPPER LEFT HAND CORNER OF M BY M MATRIX
      DIMENSION AB(M,M), ZZ(M)
      EPS = 1.0E-100
      DTRMNT = 1.0
      NM1=N-1
      DO 40 J=1,NM1
      J1=J+1
      LMAX=J
      RMAX=ABS(AB(J,J))
      DO 8 K=J1,N
      RNEXT=ABS(AB(K,J))
      IF (RMAX .GE. RNEXT) GO TO 8
      RMAX=RNEXT
      LMAX=K
    8 CONTINUE
      IF (LMAX .NE. J) GO TO 10
      IF(ABS(AB(J,J)).LT.EPS) GO TO 94
       GO TO 20
   10 DO 12 L=J,N
      W= AB(J,L)
      AB(J,L)= AB(LMAX,L)
      AB(LMAX,L)=W
   12  CONTINUE
       DTRMNT = -DTRMNT
   20 ZZ(J)= 1.0/AB(J,J)
      DO 30 K=J1,N
      IF (AB(J,K) .EQ. 0.) GO TO 30
      W=-ZZ(J)*AB(K,J)
      DO 24 L=J1,N
      AB(K,L)=W*AB(J,L)+AB(K,L)
   24  CONTINUE
   30 CONTINUE
   40 CONTINUE
   70 DO 72 J=1,N
   72 DTRMNT=DTRMNT*AB(J,J)
      RETURN
   94 DTRMNT = 0.0
      RETURN
      END
       SUBROUTINE FITLAG (X,X1,X2,X3,Y1,Y2,Y3, Y)
       AA = Y1 / ((X1-X2) * (X1-X3))
       BB = Y2/((X2-X1) * (X2-X3))
       CC = Y3/((X3-X1) * (X3-X2))
       A = AA + BB + CC
       B = - ((X2+X3)*AA + (X1+X3)*BB + (X1+X2)*CC)
       C = X2*X3*AA + X1*X3*BB + X1*X2*CC
       Y = ((A*X + B)*X + C)
       RETURN
      END


        FUNCTION YCOMP (N,B,Z,MDIM)
       DIMENSION B(1),Z(MDIM,2)
C     FITTING FUNCTION
      YCOMP=B(1)+B(2)*Z(2,N)+B(3)*(Z(2,N)**2)+B(4)*(Z(2,N)**3)
       RETURN
      END


      BLOCK DATA
      COMMON/PROPS/S(20),E(20),W(20),DELTA(20)
      REAL NAME(20)
      DATA (NAME(I),W(I),DELTA(I),S(I),E(I),I= 1,8)/
     1 2HO2, 32.0, 0.0, 3.467, 106.7,
     2 2HCO, 28.01, 0.0, 3.69, 9.17,
     3 3HCO2, 44.01, 0.0, 3.941, 195.2,
     4 3HH2O, 18.01, 1.2, 2.71, 506.0,
     5 2HH2, 2.016, 0.0, 2.915, 38.0,
     6 2HN2, 28.0, 0.0, 3.798, 71.4,
     7 2HOH, 17.0, .754, 2.662, 506.,
     6 4HH2CO, 30.0, 0.0, 4.232, 205.0/
       END
```

APPENDIX 3A

```
C    PROGRAM TO REDUCE MASS SPECTROMETER DATA


       SUBROUTINE MSDATA (FR,XMFC,XMFH,XMFO,XMFA)
      DIMENSION A(50,10),B(50,11),X(10,11),U(50,11),SUM(11),W(10,21),
     1WT(50),STDERR(10), SPECIE(10),MOLWT(10),NPEAKS(10),SENS(10),
     2MASNO (50,10),RELINT(50,10),HT(50),MNODAT(50),D(10),P(10),XF(10),
     3DIV(50,10), C(10),DXFDX(10,10),QUAN1(10),QUAN2(10,10),TERM1(10),
     4TERM2(10),TERM2A(10),ERRXF(10)
      DIMENSION FR(20,20)
C    READ COMPONENT SPECTRA DATA  (JMAX COMPONENTS)
       INPT=1
    5 J= 0
   10 J=J+1
      READ 100, SPECIE(J), MOLWT(J), NPEAKS(J), SENS(J)
  100 FORMAT(A10,I5,I2,F5.0)
      IF(MOLWT(J).EQ.0) GO TO 15
      NPKS = NPEAKS(J)
      READ 110, (MASNO(K,J), RELINT(K,J), K=1,NPKS)
  110 FORMAT (10(I3,F5.0))
      GO TO 10
   15 JMAX = J-1
C    READ UNKNOWN SPECTRA DATA
   16 READ 115, CASEID, NDATPK, (MNODAT(I),HT(I),I=1,NDATPK)
  115 FORMAT(A6,I2,9(I3,F5.0)/(10(I3,F5.0)))
C    ARRANGE THE DATA INTO THE A(I,J) MATRIX
C    I = NO OF UNKNOWN MASS PEAK
   17 DO 35 I=1,NDATPK
C    FIND A(I,J) J=1-N
      M = MNODAT(I)
C    SEARCH EACH COMPONENT TO FIND ANY PEAK AT M
      J=0
   20 J=J+1
C    J = COMPONENT NO
      IF(MOLWT(J).EQ.0) GO TO 35
      K=0
   22 K=K+1
C    K = PEAK NO FOR JTH COMPONENT
      IF(K.GT.NPEAKS(J)) A(I,J)=0.
      IF(K.GT.NPEAKS(J)) GO TO 20
      IF(MASNO(K,J).EQ.M) GO TO 30
      GO TO 22
   30 A(I,J)=RELINT(K,J)
      GO TO 20
   35 CONTINUE
C    GENERATE RIGHT SIDE MATRIX B
      DO 45 I=1,NDATPK
      B(I,1) = HT(I)
   45 CONTINUE
C    OTHER DATA FOR SOLUTION ROUTINE
      M = NDATPK
      N = JMAX
      IP = 1+N
      WT(1) = -1
      INVRSE = 1
      DO 46 J=2,IP
      DO 46 I=1,M
   46 B(I,J) =0.
      PRINT 130
      PRINT 119, CASEID
  119 FORMAT(5X,8HCASE NO ,A6//)
C
C   CALIBRATION SPECTRA OUTPUT
      PRINT 120,(SPECIE(J),J=1,JMAX)
  120 FORMAT(10X38HCALIBRATION SPECTRA FOR OBSERVED PEAKS//4X3HM/E,3X,
     1(12A10)/)
      DO 60 I=1,NDATPK
      PRINT 121, MNODAT(I), (A(I,J),J=1,JMAX)
   60 CONTINUE
      PRINT 132, (SENS(J),J=1,JMAX)
  132 FORMAT(3X4HSENS3X,(12(F7.3,3X)))
  121 FORMAT(4X,I2,4X,(12(F7.3,3X)))
C   SOLVE THE AX=B MATRIX
      CALL GLSP(A,M,N,B,IP,X,U,SUM,WT,INVRSE,STDERR)
C   CALCULATE PARTIAL PRESSURES AND MOLE FRACTIONS
      DO 50 J=1,JMAX
      P(J) = X(J,1)*100./SENS(J)
      IF(J.NE.1) GO TO 47
       TOT = P(J)
      GO TO 50
   47 PTOT = PTOT+P(J)
   50 CONTINUE
      DO 48 J=1,JMAX
      XF(J) = P(J)/PTOT
   48 CONTINUE
      DO 52 K=1,NDATPK
      DO 51 J=1,JMAX
      DIV(K,J) = X(J,1)*A(K,J)
   51 CONTINUE
   52 CONTINUE
      IF (M.EQ.N) GO TO 90
C   ERROR CALCULATIONS
C   1.  PARTIAL DERIVATIVES
      DO 80 J=1,JMAX
   80 C(J) = 1./SENS(J)
C   PARTIAL XF(I) PARTIALX(J,1) = DXFDX(I,J)
      DO 82 I=1,JMAX
      DO 82 J=1,JMAX
      IF(I.EQ.J) GO TO 81
      DXFDX(I,J)=-C(J)*XF(I)**2/(C(I)*X(I,1))
      GO TO 82
   81 DXFDX(I,J)=XF(I)*(1.-XF(I))/X(I,1)
   82 CONTINUE
C   2.  ERRORS
      DO 89 J=1,JMAX
      DO 84 I=1,JMAX
      L=I+1
      QUAN1(I)=X(I,L)*DXFDX(J,I)**2
      IF(I.NE.1) GO TO 83
      TERM1(J)=QUAN1(I)
      GO TO 84
   83 TERM1(J) =TERM1(J)+QUAN1(I)
   84 CONTINUE
      DO 88 I=1,JMAX
      DO 86 K=I,JMAX
      L=K+1
      QUAN2(I,K) = 2.*X(I,L)*DXFDX(J,I)*DXFDX(J,K)
      IF(K.NE.I) GO TO 85
      TERM2A(I) = QUAN2(I,K)
      GO TO 86
   85 TERM2A(I) = TERM2K(I)+QUAN2(I,K)
   86 CONTINUE
      IF(I.NE.1) GO TO 87
      TERM2(J)=TERM2A(I)
      GO TO 88
   87 TERM2(J) = TERM2(1) + TERM2A(I)
   88 CONTINUE
   89 ERRXF(J)= SQRT(TERM2(J)-TERM1(J))
C
C    *****DATA OUTPUT
C
C    CALCULATED DATA
   90 PRINT 140
      DATA RESD/9HRESIDUALS/
      PRINT 122,(SPECIE(J),J=1,JMAX),RESD
  122 FORMAT(21X16HMIXTURE ANALYSIS//4X3HM/E,3X9HMIX SPECT,1X,
     1(11(A10)/))
      DO 65 K=1,NDATPK
      PRINT 123, MNODAT(K),HT(K), (DIV(K,J), J=1,JMAX),U(K,1)
   65 CONTINUE
  123 FORMAT(4X,I2,5X,F7.2,2X,(11(F7.2,3X)))
      PRINT 125,(XF(J),J=1,JMAX)
      CALL CORRT(XF,XMFO,XMFC,XMFH,XMFA,JMAX)
      PRINT 125, (XF(J),J=1,JMAX)
      DO 231 IS=1,JMAX
      FR(IS,INPT) = XF(IS)
  231 CONTINUE
      INPT= INPT+1
  125 FORMAT(1X,/1X13HMOLE FRACTION,6X,(11(F7.6,3X)))
C    ERROR DATA
      IF (M.EQ.N) GO TO 91
      PRINT 131, (ERRXF(J),J=1,JMAX)
   91 PRINT 126, SUM(1)
  126 FORMAT(1X//,5X29HSUM OF SQUARES OF RESIDUALS =,E12.5)
  130 FORMAT(1H1)
  131 FORMAT(1X14HSTANDARD ERROR,5X,(11(F7.6,3X)))
  139 FORMAT(1X,//)
  140 FORMAT(1X,/////)
      READ 141, NSTOP
  141 FORMAT(I1)
      IF(NSTOP.EQ.2) GO TO 5
      IF(NSTOP.EQ.1) GO TO 16
      RETURN
      END
C       SMITHSONIAN ASTROPHYSICAL OBSERVATORY**SUBROUTINE GLSP**                001
CSIGLSP     GENERAL LEAST SQUARES PROGRAM                                       004
```

```
      SUBROUTINE GLSP(A,MM,NN,B,IPP,X,U,SUM,WT,INVRS,STDERR)
      DIMENSION A(50,10),B(50,11),X(10,11),U(50,11),SUM(11),W(10,21),
     1WT(50),STDERR(10)
      M=MM
      N=NN
      IP=IPP
      INVRSE=INVRS
C     AX=B,NORMAL EQUATIONS,A IS RECTANGULAR MATRIX,WITH M ROWS,N COLUMNS
C     WX=W1 ,NEW SET OF NORMAL EQUATIONS, W=TR(A)*A ,W1= TR(A)*B..
C     TO FORM MATRIX  W ,WITH N ROWS AND N COLUMNS. (TR= TRANSPOSE )
C  WT = -1. MEANS  NO WEIHGTS  IN PROG.   ASSIGN   WEIGHTS = 1.
C  INVRSE = 0. MEANS NO CALCULATIONS OF STD. ERRORS OF ( X )*********
C  INVRSE = 1. MEANS  STD. ERRORS ARE CALCULATED.
C  STDERR  = STANDARD ERRORS OF  UNKNOWNS ( X ) .
      KK=N+1
      IF(M-N) 80,83,81
   81 DO 5 J=1,N
      DO 5 JJ=1,N
      W(J,JJ) = 0.
      IF ( WT) 611,622,622
C   NO WEIGHTS CASE
 611  DO 51 I= 1,M
 51   W(J,JJ) = W(J,JJ) + A(I,J) * A(I,JJ)
      GO TO 5
C   WEIGHTS ARE PRESENT
 622  DO 52 I=1,M
 52   W(J,JJ) = W(J,JJ) + A(I,J) * A(I,JJ)  * WT(I)
 5    CONTINUE
C     TO FORM  MATRIX W2 , WHICH IS STORED IN N+1 TO N+P COLUMNS OF W.
C     W1 ,WITH N ROWS AND IP COLUMNS.
      IF ( INVRSE ) 201,203,201
 203  KIP = IP
      GO TO 200
 201  KIP = 1
 200  DO 8 K = 1, KIP
      DO 7 J=1,N
      W(J,KK) = 0.
      IF ( WT) 612,623,623
 612  DO 511 I=1,M
 511  W(J,KK) = W(J,KK)+A(I,J)* B(I,K)
      GO TO 7
 623  DO 522 I= 1,M
 522  W(J,KK) = W(J,KK)+A(I,J)* B(I,K)  * WT(I)
 7    CONTINUE
   8  KK = KK + 1
      GO TO 106
   83 DO 12 I=1,N
      IF ( WT) 613,624,624
 613  DO 512 J=1,N
 512  W(I,J) = A(I,J)
      GO TO 12
 624  DO 523 J=1,N
 523  W(I,J) = A(I,J) * WT(I)
 12   CONTINUE
      KKK = N+IP
      J=1
      IF ( INVRSE ) 401,403,401
 403  KKK = KKK
      GO TO 400
 401  KKK = KK
 400  DO 13 JJ= KK,KKK
      IF ( WT ) 614,625,625
 614  DO 513 I= 1,N
 513  W(I,JJ) = B(I,J)
      GO TO 13
 625  DO 524 I= 1,N
 524  W(I,JJ) = B(I,J) * WT(I)
   13 J=J+1
 106  IF ( INVRSE ) 71,72,71
 71   K2 = N + 2
      KIP = N + IP
      KK = N + 1
      DO 75 I=1,N
      DO 75 J = K2,KIP
      IF ( J - I - KK ) 73,74,73
  74  W(I,J) = 1.
      GO TO 75
 73   W(I,J) = 0.
 75   CONTINUE
 72   CALL  TRIANG (W,N,IP, DET )
C     WHERE W IS THE MATRIX WITH N ROWS AND(N+IP)COLUMNS TO BE TRIANGULA
C     RIZED
C     TO TEST THE SINGULARITY OF MATRIX  W., W = TR(A)*A  , W*X = W1.
      IF ( DET ) 82,80,82
   82 CONTINUE
      GO TO 103
   80 SUM = -1
      GO TO 104
  103 CALL  SOLVE  (W,N,IP,X)
C     WHERE W IS THE TRIANGULARIZED, X IS THE SOLUTION  MATRIX  WITH
C     N ROWS AND  IP  COLUMNS.
C     TO COMPUTE RESIDUAL MATRIX , U = A*X - B ,U IS RESIDUAL MATRX(M,P)
  105 DO 16 I=1,M
      DO 16 K=1,IP
      U(I,K) =0.
      DO 15 J=1,N
   15 U(I,K) = U(I,K) + A(I,J) * X(J,K )
 16   U(I,K) = B(I,K) - U(I,K)
      DO 18 K=1,IP
      SUM(K) = 0.
      DO 18 I=1,M
   18 SUM(K) =SUM(K) +(U(I,K))**2
      IF (M.EQ.N) GO TO 104
      IF ( INVRSE ) 722,104,722
 722  DO 723  I = 1,N
      DO  723 J= 2,IP
  723 X(I,J)=X(I,J)*(SUM(1)/FLOAT (M-N))
      DO 724 I = 1,N
      STDERR(I) = 0.
      II = I + 1
 724  STDERR(I) = SQRT ( X(I,II))
  104 RETURN
```

```
      END
CTRIANG  TO BE USED WITH SURROUTINF GLSP
      SUBROUTINE TRIANG(A,M,N,DET )
C .                 WHERE A IS THE MATRIX WITH M ROWS AND M+N COLUMNS TO
C                   BE TRIANGULARIZED.
      DIMENSION A(10,21)
      DET=1.
      MM1=M-1
      MPN=M+N
      DO 5 J=1,MM1
      MAXX = J
      VALUE = ARS  ( A(J,J))
      JP1=J+1
      DO 1 K=JP1,M
      IF ( VALUE - ARS (A(K,J)))  2,1,1
    2 VALUE = ARS (A(K,J))
      MAXX=K
    1 CONTINUE
      DO 3 L=J,MPN
      TEMP = A(MAXX,L)
      A(MAXX,L) = A(J,L)
    3 A(J,L) = TEMP
      IF ( MAXX-J) 7,6,7
    7 DET  = - DET
    6 DET = DET*A(J,J)
      ROW = A(J,J)
      DO 4 L=J,MPN
    4 A(J,L) = A(J,L)/ROW
      DO 5 K=JP1,M
      ROW = A(K,J)
      DO 5 L=J,MPN
    5 A(K,L) = A(K,L)-ROW*A(J,L)
      DFT = DFT*A(M,M)
      ROW = A(M,M)
      DO 9 L = M,MPN
    9 A(M,L) = A(M,L)/ROW
      RETURN
      END
CSOLVE   TO BE USED WITH SURROUTINF GLSP


      SUBROUTINE SOLVE(A,M,N,X)
C                   WHERE A IS THE TRIANGULARIZED MATRIX WITH M ROWS AND
C                   M+N COLUMNS.
C                             X IS THE SOLUTION MATRIX WITH M ROWS AND N
C                   COLUMNS.
      DIMENSION A(10,21),X(10,11)
      MM1=M-1
      DO 2 L=1,N
      MPL=M+L
      DO 2 K=1,MM1
      MMK=M-K
      MMKP1=MMK+1
      X(M,L)=A(M,MPL)/A(M,M)
      SUM=0.
      DO 3 I=MMKP1,M
```

```
3     SUM=SUM+A(MMK,I)*X(I,L)
2     X(MMK,L)=A(MMK,MPL)-SUM
      RETURN
      END


      SUBROUTINE CORRT(XF,XMFO,XMFC,XMFH,XMFA,JMAX)
      COMMON/PROPS/S(20),F(20),W(20),DELTA(20)
      DIMENSION XF(10),XMF(10)
      K=1
      PMLWT =0.0
      DO 102 I= 1,JMAX
      PMLWT= PMLWT+ XF(I)*W(I)
  102 CONTINUE
      DO 103 I= 1, JMAX
  103 XMF(I)= XF(I)*W(I)/PMLWT
  114 TXMO= XMF(1)+XMF(2)*16./28.+ XMF(3)*32./44.+ XMF(5)*16./18.
      DMO = XMFO-TXMO
      XMF(1) = XMF(1)+XMF(1)*DMO/TXMO
      XMF(2) = XMF(2)+(XMF(2)*DMO*16.)/(TXMO*28.)
      XMF(3)= XMF(3)+ (XMF(3)*DMO*32.)/(TXMO*44.)
      XMF(5) = XMF(5)+(XMF(5)*DMO*16.)/(TXMO*44.)
      TXMC= XMF(2)*12./28.+XMF(3)*12./44.+ XMF(4)*24./30.
      DMC= XMFC-TXMC
      XMF(2)= XMF(2)*12.*DMC/(28.*TXMC)+ XMF(2)
      XMF(3)= (XMF(3)*12.*DMC)/(44.*TXMC)+XMF(3)
      XMF(4) =(XMF(4)*24.*DMC)/(30.*TXMC)+XMF(4)
      TMH= XMF(4)*6./30.+ XMF(5)*2./18.+ XMF(6)
      DMH = XMFH-TMH
      XMF(4)=XMF(4)+XMF(4)*DMH*6./(30.*TMH)
      XMF(6)= XMF(6)+ XMF(6)*DMH/TMH
      XMF(5)= XMF(5)+XMF(5)*DMH*2./(TMH*18.)
      TXMO= XMF(1)+XMF(2)*16./28.+ XMF(3)*32./44.+ XMF(5)*16./18.
      DMO = XMFO-TXMO
      PDMO = DMO*100./TXMO
      TXMH = XMF(4)*6./30.+XMF(6)+XMF(5)*2./18.
      DMH = XMFH-TXMH
      PDMH = DMH*100./TXMH
      TXMC= XMF(2)*12./28.+XMF(3)*12./44.+ XMF(4)*24./30.
      DMC= XMFC-TXMC
      PDMC= DMC*100./TXMC
      PDMA= (XMFA-XMF(7))*100./XMF(7)
      K=K+1
      IF (K.GT.20) GO TO 112
      IF(ABS(PDMO)-2.0)131,131,114
  131 IF(ABS(PDMC)-2.0)132,132,114
  132 IF(ABS(PDMH)-2.0) 112,112,114
  112 PRINT 130,K,PDMC,PDMH,PDMO,PDMA
  130 FORMAT(1H0,*K PDM C H O A *,I2,4(2X,F8.5))
      SUM=0.0
      DO 117 I=1,JMAX
      SUM= SUM+ XMF(I)/W(I)
      XF(I) = XMF(I)/W(I)
  117 CONTINUE
      PMLWT=0.0
      DO 118 I=1, JMAX
      XF(I) = XF(I)/SUM
      PMLWT = PMLWT+ XF(I)*W(I)
  118 CONTINUE
      PRINT 120, PMLWT
  120 FORMAT( 1H0,*PMLWT*,F8.5)
      RETURN
      END
```

APPENDIX 3B

PROGRAM OHCONC FOR CALCULATION OF OH CONCENTRATION AND TEMPERATURE

```
      PROGRAM OHCONC( INPUT, OUTPUT)
      DIMENSION AMN(15), ENGY(15), WVL(15),BIO(15),BIA(15),PKOL(15),
     1 DOP(15),BIB(15), JJ(15), CONC(15), ERT(15), TCONC(15)
       DIMENSION BB(15),TM(20),TMR(20),DLR(20),CMCC(20),FROH(20)
      INTEGER CNTROL(10),BDIM
      REAL B(12,5),Z(8,20),A(12,12)
      DATA (WVL(I),I=1,12)/3085.2, 3086.2, 3087.4, 3092.4, 3092.8,
     1 3094.618, 3095.342, 3096.83, 3098.386,3101.229, 3105.663,
     2 3106.542/
      DATA(AMN(I),I=1,12)/42.2,12.7,50.6,67.5,42.6,51.0,75.8,59.3,
     1 84.1, 24.5, 84.2, 28.6/
      DATA(ENGY(I),I=1,12)/543.54,83.7,767.45,1321.25,824.48,1077.8,
     1 1650.14, 1367.54, 2014.95, 543.54, 2450.15, 767.45/
      DATA(JJ(I),I=1,12)/12,6,14,18,12,14,20,16,22,12,22,14/
  406 M=1
      READ 321,NSETS ,P
  321 FORMAT(I5,F10.6)
      PRINT 322,NSETS,P
  322 FORMAT(1X,* NSETS P*,2X,I5,2X,F10.6)
   62 READ 201,(CNTROL(I),I=1,10)
  201 FORMAT( 10I6)
      MDIM=8
      NDIM=20
      BDIM=12
    3  FORMAT (8F10.4)                                                 NLIN 600
    4  FORMAT  (32H1 NONLINEAR REGRESSION CONTROLS       10I6 //        NLIN 610
     1   30H NUMBER OF PARAMETERS                     I12 /             NLIN 620
     2   30H NUMBER OF DATA POINTS                    I12 /             NLIN 630
     3   30H NUMBER OF VARIABLES                      I12 /             NLIN 640
     4   30H LIMIT ON NUMBER/ITERATIONS               I12 /    )        NLIN 650
       NB = IABS(CNTROL(1))                                             NLIN 660
       IF (NB .EQ. 0)   STOP                                            NLIN 670
       NPTS = IABS(CNTROL(2))                                           NLIN 680
       NVARS = IABS(CNTROL(3))                                          NLIN 690
       LIMIT = IABS(CNTROL(4))                                          NLIN 700
       PRINT 4, (CNTROL(I), I=1,10), NB,NPTS,NVARS,LIMIT                NLIN 710
       IF (CNTROL(5) .EQ. 0)   PRINT 11                                 NLIN 720
       IF (CNTROL(5) .GE. 4)   PRINT 10                                 NLIN 730
       IF (MOD(CNTROL(5),2) .NE. 0)   PRINT 9                           NLIN 740
       IF (CNTROL(6) .EQ. 0)   PRINT 16                                 NLIN 750
       IF (CNTROL(6) .NE. 0)   PRINT 12                                 NLIN 760
       IF (CNTROL(10) .EQ. 0)   PRINT 15                                NLIN 770
       IF (CNTROL(10) .NE. 0)   PRINT 14                                NLIN 780
       PRINT 8, MDIM, NDIM, BDIM                                        NLIN 820
    7  FORMAT (42H0 STARTING GUESSES FOR THE PARAMETERS B(J)   )        NLIN 910
    8  FORMAT (48H0 NONLINEAR REGRESSION ARRAY DECLARATIONS ARE       / NLIN 920
     1  4H  Z( I2,  1H, I3,  8H) AND B(   I2, 1H) /1H0)                 NLIN 930
                                                                        NLIN 940
    9  FORMAT (53H CNTROL(5) .NE. 0 (MOD 2), SO PRINT INPUT DATA.      )NLIN 950
   10  FORMAT (53H CNTROL(5) .GE. 4, SO PRINT MATRICES FOR NORMAL EQS. )NLIN 960
```

```
 11  FORMAT (* CNTROL(5) = 0, SO NO INTERMEDIATE OUTPUT *)
  12  FORMAT (* CNTROL(6) .NE. 0, SO MINIMIZE RELATIVE LEAST SQUARES.*)NLIN 980
  14  FORMAT (52H CNTROL(10) NONZERO, PARAMETERS CAN CHANGE BY AT     /NLIN1000
   C          35H  MOST TEN PER CENT PER ITERATION        )             NLIN1010
  15  FORMAT (* CNTROL(10) = 0, SO UNCONSTRAINED PARAMETER CHANGES *)  NLIN1020
  16  FORMAT (* CNTROL(6) = 0, SO MINIMIZE LEAST SQUARES *)            NLIN1030
      IF (CNTROL(8) .EQ. 0)   PRINT 57
      IF (CNTROL(8) .EQ. 1)   PRINT 27
      IF (CNTROL(8) .EQ. 2)   PRINT 37                                 NLIN 170
      IF (CNTROL(8) .EQ. 3)   PRINT 47                                 NLIN 180
      IF (CNTROL(8) .EQ. 4)   PRINT 57                                 NL+N 1 0
      IF (CNTROL(8) .EQ. 5)   PRINT 6  7                               NLIN 200
  27  FORMAT (*0 TERMINATION DUE TO RELATIVE CHANGE OF LESS THAN *,/,  NLIN 210
   1  *    1.0E-8 IN AVERAGE SUM OF SQUARES.  THE SUM OF SQUARES *,/   NLIN 230
   2  *    HAS BEEN REDUCED. *)                                        NLIN 240
  37  FORMAT (*0 TERMINATION DUE TO NEGLIGIBLE CHANGE IN SUM/SQUARES *)NLIN 250
  47  FORMAT (*0 TERMINATION DUE TO LIMIT ON NUMBER OF ITERATIONS *)   NLIN 260
  57  FORMAT (*0 TERMINATION DUE TO SINGULARITY OF NORMAL EQS *)       NLIN 270
  67  FORMAT (*0 TERMINATION DUE TO NEGLIGIBLE CHANGE IN PARAMETERS.*) NLIN 280
     READ 3,(B(IB),IB=1,NB)                                            NLIN 290
      PRINT 7
      PRINT 3, (B(I), I=1,NB)                                          NLIN 800
     P= P/82.059                                                       NLIN 810
C BIB  ABSORPTION= PEAK HT * HALF WIDTH
C BIA  TRANSMITTED INTENSITY
C  BIO  INITIAL INTENSITY
      READ 301,(BIA(I),I=1,NPTS)
       PRINT 401,(BIA(I),I=1,NPTS)
       READ 301,(BIO(I),I=1,NPTS)
      PRINT 4-1,(BIO(I),I=1,NPTS)
      DO 411 I=1,NPTS
  411 BIB(I) = 0.23*(BIO(I)-BIA(I))
      PRINT 401,(BIB(I),I=1,NPTS)
  401 FORMAT(1X,*BI*,12(1X,F8.4))
  301 FORMAT(12F6.2)
C  CALCULATION OF TEMPERATURE FROM PEAK HEIGHT
      DO 302 I=1,NPTS
      PKOL(I)= (ALOG(BIO(I))-ALOG(BIA(I)))/8.0
      PRINT 303, PKOL(I),I
      Z(2,I)= ENGY(I)*1.44
      PKOL(I)= PKOL(I)/AMN(I)
      Z(1,I) = ALOG10(PKOL(I))
      PRINT 431,Z(1,I),Z(2,I)
  431 FORMAT(1X,* Z(1,I),Z(2,I)*, 2(2X,E15.8))
  302 CONTINUE
      CALL GAUSS(CNTROL,B,Z,MDIM,NDIM,BDIM,A)
      CALL FINALE(CNTROL,B,Z,MDIM,NDIM)
      TEMP = -0.434/B(2)
      PRINT 320,TEMP
  303 FORMAT(1X,*PK COEF*,2X,E15.8,2X,I3)
       TM(M) = TEMP
  320 FORMAT(1X,*TEMP*,2X,F12.6)
      DO 326 I =1,NPTS
      DOP(I)= 1.245*1.E-7*SQRT(TEMP)*WVL(I)
      PRINT 325, DOP(I)
       BIB(I)= BIB(I)*1.13/(BIO(I)*DOP(I))
C BIB= ABSORPTION* 2./(SQRT(PI)*DOP WIDTH)
```

```
325 FORMAT(1X,* DOPPLER WIDTH*,2X,E15.8)
     IF (BIB(I) . LE. 1.05 ) GO TO 403
     IF (BIB(I) . LE. 1.488) GO TO 441
     IF (BIB(I) . LE. 1.860) GO TO 442
     IF (BIB(I) . LE. 2.040) GO TO 443
     IF (BIB(I) . LE. 2.340) GO TO 444
     IF (BIB(I) . LE. 2.520) GO TO 445
     IF (BIB(I) .GT.2.52) GO TO 446
403   PKOL(I)= 0.00852818+0.8870335*BIB(I)+0.67322129*BIB(I)**2
     GO TO 404
441   PKOL(I) = 9.615-15.55*BIB(I)+ 7.895*BIB(I)**2
     GO TO 404
442 PKOL(I) = 35.99-5K.88*BIB(I)+20.40*BIB(I)**2
     GO TO 404
443 PKOL(I) = 176.0-205.5 *BIB(I) +62.50*BIB(I)**2
     GO TO 404
444 PKOL(I) = 731.4-752.3 *BIB(I)+ 197.1*BIB(I)**2
     GO TO 404
445 PKOL(I) = 1116.0-1133.0* BIB(I) +289.4*BIB(I)**2
     GO TO 404
446 PKOL(I) = 21870.0 - 17250.0*BIB(I) + 3418.0*BIB(I)**2
404 CONC(I)= 41.0*1.E21*DOP(I)*JJ(I)*PKOL(I)/((WVL(I)**2)*AMN(I))
      ERT(I) = ENGY(I)*1.44/TEMP
     AC = 2655.0/TEMP
     AD = 7760.0/TEMP
     QRV= TEMP/26.7*(1./EXP(AC)+1/EXP(AD))
     TCONC(I)= CONC(I)*QRV*EXP(ERT(I))/JJ(I)
     PRINT 306, BIB(I), PKOL(I),CONC(I),ERT(I), QRV, TCONC(I)
306 FORMAT(1X,*BI PK CON ERT QR TCN*,7(1X,F13.6))
     PKOL(I) = PKOL(I)/(AMN(I)*8.0)
     BB(I)= 0.23*(BIO(I)-BIA(I))/(BIO(I)*AMN(I))
326 Z(1,I) = ALOG10(BB(I))
     CALL GAUSS(CNTROL,B,Z,MDIM,NDIM,BDIM,A)

     TEMPR = -0.434/B(2)
     CEMP=(TEMP+TEMPR)/2.0
     DELTA= TEMPR - TEMP
     PRINT 331, TEMPR,DELTA
331 FORMAT(1X,*TEMP DELTA*,2(2X,F12.5))
319  SM=0.0
    DO 314 I=1,NPTS
314 SM= SM+ TCONC(I)
     SM= TCONC(7)
    XOH= SM*TEMP/(6.025*1.0E23* P)
    PRINT 315, SM,XOH
315 FORMAT(1X,* MOLECULES CC MOLE FRC*,2(2X,F15.8))
    TMR(M) = TEMPR
     DLR(M) = DELTA
    CMCC(M) = SM
    FROH(M) = XOH
    M= M+1
     IF (NSFTS.GE.M) GO TO 62
     PRINT 351
351 FORMAT(1X,*TEMP PK HT*,10X,*TEMP AREA*,10X,*DELTA*,10X,
   1 *CONC OH*,10X,*MOLE FR OH*)
    DO 353 I =1,M
    PRINT 471,I
```

```
      PRINT 352, TM(I),TMR(I),DLR(I),CMCC(I),FROH(I)
  471 FORMAT(1X,*M*,2X,I2)
  352 FORMAT(1X,E11.4,4(8X,E11.4))
  353 CONTINUE
  311 FORMAT(1X,*ABSRPTION GT 1.05 NO SOLUTION*)
       READ 405, MN
  405 FORMAT(I1)
      IF (MN. EQ. 2) GO TO 406
        END
```

APPENDIX 3C

```
C     PROGRAM INTEG FOR NUMERICAL INTEGRATION OF FLAME EQUATIONS

      PROGRAM INTEG(INPUT,OUTPUT)
      DIMENSION B(10,20),Y(20),F(40),AEX(20),XN(20),XT(30),EE(20),
     1TCONC(20),RCONST(20),DF(20,20),PMLWT(20),KX(20),KC(20,20),
     2 NSTCH(40,20),NEXPT(40,20),MLWT(20),KMLWT(20),YP(20),D(40),
     3DDX(20), G(20),VA(20),KA(20),T(9,40),P(40),E(40),XX(20)
C       CALCULATIONS OF REACTION RATES
      COMMON/INFO/F,D,P,T,X,H,E,XP,LFLAG,N
      COMMON/PROPS/S(20),EF(20),W(20),DELTA(20)
      DATA NBLANK/7H       /
  801 READ 298,NSS
      PRINT 299, NSS
      READ 802,(W(I),I=2,NSS)
      PRINT 803, (W(I),I=1,NSS)
      READ 802, (DELTA(I),I=1,NSS)
      PRINT 803,( DELTA(I), I=1,NSS)
      READ 802, (S(I),I=1,NSS)
      PRINT 803, (S(I),I=1,NSS)
      READ 802, (EF(I), I=1,NSS)
      PRINT 803, (EF(I), I=1,NSS)
   49 READ 283,NCASE
      PRINT 284,NCASE
      READ 55,NREACT,NS,NPTS
      PRINT 56,NREACT,NK,NPTS
      N = 2*NS
      DO 200 J=1,NREACT
      READ 11,(KC(J,I) ,I=1,6),AEX(J),EE(J),XN(J)
      PRINT 11,(KC(J,I),I=1,6),AEX(J),EE(J),XN(J)
  200 CONTINUE
      READ 12,(KX(IS),KMLWT(IS),IS=1,NS)
      PRINT 12,(KX(IS),KMLWT(IS),IS=1,NS)
      READ 804, XK, XM
      PRINT 805, XK, XM
      READ 295,ERR
      PRINT 296,ERR
  117 IS=0
      DO 15 JJ=1,NREACT
      DO 16 L=1,6
      KCHECK=KC(JJ,L)
      IF(KCHECK.EQ.NBLANK) GO TO 16
      IS=IS+1
      DO 17 MJ=1,NREACT
       NSTCH(MJ,IS)=0
      NEXPT(MJ,IS)=0
   17 CONTINUE
      KA(IS)=KCHECK
      DO 18 J=1,NREACT
       DO 19 LM=1,6
      IF(KA(IS).EQ.KC(J,LM)) GO TO 20
      GO TO 19
   20 KC(J,LM)=NBLANK
```

```
      IF (LM-3)21,21,22
   21 NSTCH(J,IS)=NSTCH(J,IS)-1
       NEXPT(J,IS)=NEXPT(J,IS)+1
       GO TO 19
   22 NSTCH(J,IS)=NSTCH(J,IS)+1
   19 CONTINUE
   18 CONTINUE
   16 CONTINUE
   15 CONTINUE
      IF(IS.NE.NS)GO TO 101
  100 DO 23 IS=1,NS
      DO 24 JS=1,NS
      IF(KA(IS).EQ.KX(JS))GO TO 25
      GO TO 24
   25 TEMP=KMLWT(JS)
      MLWT(IS)=TEMP
   24 CONTINUE
   23 CONTINUE
      PRINT 291,(KA(IS),IS=1,NS)
      PRINT 256, (MLWT(IS), IS=1,NS)
      KTR = 0
  297 READ 303,(Y(IS),IS=1,NS)
      READ 303,( G(IS),IS=1,NS)
      READ 10,(XT(I),I= 1,NPTS)
      PRINT 57,(XT(I),I=1,NPTS)
      READ 301, ROW, V, PP
      PRINT 155, ROW, V, PP
        PR=PP/82.059
      GT=XT(2)
      CALL DMULTI(DF,PP,GT,Y,NS)
      DO 125 IS=1,NS
      PRINT 811,(DF(IS,SS),JS=1,NS)
  125 CONTINUE
      CALL SIM(Y,G,DF,ROW,V,PP,GT,W)
       PRINT 165,(Y(IS),IS=1,NS)
      PRINT 268, (G(IS),IS=1,NS)
      DO 30 IS=1,NS
      JJ= IS+NS
   30 Y(JJ)=G(IS)
      H= XM/2.0
      DO 302 I=1,N
  302 E(I) = ERR
  804 FORMAT(5F6.3)
  805 FORMAT(1X, * X  STFP*, 5(2X,F6.3))
      CALL ADSET(1)
C     SET INITIAL CONDITIONS
       X= XK
      DO 321 I=1,N
  321 F(I)= Y(I)
      M= 1
      SM=M
      XP = X+ XM
  175 GT = XT(M)
      PM= PR/XT(M)
      PTM= ROW*V*XT(M)/PR
      DO 322 I =1,N
      IF (M.EQ.1) GO TO 322
      Y(I) = P(I)
      F(I)= P(I)
  322 CONTINUE
  811 FORMAT(1X,*DF*, 10(1X,E11.4))
C     INTEGRATE
  308 DO 304 ISTE= 1,50
      IF (X.GT.XP) GO TO 305
      CALL ADSET(2)
    2 DO 61 J=1,NREACT
      R= 0.0019826*XT(M)
      R1=(10.0)**AEX(J)
      R2 = XT(M)**XN(J)
      R3 = 1.0/(EXP(EE(K)/R))
      RCONST(J)=R1*(R2*R3)
   61 CONTINUE
      DO 843 I=1,N
      Y(I)= F(I)
  843 CONTINUE
      DO 844 I=1,NS
      IF((I.LE.9).AND.(F(I).LE. 0.0)) GO TO 841
  844 CONTINUE
      GO TO 851
  841 CAL3 STDY(Y,DDX,PM)
      PRIST 845
  851 CONTINUE
      DO 62 J=1,NREACT
      DDX(J)= RCONST(J)
      TCONC(J)=RCONST(J)
      DO 63 IS=1,NS
      IF(NEXPT(J,IS)-1)63,64,65
   64 TCONC(J) = TCONC(J)*Y(IS)*PR/XT(M)
       GO TO 63
   65 TCONC(J) = TCONC(J)*(( Y(IS)*PR/XT(M))**NEXPT(J,IS))
   63 CONTINUE
   62 CONTINUE
      DO 66 IS=1,NS
      SUM=0.0
      DO 67 JS=1,NS
      J=NS+IS
      JJ=NS+JS
      IF(JS.EQ.IS) GO TO 67
      SUM1 = Y(IS)*MLWT(IS)*Y(JJ)
      SUM2 = Y(JS)*MLWT(JS)*Y(J)
      SUM3= MLWT(IS)*MLWT(JS)*DF(IS,JS)
      SUM= SUM+(SUM1-SUM2)*PTM/SUM3
   67 CONTINUE
      D(IS)= SUM
   66 CONTINUE
      DO 68 IS=1,NS
      SAM=0.0
      DO 69 J=1,NREACT
      IF(NSTCH(J,IS).EQ.0)GO TO 69
      SAM= SAM+ TCONC(J)*NSTCH(J,IS)
   69 CONTINUE
      YP(IS) = SAM
   68 CONTINUE
      DO 71 IS=1,NS
      J=NS+IS
      D(J) = (MLWT(IS)*YP(IS))/(ROW*V)
   71 CONTINUE
       CALL ADSET(3)
      IF(LFLAG.EQ.1) GO TO 2
  304 CONTINUE
  305 CALL ADSET(4)
      PRINT 50,XP
      PRINT 281,(DDX(J),J=1,NREACT)
      PRINT 282,(D(J),J=1,N)
      PRINT 122,(KA(IS),IS=1,NS)
  122 FORMAT(1X,10X,9(A4,7X))
      DO 874 IS=1,NS
      IF(P(IS).LE. 0.0) GO TO 875
  874 CONTINUE
      GO TO 876
  875 CALL STDY(P,DDX,PM)
      PRINT 845
  845 FORMAT(1X,* STDY CALLES*)
  876 CONTINUE
      PRINT 87, (P(JJJ),JJJ=1,NS)
      JS= 1+NS
      PRINT 87,(P(JJJ), JJJ=JS,N)
      SM=0.0
      DO 872 I=1,NS
      SM= SM+P(I)
  872 CONTINUE
      PRINT 87,SM
      DEL= SM-1.0
      DEL= ABS(DEL)
      IF(DEL.GT. 0.10) GO TO 806
      M=M+1
      SM= M
      IF ( M .GT. NPTS) GO TO 808
      XP =XP+XM
      GO TO 175
  808 KTR = KTR+1
  806 READ 807,ML
      IF ( ML.EQ. 1) GO TO 49
      IF (ML.EQ.2) GO TO 297
      IF (ML.EQ.3) GO TO 801
  807 FORMAT(I1)
   10 FORMAT(10F8.3)
   11 FORMAT(6A7,3F8.4)
   12 FORMAT(8(A7,I3))
   13 FORMAT(3F10.6)
   14 FORMAT(20F4.2)
   50 FORMAT(1H0,55X,*X*,F10.6)
   55 FORMAT(5I4)
   56 FORMAT(1H0,8H NREACT=,I4,2X,5H NS =,I4,2X,6H NPTS=,I4)
   57 FORMAT(1H0,6F10.4)
   87 FORMAT(1X,*Y(IS)*,9(1X,E10.4))
  105 FORMAT(1H0,*ERROR IN NUMBER OF SPECIES*)
  115 FORMAT( 1H0,*XX*,20(2X,F4.3))
  133 FORMAT(8F10.5)
  155 FORMAT(1H-,*ROW V P*,3(1X,E11.4))
  165 FORMAT(1H0,*Y(IS)*,10(1X,F8.6))
```

```
256 FORMAT(12X, 10(I4,5X))
257 FORMAT(1-F8.5)
258 FORMAT (1H0,*DDX*, 10(1X,F8.5))
268 FORMAT (1H0,*G(IS)=*,10(1X,F8.6))
271 FORMAT(1H0,*DF(IS,JS)*, 9(2X,E11.4)/,
   1 1X,*DF(XXXX)*, 9(2X,E11.4))
282 FORMAT(1X,*D(J)*,8(2X,E11.4)/,5(5X,8(2X,E11.4)/)//)
281 FORMAT(1X,*RCONST(J)*,8(2X,E11.4)/,5(10X,8(2X,E11.4)/)//)
283 FORMAT(I3)
284 FORMAT(1X,* CASE NO= *,I3)
291 FORMAT(1H0,12X,10(A4,5X))
295 FORMAT( E10.4)
296 FORMAT(2X,*ERROR LIMIT*,2X,E11.4)
298 FORMAT(I2)
299 FORMAT(1X,*NMBER OF SPECIES=*,2X,I2)
301 FORMAT (F10.8,7F10.4)
303 FORMAT(10F8.6)
601 FORMAT(1X,*J=*,I3,2X/,1X,*NSTCH*,20(2X,I3)/)
602 FORMAT(1X,*NEXPT*,20(2X,I3)/)
711 FORMAT(10F8.4)
712 FORMAT(1H0,*PMLWT*,10(2X,F8.4))
802 FORMAT(10F8.3)
803 FORMAT(1X,* W DELTA S E*,10(3X,F8.3)//)
101 PRINT 105
 47 STOP
    END


    SUBROUTINE STDY(P,DDX,PM)
    DIMENSION RCONST(20),P(20),DDX(20)
    BF= (DDX(4)*P(2)+DDX(5)*P(7))*PM
    DG= (DDX(1)*P(1)*P(2) +DDX(7)*P(7)*P(2))*PM**2.0
    C= DDX(4)*DDX(8)*P(8)*P(2)*(PM**2.0)+
   1   DDX(4)*DDX(1)*P(1)*P(2)*(PM**2.0)+
   1   DDX(5)*DDX(8)*P(8)*P(7)*(PM**2.0)+
   1   DDX(5)*DDX(1)*P(1)*P(7)*(PM**2.0)
    P(4) = DG*BF/(C*PM)
    P(6)= (DDX(3)*P(4)*P(5)+DDX(6)*P(4)*P(2))*PM/BF
    RETURN
    END
```

```
        SUBROUTINE ADSET  (NWHERE)
C.... GLAUZ-ADAMS METHOD OF INTEGRATION.
C.... WITH QUASI-DOUBLE PRECISION INCREMENTING OF X AND Y.
C.... IN T(J,I), I=1...N REFERS TO THE EQUATION.  LET FN = THE FUNCTION
C        VALUE AT X, FP = PREDICTED FUNCTION VALUE AT X+H, FC = CORRECTED
C        FUNCTION VALUE AT X+H.  THEN J=1 REFERS TO LOCATION CONTAINING
C        DIFFERENCES AT X.
C        DERIVATIVE AT X, J=5...8 REFER TO THE FIRST FOUR BACKWARD
C        FC-FN, J=2 REFERS TO FP-FN, J=3 REFERS TO FN, J=4 REFERS TO THE
C        J=9 REFERS TO THE ROUND-OFF ERROR IN INCREMENTING FN, TO BE
C        ADDED ON FOR QUASI-DOUBLE PRECISION (NOT USED IN ADIN2).

        COMMON /INFO /  F,D,P,T,X,H,E,XP,LFLAG,N
      DIMENSION F(40),D(40),P(40),T(9,40),E(40),TP(5)
      DIMENSION COEFP(5),COEFC(6),TDBL(8),THAL(10),TPBL(10)

       NWAY = MOD(NWHERE,4) + 1
       GO TO (305,5,55,155),NWAY

C.... INITIALIZE STORAGE AREAS
    5  CONTINUE
      IFLAG=0
      DO 20 J=5,9
      DO 10 I=1,N
   10 T(J,I)=0
   20 CONTINUE
      NCOUNT=4
      XERR=0.
      ACCSLP=2.0**(-21)
      DO 40 I=1,N
      IF (E(I) .LE. 0.0)  E(I) = 1.0E-8
   40 CONTINUE
      RETURN


C.... INTEGRATE TO GET PREDICTED COMPONENTS OF F.
   55  CONTINUE
       IF (IFLAG .EQ. 0)  RETURN
       LFLAG = 0

C.... SAVE OLD FUNCTION VALUES.
  110 DO 120 I=1,N
  120 T(3,I)=F(I)
      X1=X

C.... COMPUTE PREDICTED FUNCTION VALUES.
  130 DO 134 I=1,N
      TEMP=0
      DO 132 J=4,8
  132 TEMP=T(J,I)*COEFP(J-3)+TEMP
      T(1,I)=H*TEMP
  134 F(I)=T(3,I)+(T(1,I)+T(9,I))
      X=X1+(H+XERR)
      RETURN
```

```
C.... COMPUTES CORRECTED VALUE OF F, TESTS ACCURACY.
  155  CONTINUE
       IF (IFLAG .EQ. 0)  GO TO 280
       IDBL = 0

C.... COMPUTE CORRECTED FUNCTION VALUES.
      DO 204 I=1,N
      TEMP=0
      DO 202 J=4,7
  202 TEMP=T(J,I)*COEFC(J-3)+TEMP
      T(2,I)=H*(TEMP+COEFC(6)*D(I))
  204 F(I)=T(3,I)+(T(2,I)+T(9,I))
C.... SET ACCURACY.
      DO 220 I=1,N
      ACCUR=ABS(ACCSLP*F(I))
      IF (ACCUR .LT. E(I)) ACCUR=E(I)
      CPDIFF=ABS(T(2,I)-T(1,I))
C.... IF FC-FP .GE. ACCUR THEN HALVE H.
      IF (CPDIFF .GE. ACCUR) GO TO 270
C.... IF FC-FP .GE. ACCUR/32 THEN DO NOT DOUBLE H.
       IF (ACCUR .LE. 32.0*CPDIFF)  IDBL = I
  220 CONTINUE

C.... RECOMPUTE DIFFERENCES.
      DO 240 I=1,N
      OLD=T(4,I)
      T(4,I)=D(I)
      DO 230 J=4,NCOUNT
      TEMP=T(J,I)-OLD
      OLD=T(J+1,I)
  230 T(J+1,I)=TEMP
  240 T(9,I)=(T(2,I)+T(9,I))-(F(I)-T(3,I))
      XERR=(H+XERR)-(X-X1)
      IF (NCOUNT .LT. 7) NCOUNT=NCOUNT+1
      IF (IDBL.NE.0) GO TO 260

C.... DOUBLE INTERVAL H.
C.... (ONLY OCCURS IF ALL EQUATIONS HAVE FC-FP .LT. ACCUR/32.)
       DO 256 I = 1,N
      T(5,I)=T(5,I)*TDBL(1)+T(6,I)*TDBL(2)
      L=3
      DO 254 J=6,8
      TEMP=0
      DO 252 K=J,8
      TEMP=T(K,I)*TDBL(L)+TEMP
  252 L=L+1
  254 T(J,I)=TEMP
  256 CONTINUE
      H=2.0*H

  260  LFLAG = 0
       RETURN

C.... HALVE INTERVAL H.
C.... (OCCURS IF ANY ONE EQUATION HAS FC-FP .GE. ACCUR.)
```

```
  270 DO 276 I=1,N
      L=1
      DO 274 J=5,8
      TEMP=0
      DO 272 K=J,8
      TEMP=T(K,I)*THAL(L)+TEMP
  272 L=L+1
  274 T(J,I)=TEMP
  276 CONTINUE

      X=X1
      LFLAG=1
      IF (H.LE.1.0E-05) GO TO 130

      H=.5*H
      GO TO 130

C.... INITIALIZE DIFFERENCE TABLE.
  280 IFLAG=1
      DO 290 I=1,N
  290 T(4,I)=D(I)
      LFLAG=1
      GO TO 110


C.... INTEGRATE A PARTIAL STEP FORWARD TO GET VALUE OF F AT XP.
  305  CONTINUE
      PRINT 401, XP, X, XERR, H
  401 FORMAT(1X,*XP X XER H*,4(2X,E14.7))
      TP(1)=((XP-X)-XERR)/H
      DO 310 K=2,5
  310 TP(K)=TP(K-1)*TP(1)
      L=1
      K=5
C.... COMPUTE COEFFICIENTS OF DIFFERENCES.
      DO 330 J=1,4
      TEMP=0.
      DO 320 I=2,K
      TEMP=TPBL(L)*TP(I)+TEMP
  320 L=L+1
      TP(K)=TEMP
  330 K=K-1

C.... COMPUTE FUNCTION VALUES AT XP.
      DO 344 I=1,N
      TEMP=0
      DO 342 J=4,8
  342 TEMP=T(J,I)*TP(J-3)+TEMP
  344 P(I)=F(I)+(H*TEMP+T(9,I))
      RETURN


      DATA COEFP/1.0,.5,.416666667,.375,.348611111/
      DATA COEFC/.651388889,.151388889,.0680555556,.0263888889,.0,
     1.348611111/
      DATA THAL/.5,.125,.0625,.0390625,.25,.125,.078125,.125,.09375,
     1.0625/
```

```
      DATA TDBL/2.0,-1.0,4.0,-4.0,1.0,8.0,-12.0,16.0/                   ADIN 165
      DATA TPBL/.125,.152777778,.0625,.00833333333,2*.166666667,        ADIN 166
     1.0416666667,.25,.166666667,.5/
      END


      SUBROUTINE SIM(Y,G,DF,ROW,V,PP,GT,W)
      REAL MWT
      DIMENSION A(8,8),B(8,1),Z(8)
      DIMENSION MWT(10),Y(20),G(10),DF(20,20),FR(10),DR(10) ,W(20)
      N1=1
      NDIM=8
      N=8
      NS=9
      SCALE=1.0
      DO 16 IS=1,NS
      MWT(IS)=W(IS)
      DR(IS)=G(IS)
      FR(IS)=Y(IS)
   16 CONTINUE
      PT= PP/(82.059*GT)
      PTM= ROW*V/PT
      NS=8
       DO 21 IS=1,NS
      DO 21 JS=1,NS
       IF (IS.EQ.JS) GO TO 23
       A(IS,JS)= PTM*FR(IS)/(MWT(JS)*DF(IS,JS))
      A(IS,JS)= A(IS,JS)-PTM*FR(IS)/ (MWT(9)*DF(IS,9))
      GO TO 21
   23 SM=0.0
      NN=NS+1
      DO 24 KS=1,NN
      IF (IS.EQ.KS) GO TO 24
      SM= SM+FR(KS)*PTM,(MWT(IS)*DF(IS,KS))
   24 CONTINUE
      SM= SM    + PTM*FR(IS)/(MWT(9)*DF(IS,9))
      A(IS,JS)= -SM
   21 CONTINUE
      DO 25 IS=1,NS
      B(IS,1)= DR(IS)- PTM*FR(IS)/(MWT(9)*DF(IS,9))
   25 CONTINUE
       L= LNEQF(NDIM,N,N1,A,B,SCALE,Z)
       PRINT 27,L
   27 FORMAT(1X,*L*, I4)
      PRINT 26,(Z(I),I=K,N)
   26 FORMAT(1X,*Z*,10(E11.4,1X)/)
      DO 32 I=1,N
      PRINT 33,(A(IS,I),IS=1,NS)
   32  CONTINUE
      PRINT 33,(B(IS,1),IS=1,NS)
   33 FORMAT(1X,*A B*,9(E11.4,1X))
      SM= 0.0
       DO 28 IS=1,NS
   28 SM=SM+B(IS,1)
       PRINT 26, SM
      DO 42 IS=1,NS
      G(IS)=B(IS,1)
   42 CONTINUE
      G(9)= 1.0-SM
      RETURN
       END
```